Studies on the skin penetration mechanisms of liposomal formulations

seit 1558

Dissertation

To fulfill the requirements for the degree of

'*Doctor rerum naturalium*' (Dr. rer. nat.)

Submitted to

Council of the Faculty of Biology and Pharmacy of

Friedrich Schiller University Jena

Submitted by Mukul Ashtikar

Master of Pharmaceutical Sciences (MS)

Born on 26th April 1985 in Mumbai, India

Studies on the skin penetration mechanisms of liposomal formulations

seit 1558

Dissertation

zur Erlangung des akademischen Grades

„*Doctor rerum naturalium*“ (Dr. rer. nat.)

vorgelegt dem Rat der Biologisch-Pharmazeutischen Fakultät

der Friedrich-Schiller- Universität Jena

von Mukul Ashtikar

Master of Pharmaceutical Sciences (MS)

Geboren am 26.04.1985 in Mumbai, Indien

Reviewers

Reviewer 1: **Prof. Dr. Rolf Daniels**
Eberhard Karls Universität Tübingen

Reviewer 2: **Emeritus Prof. Dr. Alfred Fahr**
Friedrich Schiller Universität Jena

Reviewer 3: **Prof. Dr. Dr. Jürgen Lademann**
Charité Universitätsmedizin Berlin

Date of defense: 2nd March 2016

"Equipped with his five senses, man explores the universe around him and calls the adventure Science."

- Edwin Hubble

Table of Contents

1. Introduction

Drug delivery to skin includes a wide array of therapeutic technologies and pharmaceutical applications. In general, these techniques can be broken down into 1) topical applications, when the drugs are delivered locally to treat skin conditions and 2) transdermal applications, when drug is delivered across the skin for absorption into the systemic circulation for therapeutic effect somewhere else in the body. Examples of topically delivered drugs include antifungals, antibacterials, antivirals, corticosteroids, local anesthetics, anticancer drugs etc. Transdermal delivery on the other hand is an alternative route for the systemic drug delivery and as a result has much broader applications. Transdermal delivery offers advantages like, avoiding the first pass effect, control over rate of drug release, better patient compliance, possibility of immediate termination of the therapy etc. Advantages of topical drug delivery over oral delivery include, fast onset of action and substantially reduced dose of drug as formulation is applied directly to the affected area region of the body.

According to 2012 statistics, transdermal drug delivery systems represent over 12% of global market share in pharmaceutical sales with topical delivery systems accounting for about 6% (Markets and Markets, 2013). Since their introduction in 1981, twenty-two transdermal prescription products were approved by the US-FDA till 2014. Despite their success and market growth, only a handful molecules have been approved for transdermal delivery. This is mainly because skin forms a very effective barrier against drugs and to passively transport drugs across this barrier drugs must be in a narrow window of physicochemical properties. These ideal properties include, low molecular weight (preferably < 600 Da), adequate solubility in water and oil (water/octanol partition coefficient in the range of 1 – 3) and low melting point (Barry, 2001). Apart from physicochemical requirements, drugs must also possess relatively high potency otherwise large doses of drug can render dimensions of the transdermal system impractical. Also skin barrier properties can change significantly based on age, race, location of application etc. (Kenneth and Michael, 2002). All these requirements mean that number of available drugs that are suitable for transdermal drug delivery are limited. To overcome this limitation, several strategies have been introduced which range from using penetration enhancers to assist the drug penetrate into the skin by modulating the barrier function of the stratum corneum (SC) to physically bypassing the SC using techniques such as microneedles, laser ablation etc. The following section will focus on structure of the skin and understanding the role of liposomes in the grand theme of drug delivery to the skin followed by a brief introduction to the tip-enhanced Raman scattering spectroscopy.

1.1 Structure of skin

Skin is the largest organ of the human body weighing at approximately 10 % of the body weight in adults and with an impressive surface area of about 20,000 cm² (Schaefer and Redelmeier, 1996). Skin forms a vital barrier between the environment and our organs. This barrier function protects us from harmful effects of chemicals, microorganisms, allergens and UV radiation. Skin barrier is 100 – 10,000 times less permeable compared to a blood capillary wall (Cevc and Vierl, 2010). Other major functions

of the skin include homeostasis by thermoregulation and sensory function by detecting heat, pressure, pain and allergen mediated stimuli. Thickness of skin varies between 0.5 – 4 mm depending upon the anatomical location, which subsequently means based on the location, skin barrier can also vary considerably. Briefly, skin can be considered to be divided in four layers, outermost stratum corneum (non-viable epidermis), viable epidermis, dermis, and bottom most subcutaneous tissue. Apart from different layers, skin also contains appendages like hair follicles, sweat glands and sebaceous glands. **Figure 1** shows a schematic representation of the human skin. For many years role of appendages has been neglected as they cover less than 0.1 % of surface area on the skin however, in the last decade drug delivery through the appendages has gained interest (Patzelt and Lademann, 2013).

1.1.1 Stratum corneum

Stratum corneum is the outermost layer of the epidermis formed by 10-15 layers of highly flattened, highly differentiated, non-nucleated cells called corneocytes. Typically the SC is 10-20 μm thick however, its thickness can vary greatly depending on body site, age, gender and race (Cevc and Vierl, 2010). Corneocytes are terminally differentiated keratinocytes originating from basal layers of viable epidermis. Corneocytes typically have a diameter of 40 – 50 μm and are 0.5 – 1 μm in thickness. Corneocytes are devoid of any cytoplasmic organelle, their plasma membrane is replaced by a cornified envelope and they chiefly contain bundles of keratin and lipids. Intercellular spaces within the corneocytes are surrounded by complex lipid domains which are secreted by the terminally differentiating keratinocytes from viable epidermal layer called *stratum granulosum* (Schaefer and Redelmeier, 1996). Intercellular spaces are typically 0.2 μm wide and contain high concentrations of saturated lipids. In a simplistic approach, arrangement of corneocytes and intercellular lipid can be described by the 'brick and mortar' model where corneocytes form the bricks (proteins) and intercellular lipids form the mortar (lipids) holding the bricks together (Elias, 1983). This stacked arrangement of alternating hydrophilic and lipophilic layers is responsible for the barrier properties of the SC.

Intercellular lipids mainly contain ceramides, cholesterol and free fatty acids. Ratios of these lipids depend upon location within the epidermis. SC lipid contains approximately 50 % by weight of ceramides. So far, 342 different ceramides belonging to 11 different classes have been extracted and identified in the human SC. Typically, the SC lipids are characterized by long saturated acyl chains ranging from 18 to 72 carbon atoms (Masukawa *et al.*, 2008). Within the intercellular spaces lipids are arranged in multi-lamellae with alternating wide bands (6.5 nm) and narrow bands (4.5 nm) (Iwai *et al.*, 2012). It must be pointed out that there is no clear consensus between the scientists about the molecular arrangements in the lipid lamellae. Different theories for molecular arrangement predict different lamellar repeat distances ranging from 4.5 nm up to 13 nm (Bouwstra *et al.*, 1991; Garson *et al.*, 1991; Madison *et al.*, 1987; White *et al.*, 1988).

Corneocytes are connected to each other by structural proteins called 'corneodesmosomes' (Skerrow *et al.*, 1989). In the SC these proteins do not have any other function but supporting the neighboring

corneocytes. SC can be divided further in two layers, *stratum disjunctum* which comprises of top 3-5 layers of the SC and *stratum compactum* located at the bottom. *Stratum compactum* as the name suggests contains more compact arrangement of the corneocytes whereas corneocytes in the *stratum disjunctum* are relatively loosely arranged due to a process called 'desquamation' which is responsible for shedding of the skin (Fartasch, 1996). An important feature of the SC is its low water content. SC contains only 15 – 30 % water by weight as compared to about 70 % water present in the viable epidermis (von Zglinicki *et al.*, 1993).

It is well established that the SC is responsible for a major fraction of the barrier to the percutaneous absorption of topically applied compounds. A strong evidence for this was provided in the form of increased transdermal flux for different penetrating compounds when the SC was physically removed by tape stripping (Feldmann and Maibach, 1965; Kranz *et al.*, 1977; Malkinson, 1962; Schaefer *et al.*, 1982; Scheuplein and Blank, 1971; Washitake *et al.*, 1973). Removal of the SC can increase transdermal permeability by a factor of 10 – 20 (Schaefer and Redelmeier, 1996). Also skin disorders such as ichthyosis and dermatitis which alter structure of *stratum corneum* have been associated with increased trans-epithelial water loss and higher absorption of compounds like hydrocortisone, hexyl nicotinate etc. (Aalto-Korte, 1995; Lavrijsen *et al.*, 1993; Levin *et al.*, 2013). Although SC is the major skin barrier, deeper layers also possess a small barrier function.

1.1.2 Viable epidermis

Viable epidermis is the layer directly below SC and is responsible for producing the highly differentiated corneocytes of the SC. Viable epidermis is typically 50 – 100 µm thick and contains three distinct layers based on the state differentiation of keratinocytes. At the bottom, *stratum basale* which produces columnar keratinocytes capable of undergoing large but finite number of cell divisions. After detachment from *stratum basale*, keratinocytes migrate through *stratum spinosum* and *stratum granulosum*. Cytoplasm of keratinocytes in granulosum is characterized by granules of keratohyalin (Schaefer and Redelmeier, 1996). As differentiating keratinocytes migrate upwards, they begin to flatten and the transition between *stratum granulosum* and *stratum corneum* is characterized by excretion of lamellar bodies into the extracellular space which forms the intercellular lipid matrix of the *stratum corneum*. Apart from keratinocytes viable epidermis also contains Langerhans cells responsible for immune response, melanocytes which produce melanin and Merkel cells which are involved in the somatosensory functions (Winkelmann and Breathnach, 1973). Viable epidermis does not contain any blood capillaries but does contain nerve fibers (Nolano *et al.*, 1999). Due to a lack of vascular network, nutrients are delivered to the keratinocytes by passive diffusion through the interstitial fluid. Water content of the viable epidermis is approximately 70% by weight (Schaefer and Redelmeier, 1996).

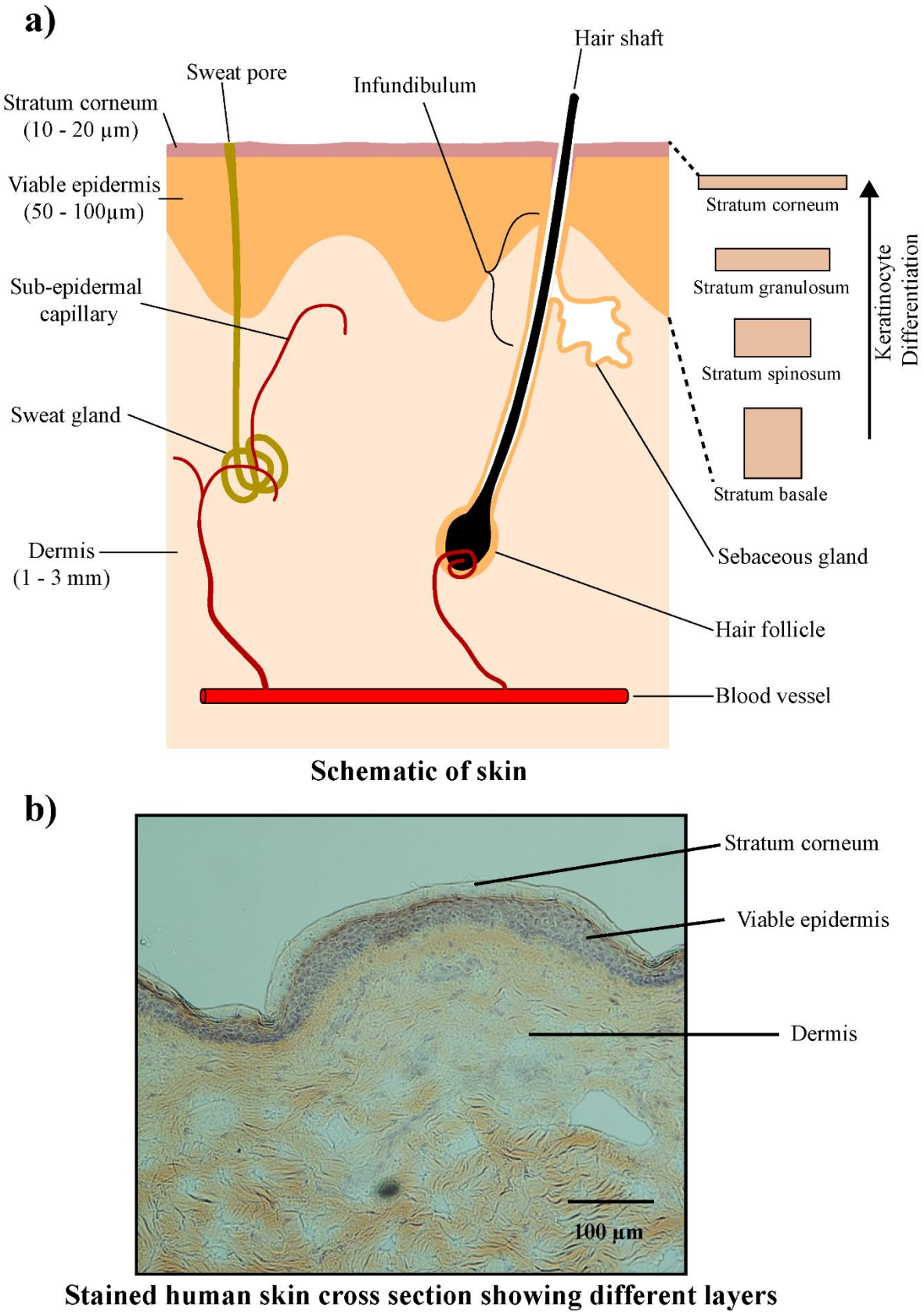

Figure 1: a) Schematic diagram of human skin showing different layers and appendages. Reproduced from Barry (2005) b) Human skin cross section stained using Mayer's hemalaun and congo red (Unpublished data).

1.1.3 Dermis

Dermis is the layer below viable epidermis, it forms the major bulk of the skin and is the thickest layer of the skin at 0.5 – 3 mm depending on the location on the body. Dermis is divided in to outer *papillary dermis* and inner *reticular dermis*. Papillary dermis contains papillae which interdigitate with the *stratum basale* of the viable epidermis. A large proportion of the dermis by weight contains a relatively loose fibrous connective tissue matrix. Cellular component of the dermis comprises of fibroblasts, epithelial cells, mast cells and cells of immune system such as lymphocytes and leukocytes. Fibroblasts, as the name suggests are responsible for producing connective tissue components like collagen, elastin, fibronectin etc. Mast cells play an important role in tissue regeneration and provide defense reactions against invading pathogens through release of histamine, protease enzymes and chemotactic factors (Goldsmith and Fitzpatrick, 2012; Schaefer and Redelmeier, 1996). The connective tissue matrix is composed of high amounts (approximately 70 % of dry weight of dermis) of collagenous fibers (Cevc and Vierl, 2010). Elastin fibers present in the connective tissue provide elasticity to this layer. The water retaining ability of the dermis originates from a class of compounds known as proteoglycans and glycosaminoglycans which are present in the connective tissue matrix. These compounds can retain water up to 1000 times their own weight. Dermis also provides physical support for skin appendages, nerve fibers and network of lymphatic and blood vessels. Microvasculature of the dermis is responsible for maintaining the sink conditions for the drug molecules that have penetrated through the primary skin barrier into the dermis (Ng and Lau, 2015). Dermis does not pose as a major barrier to drugs unless drugs are susceptible to enzymatic degradation then dermis can pose as a relevant barrier for absorption of drugs into systemic circulation.

1.1.4 Skin appendages

Most important skin appendages include, sweat glands, hair follicles and sebaceous glands. These appendages originate from lower dermis and reach the skin surface by penetrating through viable epidermis and the *stratum corneum*. Skin appendages occupy about 0.1 % of the total skin area (Higuchi, 1962) and as a result in the past they were not considered to be significant in the overall theme of percutaneous absorption. In past couple of decades better understanding of the structure of these appendages has reignited the interest in trans-appendageal drug delivery for both local and systemic delivery.

Amongst all appendages *sweat glands* are the most abundant with approximately 400 glands/cm² (Schaefer and Redelmeier, 1996). There are two types of sweat glands, ‘eccrine’ glands which are more abundant and are located throughout the body and ‘apocrine’ glands which are limited to axilla, anus and areolar regions of the breast. Eccrine glands are highly coiled and extend from deep dermis or upper subcutaneous regions (Eroschenko and Fiore, 2013). Their secretions are watery, hypotonic and are mainly responsible for temperature regulation of the body surface. Apocrine glands on the other hand

are associated with hair follicles and secrete viscous fluids which has an unpleasant odor after bacterial decomposition.

Hair follicles are the second most abundant skin appendages. Entire human body is covered with hair follicles except on the palms and soles. Humans on average have about 5 million hair follicles in total, about 80,000 to 150,000 are located on the scalp (Krause and Foitzik, 2006). Based on their length, hair can be classified as 'vellus' hair which extend about 1 mm into the dermis and 'terminal' hair which give rise to relatively coarse hair and extend more than 3 mm into the subcutaneous tissue. In brief, hair follicles consist of a hair bulb and a hair shaft. Hair bulb contains hair papilla and hair matrix and are responsible for the growth of the hair. *Infundibulum* is a funnel shaped region of the hair follicle near the opening of the hair follicle on surface of the skin. *Infundibulum* is about 0.6 – 0.8 mm in length and is characterized by lining of epithelial cells which are well perfused due to the capillary network in the surrounding region (Krause and Foitzik, 2006). Upper part of the *infundibulum* is lined with keratinized epidermis and has a structure similar to the SC however; in the lower region of the *infundibulum* the epithelial lining is interrupted. Due to this structural peculiarity transfollicular drug delivery is conceivable and has gained momentum in the past years (Patzelt and Lademann, 2013). Due to secretion of sweat, pH of the skin surface is mildly acidic and can be in the range of 4 – 7.0 (Herrmann and Mandol, 1955). Skin pH is an important parameter and should be taken into consideration during formulation development as variation in pH could affect the stability of the formulation or even irritate the skin.

Hair follicles are associated with one or more sebaceous glands towards the mouth of the hair follicles. Sebaceous glands are holocrine glands which secrete an oily fluid called sebum. Activity of sebaceous glands is age dependent and commonly peaks around puberty and is reduced in infants and in old age (Krause and Foitzik, 2006). Density of sebaceous glands is the highest on face and forehead. Sebum typically is composed of mixtures of triglycerides, free fatty acids, squalene and waxes. Excretion rate of sebum averages around 0.1 mg/cm²/h (Krause and Foitzik, 2006). It is a common consensus that sebum does not have a skin barrier function. However, it may have a beneficiary or a retarding effect on the percutaneous penetration of the drug applied to the skin, depending on the nature of formulation and physicochemical properties of the drug.

1.2 Strategies for overcoming the skin barrier function in dermal delivery

A very small number of drugs have the ability to effectively cross the skin barrier and reach target sites in therapeutic concentrations, therefore various strategies can be employed to help the drug cross the skin barrier effectively. In this section a brief snapshot of the various strategies developed over past decades in drug delivery to or through the skin is presented. In skin delivery, first objective must be to identify the location of target sites for action of the drug applied on the skin. Based on the distance from site of application, drug targets can be classified as 1) local, drug penetration only in the near-surface skin layers such as epidermis and dermis. For example topical formulations for treatment of skin

conditions like eczema, psoriasis etc. 2) deep local regions, drug must penetrate the skin deep in therapeutic concentrations to act on local targets 3) systemic circulation, site of application of drug and target sites are far apart (Flynn and Weiner, 1991). Identification of the target sites is an important consideration because it influences drug selection and transdermal strategy selection as different techniques tend to deposit different amounts of drug into the skin. For simplicity, strategies for topical drug delivery are classified topical, chemical and physical. For in-depth overview about transdermal penetration strategies, interested readers are urged to discover following publications, Atkinson *et al.* (2015); Barry (2005); Narasimha Murthy and Shivakumar (2010); Prausnitz and Langer (2008).

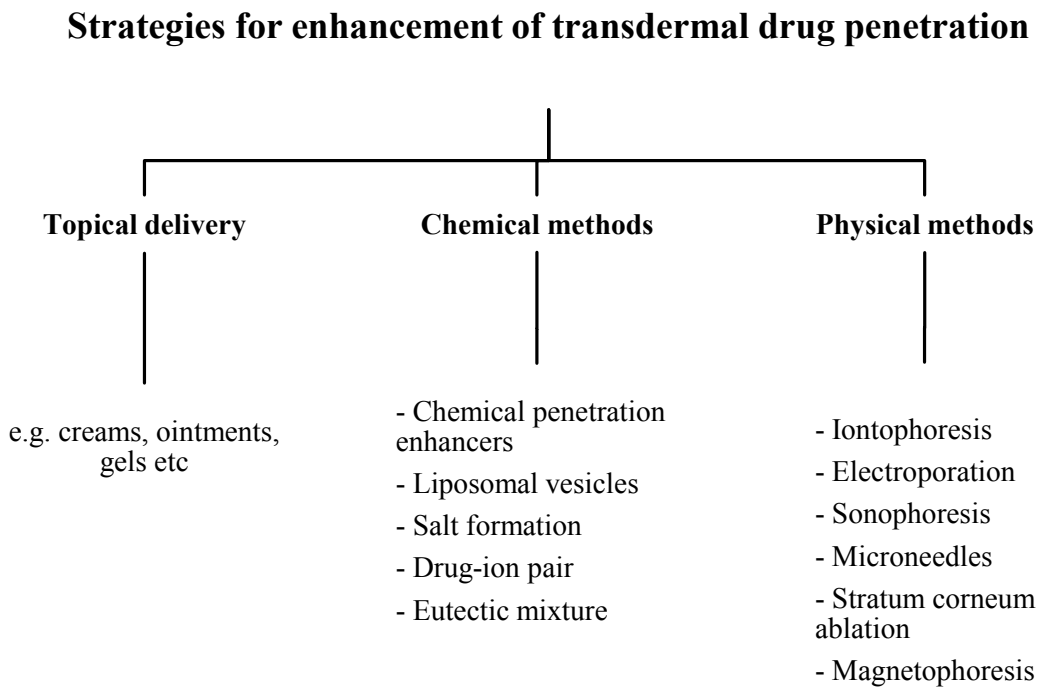

Figure 2: An overview of the various strategies for enhancing drug delivery to or through the skin

1.2.1 Topical drug delivery

Drugs delivered topically include antibiotics, antivirals, antifungals, corticosteroids, anti-inflammatory, anesthetics etc. Typically, conventional formulations like creams, ointments, gels, lotions, emulsions, solutions etc. are employed in the topical drug delivery. Drug penetration from conventional formulations is usually limited to upper layers of skin only. However, conventional formulations benefit from the fact that in dermatological conditions or skin infections, the skin barrier function is impaired thus formulations typically do not employ complex penetration enhancing strategies to improve drug penetration into the skin. It does not mean however that conventional formulations cannot be used for transdermal applications. Gels and creams containing chemical penetration enhancers such as short chain alcohols, propylene glycol, surfactants etc. have been employed e.g. doc® ibuprofen gel in the treatment of muscle pain.

1.2.2 Chemical methods for penetration enhancement

Chemical penetration enhancers are a wide class of compounds which temporarily reduce the skin barrier function which can lead to increased drug penetration into the skin (Barry, 2001). For example, water, short chain alcohols like ethanol, propanol, dimethylsulfoxide and analogs, fatty acids, surfactants, pyrrolidones, urea, polyols, terpenes, essential oils etc. Chemical penetration enhancement for increased drug penetration is by far the most studied strategy as these penetration enhancers can enhance penetration of a wide variety of drugs (Atkinson *et al.*, 2015). For example, fatty acids have shown to increase skin penetration of flurbiprofen (Chi *et al.*, 1995), vasopressin, levosimendan (Valjakka-Koskela *et al.*, 2000), diclofenac sodium (Escribano *et al.*, 2003), ondansetron (Takahashi and Rytting, 2001), tenoxicam (Gwak and Chun, 2002) etc. Increased drug penetration is achieved by one or more of the following mechanisms depending on the chemical nature of the penetration enhancer; 1) lipid modification – by disrupting the intercellular lipid organization in the SC 2) protein modification – by interacting with the corneocyte proteins 3) partitioning promotion – alters the chemical environment of the SC which increases partitioning of drug into the SC (Barry, 2005). Chemical penetration enhancers are usually only effective in increasing drug penetration of small molecules. Also to achieve a substantial penetration enhancement, high concentrations of penetration enhancers are required which can be irritating to the skin. Due to the irritation potential of these chemical agents, they are not used as a stock vehicle for the drug but rather used in small concentrations as excipients in creams, gels, transdermal patches etc.

Phospholipid vesicles (liposomes) are spherical, self-contained amphiphilic bilayer membranes containing an aqueous interior, usually in the colloidal size range. As the name suggests, most commonly liposomes are prepared from phospholipids and can contain excipients like surfactants, ethanol, cholesterol etc. There exists a group of liposomes which were specifically designed for dermal drug delivery, e.g. Transfersomes®, invasomes, ethosomes, niosomes etc. Role of liposomes in drug delivery to skin is discussed in much greater detail in the following section 1.3.

A group of strategies to chemically modify the drug to improve its physicochemical properties for better skin penetration include, salt formation, ion-pair formation and prodrug formation. Solubility of the drug in a vehicle or a solvent can be affected by *salt formation*. Such increase in solubility can often lead to increased transdermal penetration. Cheong and Choi have shown that percutaneous permeation of piroxicam in hairless mouse skin can be increased significantly by forming mono and diethylamine salts of piroxicam (Cheong and Choi, 2003). Hydrophilic ionic-drugs tend to have poor skin permeability. Skin permeability of ionic drugs can be improved by using a counter ion to form a sufficiently lipophilic and neutral *drug-ion pair (Fang et al., 2015)*. Ionic species such as p-toluenesulfonic acid, 2-naphthalenesulfonic acid, 1-hydroxy-2-naphthoic acid, ethanolamines, N-(2'-hydroxyethanol)-piperidine, long chain fatty acids etc. can be used to increase the lipophilic properties of the parent drug molecule (Miller *et al.*, 2009; Xi *et al.*, 2012). Penetration behavior of such ion pairs usually depends

upon the non-drug part of the ion pair. Physicochemical properties of drugs with poor percutaneous permeation can also be improved by forming a prodrug which has suitable properties for skin permeation. Prodrugs can penetrate the SC and get converted to the active parent drug by hydrolysis or by enzymatic conversion within the viable epidermis or dermis thereby making the active parent drug available for the target site. When designing prodrug strategies for transdermal permeation, prodrug moieties are selected based upon the physicochemical properties of the parent drug (Sloan *et al.*, 2015). *Jona et al.* have shown a 10 fold improvement in transdermal flux through human cadaver skin for indomethacin when it was esterified with 3-diethylamino-1-propanol (Jona *et al.*, 1995).

Eutectic mixtures are physical mixtures of two or more components such that melting point of the mixture is lower than the melting point of the individual ingredients. It is hypothesized that lower the melting point of a drug higher the solubility of the drug in skin lipids (Benson, 2005; Kasting *et al.*, 1987; Touitou *et al.*, 1994). Therefore forming a eutectic mixture of the drug can enhance its solubility in a solvent vehicle and as a result may also increase the transdermal permeation. For example, Stott *et al.* (1998) have shown that terpenes can form eutectic mixture with ibuprofen causing a significant depression of the melting point resulting in an increased transdermal permeation.

1.2.3 Physical methods for penetration enhancement

Methods discussed in this section are relatively new and encompass a wide variety of techniques which deliver drug in the skin or through the skin either by bypassing the SC, by removing the SC or by temporarily decreasing the barrier function of the SC. These methods often use a combination of physical and chemical penetration enhancement strategies in order to maximize the amount of drug being delivered.

Iontophoresis utilizes application of low voltage electrical currents (0.5 mA/cm²) to the skin providing an electrical driving force which assists in drug permeation into the skin (Barry, 2005). Typically, electricity is applied through a drug reservoir and an electrode placed on the skin. Both charged and uncharged drugs can be delivered by iontophoresis. Charged drugs are acted upon by the electrophoretic force while weakly charged and uncharged drugs are affected by electroosmotic flow of water generated by the preferential movement of ions such as Na^+ (Barry, 2005; Prausnitz and Langer, 2008). Because, skin barrier properties are not altered in iontophoresis, drug must possess adequate physicochemical properties to be able to penetrate the SC. The biggest advantage of this method is that rate of drug delivery is proportional to the electric current applied therefore, rate of drug delivery can be controlled very effectively. However, moderate to high electrical currents passing through the skin can cause skin irritation which makes drug delivery rates dependent of skin irritation and pain experienced by the individual patient (Prausnitz and Langer, 2008). Recently, US-FDA has approved Zecuity® for delivering sumatriptan in the management of migraine and Ionsys® delivering fentanyl for management of pain in hospitalized patients.

In *electroporation*, increased drug permeation through skin is achieved by applying short (micro to millisecond) high-voltage (100 – 1000 V/cm) pulses to the skin which disrupt the intercellular lipid bilayer structures of the SC (Barry, 2005; Denet *et al.*, 2004; Lucille *et al.*, 2014). Drugs permeation through the skin is either due to short lived electrophoretic forces or by simple diffusion through the electropores which can last for a few hours. Because skin is anatomically altered, small as well large molecules can be delivered using electroporation (Blagus *et al.*, 2013; Denet and Preat, 2003). Despite their early promises transdermal drug delivery by electroporation is mainly confined to animal models and *in vitro* studies.

Sonophoresis or *phonophoresis* refer to delivering drugs through the skin with the aid of ultrasound. Both high frequency (0.7 – 16 MHz) and low frequency (20 – 100 MHz) ultrasound can be used (Polat *et al.*, 2011). In low frequency ultrasound sonophoresis, acoustic cavitation just above the skin, in the liquid or semisolid formulation, forms shockwaves which alter the inter-corneocyte lipid arrangement leading to a higher permeation of the drug (Tezel and Mitragotri, 2003). Whereas in high frequency ultrasound sonophoresis, cavitation occurs within the skin. In general, high frequency sonophoresis is more effective in increasing transdermal flux of small molecules while low frequency ultrasound sonophoresis has demonstrated capacity to deliver larger molecules like proteins, hormones, vaccines and even nanoparticles (Polat *et al.*, 2011).

Microneedles are micron sized array of solid or hollow needles which can pierce through and make channels in the SC through which drug can penetrate deep into the skin. Dimensions of the microneedles are such that they do not reach deep enough to innervate the nerves in the lower epidermis (Sivamani *et al.*, 2007). Microneedles have successfully deposited low as well as high molecular weight molecules such as proteins, DNA, vaccines (Gill and Prausnitz, 2007). For drug delivery using microneedles different strategies have been explored such as, piercing the skin with solid microneedles first followed by application of a transdermal patch; coating the solid microneedles with a drug formulation; application of hollow microneedles which can deliver drug formulation like an injection needle; drug can also be encapsulated within biodegradable microneedles and as microneedles are degrade drug is released in the skin (Atkinson *et al.*, 2015; Sivamani *et al.*, 2007). Different materials like silicon, glass, titanium, polymers and even sugars have been used in the past to manufacture microneedles (Sivamani *et al.*, 2007). Precise and reproducible fabrication of microneedles and drug loading is one of the biggest challenge in this field.

Stratum corneum ablation is controlled removal of the *SC* to produce micro-channels in the epidermis through which drug can permeate easily. Ablation can be achieved with the help of high power laser beams or precisely controlled local heating of the skin (Atkinson *et al.*, 2015). In laser ablation usually an infrared laser (λ = 1 to 5 μm) which can excite water molecules in the tissue is used. Application of laser causes local water molecules to excite and eventually epidermis undergoes an explosive evaporation which leaves a micro-pore in the epidermis through which drugs can access deeper layers

of the skin (Bachhav *et al.*, 2013). Laser can either be used in the form of a large few mm diameter beam or in the form of a large grid of micro-pores. Enhancement of transdermal delivery of small molecules, various proteins and vaccines by application of laser ablation has been demonstrated (Bachhav *et al.*, 2013; Gomez *et al.*, 2008). In thermal ablation using specialized heating blocks, surface of the skin is heated to a few hundred Celsius for very short periods. Such rapid heating can vaporize the SC cells locally and with precise control leaving micro-pores through the epidermis (Bramson *et al.*, 2003; Levin *et al.*, 2005; Park *et al.*, 2008).

Magnetophoresis, Murthy and group reported for the first time that a static magnetic field can be used for increasing transdermal penetration of drugs (Krishnan *et al.*, 2010; Murthy *et al.*, 2010). Although enhancement of various small and large molecules has been demonstrated, the exact mechanism of action behind the increased drug permeation is not clear.

Over the past few decades different strategies have evolved for improving the transdermal permeation of small as well as large therapeutic molecules. These strategies can be either employed alone or in combination to bring the drug in therapeutic concentrations to the target site. Most importantly, in transdermal drug delivery there is no 'one-stop' solution for all therapeutic requirements and each therapy must be customized as per the requirements presented by the target site, active ingredients, anatomical considerations etc. In the following section a more comprehensive overview about liposomal formulations for transdermal drug delivery is discussed.

1.3 Current status of liposomes in transdermal drug delivery systems

In the previous section, some of the strategies for delivering drug to or through the skin were discussed. This section will take a closer look at the liposomal formulations for drug delivery to skin. Liposomes were first suggested by Mezei and Gulasekharam in 1980 as a drug delivery system for depositing triamcinolone in skin (Mezei and Gulasekharam, 1980). Liposomes are phospholipid vesicles containing one or more bilayers containing an aqueous core. A detailed review for different preparation methods, characterization and properties of liposomes can be found elsewhere (Barenholz and Lasic, 1996; Gregoriadis, 2006; Torchilin and Weissig, 2003).

Liposomes in skin drug delivery applications have a rather controversial history. Ambiguity originates from the wide array of results that have been reported by various work groups. Some groups have suggested liposomes for topical drug delivery because liposomes tend to accumulate the drug in upper layers of skin and even act as drug-depot reducing the systemic absorption of the drug. Whereas some groups have found liposomes to increase transdermal drug penetration. Liposomes have been even shown to accumulate in the hair follicles (Patzelt and Lademann, 2013; Verma *et al.*, 2004; Vogt *et al.*, 2005). Liposomes have also shown the ability to improve transdermal delivery of small molecules as well as peptides and proteins (Benson, 2009; El Maghraby *et al.*, 2008b). Reasons for the disparity between different results of different studies likely originate from; differences in composition of liposomes, different physicochemical properties of the liposomal vesicles like charge, size, and different

drugs employed in the studies, additives to the liposomes such as ethanol, edge activators, penetration enhancers also modify the bilayer characteristics and drug transfer from the liposomal bilayer, use of different animal models etc.

Interactions of liposome with the skin and drug transfer from liposome to skin are influenced by the thermodynamic state of the liposomal bilayers and therefore influenced by the nature of phospholipids used in the preparation of the liposomes. Depending on the composition, liposomal bilayers can exist in *gel state*, characterized by rigid and unyielding bilayers or *liquid crystalline state* where bilayers are flexible and accommodating. Liposomal formulations in gel state are usually associated with drug accumulation in the upper layers of the skin and even reduced transdermal drug penetration (Hofland *et al.*, 1994; Knepp *et al.*, 1987; Mezei and Gulasekharam, 1980). For skin application, liposomal formulations can be divided in two broad categories as, *conventional liposomes* and *novel liposomes* (deformable or ultradeformable or elastic liposomes) (Dragicevic-Curic and Fahr, 2012). Conventional liposomes are mainly composed of pure or mixtures of phospholipid(s) and may or may not contain cholesterol. Although a few studies have suggested possibility of transdermal drug delivery using conventional liposomes, a vast number of studies suggest conventional liposomes are more suitable for topical or local delivery of drug in the skin (Deo *et al.*, 1997; Yu and Liao, 1996). Second category represents an array of different liposomal systems which apart from phospholipids contain other additives which essentially imparts the liposome bilayer deformability or elasticity which has been correlated to increased drug permeability in skin (Celia *et al.*, 2012; Cevc and Blume, 2003; Cevc *et al.*, 2008; Touitou *et al.*, 2000; Wo *et al.*, 2011). Few of such liposomal systems are described in **table 2**. A review of the important findings in the drug delivery to skin using liposomes is presented in **table 5 & 6** however a much more in depth and elaborate review is presented by Benson (2009); Elsayed *et al.* (2007); Hamishehkar *et al.* (2012).

Table 2: A brief description of the deformable or elastic liposomal systems for skin drug delivery

Formulations Work group	**Bilayer forming lipid and other additives**
Transfersomes® Cevc *et al.*	Soya phosphatidylcholine (S100, Lipoid GmbH). See table 3 for composition. Edge activators, sodium cholate, polysorbate 80, sorbitan monooleate 80 etc.
Ethosomes Touitou *et al.*	Soya phosphatidylcholine (S100, Lipoid GmbH) 10-50% ethanol by weight which fluidizes the phospholipid bilayers
Invasomes Fahr *et al.*	Soya phospholipid (NAT 8539, Lipoid GmbH) See table 4 for composition. Lyso phosphatidylcholine as an edge activator, 1% terpenes and 10% ethanol by weight as penetration enhancers
Niosomes Handjani *et al.*	Non-ionic surfactants such as dicetylphosphate, hexadecyl diglycerol ether, polysorbates, sorbitan monooleates etc and cholesterol

Table 3: Composition of soy-phosphatidylcholine LIPOID S100

Phospholipid composition			**Fatty acid composition**	
Phosphatidyl choline	> 94%		Palmitic acid	12 – 17%
Phosphatidyl ethanolamine	< 0.1%		Stearic acid	2 – 5%
N-acyl-phosphatidyl ethanolamine	< 0.5%		Oleic acid	11 – 15%
Phosphatidyl inositol	< 0.1%		Linoleic acid	59 – 70%
Lyso-phosphatidyl choline	< 3.0		Linolenic acid	3 – 7%

Table 4: Composition of soy-phosphatidylcholine NAT8539

Phospholipid composition			**Fatty acid composition**	
Phosphatidyl choline	> 73%		Palmitic acid	10 – 15%
Phosphatidyl ethanolamine	< 7%		Stearic acid	1 – 4%
Phosphatidic acid	< 7%		Oleic acid	6 – 13%
Phosphatidyl inositol	< 5%		Linoleic acid	60 – 70%
Lyso-phosphatidyl choline	< 6		Linolenic acid	4 – 7%

Table 5: A brief review of the conventional liposomes in topical drug delivery

Formulation details	Criteria investigated, test model	Results / Remarks
Drug deposition in upper layers of the skin following application of liposomal formulation		
Mezei and Gulasekharam (1980) Multilamellar liposomes, DPPC : chol (1.1:0.5) Drug: C^{14} labeled triamcinolone Liposomes dispersed in an ointment base	Drug deposition in skin, organs, blood and urine measured in New Zealand white rabbits	Approx. 4-5 times higher deposition of triamcinolone in upper skin layers from liposomal formulation compared to a conventional ointment and reduced urinary excretion of triamcinolone.
Gesztes and Mezei (1988) Soya phosphatidylcholine (7%), stearic acid (0.7%), cholesterol (0.7%) Drug: tetracaine (0.5%)	24 healthy human adults, pain scores measured using pin prick method	Liposomal tetracaine produced significantly stronger and longer lasting local anesthesia compared to a cream. Lipids and drug were dispersed in a medium containing 10% ethanol and 7% propylene glycol to prepare liposomes. Both ethanol and propylene glycol have a penetration enhancing effect
Foldvari *et al.* (1990) Soya PC : chol (6.5:1) Drug: C^{14} lidocaine MLVs were dispersed in a gelling agent to increase viscosity	Five healthy human adults, pain scores measured using pin prick method	Liposomal lidocaine produced a much stronger local anesthesia compared to lidocaine ointment.
(Fresta and Puglisi, 1996) DMPC : chol : DPPS (7:5:3) Ceramides : chol : palmitic acid : cholesteoryl sulphate (4:2.5:2.5:1) Soya phosphatidylcholine : chol (2:1) Drug/marker: [C^{14}]Inulin MLVs subjected to freeze thaw cycles	*In vitro*, permeation and penetration of [C^{14}]inulin was measured in hairless mouse skin mounted on Franz diffusion cell *In vivo*, distribution of [C^{14}]inulin in various orangs and blood was determined in female piglets	*Stratum corneum* lipid (ceramide) liposomes deposited higher amounts of [C^{14}]inulin in epidermis and dermis with very minor systemic absorption as compared to DMPC liposomes. Highest transdermal penetration of [C^{14}]inulin was observed for fluid soya phosphatidylcholine liposomes
(Kitagawa and Kasamaki, 2006) Egg PC : retinoic acid (4:1), Egg PC : DOTAP : retinoic acid (2:2:1), DMPC : DOTAP :retinoic acid (2:2:1) DPPC : DOTAP : retinoic acid (2:2:1) Drug: retinoic acid	Skin deposition of retinoic acid measured in excised guinea pig dorsal skin mounted on Franz cells	Two fold increase in deposition of retinoic acid in skin from egg PC liposomes compared to retinoic acid delivered from isopropyl myristate solution. Incorporation of cationic surfactant DOTAP further increased retinoic acid deposition by 3.7 fold compared to non-ionic egg PC liposomes. Replacing egg PC with either DMPC or DPPC did not result in significant change in retinoic acid deposition.

Chol cholesterol, DPPC dipalmitoylphosphatidylcholine, DMPC dimyristoylphosphatidylcholine, DOTAP 1,2-dioleoyl-3-trimethylammonium-propane, MLV multilamellar vesicles

Effect of change in physiochemical properties of liposomes on drug delivery to skin

Sinico *et al.* (2005) Soya PC : chol : retinoic acid : stearylamine or dicetylphosphate (5:0.6:2:1) Stearylamine => cationic liposomes Dicetylphosphate => anionic liposomes Both MLVs and UVs were prepared Drug: retinoic acid	Skin penetration and permeation studies using newborn pig skin mounted on Franz diffusion cells.	Positively charged liposomes were associated with higher and faster permeation of retinoic acid compared with negatively charged liposomes. MLVs and UVs did not have a significant effect on the penetration of retinoic acid Replacing soya PC with a hydrogenated PC increased permeation of retinoic acid by a factor of 2 to 2.35 for both cationic and anionic liposomes.
Yu and Liao (1996) Egg PC : chol (2:1) Egg PC : chol : dicetylphosphate (2:1:0.25) Egg PC : chol : stearylamine (2:1:0.25) Skin lipid liposomes: Ceramide : chol : palmitic acid : cholesteryl sulphate (4:2:2.5:1) Drug: Triamcinolone	Drug permeation study using Wistar rat skin mounted on Franz diffusion cells Effect of liposome size was tested by applying 1, 0.4 0.2 µm MLVs and SUVs.	Negatively charged SUVs showed significantly higher permeation and deposition of triamcinolone. Comparing vesicle charge in MLVs and SUVs, amount of drug permeated was not statistically significant however deposition of triamcinolone was significantly higher from cationic MLVs. Replacing Egg PC with DPPC (neutral liposomes) significantly reduced the amount of triamcinolone deposited and permeated through the skin. All liposomes showed better permeability of triamcinolone compared to ointment.
Manosroi *et al.* (2004) HPC : chol (1:1) & (7:2) HPC : chol : stearylamine (7:2:1) HPC : chol : dicetylphosphate (7:2:1) Drug: AmB (0.05mg/mg of lipid) MLVs were probe sonicated	Drug permeation and deposition was studied in full thickness abdominal skin of Wistar rats mounted on Franz diffusion cells.	Highest flux of AmB across the skin was observed for cationic liposomes while nutral liposomes showed the lowest permeated AmB. Flux for cationic liposomes (57.6 ± 29.1 ng/cm²/h) through the SC was higher than anionic liposomes (39.5 ± 6.3 ng/cm²/h) however flux through viable epidermis was higher for anionic liposomes (22.8 ± 2.5 ng/cm²/h) compared to cationic liposomes (10.9 ±3.3 ng/cm²/h)

PC phosphatidylcholine, SUV small unilamellar vesicles, HPC hydrogenated soya phosphatidylcholine, AmB amphotericin B

Delivery to hair follicles

Jung *et al.* (2006) DPPC : DPPG : chol (5:1:4) (Anionic) DPPC : DC-chol: chol (5:1:4) (Cationic) DMPC : HCS : chol (5:1:4) (Amphoteric) DMPC : TES : chol (5:1:4) (Cationic) Label: carboxyfluorescein	Pig ear skin, skin biopsies were taken after 1 hour, 1, 3, 5 and 7 days after application of liposomes. Analyzed by cryo sectioning and confocal microscope	All liposomal formulations had higher carboxyfluorescein deposition in the hair follicles compared to a carboxyfluorescein containing cream. Cationic and amphoteric liposomes reached the highest penetration depth on day-5 after application. Liposomes had size range between 200 – 450 nm.
Li and Hoffman (1997) Egg PC 10 mg/ml	In vivo application of fluorescent liposomes to dorsal skin of mice.	Deposition of calcein deep in the hair follicles was observed when applied in the form of liposomes as compared to topically applied solution.

MLVs are probe sonicated Label: Calcein or melanin Unentrapped label separated by gel filtration chromatography	Punch biopsies taken at 0.5, 1, 2, 4, 6, 16 and 24 hours. Fluorescent label deposition in skin and blood is measured along with microscopy	Melanin showed similar results to calcein but distribution of melanin was not as uniform as calcein.
Trauer *et al.* (2014) DPPC : DPPG (9:1) Invasomes (Table-2) Label: Carboxyfluorescein, Rh-DOPE MLVs extruded to obtain LUVs	Excised breast or abdominal human skin. Effect of massage and occlusion on penetration of fluorescent dye was investigated using confocal microscope	Carboxyfluorescein penetrated significantly deeper from both liposomal formulations compared to lipid marker Rh-DOPE. Massage increased the penetration achieved for fluorescent markers for both rigid and flexible liposomal formulations. Occlusive application increased penetration of carboxyfluorescein only from rigid liposomes. For invasomes penetration depth decreased after occlusive application.

DC-chol 3β-[N-(dimethylaminoethane) carbamoyl]cholesterol, TES trimethylammonium methyl sulfate, DPPG dipalmitoylphosphatidylglycerol, Rh-DOPE 1,2-Diol-eoyl-sn-glycero-3-phosphoethanolamine-N-(lissamine rhodamine B)

Table 6:

Formulation type	Drug / label, test model	Results / remarks
Transfersomes®		
Cevc and Blume (2003)	Triamcinolone. In vivo measurement of drug distribution and murine ear edema model	Triamcinolone applied from Transfersomes® showed higher and prolonged anti-inflammatory activity compared to cream and ointment formulations. Prolonged anti-inflammatory activity can decrease dose of triamcinolone by a factor of 10 compared to the conventional cream and ointment.
Cevc *et al.* (1998), Cevc (2003)	Insulin, in vivo distribution and hypoglycemia in mice and humans	Hypoglycemia induced by transfersomal insulin was comparable to insulin delivered by sub cutaneous injection. Lag time of approx. 45-145 min was observed. Mixed micelles and conventional liposomes did not induce hypoglycemia.
Cevc and Blume (2001)	Diclofenac transfersomal gel, in vivo distribution of radioactive drug in NMRI mice, Wistar rats and pigs	High levels of diclofenac was found in muscle tissue in all three animal models compared to a commercially available gel.
Gupta *et al.* (2005)	Tetanus toxoid, albino Wistar rats for immunization study	Topically applied tetanus toxoid transfersomes after secondary immunization elicited an anti-TT-IgG immune response comparable to immune response elicited by intramuscular administration of alum adsorbed tetanus toxoid.
Mishra *et al.* (2006)	Immune response to topically applied hepatitis B surface antigen in BALB/c mice	A strong immune response comparable to intramuscularly administered alum adsorbed hepatitis B surface antigen was observed. Ex vivo penetration studies revealed penetration of antigen to the Langerhan's cells

Ethosomes

Horwitz *et al.* (1999)	Acyclovir, double blind randomized clinical study to determine efficacy of acyclovir loaded ethosomes in patients with recurrent herpes labialis	Time to crusting of lesions and time to loss of crust were significantly shorter with ethosomal acyclovir as compared to a commercially available cream.
Paolino *et al.* (2005)	Ammonium glycyrrhizinate, anti-inflammatory activity was determined in healthy human volunteers and percutaneous permeation was determined using human epidermis *ex vivo*	Significantly higher anti-inflammatory activity was seen when drug was administered from ethosomes as compared with ethanolic and aqueous solutions of the drug. *Ex vivo* permeation of ammonium glycyrrhizinate was higher from ethosomes compared to its ethanolic and aqueous solutions.
Zhang *et al.* (2014)	Psoralen loaded ethosomes, ex vivo permeation studied in rat skin	Transdermal flux and skin deposition of psoralen was 3.5 and 2.15 times higher for ethosomes compared to conventional liposomal psoralen.

Invasomes

Shah *et al.* (2015)	Anti-acne efficacy of azelaic acid loaded invasomal gel was determined in vivo in by inducing acne in female Wistar rats	Invasomal gel showed significantly higher anti-acne activity compared to conventional liposomes and a cationic liposomal formulation. Complete recovery from acne was observed in 7 days in invasomal gel compared to 10 or more days for the conventional liposomes and cationic liposomes.
Dragicevic-Curic *et al.* (2008)	Photodynamic therapy using temoporfin loaded invasomes for subcutaneously implanted human colorectal tumor HT29 in mice	Invasomal temoporfin showed significantly slower increase in tumor size compared to controls
Chen *et al.* (2010)	Penetration and permeation of ferrulic acid across human epidermis was studied when delivered in the form of invasomes, ethosomes and transfersomes	Invasomal ferrulic acid penetration and permeation was about two times higher compared to conventional liposomes. Highest amount of ferrulic acid permeation was from ethosomes while for transfersomes ferrulic acid penetrated and permeated was not significantly different from invasomes.

Niosomes

Maheshwari *et al.* (2011)	Niosomes encapsulating Hepatitis B surface antigen and cholera toxin B as an adjuvant were tested on human cadaver skin *ex vivo* to test skin deposition and permeation. Immune response was tested in vivo using BALB/c mice	Permeation of the antigen was significantly higher when delivered from niosomes compared to application of aqueous solution. Immune response measured by determining IgG titers 21 days after topical immunization was similar to intramuscular injection of alum adsorbed Hepatitis B antigen.
Manosroi *et al.* (2012)	Follicular penetration from cationic niosomes encapsulating semipurified fraction of Oryza sativa containing unsaturated fatty acids (treatment against male pattern baldness) was determined in excised porcine skin	Enhanced delivery of unsaturated fatty acids from cationic niosomes was observed compared to neutral niosomes.
Lakshmi *et al.* (2007)	Efficacy study of niosomal methotrexate gel in a double blind clinical trial in patients with psoriasis	Significantly reduced erythema scores were obtained when methotrexate was delivered via niosomal gel compared to a commercially available methotrexate gel

1.4 Mechanisms of drug penetration in skin from liposomes

Previous section demonstrated that application of liposomes as a drug delivery to or through the skin is dependent on the lipid composition of liposomal bilayers, size and charge of the vesicles, physicochemical properties of the drug and state of the skin barrier. Despite the variability seen in the outcomes from liposomal drug delivery to skin, some general rules can be established. Liposomes with rigid bilayers tend to confine the drug locally in the skin. For deeper penetration, liposomes with flexible bilayers perform better. This flexibility is often induced by incorporation of surfactants often termed as 'edge activators' which reduce the elastic modulus of the phospholipid bilayer. Also size of liposomes is an important factor, large multilamellar vesicles are mainly associated with topical drug delivery whereas liposomes around 100 nm can deliver drug deeper in the skin or even across the skin.

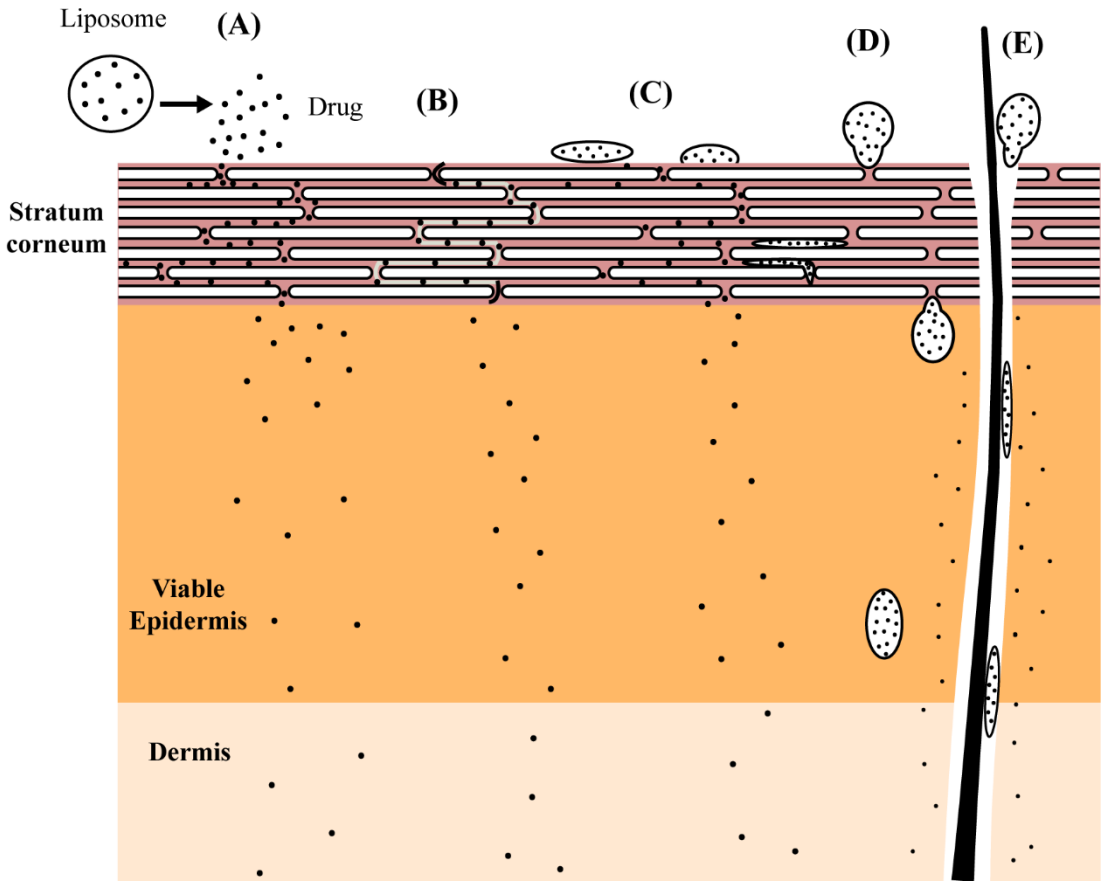

Figure 3: Schematic showing various mechanisms by which liposomes can facilitate drug delivery to skin. (A) The free drug mechanism (B) Penetration enhancement achieved by components of the liposomal formulation (C) Adsorption or fusion of liposomal vesicles with the SC (D) penetration of intact vesicles into or through the SC (E) Transfollicular delivery. Redrawn from El Maghraby *et al.* (2008a). Not to scale.

Liposomal drug delivery to the skin can be classified in five different mechanisms or pathways as shown in **Figure 3** (El Maghraby *et al.*, 2008a). According to this classification, liposomes can either act as drug carriers bringing different lipophilic and hydrophilic drugs in close proximity to the SC from where drug partitions into the SC independent of the liposomal components. Second mechanism suggests that components of the liposomes act as penetration enhancers which facilitate in the penetration of the drugs.

Third mechanism suggests that liposomal bilayers can fuse or get adsorbed on the surface of the SC where they release their drug cargo. Forth and the most controversial mechanism suggests that flexible liposomes such as Transfersomes can penetrate the SC intact and therefore taking the drug cargo along with them. Fifth mechanism is the transfollicular mechanism, where liposomes can enter the hair follicles which typically penetrate the dermis and release the drug in the hair follicles which can diffuse out in the dermis or viable epidermis from within the hair follicle. Which mechanism or combination of two or multiple mechanisms dominate in any given drug – liposomal system combination would depend on the physicochemical properties of the drug and liposomal system. Mechanisms for drug penetration are discussed in much greater detail in publication-3 and 4 and in chapter 4.

1.5 Introduction to tip-enhanced Raman scattering

Vibrational spectroscopic techniques such as infrared and Raman microscopy are able to provide a wealth of information by identifying molecular structures and conformations at cellular and molecular level without requiring dyes, stains, radioactive labels etc. Application of these techniques for diagnostic purposes and in pathophysiology of various diseases and disorders such as, carcinomas (Lasch *et al.*, 2007), brain tumors (Krafft and Salzer, 2008), bone diseases (Boskey and Mendelsohn, 2005), atherosclerosis (Kodali *et al.*, 1991), diabetes (Hosafci *et al.*, 2007), osteoarthritis (West *et al.*, 2004) etc. has been demonstrated. In skin related fields, these techniques have been used to study skin hydration status (Vyumvuhore *et al.*, 2013), penetration of various compounds like, metronidazole (Tfayli *et al.*, 2007), caffeine (Tfaili *et al.*, 2013), deuterated water (Ashtikar *et al.*, 2013), beta carotene (Ashtikar *et al.*, 2013; Ermakov *et al.*, 2004), ibuprofen (Mateus *et al.*, 2013) etc. and in diagnostics of skin related disorders such as melanoma (Gniadecka *et al.*, 2004), basal cell carcinoma (Nijssen *et al.*, 2007), squamous cell carcinoma (Lieber *et al.*, 2008) etc.

Despite the great potential of these microspectroscopic techniques, they are limited by the Abbe's diffraction limit. Which means the highest resolution for these techniques is roughly in the range of 200-300 nm. However, to study the interactions between the SC and liposomes a microspectroscopic technique with high spatial resolution is desired, especially given the liposomes used for transdermal drug delivery have size around 100 nm. Tip-enhanced Raman scattering (TERS) is capable of providing a sub-nanometer spatial resolution and spectroscopic information with single-nanometer resolution (Treffer *et al.*, 2012). Simplified, TERS can be described as a combination of scanning probe microscopy (SPM) and surface enhanced Raman scattering (SERS). SPM provides the high resolution topographical imaging mode whereas SERS provides the chemical signatures for identification and detection.

Raman scattering is an inherently weak phenomenon where about one out of a million photons undergoes an inelastic scattering or Raman scattering. In SERS, weak Raman scattering is enhanced up to a factor of 10^{14} if the compound whose Raman spectra is to be measured is adsorbed on heavy metal

nanoparticles like silver, gold, iron or copper. The SERS enhancement is due to combination of two mechanisms, electromagnetic effect and chemical effect. Incident laser light can excite the surface plasmons on the metal nanoparticles and if resonance conditions are met, electromagnetic fields involved in the scattering event can be strongly enhanced. The product of the incident laser field and the scattered Raman yields the overall *electromagnetic SERS effect* (Barber *et al.*, 1983; Wokaun *et al.*, 1982). In the *chemical enhancement effect* a charge transfer between the metal nanoparticle and the adsorbed molecule results in an amplification of the polarizability of the adsorbed molecule and enhanced Raman scattering (Moskovits, 1985).

In TERS, field enhancement is achieved by confining the SERS effect to a sharp metal tip of SPM probe (Anderson, 2000; Hayazawa *et al.*, 2001; Stöckle *et al.*, 2000). Usually, either atomic force microscope (AFM) or scanning tunneling microscope (STM) can be used for this purpose. Here, to study the interactions between the *stratum corneum* and liposomal formulations, AFM tips coated with silver nanoparticles were employed as shown in **Figure 4.** A much more comprehensive review of the TERS is presented by Bailo and Deckert (2008); Blum *et al.* (2014) and a review of the biomedical applications of TERS is presented by Deckert-Gaudig and Deckert (2011); Treffer *et al.* (2012).

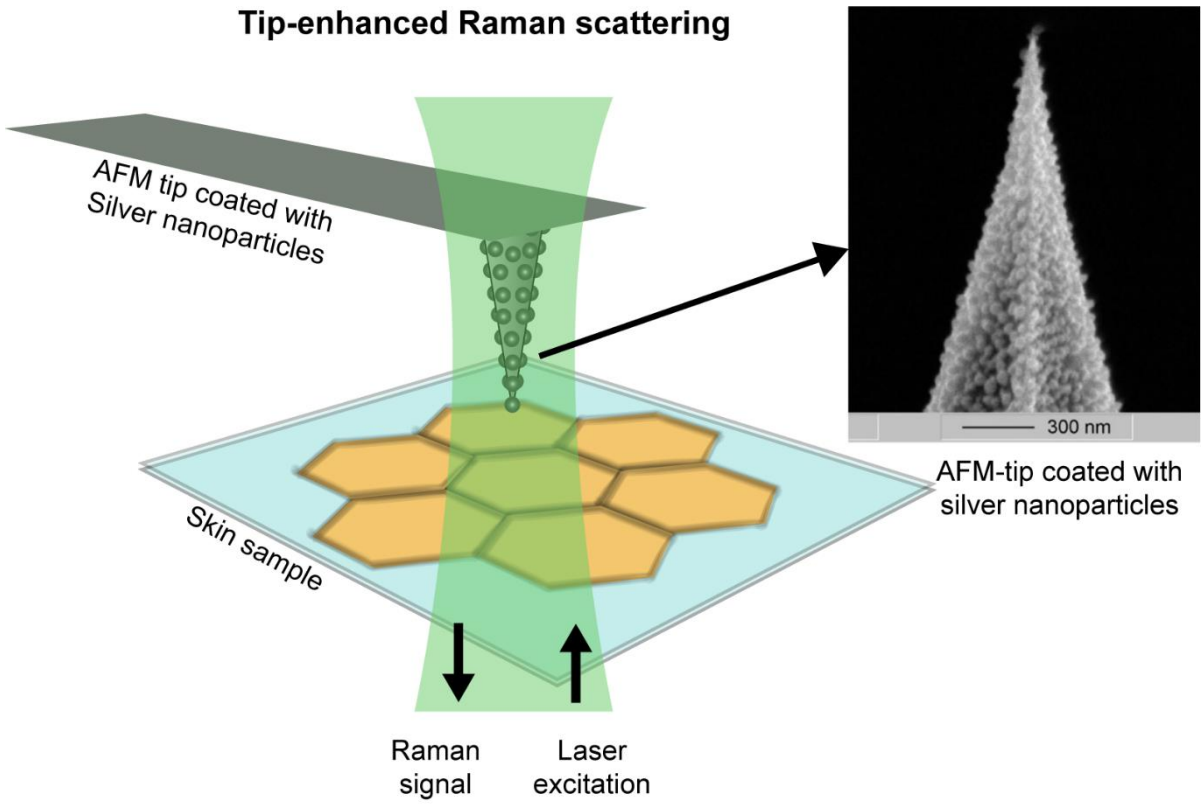

Figure 4: Schematic for the TERS setup showing AFM tip coated with silver nanoparticles. Scanning electron micrograph of the silver nanoparticle coated AFM tip was taken from (Sharma *et al.*, 2015)

1.6 Aim of the Study

Stratum corneum forms the most significant fraction of the skin barrier for percutaneous absorption of topically applied substances. Various strategies have been employed to enhance drug penetration through the SC such as chemical penetration enhancers, microneedles, iontophoresis etc. Incorporation of drugs within liposomal membranes have also shown to enhance the drug penetration within the skin as already discussed in the previous section. When drug substances are applied in the solution form to the skin, drug penetration mainly depends on the physicochemical properties of the drug however, incorporation of drugs in the liposomal membrane results in a rather complex interaction between the *stratum corneum*, phospholipid membrane and drug. Objective of this thesis was to probe the interactions between *stratum corneum* and liposomes in order to gain a better understanding of the mechanisms involved in the skin-drug delivery from topical liposomal formulations, especially 'invasomes'.

1) Confocal Raman microscopy study

Objective in this study was to study the diffusion patterns of liposomally entrapped drugs and the liposome-forming phospholipids after topical application of liposomes on intact human skin. We were particularly interested in understanding the behavior of our in-house topical liposomal system 'invasomes'. Understanding the diffusion behavior of both, drug and phospholipid can directly shed light on the mechanism(s) involved in drug delivery to skin by topically applied liposomal formulation. Confocal Raman microscopy was the preferred choice of imaging technique as it facilitates possibility of a label-free identification of externally applied substances. In the first part of this study, a method for obtaining XZ non-invasive optical biopsies in human skin was established. Second part of this study investigated co-diffusion of drug and phospholipids in the *stratum corneum* after topical application of liposomally entrapped drugs on human skin *ex vivo*.

2) Tip-enhanced Raman scattering study

Our results of Raman microscopy experiments suggested that upon topical application of phospholipids in the form of liposomes, only a fraction of applied phospholipid found its way into the skin. Similar findings were also reported by Röding and Artmann (1992) who measured diffusion of radioactive phospholipids in the pig skin. Despite of this finding, a link between liposomes and enhanced skin penetration of a wide range of drugs has been established. This study investigated the interactions between liposomes and the *stratum corneum* at a nanoscale using tip-enhanced Raman scattering (TERS) in order to get a deeper understanding of the mechanism(s) involved in the liposomal drug delivery to the skin. TERS was the tool of choice for this study as it is not limited by the Abbe's resolution limit and is an excellent tool for providing chemical and structural information in great detail.

Motivation for this study was taken from work published by the Bouwstra group (Bouwstra and Honeywell-Nguyen, 2002; Hofland *et al.*, 1995) where freeze-fracture transmission electron microscopy

was employed to study the interactions between the *stratum corneum* and liposomes. One of the objectives in the current study was to keep the sample preparation as simple as possible in order to eliminate artifacts.

3) LeciPlex, invasomes and liposomes: a skin penetration study

LeciPlex are cationic extemporaneous liposomal formulations developed by the Nagarsenkar group (Date *et al.*, 2011) whereas invasomes are deformable liposomes developed by the Fahr group (Fahr and Muller, 2003) for skin delivery. In this study three vesicular systems, cationic LeciPlex, amphoteric invasomes and conventional liposomes were compared for their ability to deliver idebenone and azelaic acid into the deeper layers of human skin. Formulations were also characterized and their efficacy was measured using *in vitro* cell assays and *in vivo* animal model. Observations were discussed based on the drug-liposomal membrane interactions.

2. Publication Overview

Publication-1

Book chapter

Confocal microscopy for visualization of skin penetration

Mukul A. Ashtikar, Daya D. Verma, Alfred Fahr

Accepted for publication after peer review in the 5th volume of book series '*Percutaneous Penetration Enhancers - Chemical methods in penetration enhancement*' Publisher - Springer-Verlag Berlin Heidelberg.

Revised proofs of the book chapter were submitted on 17th March 2013.

Abstract:

Book chapter provides an overview of various commercial confocal techniques that have emerged over a few decades discussing in brief their conception and working principle. Techniques discussed in the book chapter include, confocal laser scanning microscopy, two-photon fluorescence microscopy, confocal Raman microscopy and coherent Raman microscopy. Applications of these techniques to understand the skin penetration of various drugs, labels and chemical substances and in understanding the barrier function of skin is reviewed. Book chapter also presents different experimental results obtained in our lab, using confocal laser scanning microscopy, Raman microscopy and multimodal coherent anti-stokes Raman microscopy.

Contributions to the publication:

- Preparation of the manuscript
- Review of microscopic techniques including two-photon fluorescence microscopy, confocal Raman microscopy and coherent Raman microscopy
- Preparation of formulations, skin samples and spectral acquisition for confocal Raman microscopy and for multimodal coherent anti-stokes Raman spectroscopy and experiments

Publication-2

Research article

Non-invasive depth profile imaging of the stratum corneum using confocal Raman microscopy: First insights into the method

Mukul Ashtikar*, Christian Matthäus*, Michael Schmitt, Christoph Krafft, Alfred Fahr, Jürgen Popp

European Journal of Pharmaceutical Sciences, Vol 50 (2013) 601-608. Published on 10th June 2013.

*Equal first authorship

Abstract:

Confocal Raman microscopy offers an opportunity for label-free imaging and can provide information about the chemical integrity of the drug as well as the tissue. This publication demonstrated a relatively simple method for obtaining XZ-Raman profiles of human *stratum corneum* using a confocal Raman microscope. XZ-Raman profiles for untreated human skin and human skin treated with beta-carotene and deuterated water were measured to demonstrate the method. Vertex component analysis was employed to analyze the spectral dataset and differentiate the skin components and applied substances. The method was developed with an aim of studying the patterns of drug diffusion in the SC.

Contributions to the study:

- Study design
- Preparation of skin samples and confocal Raman microscopy measurements
- Data interpretation, data analysis except for vertex component analysis.
- Preparation of the manuscript

Publication-3

Research article

Tip-enhanced Raman scattering for tracking of invasomes in the stratum corneum

Mukul Ashtikar*, Lucas Langelüddecke*, Alfred Fahr, Volker Deckert

Manuscript in preparation.

*Equal first authorship

Abstract:

Transdermal drug delivery from liposomal vesicles has been explained based several mechanisms. Straightforward observation of the interaction between liposome and skin is difficult due to the scale of this interaction. To study the effects of treatment of invasomes in human *stratum corneum* and in turn comment on the skin penetration mechanism of liposomes, a new sampling technique was developed to enable application of tip-enhanced Raman scattering to the layers of *stratum corneum*. Individually removed layers of corneocytes from invasome treated skin were first analyzed using atomic force microscopy, where presence of flattened vesicle-like structures was observed. TER spectra measured on the surface of these vesicle-like flattened structures reveled presence of head deuterated phospholipids which confirmed that the flattened vesicles were topically applied invasomes. For the first time a spectroscopic evidence for the penetration of intact liposomal vesicles in the human SC has been presented in this study. Presence of diffused deuterated phospholipid on the surface of corneocytes was also observed. Findings of this study point towards a penetration enhancement by phospholipid diffusion through the intercellular lipids of the SC and penetration of intact invasomes in the SC.

Contributions to the study:

- Development and calibration of stripping technique
- Preparation of invasomes, preparation of supported bilayers and all skin samples for atomic force microscopy and tip-enhanced Raman scattering measurements
- Atomic force microscopy and tip-enhanced Raman scattering measurements
- Data analysis and interpretation
- Manuscript preparation

Publication-4

Research article

LeciPlex, invasomes, and liposomes: A skin penetration study

Sanket M. Shah*, Mukul Ashtikar*, Ankitkumar S. Jain, Dinesh T. Makhija, Yuvraj Nikam, Rajiv P. Gude, Frank Steiniger, Aarti A. Jagtap, Mangal S. Nagarsenker, Alfred Fahr

International Journal of Pharmaceutics, Vol 490 (2015) 391-403. Published on 19th May 2015.

*Equal first authorship

Abstract:

This study compares three liposomal systems, cationic Leciplex, invasomes and conventional liposomes for their ability to deliver idebenone and azelaic acid deep into the skin. Efficiency of all liposomal vesicles was compared based on *ex vivo* human skin penetration studies, *in vitro* cytotoxicity studies, *in vitro* antimicrobial activity studies and *in vivo* anti-acne efficacy studies in rats. In *ex vivo* human skin penetration studies, the highest deposition of idebenone was observed from Leciplex formulations whereas from invasomes least amount of idebenone penetrated the skin. For azelaic acid, this trend was reversed and highest penetration was observed for invasomes and least for Leciplex. Similar trend was observed in the *in vivo* experiments for azelaic acid formulations. These contradictory trends were explained based on different partition coefficients between the liposomal formulations and skin. The study highlights the importance of apprehending the interactions between phospholipid bilayers and drugs when designing a formulation.

Contributions to the study:

- Preparation and characterization of formulations
- Human skin preparation and ex vivo skin penetration experiments
- Data interpretation
- Preparation of manuscript

3. Publications

3.1 Publication-1

Confocal microscopy for visualization of skin penetration

Mukul A. Ashtikar, Daya D. Verma, Alfred Fahr

Accepted for publication after peer review in the 5th volume of book series '*Percutaneous Penetration Enhancers - Chemical methods in penetration enhancement*' Publisher - Springer-Verlag Berlin Heidelberg.

Revised proofs of the book chapter were submitted on 17th March 2013.

Chapter 13

Confocal microscopy for visualization of skin penetration

Mukul A. Ashtikar[1], Daya D. Verma[2], Alfred Fahr[1*]

[1]Lehrstuhl für Pharmazeutische Technologie, Friedrich-Schiller-Universität Jena, Lessingstr. 8, D-07743 Jena, Germany.

[2]Novartis Pharmaceutical Corp. East Hanover, New Jersey, USA

*Corresponding author

Prof. Dr. Alfred Fahr
Friedrich-Schiller-Universität Jena
Institut für Pharmazie
Lehrstuhl für Pharmazeutische Technologie
Lessingstraße 8
07743 Jena
Email: alfred.fahr@uni-jena.de
Phone: +49 3641 949900

Author	Email ID
Mukul Ashtikar	Mukul-arun.ashtikar@uni-jena.de
Daya D Verma	ddverma@yahoo.com
Alfred Fahr	Alfred.fahr@uni-jena.de

Abstract

Confocal microscopic techniques have been around for over 50 years. However only in the last two decades there has been a truly widespread use of this technology in life sciences. Today there are different confocal techniques available and at the heart of all these techniques is the ability to differentiate between the light originated from different planes of the specimen. This ability is quite important when studying thick biological specimen such as skin microscopically, otherwise a lot of the information can get lost in the form of blur. In addition, due to advances in the material sciences and photonics, microscopes are able to image in vitro as well as in vivo and have allowed us to couple microscopes with spectroscopic techniques which provide valuable information in identification and characterization of structures. In this book chapter, we discuss basic principles of confocal laser scanning microscopy, 2-photon fluorescence microscopy, confocal Raman microscopy, coherent Raman microscopy and their applications in understanding the skin penetration of various substances.

Key words: Confocal laser scanning microscopy; Fluorescence microscopy; Two-photon fluorescence microscopy, Confocal Raman microscopy, Coherent anti-stokes Raman scattering microscopy, Stimulated Raman scattering microscopy, Skin penetration; Liposomes; Hair follicle targeting.

Table of Contents

1. Introduction

Over the years various methods such as diffusion experiments (Addicks et al., 1987; du Plessis et al., 1994), microdialysis (Benfeldt, 1999; Fang et al., 1999; Murakami et al., 1998; Schnetz and Fartasch, 2001), visualization by microscopic techniques like conventional fluorescence microscopy (Kriwet and Müller-Goymann, 1995; Yarosh et al., 1994), electron microscopy (Bouwstra and Honeywell-Nguyen, 2002; Hashimoto et al., 1991; Hofland et al., 1995; Kanerva, 1990; Schreiner et al., 2000; van den Bergh et al., 1999), confocal laser scanning microscopy (Betz et al., 2001; Kirjavainen et al., 1996; Schatzlein and Cevc, 1998; van Kuijk-Meuwissen et al., 1998; van Kuijk-Meuwissen et al., 1998; Vardaxis et al., 1997; Veiro and Cummins, 1994) etc. have been exploited by researchers for studying percutaneous penetration and gain a better understanding of the skin barrier. Tape stripping and microdialysis experiments though extensively used to measure the amount and rate of penetration of the model compound, are lacking in providing information about the effect of the model drug on cells and lipid organization or particular pathways for the penetration of the model drug. These techniques also do not give much information about spatial distribution of the model drug inside the tissue or comment on the mechanism of penetration and more importantly, these are destructive methods where tissue has to be carefully removed or homogenized to quantify the amount of drug.

Electron microscopy has been extremely useful in understanding the structure of the stratum corneum (SC) and intercellular lipid organization. Bouwstra and coworkers have made important contributions to the understanding of the interactions between vesicles and human skin (Hofland et al., 1995; Hofland et al., 1994; Schreiner et al., 2000). They employed freeze fracture electron microscopy and small angle X-ray scattering to study the effects of vesicular formulations on the SC. Their results indicated increased diffusion of the drug due to adsorption and fusion of drug loaded vesicles to the surface of the skin. They also reported perturbations in the ultrastructure of the SC intercellular lipid domains due to mixing of liposomal components with SC lipids, which could have also enhanced penetration of the model drug. Although freeze fracture electron microscopy provides rather useful information about the effect of liposomal vesicles on the ultrastructure of the skin barrier it lacks in providing information of penetration pathways and depth up to which the model drug has penetrated.

Another widely appreciated technique is the conventional fluorescence microscopy. Evaluation of skin treated with fluorescently labeled liposomes by fluorescence microscopy has demonstrated that the fluorescent marker remained in the SC (Kriwet and Müller-Goymann, 1995) or penetrated deeper in the epidermis mainly along the hair shaft (Yarosh et al., 1994). However, during the sample preparation the tissue needs to be (cryo-) fixed which might lead to the alteration of the original specimen by the change in skin lipid organization, redistribution of the marker etc.

Confocal microscopy has evolved over last 5-6 decades and today it is an essential tool for a life-sciences laboratory; it has emerged as a sophisticated tool for tracking and studying transport phenomena of different compounds with high degree of precision. Confocal microscopy offers significant advantages over other microscopic techniques in evaluation of thick specimens due to their inherent ability to distinguish photons generated from different focal planes of the specimen. This ability is mainly achieved in two ways, either by introducing a pinhole aperture in front of the detector which limits the out of focus light or by utilizing a non-linear technique such as 2-photon fluorescence, which excites the specimen only in a very small focal plane at a time. Confocal microscopes create quite sharp images compared to conventional microscopes where light coming from different planes of the specimen is not differentiated, resulting in blurry and low resolution images. Confocal microscopy on a broad basis can be classified as an imaging and spectroscopic technique. Confocal techniques that are discussed in this chapter are confocal laser scanning microscopy (CLSM), two-photon microscopy and Raman microspectroscopic techniques. Although these techniques are based on different principles, they all have something in common and that is confocality, ability to image one small focal volume at a time to construct a high-resolution image. Thanks to the modern electronics and optics, we are able to image deeper into a thick biological specimen like skin at high resolution, high speed and in-vitro as well as in-vivo conditions. Sophisticated lasers and detection systems have enabled us to exploit non-linear excitation phenomena such as 2-photon fluorescence, coherent anti-stokes Raman scattering, stimulated Raman scattering etc. The following chapter reviews these techniques and discusses some of the results obtained pertaining to dermal delivery.

2. Confocal laser scanning microscope

In the last two decades, CLSM has been extensively used as a tool to visualize the fluorescent model compounds in the skin. CLSM examination revealed valuable additional morphological information of porcine skin in wound healing studies which was not obtained by conventional microscopy (Vardaxis et al., 1997). CLSM was also used to understand the mechanism by which nanoparticulate systems facilitate skin transport. The surface images revealed that (a) polystyrene nanoparticles accumulated preferentially in the follicular openings (b) this distribution increased in a time-dependent manner and (c) the follicular localization was favored by particles of smaller size (Alvarez-Roman et al., 2004). Simonetti et al. visualized diffusion pathways across the SC of native and in-vitro reconstructed epidermis by using CLSM (Simonetti et al., 1995).

Many researchers used CLSM to evaluate the penetration of liposomes into human or animal skin using a fluorescent compound or a fluorescent model drug. It was demonstrated that flexible liposomes penetrated deeper into the skin in non-occlusive conditions than after occlusive application (van Kuijk-Meuwissen et al., 1998) as measured by a fluorescent liposome marker. Touitou and coworkers

examined the penetration of fluorescent probes into fibroblasts and nude mice skin by CLSM and showed that ethosomes facilitated the penetration of all probes into the cells, as evident from the high-intensity fluorescence as compared to the hydroethanolic solution or conventional liposomes (Touitou et al., 2001).

Many research groups examined different lipid combinations for their potential to influence the skin. Zellmer et al. used CLSM to demonstrate that vesicles made of native human SC lipids interact rapidly with phosphatidylserine liposomes, weakly with human SC lipid liposomes and do not interact with phosphatidylcholine (PC) liposomes (Zellmer et al., 1998). Kirjavainen et al. reported that lipophilic fluorescent marker, L-α-phosphatidylethanolamine-N-lissamine rhodamine B sulfonyl (N-Rh-PE) was able to penetrate deeper into the SC from liposomal vesicles containing dioleylphosphatidyl-ethanolamine (DOPE) than from liposomes without DOPE. A pretreatment of the skin with unlabeled liposomes containing DOPE or lyso-phosphatidylcholine (lyso-PC) enhanced the subsequent penetration of the fluorescent markers, N-Rh-PE and sulforhodamine B into the skin, suggesting a possible penetration enhancing activity (Kirjavainen et al., 1996).

Procedures like iontophoresis which enhance the percutaneous flux of model drugs like calcein (Turner and Guy, 1998) and mannitol (Kirjavainen et al., 2000) were also examined by CLSM in animal models. Grams et al. used CLSM to visualize time resolved diffusion of a lipophilic dye into the hair follicle of fresh and unfixed piece of human scalp skin. The authors claimed that this technique was able to visualize the diffusion of a dye into the upper hair follicle at different time points (Grams et al., 2004). In another study, they also report that follicular accumulation of lipophilic dyes increased when applied in combination of surfactant-propylene glycol (Grams et al., 2003).

2.1. Principle of CLSM

Confocality is achieved in CLSM by using a point illumination and point detection. Marvin Minsky constructed the first confocal microscope in 1957 at Harvard (Semwogerere and Weeks, 2008). He used a zirconium arc lamp and two pinholes, one in front of the lamp and another in front of the detector to achieve the confocality, while the sample was scanned through the light beam to generate the image. Today's confocal microscopes although different are based on the same principle of point illumination and detection, and their ability to image thick samples with high resolution have enabled their use in studying skin penetration of various molecules and delivery systems.

A CLSM can create a very sharp and high-resolution image of a specimen compared to a conventional microscope. This ability arises from the fact that CLSM is able to filter light coming from parts of the specimen that are not in focus, and in the process as much as 95% of the light coming from the specimen can be blocked to generate an image. As a result, very few photons actually make it to the detector therefore a very high intensity light source in the form of laser is used in modern CLSMs. One

disadvantage of this is that more than one laser might be required in order to have multiple excitation wavelengths.

The principle of confocality is explained in the schematic diagram in figure-1A where light coming from the specimen is focused on the detector with the help of two lenses. Due to the pinhole in front of the detector only the light coming from a very small focal point reaches the detector and light from out of focus regions of the specimen is blocked by the pinhole. The second pinhole is employed in front of the light source, which limits the amount of specimen that is illuminated at any time, and as a result reduces the background scatter from out of focus region of the specimen. Two pinholes of the confocal microscope are able to significantly reduce the background blur and produce very high-resolution images (Hollricher and Ibach, 2011; Nwaneshiudu et al., 2012).

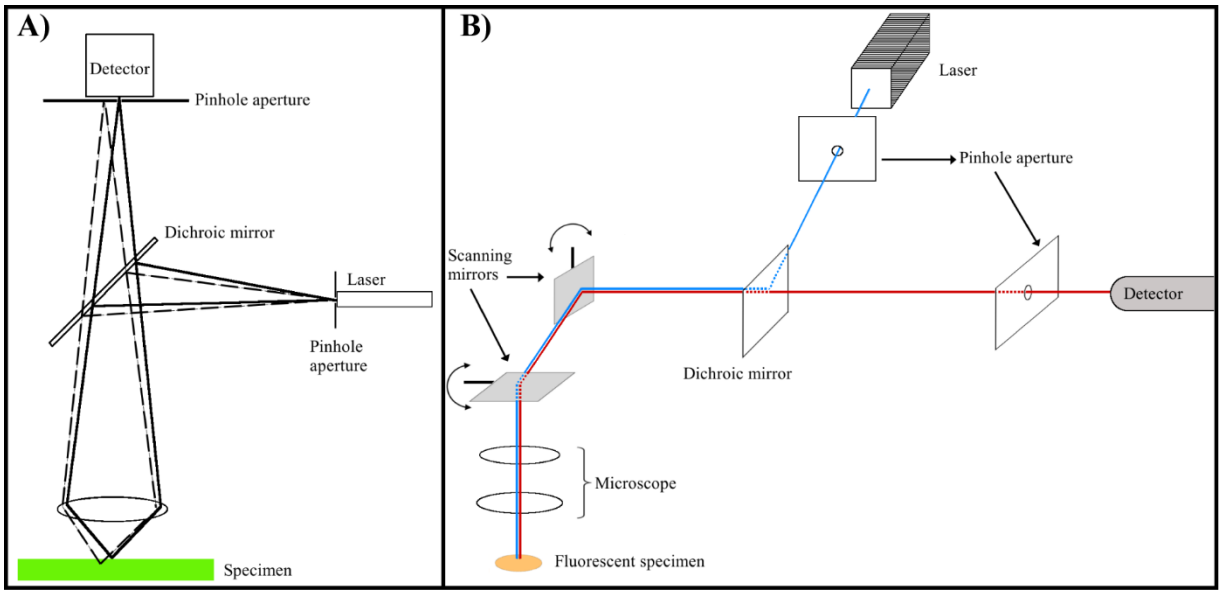

Figure-1: A) Pinhole in front of the detector rejects light emerging from out of focus regions B) Schematic representation of CLSM optics (redrawn from Semwogerere and Weeks, 2008).

Schematic representation of a CLSM is provided in figure-1B. In a modern CLSM a beam of light is provided by a laser which passes through a pinhole onto a dichroic mirror which directs the light to a scanning mirror assembly and onto the specimen through the microscope objective. The scanning mirrors scan the laser across the specimen in order to generate the image. Light reflected from the specimen is de-scanned at the scanning mirrors and passes to the photo-multiplier tube (PMT) detectors through the dichroic mirror (Semwogerere and Weeks, 2008). Light coming from out of focus regions of the specimen is blocked at the detector by a pinhole. Image of the specimen is reconstructed by a computer from the spatial coordinates and corresponding light intensity at the detector.

2.2. Major advantages of CLSM

Blurring effect observed in the conventional microscope is either eliminated or reduced to a great extent in CLSM, and as a result, images generated are very sharp, have a high contrast and a higher resolution. In practice a CLSM can have at best a horizontal resolution of 0.2 μm and a best vertical resolution of 0.5 μm. Further, a 3D sectioning or optical sectioning of the sample is possible as very small focal point is imaged at a time which also gives possibility to image thicker specimens using a confocal microscope. Using multiple lasers, it is possible to excite different fluorophores simultaneously.

2.3. Major disadvantages of CLSM

CLSM has an inherent resolution limitation of about 0.2 μm and is dependent on the wavelength of excitation. Due to the high intensity light source, photo bleaching and photo-damage in the illuminated region of the specimen is possible and repeated scans with high-energy light beam greatly reduce the viability of biological tissues and thereby the available time for studying a given specimen. For a high quality image, CLSM usually needs long scan times and as a result, CLSM is not suitable for imaging rapid physiological events in a cell or a tissue. In addition, because lasers emit light only at certain narrow bandwidths, in order to be able to excite a large range of fluorophores, multiple lasers need to be employed which along with the complex electronics, scanning mirrors and sophisticated data acquisition system raise the cost.

2.4. CLSM used for tracking liposomal formulations in the skin

Liposomes have been extensively studied and suggested as a vehicle for topical drug delivery(Chen et al., 2010; Chen et al., 2011; Dragicevic-Curic et al., 2008; Dragicevic-Curic et al., 2009; Ntimenou et al., 2012). However, the mechanism of penetration of liposomes as drug carriers into the intact skin is not fully understood. In this section, we will discuss the interactions between liposomes, containing hydrophilic and lipophilic fluorescent probes, and human as well as rat skin using CLSM.

2.4.1. Tracking skin penetration of liposomally entrapped or un-entrapped hydrophilic fluorescent model drug

The mechanism of action of liposomes as penetrable drug carriers in topical delivery is not completely understood. In order to evaluate if liposomes are able to increase skin penetration of only entrapped hydrophilic drugs or also of unentrapped hydrophilic drugs, three different liposomal formulations using carboxyfluoresceine (CF) as a fluorescent hydrophilic model drug were prepared: '$CF_{in\text{-}out}$' (non-entrapped CF was not removed), 'CF_{in}' (non-entrapped CF was removed) and 'CF_{out}' (a precalculated amount of CF was added to empty liposomes). All the liposomal formulations had similar size of liposomes and the concentration of CF was the same in all formulations (Verma et al., 2003). After 6 h incubation of the skin with different formulations, the skin was cryofixed and 7 μm thick sections were

221 cut using a cryo-microtome. These cross sections were investigated using CLSM for the skin penetration
222 of CF.

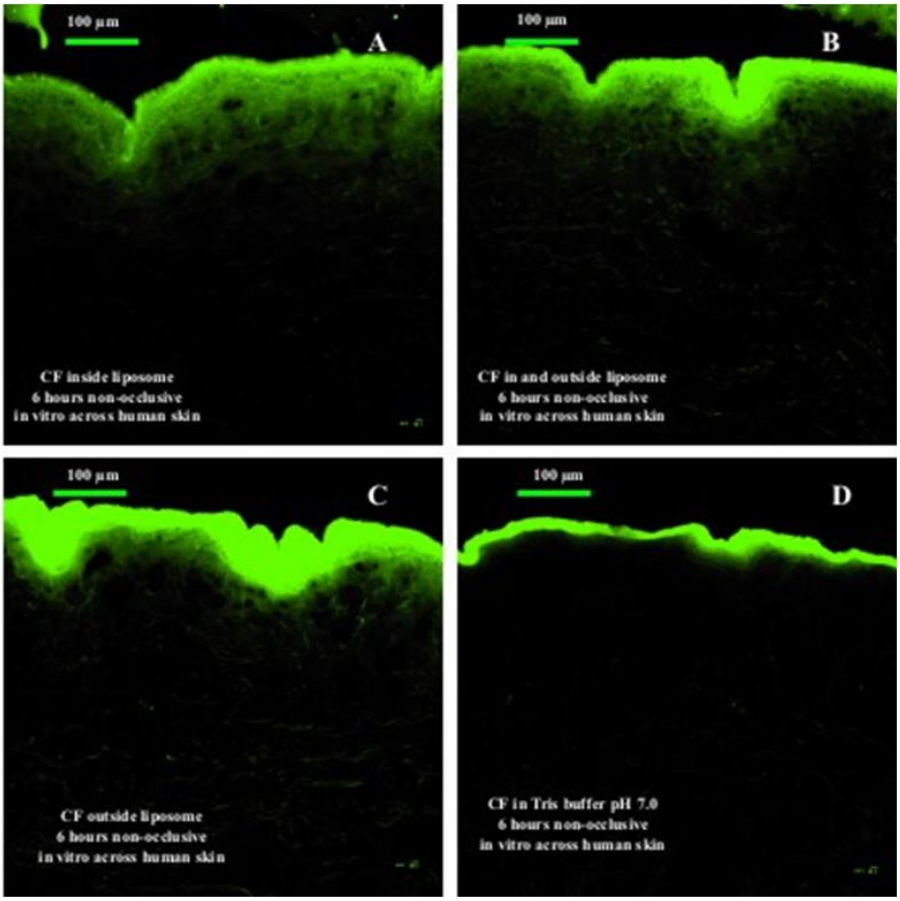

223

224 **Figure-2:** Fluorescence micrographs of cross-sections of human abdominal skin incubated on Franz diffusion cells
225 with different formulations containing CF. Formulations were applied without occlusion for 6 h. (A) liposomes
226 CF_{in}; (B) liposomes $CF_{in\text{-}out}$; (C) liposomes CF_{out}; CF outside liposomes and (D) CF dissolved in Tris buffer. Scale
227 bar represents 100 µm.

228 The penetration studies and CLSM images showed that liposomes $CF_{in\text{-}out}$ exhibited maximum
229 deposition of CF in the SC, whereas liposomes CF_{in} showed higher penetration of CF into the deeper
230 skin layers such as the viable epidermis (Figure-2), and through the skin to the acceptor compartment
231 of the Franz diffusion cell. These results were comparable to the data obtained from tape stripping
232 experiments. This study confirmed the assumption that liposomes $CF_{in\text{-}out}$ were not under osmotic stress
233 and will, therefore, transfer themselves more easily into the SC. The results indicated further that
234 phospholipid vesicles not only carry the entrapped hydrophilic substance, but also the non-encapsulated
235 hydrophilic substance into the SC and possibly to the deeper layers of the skin. Although CLSM served
236 as useful tool to estimate skin penetration, CLSM images do not provide the visualization of single
237 liposomes, so the exact mechanism of penetration of liposomes still remains an unsolved question.

238 **2.4.2.Effect of vesicle diameter on skin penetration of liposomally entrapped drugs**

239 The influence of vesicle size on the penetration of fluorescently labeled liposomes into the human skin
240 was investigated using lipophilic fluorescent label, 1,1'-dioctadecyl-3,3,3',3'-

241 tetramethylindocarbocyanine percholate (DiI) (Verma et al., 2003). In all CLSM images (Figure-3) very
242 high fluorescence was observed in the SC, which was expected due to the lipophilic nature of the
243 fluorescent label, DiI. This study indicated that large vesicles with a size ≥ 600 nm were not able to
244 deliver their contents into the deeper layers of the skin. These liposomes probably stayed in/on the SC
245 and after drying they formed a layer of lipid, which would have further strengthened the barrier
246 properties of the SC. The liposomes with size ≤ 300 nm were able to deliver their contents to some
247 extent into the deeper layers of the skin. However, the liposomes with size ≤ 70 nm were most promising
248 for dermal drug delivery into the deeper skin layers as they showed maximum fluorescence both in
249 viable epidermis, as well as in dermis.

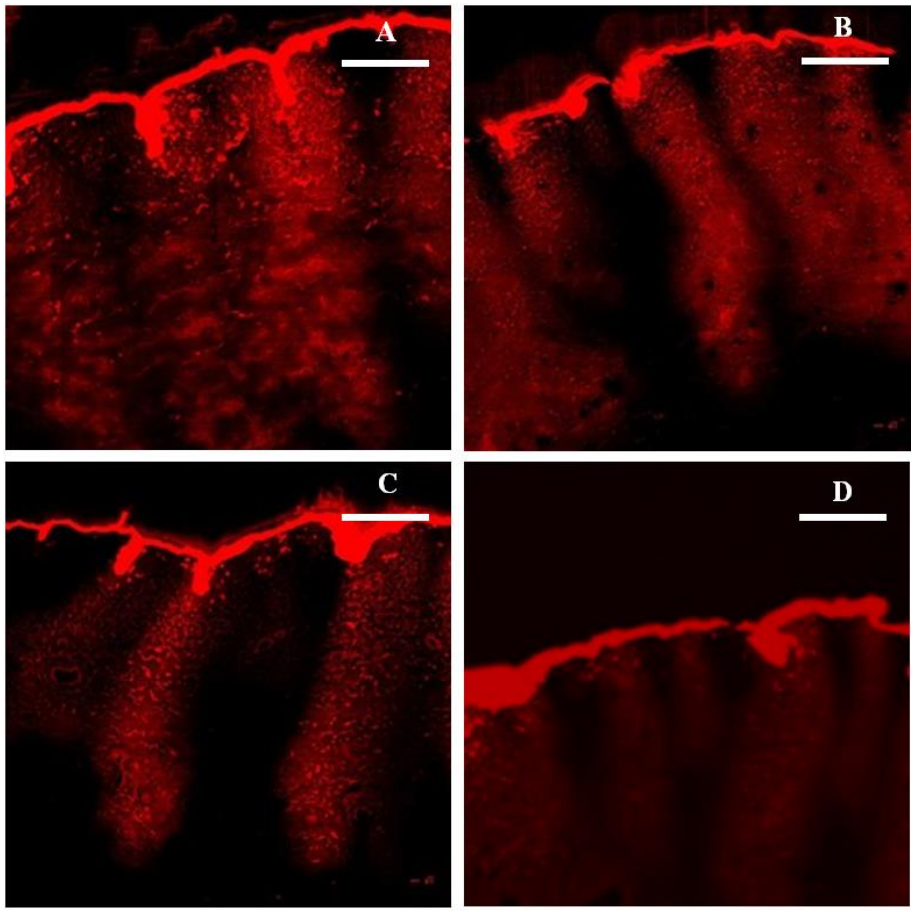

250

251 **Figure-3:** Fluorescence micrographs of cross-sections of human abdominal skin incubated on Franz diffusion cells
252 with different formulations containing DiI. The vesicles were applied non-occlusively for 12h. (A) Ethanolic
253 solution of DiI; (B) NAT8539/ethanol (10/3.3); (C) NAT8539/ethanol (10/10); (D) NAT8539/ethanol (10/20).
254 Scale bar represents 50 μm.

255 **2.4.3.Synergistic penetration enhancement effect of ethanol and phospholipids on topical drug**
256 **delivery**

257 It was observed that the composition of liposomal formulation had an appreciable effect on the
258 penetration of compounds into and through the skin (Hofland et al., 1994; Jimbo et al., 1983; Loftsson
259 et al., 1989; Tenjarla et al., 1999). Hence, the effect of lipid vesicular systems embodying ethanol in

relatively high concentrations on the percutaneous penetration of cyclosporin A (CyA) was investigated using a standardized skin stripping technique and CLSM (Verma and Fahr, 2004). Ethanol has been widely reported as an efficient skin penetration enhancer in the concentration of 5% to 100% (Bhatia and Singh, 1999; Kobayashi et al., 1994; Simonetti et al., 1995). In a preliminary study, we have seen that, not only the amount and the type of phospholipids are important for skin penetration enhancement, but also the amount of ethanol has a significant role in delivering the fluorescent model compounds into the skin (Figure-4) (Verma, 2002). We hypothesized that ethanol and phospholipids might have synergistic skin penetration enhancing effect.

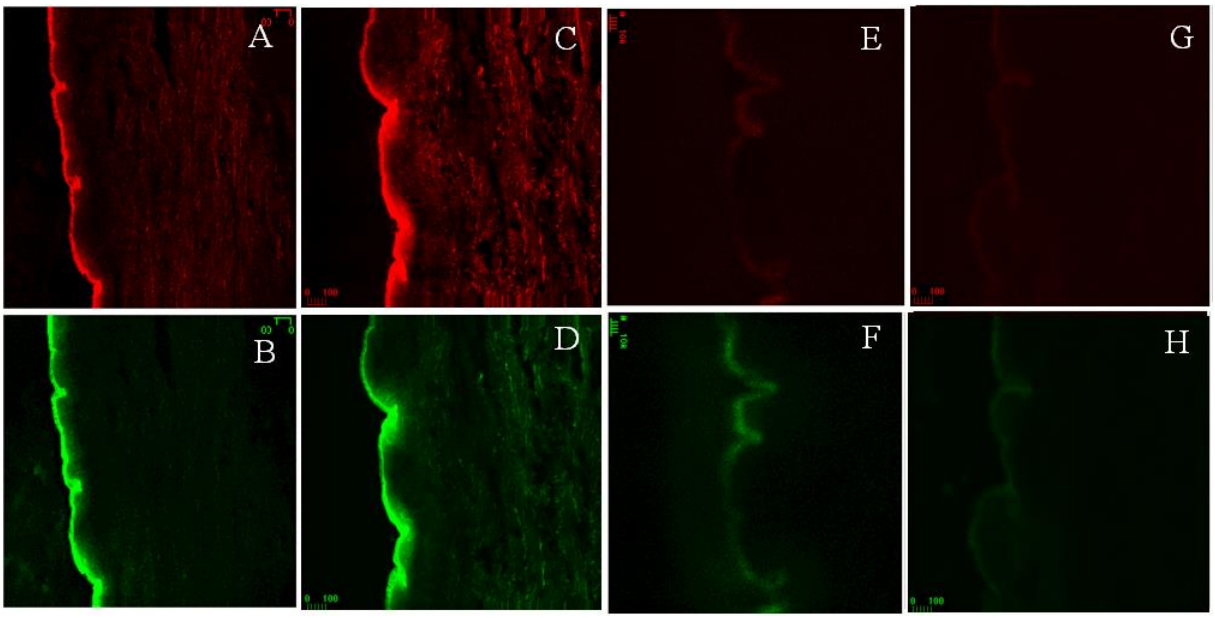

Figure-4: Fluorescence micrographs of cross sections of human skin incubated with vesicles with different lipid content for 12 h. A & B: ethanolic solution of N-Rh-PE (A) and CF (B). C & D: Flexible liposomes with N-Rh-PE (C) and CF (D). E & F: PL 90H-liposomes with N-Rh-PE (E) and CF (F); G & H: PL25 liposomes with N-Rh-PE (G) and CF (H).

In order to evaluate synergistic effect of the ethanol and phospholipids on penetration of DiI, vesicles with composition of 10% (w/v) phospholipid mixture NAT 8539 (Lipoid, Germany) and ethanol at different concentrations ranging from 0-20% w/v were prepared. The results of the CLSM studies are represented in Figure-5. Ethanolic solution of the DiI dye was able to deliver only weak fluorescence into the SC, and no fluorescence was noticeable in the viable epidermis and dermis (Figure-5A). Formulation, NAT 8539/ethanol (10/3.3), produced a homogeneous bright fluorescence throughout the SC, but no fluorescence was observed in the viable epidermis and dermis (Figure-5B). Formulation, NAT 8539/ethanol (10/10), produced a bright fluorescence throughout the SC with very weak to weak fluorescence observed in the viable epidermis and dermis (Figure-5C). Formulation NAT 8539/ethanol (10/20), produced a homogeneous bright fluorescence throughout the SC and very a weak fluorescence was noticeable in the viable epidermis and dermis (Figure-5D). CLSM experiments have shown that the ethanolic solution of DiI was not even able to deliver the fluorescent label into the SC. In contrast, all the formulations with NAT 8539 and ethanol produced a bright fluorescence homogeneously throughout

the SC. Formulations prepared with NAT 8539 containing 10 and 20% ethanol were also able to show very weak fluorescence in the viable epidermis and dermis. The results above were confirmed by in vitro penetration studies followed by tape stripping and extraction of the radioactively labeled CyA from various layers of the skin. Ethanol, together with NAT 8539 had synergistic effects on the delivery of the CyA into the skin, and the enhancement effect of ethanol was concentration dependent. Although CLSM images do not provide pure quantitative data regarding the skin penetration, they are, however, extremely useful as a comparative tool and give useful information about the distribution of the drug within the skin.

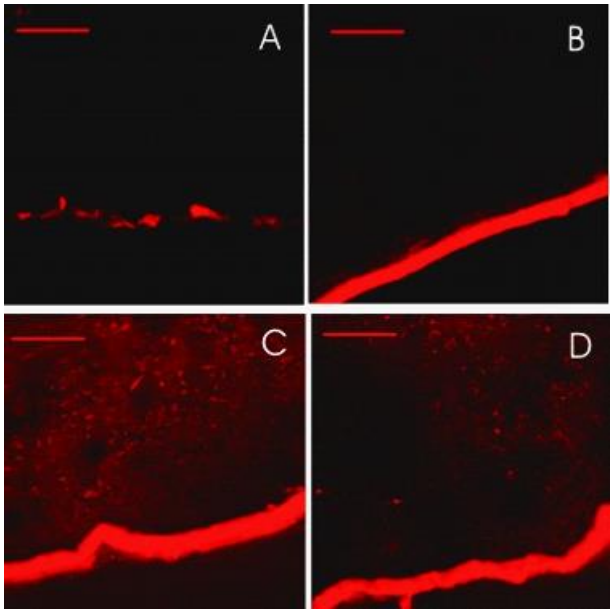

Figure-5: Fluorescence micrographs of cross-sections of human abdominal skin incubated on Franz diffusion cells with different formulations containing DiI. The vesicles were applied without occlusion for 12 h. (A) Ethanolic solution of DiI; (B) NAT8539/ethanol (10/3.3); (C) NAT8539/ethanol (10/10); (D) NAT8539/ethanol (10/20). Scale bar represents 50 μm.

2.4.4. Terpenes as penetration enhancers in liposomes

In this study, CLSM was used to investigate if incorporation of penetration enhancers (terpenes) into liposomal formulations had an effect on their percutaneous penetration enhancing ability in human and rat skin (Verma, 2002). Fluorescent derivative of CyA, D-Ala-8-CS-beta-aminebenzofurazan (Fl-CyA) and DiI, were used as lipophilic markers while Alexa Fluor-488® (Life Technologies GmbH, Germany) was used as a hydrophilic fluorescent marker. Vesicles with and without terpenes were compared with ethanolic and hydro-alcoholic solutions of the fluorescent labels. Double-labeled vesicles, vesicles containing both DiI and Alexa Fluor-488®, were applied to skin for 6 and 12h. Penetration of the fluorescent labels was visualized by CLSM both in terms of depth and intensities of the fluorescence. Fluorescent intensities of the CLSM images were semi-quantitatively scored ranging from no fluorescence to bright fluorescence. Further details regarding imaging and formulations can be found elsewhere, (Verma, 2002).

CLSM images of cross sections of rat skin incubated for 6 h with Fl-CyA liposomes prepared with and without terpenes are compared in Figure-6. A bright fluorescence was observed in the SC (Figure-6B) for skin treated with Fl-CyA liposomes without terpenes, but only a negligible or no fluorescence was observed in the viable epidermis and dermis. The skin treated with Fl-CyA liposomes containing 1% terpenes showed a relatively higher fluorescence in the SC and weak fluorescence in the epidermis, suggesting diffusion of the Fl-CyA from SC to the epidermis (Figure-6C). Ethanolic solution of Fl-CyA showed a very weak fluorescence in the SC and no fluorescence was observed in the viable epidermis and dermis (Figure-6A). Based on the fluorescence scores obtained from CLSM images, results indicate that penetration enhancers do play an important role in the penetration of fluorescent labels into the skin.

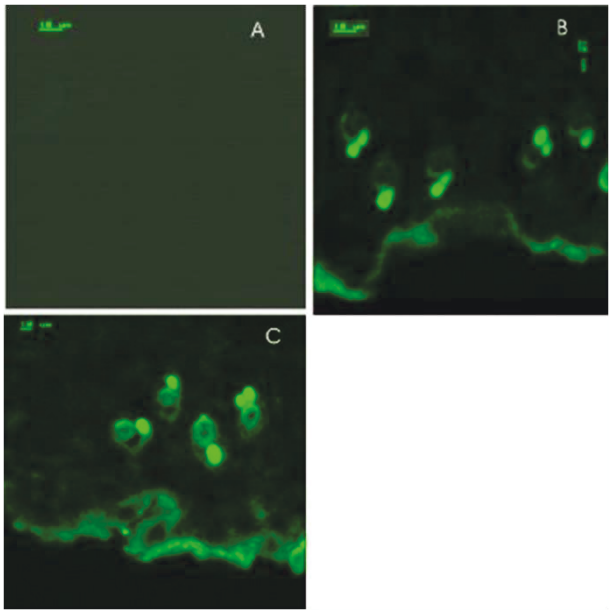

Figure-6: Cross sections of rat skin incubated with different formulations containing Fl-CyA. The vesicles were applied non-occlusively for 6 h on rat skin. (A) Ethanolic solution of Fl-CyA, (B) Fl-CyA liposomes without terpenes, and (C) liposomes containing 1% terpenes. The length bar represents 10 µm. Arrows represent hair follicles in the dermis.

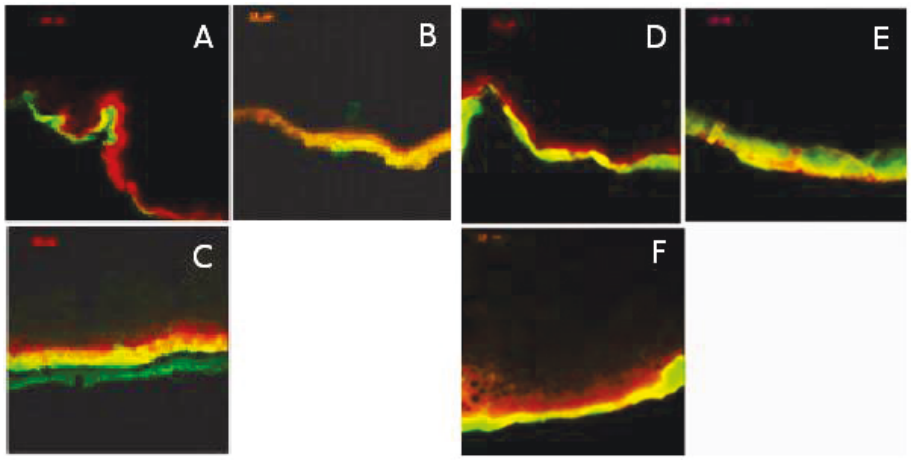

Figure-7: Cross sections of human abdominal skin treated with formulations containing two fluorescent markers, DiI and Alexa Fluor 488®. The formulations were applied without occlusion for 6h (A-C) and 12h (D-F). A & C: Hydroalcoholic solution of DiI and Alexa Fluor 488, B & E: double-labeled liposomes without terpenes C & F: double-labeled vesicles containing 1% terpenes. The bar represents 10 µm.

Cross sections of human skin treated with double-labeled (DiI and Alexa Fluor 488®) liposomes with and without terpenes are represented in Figure-7. Incubation period of formulation with the skin was 6 h (Figure-7A-C) and 12 h (Figure-7D-F). Control was provided by skin samples treated with hydro alcoholic solution containing both dyes mentioned above. In all the samples the fluorescence was restricted mainly to the SC and to a smaller or larger extent, to the viable epidermis. Samples treated with hydroalcoholic solutions of the dyes exhibited fluorescence for both DiI and Alexa Fluor-488® only in the SC. Increasing the incubation period from 6 h to 12 h only increased the fluorescence intensities for both the labels (Figure-7A & 7D). In samples treated with dual labeled liposomes without terpenes, fluorescent markers after 6 h diffusion are restricted to the SC only. DiI penetrated upto deeper layers of the SC however no fluorescence was observed in the viable epidermis and dermis (Figure-7B). Increasing the incubation period to 12 hours did not have marked improvement in penetration depths. CLSM images (Figure-7E) show higher intensities and slightly higher penetration up to viable epidermis achieved for both the dyes. Although distribution of Alexa Fluor-488® appears uniform for both 6 and 12 h diffusion samples, distribution of lipophilic dye DiI, was not uniform for 12 h samples. For skin treated with liposomal formulations containing 1% terpenes, much higher intensities were observed for both the fluorescent dyes in the SC (Figure-7C & 7F). For sample with 6 h incubation, very weak fluorescence for Alexa Fluor-488® while weak fluorescence for DiI, was observed in the viable epidermis. For 12 h incubation samples, fluorescence intensity scores were bright-fluorescence at SC for both the dyes and moderate fluorescence intensities were observed in the viable epidermis. Surprisingly, the reddish fluorescence continued from the epidermis towards the dermis, indicating a diffusion of the lipophilic marker. It was observed that liposomal formulations containing terpenes as penetration enhancer were able to deliver relatively higher amounts of fluorescent labels into the SC, epidermis and, to a small extent the dermis. In this study we clearly demonstrated the ability of CLSM to simultaneously image two fluorescent dyes.

2.5. Tracking the penetration of fluorescence labels into hair follicles

2.5.1. Tracking of fluorescently labeled cyclosporin A into rat hair follicles

CLSM has been successfully used to track follicular penetration of drugs. Topical application of the CF-loaded liposomes has been reported to significantly increase the accumulation of CF in the pilosebaceous units compared to other non-liposomal formulations (Lieb et al., 1992). Using CLSM, Patzelt et al. demonstrated that follicular penetration for nano-particles was size dependent (Patzelt et al., 2011). The effect of terpenes as penetration enhancers in liposomes for targeting hair follicles was investigated using Fl-CyA vesicles (as mentioned above), with and without terpenes, in rat skin. Figure-6 also depicts the role of the pilosebaceous unit in the penetration of drugs into the skin. A bright fluorescence was observed in the pilosebaceous units (bright green fluorescent regions in dermis in Fig.6B and 6C identified as the hair shaft, a part of the pilosebaceous unit) for both formulations, with and without PE.

The fluorescence was also visualized in the outer root sheath of the hair shaft (Figure-6B-C & Figure-8) (Verma, 2002). The images presented here demonstrate that the liposomal vesicles can enter the pilosebaceous unit and deliver their content to the hair follicle and possibly to the hair bulb. Importance of this was stressed upon by the fact that ethanolic solution of Fl-CyA failed to deliver any fluorescence into the skin. These CLSM results were supported by in-vivo studies with Dundee Experimental Bald Rats model (Verma et al., 2004) and other published reports (Agarwal et al., 2000; Bohm and Luger, 1998; Lieb et al., 1992; Niemiec et al., 1995). The CLSM investigations enabled us to visualize the accumulation of fluorescent label in the pilosebaceous units which is not possible with tape stripping.

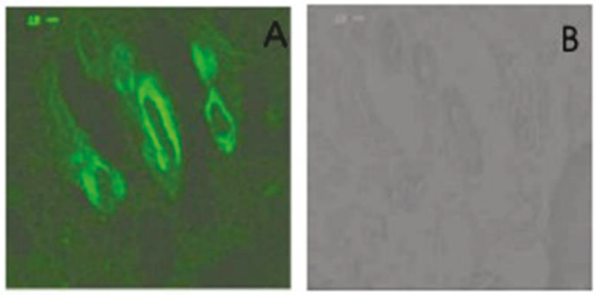

Figure-8: Fl-CyA liposomes treated rat skin cross section demonstrating the role of pilosebaceous units in the penetration of substance into the skin. The bar represents 10 µm.

2.5.2.Accumulation of CF and N-Rho-PE loaded liposomes in the human hair follicles

In this study, liposomal formulations containing CF and N-Rh-PE were prepared (Verma, 2002). Liposomal formulations were able to deliver both the hydrophilic and lipophilic fluorescent labels to the human hair follicles as seen in Figure-9A and 9B respectively. Studies represented in Figures-6, 8, and 9 demonstrated that the presence of hair follicles plays a significant role in the skin penetration of drugs, as well as that the presence of penetration enhancers helps the formulation in enhancing the follicle delivery of drugs.

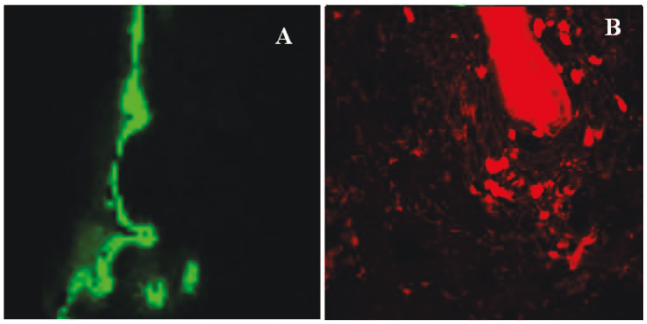

Figure-9: Delivery of CF (left) and Rhodamine (right) encapsulated in liposomes to the hair follicles.

2.6. The efficacy of Dermaroller® to enhance penetration into the skin

CLSM was also used to investigate the efficacy of the micro-perforation devices, Dermaroller® (Horst Liebl ETS, France) in increasing the skin penetration of a fluorescent lipophilic model compound DiI encapsulated in liposomes (Verma, 2002). Three types of Dermarollers® were tested in this study,

namely Dermaroller® C8 0.13-15°, M8 1.5-15° and M8 1.5-30°. Control was provided by the skin not treated with Dermarollers®.

Bright intensity of fluorescence was observed in SC for all samples treated with Dermaroller and for control (Figure-10). For control samples however fluorescence intensities in the viable epidermis and dermis were very low. For Dermaroller® C8 0.13-15°, highest fluorescence was observed in the SC and fluorescence intensities rapidly decreased in the viable epidermis and dermis (Figure-10B). Dermaroller® C8 0.13-15° was intended for delivering drugs to the SC whereas Dermaroller® M8 1.5-15° and M8 1.5-30° were optimized for delivering drugs to the deeper regions of skin. Both M8 Dermarollers® did show very high fluorescence intensities in the dermis region (Figure-10C-D). We observed that, samples treated with both M8 Dermarollers® showed only a weak fluorescence in the viable epidermis region and showed weak lateral diffusion of the fluorescent label from the pores. This might be because, Dermaroller® was able to deliver the liposomes into the deeper layers quickly during application of the Dermaroller but after the application, liposomes probably were not able to diffuse to a great extent from the surface of the skin to the deeper layers in the skin. In this study we emphasized on the spatial distribution of the fluorescent label which helped us to get a better understanding of the mode of action of the micro-perforation device, Dermaroller®.

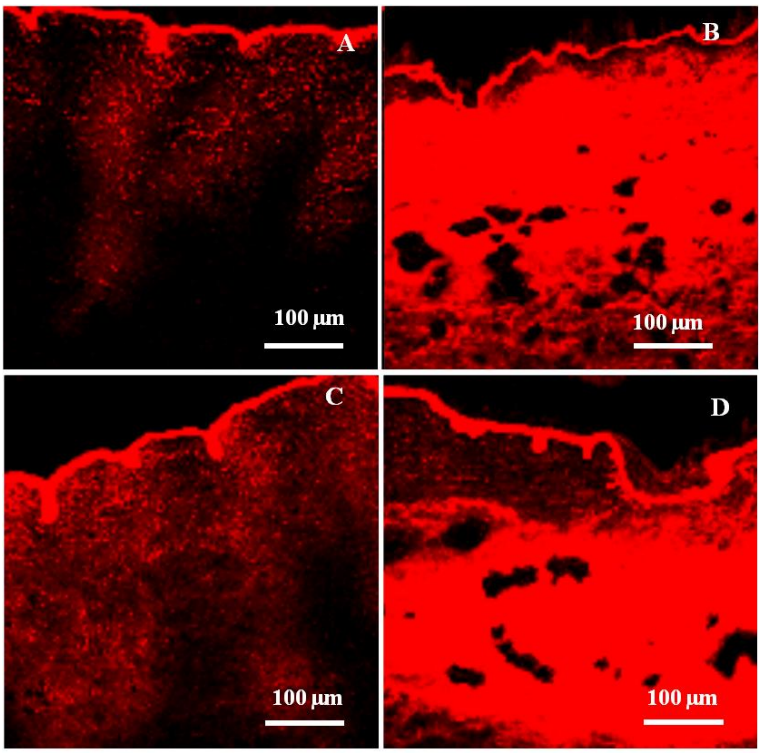

Figure-10: Fluorescent micrographs of cross-sections of human abdominal skin pretreated with Dermaroller® and incubated on a Franz diffusion cell with liposomes containing lipophilic fluorescent label DiI. The liposomes were applied without occlusion for 3 h. (A) Control; (B) Model C 8 0.13-15°; (C) Model M 8 1.5-15°; (D) Model M 8 1.5-30°.

3. Two-photon fluorescence microscopy

3.1. Principle of two-photon fluorescence microscopy

As seen from aforementioned studies, CLSM is a very good technique for imaging of biological samples, however, it suffers from some disadvantages. One of the most important limitations of the CLSM is that because only a small fraction of the incident light reaches the detector, relatively high intensities of light are required to achieve high signal to noise ratios. This results in high total energy transfer to the specimen during imaging. Also the laser beam excites the fluorophores in the specimen above and below the focal plane that is under investigation and this can cause severe photo bleaching, photo damage and even dehydration of the biological specimen. Many fluorophores generate free radicles or singlet oxygen when excited which can be toxic if imaging living cells or tissue. CLSM also suffers from low axial resolution especially when imaging deep within a thick tissue. The poor axial resolution results from the scattering of light by the specimen itself, which can lead to detection of light that is not generated from the observed focal plane. Also CLSM employs short wavelength excitation sources and shorter wavelengths are scattered stronger (scattering intensity is inversely proportional to fourth power of the wavelength) hence these excitation sources are not very efficient at deep tissue imaging. Due to limitations in deep tissue imaging, when adopting a CLSM for imaging skin, the sample must be cryo-sectioned and this is not always possible and desirable.

Multiphoton excitation phenomenon was proposed in 1931, however Kaiser & Garret were able to validate it only in 1961 after the development of lasers which were sufficiently powerful to generate the high photon flux required for two-photon excitation. Figure-11A explains the energy transfer during one photon and two-photon excitation. In single-photon fluorescence, the fluorescence photon is generated when a high energy photon is incident on the fluorophor which results in raising the energy level of one of the electron to an excited state. In two-photon excitation, if two low energy photons arrive together within 10^{-18} sec of one another, the combined energy transfer of the two low energy photons is sufficient to raise the same electron to a higher energy level (Dunn and Young, 2006). A low energy photon is too weak to illicit the two-photon fluorescence phenomenon in the fluorophor. Hence, in order to increase the probability of simultaneous incidence of photons a laser with very high photon flux is required. Setup of a two-photon microscope is quite similar to that of a confocal scanning microscope with two major differences. One is the light source, two-photon microscopes use a tunable Ti-sapphire high frequency pulsed laser which has a pulse length of approximately a few hundred femtoseconds. Second important difference is the lack of any pinholes in front of the detector to avoid detecting scattered light from out of focus plane.

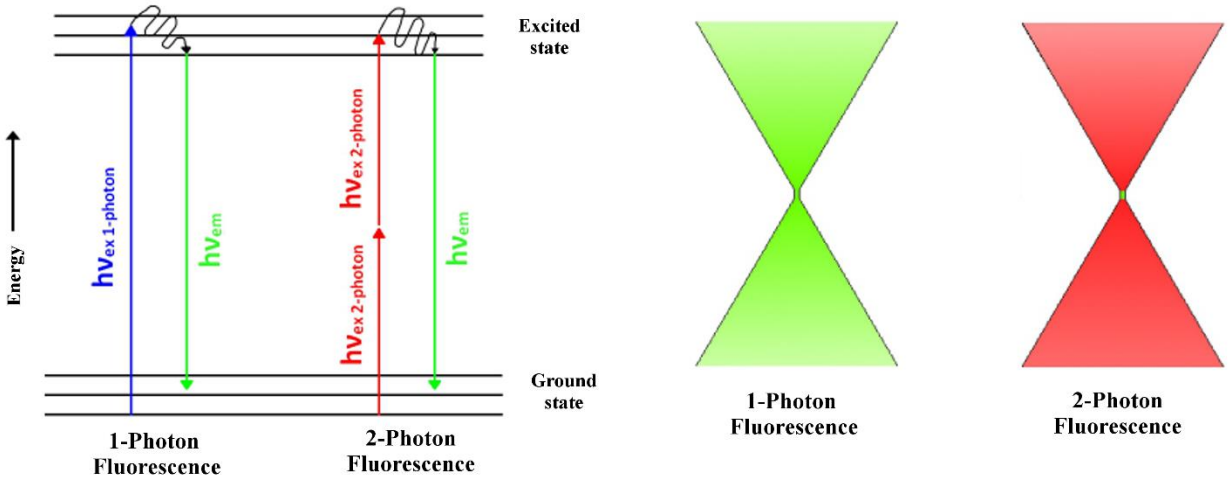

Figure-11:(A) Jablonski diagram elucidating the differences between single photon fluorescence and two photon fluorescence phenomenon. (B) Excitation volume in one-photon and two-photon fluorescence phenomena.

One of the important advantages of 2-PFM is that total energy delivered to the specimen is much lower as compared to a CLSM. Also the two-photon excitation phenomenon occurs only at a very small focal volume (Figure-11B) and as a result fluorophores in a very small volume of the specimen are excited which reduces the probability of photo-bleaching, photo-damage. In addition, no confocal pinhole aperture is required to block the scattered light from out of focus planes. The near-infrared (NIR) light source used in a 2-PFM is very efficient at imaging deeper regions of the biological samples, as it is least scattered and absorbed by the biological samples. These advantages mean that the skin samples can be studied without cryofixing and cutting. Disadvantages of a two-photon microscope include a relatively high price of the ultra-short pulsed Ti-sapphire lasers and the fact that they require an elaborate cooling system. Also, 2-PFM has lower lateral resolution compared to CLSM, but in practice the difference in their resolution is not significant.

3.2. Application of two-photon microscopy in skin penetration experiments

Carrer et al. used 2-PFM to study the architecture and physical properties of the pig skin epidermis and permeability of different liposomal formulations in the pig skin (Carrer et al., 2008). In this study, authors were able to easily distinguish different layers of the pig epidermis based on their morphological differences without any significant sample preparation. To study the hydration/polarity of different layers of the epidermis they used Laurdan generalized polarization (Laurdan-GP) values as an indicator of polarity. As expected, the Laurdan-GP values were highest for SC and decreased for deeper layers of the skin indicating an increase in fluidity or hydration. The authors report an interesting observation in the intercluster region (canyons or wrinkles as in human skin), the Laurdan-GP values in the canyons were quiet high, comparable to that of SC and they did not change with depth (from surface of SC to dermis), indicating that canyons might show environment similar to SC. To study the penetration of liposomal formulations, Lissamine rhodamine B 1,2-dihexadecanoyl-*sn*-glycero-3-

phosphoethanolamine, was incorporated in the liposomal membrane. After 16-h diffusion, image stacks were collected and penetration was measured in the form of ratio of fluorescence intensity of rhodamine and autofluorescence of the skin. Authors report that the liposomes with lower lipid content (10mg/ml) were able to deliver more fluorescent label to the lower parts of viable epidermis compared to the formulations with higher lipid content (25 and 50mg/ml).

van den Bergh et al. elucidated the mechanism of interactions of elastic and rigid liposomal vesicles with human skin (van den Bergh et al., 1999). Using 2-PFM and different electron microscopic techniques they studied interactions between skin and various elastic liposomal formulations to understand the modulation of the skin barrier. They observed that fluorescently labeled elastic vesicles primarily affected the intercellular lipid lamellae of the SC, while the underlying layers of the viable epidermis remained relatively unchanged. This effect was visualized using 2-PFM, in the form of small penetration pathways that were confined to the SC only. Authors also reported that the penetration enhancing ability of elastic vesicles was dependent on whether vesicles were applied with or without occlusion.

Oleic acid is a good penetration enhancer and has been found to increase transdermal penetration of both hydrophilic and hydrophobic drugs by modulating the intercellular lipid domains in the SC. Yu et al. used a high-speed two-photon microscope with dual channels capable to simultaneous monitoring of autofluorescence of skin and fluorescence from rhodamine as a model drug (Yu et al., 2003). Treatment of human skin with oleic acid as a penetration enhancer was found to induce increased intra-corneocyte diffusion of the hydrophilic model drug (sulforhodamine-B), while causing localization of the hydrophobic model drug (Rhodamine-B hexyl ester) to the intercellular region. Hence, Yu et al. provided evidence that for chemical penetration enhancers, intra-corneocyte diffusion is an important enhancement mechanism along with fluidization of intercellular lipid domains, and physicochemical properties of the drug would determine which pathway predominates in the penetration enhancement.

In 2002, Jenlab GmbH introduced a dual-channeled non-invasive multi-photon tomograph capable of in vivo optical biopsies with subcellular spatial resolution based on near-IR femtosecond pulsed laser. König et al. reported the potential of this microscope to acquire high-resolution images from deep within the skin in vitro and in vivo (Konig et al., 2006; Schenke-Layland et al., 2006). The microscope utilized the second harmonic generation (SHG) signal to monitor the position of the microscope in the skin, while the fluorescence channel was used to detect either autofluorescence from the NAD(P)H, flavins, melanin etc or to detect exogenous fluorophores. In vivo imaging capabilities of 2-PFM promises great advances in cancer diagnostics and skin diseases, as well as in understanding the mechanisms involved in dermal drug delivery.

2-PFM is, as already mentioned, a relatively young technology. Bio-Rad Laboratories (USA) introduced first commercial two-photon microscope in 1996 and since then this technology has seen exponential

503 growth in its use and applications. Its ability to take high-resolution optical biopsies of the intact skin or
504 even do live imaging in vivo holds a great potential to unlock the secrets that were kept in the dark by
505 nature.

506 4. Confocal Raman Microscopy

507 4.1. Principles of Raman microscopy

508 Fluorescence microscopy has seen a lot of evolution in the last couple of decades and modern
509 microscopic techniques, like CLSM, multi-photon microscopy and various imaging modes such as
510 fluorescence life-time imaging, Förster resonance energy transfer etc., have increased the applications
511 and flexibility of the fluorescence imaging. However, fluorescence microscopy still has certain
512 disadvantages; mainly, fluorescence microscopy still utilizes exogenous dyes to label the drug or
513 formulation. These labels are often toxic or could cause perturbations in the cells or other physiological
514 processes. The biggest limitation for studying skin penetration is that often the fluorescent label and the
515 formulation or the drug do not travel together and consequently fluorescence imaging could give
516 incorrect interpretation of the observations.

517 Due to the disadvantages of fluorescent labeling to monitor the penetration depth in the skin, label free
518 vibrational spectroscopic techniques have gained importance. Vibrational spectroscopy is an
519 identification technique based on the principle that it is possible to interfere with the vibrational state of
520 a molecule by irradiating it with light of certain frequencies. Such interactions can be recorded in the
521 form of spectra which are representative of the bonds present in the molecule. Because each molecule
522 has its unique atomic structure and as a result a characteristic vibrational state, the vibrational spectra
523 can provide a host of information about the structure of the molecule. Vibrational spectroscopy involves
524 different techniques such as mid infrared (IR) spectroscopy, NIR spectroscopy, Raman spectroscopy
525 etc, but for this chapter we shall only review the Raman spectroscopic techniques. In addition, because
526 water content in the biological specimen interferes strongly with IR spectroscopy, Raman techniques
527 are more suitable for studying the drug penetration into the skin.

528 When a monochromatic beam of light is incident on the sample, most of the light is scattered by the
529 sample such that, the scattered light has the same wavelength as the incident light, this phenomenon is
530 known as elastic scattering or Rayleigh scattering. However, a small fraction of photons do interact with
531 the molecules of the sample and as a result, scattered photons have a different energy compared to the
532 incident photons which manifests in the form of a shift in the wavelength of the scattered photons. This
533 phenomenon is known as inelastic scattering or Raman scattering. Raman effect was first observed by
534 C.V. Raman in 1928 (Raman and Krishnan, 1928). It is a very weak phenomenon, about one photon
535 undergoes Raman scattering in a million Rayleigh scattered photons. Due to low signal to noise ratio,
536 Raman spectroscopic techniques were not very practical as they needed an intense source of light and a

sophisticated detection system. After the discovery of lasers and charged coupled detectors (CCD) however Raman spectroscopy has seen tremendous increase in its application (Hollricher, 2011).

To understand the Raman effect, we shall first have a look at the Rayleigh scatter. According to the classical theory, when photons are incident on the sample, they are absorbed by the molecules of the sample and are excited to a virtual state. When molecules relax back, if they relax to the same energy level as they started in, the emitted photons have the same energy as the incident photons and this type of scattering is called Rayleigh scattering. This effect is explained schematically in the Figure-12. In Raman scattering, a molecule relaxes back to a higher energy level after absorbing a photon, and as a result the emitted photon has lower energy by an amount required to vibrationally excite the molecule. Reemitted photon exhibits red shift and hence this effect is also called 'Stokes Raman scattering'. If after absorbing the photon, molecule loses a fraction of vibrational energy i.e. if molecule relaxes back to a lower energy state compared to its energy state before absorbing the photon, then the emitted photon has higher energy compared to the incident photon. This phenomenon is called the 'anti-stokes Raman scattering'. Raman spectrum is a plot of wavenumber shifts observed between Raman radiation and excitation radiation. Raman effect and fluorescence are distinct phenomena, in the later, incident photons are absorbed and molecules transition from ground state to an electronic excited state due to the resonance between vibrational frequency of the molecule and incident photons. As a result for a given molecule, fluorescence can be observed only at a certain fixed frequency range. However, Raman effect is not a resonant effect and can take place for wider range of excitation wavelengths. In addition, fluorescence phenomenon lasts much longer in terms of few nanoseconds, while Raman scattering is much short lived, i.e. less than a picosecond.

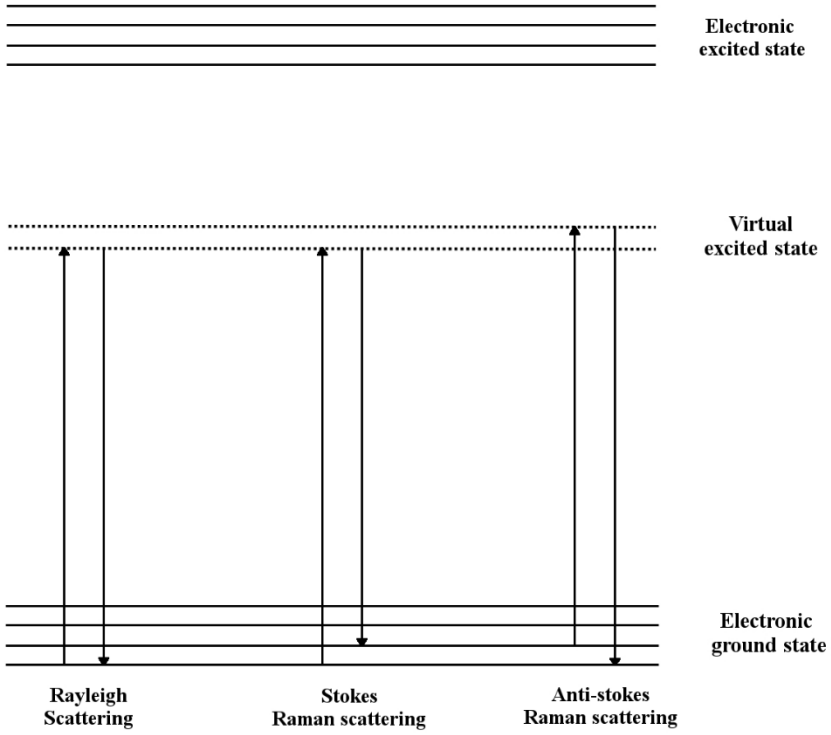

Figure-12: Jablonski diagram representation of Rayleigh and Raman scattering.

In modern Raman microscopes, light source is provided by a laser and is focused onto the sample with the help of an objective with high numerical aperture. Scattered light is collected by the same objective and passed through a diachroic mirror then to a spectrometer to resolve the Raman shifts, which are detected by a sensitive CCD camera. Raman map of the sample is usually generated by scanning the sample with the help of a piezo driven stage through the laser beam. In order to improve the signal to noise ratio most microscopes employ a confocal detection to reduce the scattered light from out of focus planes. Raman scattering intensity is proportional to fourth power of the frequency of incident photons. Hence, excitation at 400nm would give a 16 times more intense Raman signal compared to excitation at 800nm (Hollricher, 2011). However, skin has a very strong autofluorescence in the range of 400-700 nm and hence lower wavelengths are not ideal for Raman mapping of the skin. Higher wavelengths although useful for imaging thick specimen, according to the Rayleigh criterion, the lateral resolution is directly proportional to the wavelength, in other words lower wavelength would give better resolution. As a result selecting the right wavelength of excitation is very important in order to maintain a good balance between resolution and signal quality. For collecting Raman spectra from skin, usually lasers with wavelength of 633, 660 or 785nm are preferred.

4.2. Confocal Raman microscopy for skin penetration experiments

There are several studies which report application of confocal Raman microscopy (CRM) in determining the penetration of various ingredients into the skin, such as retinol (Failloux et al., 2004; Forster et al.,

578 2011; Mélot et al., 2009), dimethyl sulfoxide (Caspers et al., 2002), water (Caspers et al., 2000), urea
579 (Wascotte et al., 2007), 5-fluorouracil (Zhang et al., 2007) etc. Xiao et al. demonstrated the ability of
580 CRM to study and understand the penetration mechanism of phospholipids from liposomal formulations,
581 in pig skin (Xiao et al., 2005). Penetration of two liposomal formulations was tested, liposomes in gel
582 crystalline state were prepared from 1,2-dipalmitoyl (d62)-sn-glycero-3-phosphocholine (DPPC-d62),
583 while liposomes in liquid crystalline state were prepared from 1-palmitoyl(d31)-2-oleoyl-sn-glycero-3-
584 phosphocholine (P-d_{31}OPC). After the application of liposomes to pig skin, Raman spectra were
585 obtained using a CRM employing laser at 785nm and spectra were recorded in the region of 100 -
586 3450cm^{-1}. Exogenous phospholipids were monitored by observing the CD_2 and CD_3 stretching vibration
587 bands at 2080 and 2220cm^{-1} respectively, while the skin was monitored using the Phenylalanine-ring
588 breathing mode at 1004cm^{-1} and the amide-I band at 1652cm^{-1}. The results indicated that the liquid state
589 phospholipid P-d_{31}OPC penetrated 40-48µm deep into the skin as compared to the gel state phospholipid
590 DPPC-d_{62}, which was found to penetrate only 10-15µm deep.

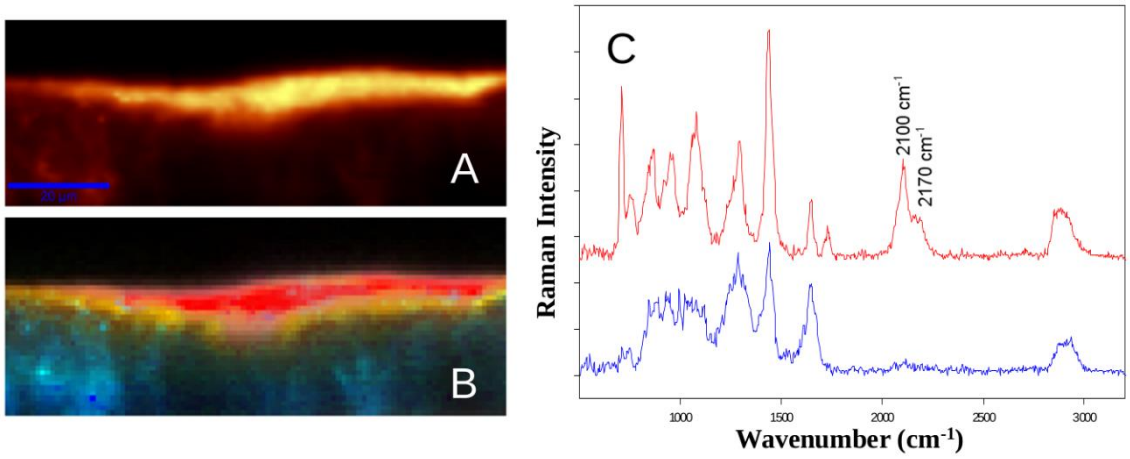

591

592 Figure-13: XZ-profiles recorded on a full thickness human skin treated with deuterated invasomes. (A) Raman
593 map generated by integrating C-H stretching intensities from 2800 - 3100 cm-1 (B) False color image showing
594 dissimilar spectral mixing. Red color represents highest C-D signal while blue represents signal from endogenous
595 skin tissue. (C)The red spectra on the right is representative of the applied P-d31OPC invasomes while blue spectra
596 representative of the skin. Peaks at 2100 and 2170 cm-1 represent C-D stretching vibrations. Scale bar = 20 µm.

597 We reported a method for recording depth profiles using CRM in excised human skin biopsies to study
598 diffusion patterns of drugs and components of the formulation system (Ashtikar et al., 2012). Figure-13
599 shows a XZ-penetration profile, where every pixel represents intensity of Raman signal obtained from
600 intact human skin treated with deuterated invasomes (P-d_{31}OPC). The depth profile scans (XZ-scans)
601 were collected using WITec Alpha 300R CRM. Excitation was provided by 785nm laser and step size
602 for collecting the depth profiles was 1µm with illumination time of 0.5sec/spectra. In Figure-13B,
603 penetration profile of deuterated phospholipid is plotted as a gradient from red to yellow, where red
604 color corresponds to the highest concentration of P-d_{31}OPC. The protein distribution of the skin is
605 plotted in blue. Spectra corresponding to the invasomes and stratum corneum are represented in Figure-

606 13C. Penetration profile was constructed using spectral unmixing algorithm, vertex component analysis,
607 which decomposes a given dataset into fractions of most dissimilar spectral information and reconstructs
608 the image by plotting their individual abundances (Du et al., 2008; Winter, 1999). P-d_{31}OPC penetrated
609 to a depth of ~10 to 15µm after application of flexible Invasomes, also it was interesting to note that the
610 penetration profile of the phospholipid was not uniform throughout the stratum corneum.

611 Retinol is a common ingredient of the anti-aging creams, which is highly lipophilic and does not
612 penetrate the skin very well. Raman microscopy is widely employed for studying penetration profiles
613 of retinol as it has a characteristic Raman peak at 1594cm^{-1}, which can easily be traced through the
614 various layers of the skin. In vitro penetration profile of retinol in human skin biopsies was studied by
615 Failloux et al. using CRM. They have reported that retinol penetrated the SC faster when it was applied
616 in the form of microspheres as compared to an oil in water emulsion (Failloux et al., 2004). Förster et
617 al. studied the penetration of retinol from various emulsions and also monitored penetration of oil and
618 aqueous components of the emulsion by using D(26)-n-dodacane and deuterated water respectively.
619 Their results show that retinol penetration from an emulsion depends on the nature of the surfactant used
620 and that an emulsified retinol can penetrate deeper in the skin, while micellar retinol is localized in the
621 SC (Forster et al., 2011). Mélot at al studied the effect of penetration enhancers to deliver retinol into
622 human skin in vivo. The in vivo measurements were carried out using an inverted Raman microscope
623 customized for fast in vivo spectral acquisition from volar forearm. Formulations containing penetration
624 enhancers like oleic acid, polyethylene glycol showed to have improved penetration of retinol into SC
625 after 6 hours of application time (Mélot et al., 2009).

626 Caspers et al. used CRM to study the interactions between human skin and dimethyl sulfoxide (DMSO)
627 in vivo (Caspers et al., 2002). DMSO shows strong C-S-C symmetric and asymmetric vibration modes
628 at 671 & 702 cm^{-1}, while the position of the microscope in the skin was determined using the natural
629 moisturizing factor to protein ratio (NMF, 885 & 1415 cm^{-1}). Authors reported that DMSO penetrated
630 the SC within 20 minutes, however traces of DMSO could be found in the SC even after 72 hours.
631 Caspers et al. also reported the use of CRM for monitoring in vivo water profiles in the SC. Water
632 content at various depths was determined by calculating the ratio of the water intensities (3350-3550cm^{-1}) and protein intensities (CH_3 stretching mode 2910-2965cm^{-1}). Chrit et al. also reported application of
634 CRM for in vitro and in vivo measurement of water in human skin, and they were able to demonstrate
635 the hydration efficiency of a cosmetic product containing hydrating polymers in microcapsules (Chrit et
636 al., 2007).

637 CRM was used to follow the penetration of metronidazole dissolved in diethylene glycol monoethyl
638 (Transcutol®, Gattefossé, France) in human skin (Tfayli et al., 2007). Metronidazole was tracked in the
639 skin by monitoring (υ C-N) stretching vibrations at 1191 cm^{-1} and 1369 cm^{-1}, while the skin proteins
640 were tracked from the amide-I, amide-III, Phenylalanine -ring breathing mode and other weaker spectral
641 features. Spectra were collected from full thickness skin 1 and 2 hours after the application of

metronidazole solution at different z-planes with 4µm steps. Maximum penetration depth achieved for metronidazole was ~25µm in the SC. Several changes were noted in the Raman shifts for C-H vibration bands associated with skin endogenous proteins and lipids. Zhang et al. took advantage of differences in the Raman spectra of 5-fluorouracil (5-FU) and the prodrug of 5-FU (1-ethoxycarbonyl-5-fluorouracil) to determine the spatial distribution and the transformation of prodrug to 5-FU in skin (Zhang et al., 2007).

5. Coherent Raman microscopy

In spontaneous Raman microscopy, images are recorded using the mapping mode where Raman spectra from each point on the sample is collected. Due to the inherent weak nature of the Raman scattering, acquisition of such images can take several hours. This is a problem for biological samples as they can undergo dehydration or photo damage due to high exposure to the intense laser radiation. Today several variants of Raman microscopy are available, such as, coherent anti-Stokes Raman scattering microscopy (CARS), stimulated Raman scattering microscopy (SRS), surface enhanced Raman scattering (SERS) etc., which have an advantage of higher S/N ratio. In this part, we would like to introduce CARS and SRS in brief with some examples of their application in transdermal delivery research, but it is out of scope of this book to go in depth into the principles and instrumentation of these techniques; further references can be found elsewhere (Chabay et al., 1976; Cheng, 2007; Eesley, 1981; Nandakumar et al., 2009; Scholten and Scholten, 1989; Scholten et al., 1989)

CARS and SRS are non-linear enhancement techniques, which enhance the weak Raman signal and as a result reduce the imaging duration to a few minutes or even seconds (Hanson and Bardeen, 2009). In both techniques the molecular vibrations are excited by using a Stokes and pump laser beams. CARS is a complex process in which three laser beams stokes (ω_s) pump (ω_p) and probe (ω_{pr}) interact with the sample to generate anti-stokes emission. When difference in the ω_s and ω_p frequencies approach the vibrational frequency of a molecular bond (ω_v), such that; $\omega_v = \omega_p - \omega_s$, the electrons in the electron cloud around the molecular bond are in the virtual excited vibrational state. Such vibrational excitations only take place in small focal volume where both stokes and pump beams are coherently in phase. To probe the virtual excitations, a third beam (ω_{pr}) is applied, which gets scattered off and generates anti-stokes radiation (ω_{as}) modulated at difference frequency such that, $\omega_{as} = \omega_{pr} + (\omega_p - \omega_s)$ (Min et al., 2011). The emitted photon is blue shifted and as a result can be easily separated from the incident laser beams. Due to the nature of the excitation source of CARS microscope, it also generates 2-photon fluorescence and second harmonic generation (SHG) signal, and a multimodal detection system could be employed to detect these signals (Le et al., 2007; Potma et al., 2001; Wang et al., 2008).

Capability to identify endogenous and exogenous components by a multimodal-imaging mode is demonstrated in Figure-14 which shows CARS, SHG and 2-photon fluorescence signals collected from a human skin cross section (Heuke et al., 2012). Figure-14a shows the anti-stokes Raman shifts recorded

for C-H stretching mode at 2850cm^{-1}, which are mainly generated by the intercellular lipids and adipocytes. Figure-14b shows the SHG signal, which is generated mainly from the collagen fibers of the dermis. Figure-14c shows 2-photon fluorescence detected at 435-485nm, and figure-14d shows a false color image generated by overlapping all the singals, where CARS signal is represented as green, SHG as white and two-photon fluorescence as red.

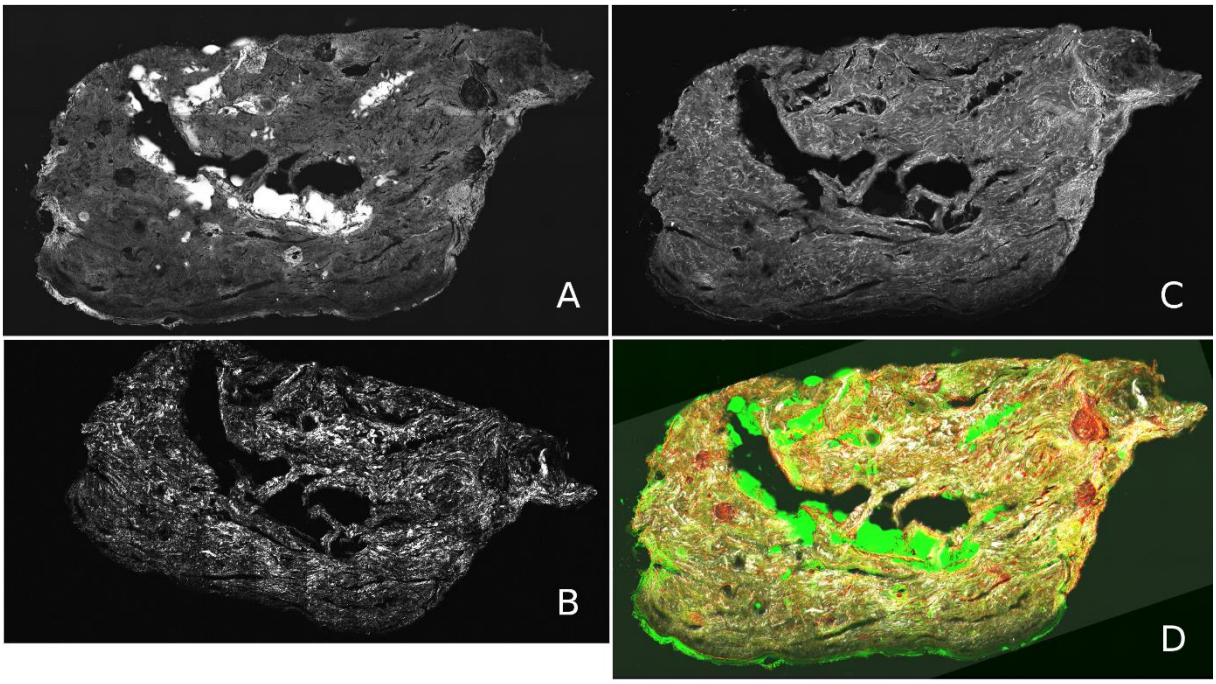

Figure-14: Multimodal CARS image of an untreated skin cross section to demonstrate the scope of multimodal microscopy. (A) CARS map for CH_2 symmetrical stretching vibrations (B) SHG image (C) two-photon fluorescence image (D) False color image showing overlap of CARS (green), SHG (white) and two-photon fluorescence (red) signals.

In vivo real-time video-rate epi-CARS (backscattered CARS) imaging was demonstrated by Evans et al. on anesthetized female mice (Evans et al., 2005). The excitation source was tuned in order to excite the CH_2 stretching vibrations and anti-Stokes photons were detected with the help of a sensitive PMT detector. The microscope had lateral resolution of 0.3µm and axial resolution of 1.5µm. Authors were able to image the mouse skin at various depth up to 100µm and identified lipid rich structures such as sebaceous glands and adipocytes. Real time diffusion of the topically applied mineral oil was also observed in the mouse skin. The mineral oil penetrated the SC within 20 minutes, however it remained confined to the viable epidermis and was not able to penetrate the dermis. Zimmerly et al. used CARS microscopy to generate quantitative concentration maps of deuterated water and d-glycine in human hair (Zimmerley et al., 2009), while Breunig et al. demonstrated application of in vivo multimodal CARS microscopy in healthy and diseased human skin (Breunig et al., 2012). In healthy human skin, they were able to follow a topically applied emulsion cream, while in skin affected with psoriasis they were able to identify differences in the SC intercellular lipid domains compared to the healthy skin.

CARS microscopy is more sensitive than spontaneous Raman microscopy; however, it has some drawbacks such as presence of non-resonant background and more importantly anti-Stokes shifts are slightly different from stokes Raman shifts, which makes spectral interpretation more complicated. In SRS, pump beam and stokes beam coincide the sample such that difference in the frequencies between Stokes and pump-beams matches a molecular vibration. This results in an increase in the rate of molecular vibrations. The energy required for this excitation is taken up from the pump laser field and as a result pump beam experiences loss in intensity (stimulated Raman loss). Stokes beam experiences a gain in intensity due to the emission of stokes photons as the molecular vibrations return to ground state (stimulated Raman gain). In SRS microscopy, either stimulated Raman loss or gain can be used as a contrast mechanism (Min et al., 2011; Nandakumar et al., 2009). Using SRS microscopy, Saar et al. were able to determine penetration profiles of ibuprofen and ketoprofen from solutions in propylene glycol applied topically onto mouse skin (Saar et al., 2011). Ketoprofen was tracked in the skin by following the aromatic C-H stretching vibrations at 1599 cm^{-1}, ibuprofen and propylene glycol were deuterated and were monitored at 2120cm^{-1}, while skin lipid architecture was imaged from CH_2 stretching vibrations at 2845cm^{-1}. Ketoprofen and propylene glycol penetrated the SC mainly via intercellular lipid pathways and through hair follicles. From time resolved images at various depths, the authors showed that propylene glycol penetrated deeper and faster than ketoprofen into the skin. In addition, penetration of propylene glycol via hair follicle was much faster and reached a steady state in less than 30 minutes compared to ~2 hours via intercellular lipid penetration in the SC to reach similar levels. Penetration profiles of ibuprofen were similar to that of ketoprofen. Ibuprofen crystals on the surface of the SC during penetration also indicated faster penetration of the solvent propylene glycol compared to ibuprofen. Freudiger et al. reported application of SRS microscopy to construct three dimensional diffusion profiles of DMSO and retinoic acid in mouse skin. From the diffusional profiles they were able to show that DMSO mainly penetrated the SC via the protein phase while retinoic acid penetrated mainly via the lipid rich intercellular spaces (Freudiger et al., 2008).

Coherent Raman microscopy is a label free and more sensitive approach of tapping into the advantages of Raman effect compared to the spontaneous Raman microscopy. Due to the enhancement of the Raman effect, the image acquisition is much faster and hence more suitable for biological samples compared to spontaneous Raman microscopy. Also the non-linear excitation approach in the generation of CARS and SRS signal is limited to a very small focal volume, which increases the resolution of these techniques without using the confocal detection setup. CARS and SRS microscopic techniques are relatively young compared to other techniques discussed here. Today these microscopes are mainly confined to the photonics labs; however, both the techniques hold a great promise for mainstream applications.

6. Conclusion

Microscopic techniques are very important in understanding the mechanisms involved in skin penetration as they enable spatial visualization of the drug in the skin. In this chapter we report almost 50 years of development in the microscopic techniques and at least today, no technique holds superiority in all the aspects of imaging such as resolution, signal quality, specificity, speed, sample preparation, sample stability etc. These are rather complementary techniques, which are able to provide a host of information according to the requirements and objectives of the experiments. For skin penetration experiments, 2-PFM was first to set high standards owing to its ability to acquire high-resolution optical biopsies, in vitro as well as in vivo. Raman microscopic techniques provide a unique opportunity for label free imaging. With development of modern Raman variants like CARS and SRS microscopy, signal to noise ratio has been greatly improved and high speed, label free, 3D imaging is now possible however complex nature of these microscopes and expensive optics have limited their wide spread application.

Acknowledgement:

Authors would like to acknowledge Prof. Dr. Benjamin Dietzek and Prof. Dr. Jürgen Popp from Institut für Photonische Technologien, Jena, Germany for their cooperation in acquiring multimodal CARS images on the human skin cross sections.

751 **References:**

752 Addicks WJ, Flynn GL, Weiner N. Validation of a flow-through diffusion cell for use in transdermal research.
753 Pharmaceutical Research. 1987 Aug;4(4):337-41

754 Agarwal R, Katare OP, Vyas SP. The pilosebaceous unit: a pivotal route for topical drug delivery. Methods Find
755 Exp Clin Pharmacol. 2000 Mar;22(2):129-33

756 Alvarez-Roman R, Naik A, Kalia YN, Guy RH, Fessi H. Skin penetration and distribution of polymeric
757 nanoparticles. J Control Release. 2004 Sep 14;99(1):53-62 doi:10.1016/j.jconrel.2004.06.015.

758 Ashtikar M, Matthäus C, Krafft C, Popp J, Fahr A. Non-invasive imaging of transdermal drug penetration profiles
759 using Raman microscopy. 9th International conference and workshop on Biological Barriers - in vitro and in silico
760 tools for drug delivery and nanosafety research; 29 Feb - 9 Mar 2012; Saarland University, Saarbrücken,
761 Germany2012.

762 Benfeldt E. In vivo microdialysis for the investigation of drug levels in the dermis and the effect of barrier
763 perturbation on cutaneous drug penetration. Studies in hairless rats and human subjects. Acta Derm Venereol Suppl
764 (Stockh). 1999;206:1-59

765 Betz G, Imboden R, Imanidis G. Interaction of liposome formulations with human skin in vitro. Int J Pharm. 2001
766 Oct 23;229(1-2):117-29

767 Bhatia KS, Singh J. Effect of linolenic acid/ethanol or limonene/ethanol and iontophoresis on the in vitro
768 percutaneous absorption of LHRH and ultrastructure of human epidermis. Int J Pharm. 1999 Apr 15;180(2):235-
769 50

770 Bohm M, Luger TA. The pilosebaceous unit is part of the skin immune system. Dermatology. 1998;196(1):75-9

771 Bouwstra JA, Honeywell-Nguyen PL. Skin structure and mode of action of vesicles. Adv Drug Deliv Rev. 2002
772 Nov 1;54 Suppl 1:S41-55

773 Breunig HG, Buckle R, Kellner-Hofer M, Weinigel M, Lademann J, Sterry W, et al. Combined in vivo multiphoton
774 and CARS imaging of healthy and disease-affected human skin. Microsc Res Tech. 2012 Apr;75(4):492-8
775 doi:10.1002/jemt.21082.

776 Carrer DC, Vermehren C, Bagatolli LA. Pig skin structure and transdermal delivery of liposomes: a two photon
777 microscopy study. J Control Release. 2008 Nov 24;132(1):12-20 doi:10.1016/j.jconrel.2008.08.006.

778 Caspers PJ, Lucassen GW, Bruining HA, Puppels GJ. Automated depth-scanning confocal Raman
779 microspectrometer for rapid in vivo determination of water concentration profiles in human skin. Journal of Raman
780 Spectroscopy. 2000;31(8-9):813-8 doi:10.1002/1097-4555(200008/09)31:8/9<813::AID-JRS573>3.0.CO;2-7.

781 Caspers PJ, Williams AC, Carter EA, Edwards HG, Barry BW, Bruining HA, et al. Monitoring the penetration
782 enhancer dimethyl sulfoxide in human stratum corneum in vivo by confocal Raman spectroscopy. Pharmaceutical
783 Research. 2002 Oct;19(10):1577-80

784 Chabay I, Klauminzer GK, Hudson BS. Coherent anti-Stokes Raman spectroscopy (CARS): Improved
785 experimental design and observation of new higher-order processes. Applied Physics Letters. 1976
786 01/01/;28(1):27-9

787 Chen M, Liu X, Fahr A. Skin delivery of ferulic acid from different vesicular systems. J Biomed Nanotechnol.
788 2010 Oct;6(5):577-85

789 Chen M, Liu X, Fahr A. Skin penetration and deposition of carboxyfluorescein and temoporfin from different lipid
790 vesicular systems: In vitro study with finite and infinite dosage application. Int J Pharm. 2011 Apr 15;408(1-
791 2):223-34 doi:10.1016/j.ijpharm.2011.02.006.

792 Cheng JX. Coherent anti-Stokes Raman scattering microscopy. Appl Spectrosc. 2007 Sep;61(9):197-208

793 Chrit L, Bastien P, Biatry B, Simonnet JT, Potter A, Minondo AM, et al. In vitro and in vivo confocal Raman
794 study of human skin hydration: assessment of a new moisturizing agent, pMPC. Biopolymers. 2007
795 Mar;85(4):359-69 doi:10.1002/bip.20644.

796 Dragicevic-Curic N, Grafe S, Albrecht V, Fahr A. Topical application of temoporfin-loaded invasomes for
797 photodynamic therapy of subcutaneously implanted tumours in mice: a pilot study. J Photochem Photobiol B. 2008
798 Apr 25;91(1):41-50 doi:10.1016/j.jphotobiol.2008.01.009.

Dragicevic-Curic N, Scheglmann D, Albrecht V, Fahr A. Development of different temoporfin-loaded invasomes-novel nanocarriers of temoporfin: characterization, stability and in vitro skin penetration studies. Colloids Surf B Biointerfaces. 2009 May 1;70(2):198-206 doi:10.1016/j.colsurfb.2008.12.030.

du Plessis J, Ramachandran C, Weiner N, Müller DG. The influence of particle size of liposomes on the deposition of drug into skin. International Journal of Pharmaceutics. 1994 3/30/;103(3):277-82 doi:10.1016/0378-5173(94)90178-3.

Du Q, Raksuntorn N, Younan NH, King RL. End-member extraction for hyperspectral image analysis. Appl Opt. 2008 10/01;47(28):F77-F84

Dunn KW, Young PA. Principles of Multiphoton Microscopy. Nephron Experimental Nephrology. 2006;103(2):e33-e40

Eesley GL. Coherent Raman spectroscopy / G. L. Eesley. Oxford ; New York :: Pergamon Press; 1981.

Evans CL, Potma EO, Puoris'haag M, Cote D, Lin CP, Xie XS. Chemical imaging of tissue in vivo with video-rate coherent anti-Stokes Raman scattering microscopy. Proc Natl Acad Sci U S A. 2005 Nov 15;102(46):16807-12 doi:10.1073/pnas.0508282102.

Failloux N, Baron MH, Abdul-Malak N, Perrier E. Contribution of encapsulation on the biodisponibility of retinol. Int J Cosmet Sci. 2004 Apr;26(2):71-7 doi:10.1111/j.0412-5463.2004.00206.x.

Fang JY, Hsu LR, Huang YB, Tsai YH. Evaluation of transdermal iontophoresis of enoxacin from polymer formulations: in vitro skin permeation and in vivo microdialysis using Wistar rat as an animal model. Int J Pharm. 1999 Apr 15;180(2):137-49

Forster M, Bolzinger MA, Ach D, Montagnac G, Briancon S. Ingredients tracking of cosmetic formulations in the skin: a confocal Raman microscopy investigation. Pharmaceutical Research. 2011 Apr;28(4):858-72 doi:10.1007/s11095-010-0342-0.

Freudiger CW, Min W, Saar BG, Lu S, Holtom GR, He C, et al. Label-free biomedical imaging with high sensitivity by stimulated Raman scattering microscopy. Science. 2008 Dec 19;322(5909):1857-61 doi:10.1126/science.1165758.

Grams YY, Alaruikka S, Lashley L, Caussin J, Whitehead L, Bouwstra JA. Permeant lipophilicity and vehicle composition influence accumulation of dyes in hair follicles of human skin. Eur J Pharm Sci. 2003 Apr;18(5):329-36

Grams YY, Whitehead L, Cornwell P, Bouwstra JA. Time and depth resolved visualisation of the diffusion of a lipophilic dye into the hair follicle of fresh unfixed human scalp skin. J Control Release. 2004 Aug 27;98(3):367-78 doi:10.1016/j.jconrel.2004.05.010.

Hanson KM, Bardeen CJ. Application of nonlinear optical microscopy for imaging skin. Photochem Photobiol. 2009 Jan-Feb;85(1):33-44 doi:10.1111/j.1751-1097.2008.00508.x.

Hashimoto K, Kagetsu N, Taniguchi Y, Weintraub R, Chapman-Winokur RL, Kasiborski A. Immunohistochemistry and electron microscopy in Langerhans cell histiocytosis confined to the skin. J Am Acad Dermatol. 1991 Dec;25(6 Pt 1):1044-53

Heuke S, Ashtikar M, Matthäus C, Fahr A, Dietzek B, Popp J. Unpublished Work: Coherent anti-stokes Raman scattering microscopy of human skin. 2012.

Hofland HE, van der Geest R, Bodde HE, Junginger HE, Bouwstra JA. Estradiol permeation from nonionic surfactant vesicles through human stratum corneum in vitro. Pharm Res. 1994 May;11(5):659-64

Hofland HE, Bouwstra JA, Bodde HE, Spies F, Junginger HE. Interactions between liposomes and human stratum corneum in vitro: freeze fracture electron microscopical visualization and small angle X-ray scattering studies. Br J Dermatol. 1995 Jun;132(6):853-66

Hollricher O. Raman Instrumentation for Confocal Raman Microscopy. In: Dieing T, Hollricher O, Toporski J, editors. Confocal Raman Microscopy. Springer Series in Optical Sciences. 158: Springer Berlin Heidelberg; 2011. p. 43-60.

Hollricher O, Ibach W. High-Resolution Optical and Confocal Microscopy. In: Dieing T, Hollricher O, Toporski J, editors. Confocal Raman Microscopy. Springer Series in Optical Sciences. 158: Springer Berlin Heidelberg; 2011. p. 1-20.

Jimbo Y, Ishihara M, Osamura H, Takano M, Ohara M. Influence of vehicles on penetration through human epidermis of benzyl alcohol, isoeugenol and methyl isoeugenol. J Dermatol. 1983 Jun;10(3):241-50

Kanerva L. Electron microscopy of the effects of dithranol on healthy and on psoriatic skin. Am J Dermatopathol. 1990 Feb;12(1):51-62

Kirjavainen M, Urtti A, Jaaskelainen I, Suhonen TM, Paronen P, Valjakka-Koskela R, et al. Interaction of liposomes with human skin in vitro--the influence of lipid composition and structure. Biochim Biophys Acta. 1996 Dec 13;1304(3):179-89

Kirjavainen M, Urtti A, Monkkonen J, Hirvonen J. Influence of lipids on the mannitol flux during transdermal iontophoresis in vitro. Eur J Pharm Sci. 2000 Apr;10(2):97-102

Kobayashi D, Matsuzawa T, Sugibayashi K, Morimoto Y, Kimura M. Analysis of the combined effect of 1-menthol and ethanol as skin permeation enhancers based on a two-layer skin model. Pharmaceutical Research. 1994 Jan;11(1):96-103

Konig K, Ehlers A, Stracke F, Riemann I. In vivo drug screening in human skin using femtosecond laser multiphoton tomography. Skin Pharmacol Physiol. 2006;19(2):78-88 doi:10.1159/000091974.

Kriwet K, Müller-Goymann CC. Diclofenac release from phospholipid drug systems and permeation through excised human stratum corneum. International Journal of Pharmaceutics. 1995 10/31/;125(2):231-42 doi:10.1016/0378-5173(95)00130-B.

Le TT, Langohr IM, Locker MJ, Sturek M, Cheng JX. Label-free molecular imaging of atherosclerotic lesions using multimodal nonlinear optical microscopy. J Biomed Opt. 2007 Sep-Oct;12(5):054007 doi:10.1117/1.2795437.

Lieb LM, Ramachandran C, Egbaria K, Weiner N. Topical delivery enhancement with multilamellar liposomes into pilosebaceous units: I. In vitro evaluation using fluorescent techniques with the hamster ear model. J Invest Dermatol. 1992 Jul;99(1):108-13

Loftsson T, Somogyi G, Bodor N. Effect of choline esters and oleic acid on the penetration of acyclovir, estradiol, hydrocortisone, nitroglycerin, retinoic acid and trifluorothymidine across hairless mouse skin in vitro. Acta Pharm Nord. 1989;1(5):279-86

Mélot M, Pudney PDA, Williamson A-M, Caspers PJ, Van Der Pol A, Puppels GJ. Studying the effectiveness of penetration enhancers to deliver retinol through the stratum cornum by in vivo confocal Raman spectroscopy. Journal of Controlled Release. 2009 8/19/;138(1):32-9 doi:10.1016/j.jconrel.2009.04.023.

Min W, Freudiger CW, Lu S, Xie XS. Coherent nonlinear optical imaging: beyond fluorescence microscopy. Annu Rev Phys Chem. 2011;62:507-30 doi:10.1146/annurev.physchem.012809.103512.

Murakami T, Yoshioka M, Yumoto R, Higashi Y, Shigeki S, Ikuta Y, et al. Topical delivery of keloid therapeutic drug, tranilast, by combined use of oleic acid and propylene glycol as a penetration enhancer: evaluation by skin microdialysis in rats. J Pharm Pharmacol. 1998 Jan;50(1):49-54

Nandakumar P, Kovalev A, Volkmer A. Vibrational imaging based on stimulated Raman scattering microscopy. New Journal of Physics. 2009;11(3):033026

Niemiec SM, Ramachandran C, Weiner N. Influence of nonionic liposomal composition on topical delivery of peptide drugs into pilosebaceous units: an in vivo study using the hamster ear model. Pharmaceutical Research. 1995 Aug;12(8):1184-8

Ntimenou V, Fahr A, Antimisiaris SG. Elastic vesicles for transdermal drug delivery of hydrophilic drugs: a comparison of important physicochemical characteristics of different vesicle types. J Biomed Nanotechnol. 2012 Aug;8(4):613-23

Nwaneshiudu A, Kuschal C, Sakamoto FH, Anderson RR, Schwarzenberger K, Young RC. Introduction to confocal microscopy. J Invest Dermatol. 2012 Dec;132(12):e3 doi:10.1038/jid.2012.429.

Patzelt A, Richter H, Knorr F, Schäfer U, Lehr C-M, Dähne L, et al. Selective follicular targeting by modification of the particle sizes. Journal of Controlled Release. 2011 2/28/;150(1):45-8 doi:http://dx.doi.org/10.1016/j.jconrel.2010.11.015.

Potma EO, de Boeij WP, van Haastert PJM, Wiersma DA. Real-time visualization of intracellular hydrodynamics in single living cells. Proceedings of the National Academy of Sciences. 2001 February 13, 2001;98(4):1577-82 doi:10.1073/pnas.98.4.1577.

Raman C, Krishnan K. A new type of secondary radiation. Nature. 1928;121(3048):501-2 doi:doi:10.1038/121501c0.

900 Saar BG, Contreras-Rojas LR, Xie XS, Guy RH. Imaging drug delivery to skin with stimulated Raman scattering
901 microscopy. Mol Pharm. 2011 Jun 6;8(3):969-75 doi:10.1021/mp200122w.

902 Schatzlein A, Cevc G. Non-uniform cellular packing of the stratum corneum and permeability barrier function of
903 intact skin: a high-resolution confocal laser scanning microscopy study using highly deformable vesicles
904 (Transfersomes). Br J Dermatol. 1998 Apr;138(4):583-92

905 Schenke-Layland K, Riemann I, Damour O, Stock UA, Konig K. Two-photon microscopes and in vivo
906 multiphoton tomographs--powerful diagnostic tools for tissue engineering and drug delivery. Adv Drug Deliv Rev.
907 2006 Sep 15;58(7):878-96 doi:10.1016/j.addr.2006.07.004.

908 Schnetz E, Fartasch M. Microdialysis for the evaluation of penetration through the human skin barrier - a promising
909 tool for future research? Eur J Pharm Sci. 2001 Jan;12(3):165-74

910 Scholten T, Scholten TAHM. Coherent Anti-stokes Raman Scattering (CARS): Technique and Application to
911 Biophysical Studies ; the Potentials of CARS Microscopy1989.

912 Scholten TA, Lucassen GW, De Mul FF, Greve J. Nonresonant background suppression in CARS spectra of
913 dispersive media using phase mismatching. Appl Opt. 1989 Apr 1;28(7):1387-400 doi:10.1364/ao.28.001387.

914 Schreiner V, Gooris GS, Pfeiffer S, Lanzendorfer G, Wenck H, Diembeck W, et al. Barrier characteristics of
915 different human skin types investigated with X-ray diffraction, lipid analysis, and electron microscopy imaging. J
916 Invest Dermatol. 2000 Apr;114(4):654-60 doi:10.1046/j.1523-1747.2000.00941.x.

917 Semwogerere D, Weeks ER. Confocal Microscopy. Encyclopedia of Biomaterials and Biomedical Engineering:
918 Informa Healthcare; 2008. p. 705-14.

919 Simonetti O, Hoogstraate AJ, Bialik W, Kempenaar JA, Schrijvers AH, Bodde HE, et al. Visualization of diffusion
920 pathways across the stratum corneum of native and in-vitro-reconstructed epidermis by confocal laser scanning
921 microscopy. Arch Dermatol Res. 1995;287(5):465-73

922 Tenjarla SN, Kasina R, Puranajoti P, Omar MS, Harris WT. Synthesis and evaluation of N-acetylprolinate esters
923 - novel skin penetration enhancers. Int J Pharm. 1999 Dec 10;192(2):147-58

924 Tfayli A, Piot O, Pitre F, Manfait M. Follow-up of drug permeation through excised human skin with confocal
925 Raman microspectroscopy. Eur Biophys J. 2007 Nov;36(8):1049-58 doi:10.1007/s00249-007-0191-x.

926 Touitou E, Godin B, Dayan N, Weiss C, Piliponsky A, Levi-Schaffer F. Intracellular delivery mediated by an
927 ethosomal carrier. Biomaterials. 2001 Nov;22(22):3053-9

928 Turner NG, Guy RH. Visualization and quantitation of iontophoretic pathways using confocal microscopy. J
929 Investig Dermatol Symp Proc. 1998 Aug;3(2):136-42

930 van den Bergh BA, Vroom J, Gerritsen H, Junginger HE, Bouwstra JA. Interactions of elastic and rigid vesicles
931 with human skin in vitro: electron microscopy and two-photon excitation microscopy. Biochim Biophys Acta.
932 1999 Nov 9;1461(1):155-73

933 van Kuijk-Meuwissen ME, Junginger HE, Bouwstra JA. Interactions between liposomes and human skin in vitro,
934 a confocal laser scanning microscopy study. Biochim Biophys Acta. 1998 Apr 22;1371(1):31-9

935 van Kuijk-Meuwissen ME, Mougin L, Junginger HE, Bouwstra JA. Application of vesicles to rat skin in vivo: a
936 confocal laser scanning microscopy study. J Control Release. 1998 Dec 4;56(1-3):189-96

937 Vardaxis NJ, Brans TA, Boon ME, Kreis RW, Marres LM. Confocal laser scanning microscopy of porcine skin:
938 implications for human wound healing studies. J Anat. 1997 May;190 (Pt 4):601-11

939 Veiro JA, Cummins PG. Imaging of skin epidermis from various origins using confocal laser scanning microscopy.
940 Dermatology. 1994;189(1):16-22

941 Verma D. Invasomes - Novel vesicular carriers for enhanced topical delivery: characterization and skin penetration
942 properties. Marburg: Philipps-Universität Marburg; 2002.

943 Verma DD, Verma S, Blume G, Fahr A. Particle size of liposomes influences dermal delivery of substances into
944 skin. Int J Pharm. 2003 Jun 4;258(1-2):141-51

945 Verma DD, Verma S, Blume G, Fahr A. Liposomes increase skin penetration of entrapped and non-entrapped
946 hydrophilic substances into human skin: a skin penetration and confocal laser scanning microscopy study. Eur J
947 Pharm Biopharm. 2003 May;55(3):271-7

948 Verma DD, Fahr A. Synergistic penetration enhancement effect of ethanol and phospholipids on the topical
949 delivery of cyclosporin A. J Control Release. 2004 May 31;97(1):55-66 doi:10.1016/j.jconrel.2004.02.028.

950 Verma DD, Verma S, McElwee KJ, Freyschmidt-Paul P, Hoffmann R, Fahr A. Treatment of alopecia areata in the
951 DEBR model using cyclosporin A lipid vesicles. Euro J of Dermatology. 2004;14(5):1-7

952 Wang HW, Le TT, Cheng JX. Label-free Imaging of Arterial Cells and Extracellular Matrix Using a Multimodal
953 CARS Microscope. Opt Commun. 2008 Apr 1;281(7):1813-22 doi:10.1016/j.optcom.2007.07.067.

954 Wascotte V, Caspers P, de Sterke J, Jadoul M, Guy RH, Preat V. Assessment of the "skin reservoir" of urea by
955 confocal Raman microspectroscopy and reverse iontophoresis in vivo. Pharm Res. 2007 Oct;24(10):1897-901
956 doi:10.1007/s11095-007-9314-4.

957 Winter ME. N-FINDR: an algorithm for fast autonomous spectral end-member determination in hyperspectral
958 data. 1999:266-75 doi:10.1117/12.366289.

959 Xiao C, Moore DJ, Rerek ME, Flach CR, Mendelsohn R. Feasibility of tracking phospholipid permeation into skin
960 using infrared and Raman microscopic imaging. J Invest Dermatol. 2005 Mar;124(3):622-32 doi:10.1111/j.0022-
961 202X.2004.23608.x.

962 Yarosh D, Bucana C, Cox P, Alas L, Kibitel J, Kripke M. Localization of liposomes containing a DNA repair
963 enzyme in murine skin. J Invest Dermatol. 1994 Oct;103(4):461-8

964 Yu B, Kim KH, So PT, Blankschtein D, Langer R. Visualization of oleic acid-induced transdermal diffusion
965 pathways using two-photon fluorescence microscopy. J Invest Dermatol. 2003 Mar;120(3):448-55
966 doi:10.1046/j.1523-1747.2003.12061.x.

967 Zellmer S, Reissig D, Lasch J. Reconstructed human skin as model for liposome-skin interaction. J Control
968 Release. 1998 Nov 13;55(2-3):271-9

969 Zhang G, Moore DJ, Sloan KB, Flach CR, Mendelsohn R. Imaging the prodrug-to-drug transformation of a 5-
970 fluorouracil derivative in skin by confocal Raman microscopy. J Invest Dermatol. 2007 May;127(5):1205-9
971 doi:10.1038/sj.jid.5700690.

972 Zimmerley M, Lin C-Y, Oertel DC, Marsh JM, Ward JL, Potma EO. Quantitative detection of chemical
973 compounds in human hair with coherent anti-Stokes Raman scattering microscopy. Journal of Biomedical Optics.
974 2009;14(4):044019- doi:10.1117/1.3184444.

975

3.2 Publication-2

Non-invasive depth profile imaging of the stratum corneum using confocal Raman microscopy: First insights into the method

Mukul Ashtikar, Christian Matthäus, Michael Schmitt, Christoph Krafft, Alfred Fahr, Jürgen Popp

European Journal of Pharmaceutical Sciences, Vol 50 (2013) 601-608.

Published on 10th June 2013.

European Journal of Pharmaceutical Sciences 50 (2013) 601–608

Contents lists available at SciVerse ScienceDirect

European Journal of Pharmaceutical Sciences

journal homepage: www.elsevier.com/locate/ejps

Non-invasive depth profile imaging of the stratum corneum using confocal Raman microscopy: First insights into the method

Mukul Ashtikar [a,*,1], Christian Matthäus [b,1], Michael Schmitt [c], Christoph Krafft [b,c], Alfred Fahr [a], Jürgen Popp [b,c]

[a] Friedrich-Schiller-Universität Jena, Institut für Pharmazie, Lehrstuhl für Pharmazeutische Technologie, Lessingstraße 8, 07743 Jena, Germany
[b] Institut für Photonische Technologien e.V., Albert-Einstein-straße 9, 07745 Jena, Germany
[c] Institut für Physikalische Chemie und Abbe Center für Photonik, Friedrich-Schiller-Universität Jena, Helmholtzweg 4, 07743 Jena, Germany

ARTICLE INFO

Article history:
Received 22 February 2013
Received in revised form 21 May 2013
Accepted 31 May 2013
Available online 10 June 2013

Keywords:
Stratum corneum
Skin penetration
Confocal Raman microscopy
Vertex component analysis
Deuterated water
Beta-carotene

ABSTRACT

The stratum corneum is a strong barrier that must be overcome to achieve successful transdermal delivery of a pharmaceutical agent. Many strategies have been developed to enhance the permeation through this barrier. Traditionally, drug penetration through the stratum corneum is evaluated by employing tape-stripping protocols and measuring the content of the analyte. Although effective, this method cannot provide a detailed information regarding the penetration pathways. To address this issue various microscopic techniques have been employed. Raman microscopy offers the advantage of label free imaging and provides spectral information regarding the chemical integrity of the drug as well as the tissue. In this paper we present a relatively simple method to obtain XZ-Raman profiles of human stratum corneum using confocal Raman microscopy on intact full thickness skin biopsies. The spectral datasets were analysed using a spectral unmixing algorithm. The spectral information obtained, highlights the different components of the tissue and the presence of drug. We present Raman images of untreated skin and diffusion patterns for deuterated water and beta-carotene after Franz-cell diffusion experiment.

1. Introduction

Trans-dermal drug delivery has received considerable attention over the past decade. Apart from being used in the treatment of skin diseases, trans-dermal delivery can be a good alternative to deliver drugs systemically, as skin offers a large surface area to which drugs can be applied. The non-invasive nature of the application, high patient compliance, controlled release kinetics of the drug etc. are some of the advantages, which make transdermal application an attractive route for drug administration. A major hurdle in achieving this is, however, the low permeability of the skin and especially of the stratum corneum (Walters and Brain, 2002; Walters and Roberts, 2002). One of the most important functions of the skin is to protect the organism against detrimental effects of the environment; for this purpose stratum corneum has evolved into a very tight barrier, which has proven difficult to overcome. First generation transdermal delivery systems such as creams, gels and patches have been successfully employed to deliver drugs such as ibuprofen (Ibuleve®), fentanyl (Duragesic®), nicotine (Nicotinell®). However application of these systems has only been successful for a limited number of drugs; traditional delivery systems do not readily cross the stratum corneum and skin permeation was found to be dependent upon the drug's physiochemical properties like lipophilicity, molecular weight and molecular shape (Grice et al., 2010). Recently, 2nd and 3rd generation delivery systems were developed involving modification of the barrier properties of the stratum corneum by means of chemical penetration enhancers, iontophoresis, microneedles, laser ablation etc. (Prausnitz and Langer, 2008).

The stratum corneum is a 10–20 μm thick tightly packed layer of flattened cells, called corneocytes, originating from keratinocytes in the stratum basale, i.e., the bottom layer of the epidermis. Intercellular spaces are filled with laterally packed lamellar lipid domains (Bouwstra et al., 1991) and play an essential role in the barrier function but also provide a pathway through which drug molecules may diffuse during the transdermal delivery. The traditional method of studying skin penetration is by tape stripping, where layers of SC are progressively removed and the drug is quantified by analytical methods such as UV spectroscopy, fluorescence spectroscopy, and radioactivity measurement (Breternitz et al., 2007; Pinkus, 1951). Although a very powerful technique, tape stripping is an invasive technique. In addition, tape stripping is not an ideal technique for studying penetration pathways of the drug within the SC over several time points. Microscopic

* Corresponding author.
E-mail address: mashtikar@gmail.com (M. Ashtikar).
[1] These authors contributed equally to this work.

0928-0987/$ - see front matter © 2013 Elsevier B.V. All rights reserved.
http://dx.doi.org/10.1016/j.ejps.2013.05.030

techniques such as confocal laser scanning microscopy (Alvarez-Roman et al., 2004; Fink-Puches et al., 1995; Schatzlein and Cevc, 1998; Verma et al., 2003a), two-photon fluorescence microscopy (Carrer et al., 2008; Schenke-Layland et al., 2006; van den Bergh et al., 1999; Yu et al., 2003) have been exploited for studying the detailed spatial distribution in the SC. A major drawback of both techniques is that they rely on a fluorescent signal limiting the method to fluorescent or fluorescently labelled drugs. Also the attachment of a fluorescent label to the drug might affect its diffusion profile.

Raman microscopy is commonly used to study the biological composition of especially diseased tissues and has been applied to tissue biopsies of virtually every organ (Krafft et al., 2009). Raman microscopy as well as the complementary infra-red (IR) microscopy have been utilised to image skin cross sections. Raman spectroscopy has also been employed to study the penetration of caffeine (Franzen et al., 2012) and anti-oxidants (Uragami et al., 2012). Confocal Raman microscopy provides a useful depth profiling technique as it allows label free imaging (Baia et al., 2002; Schmitt et al., 2003). The obtained spectral information allows imaging the distribution of substances or tissue features based on their chemical composition. Apart from penetration depth, the spectral information could be useful to identify chemical integrity (Zhang et al., 2007), hydration state (Chrit et al., 2007), oxidative stress (Ermakov et al., 2004) and the ability to individually track various ingredients of a formulation (Xiao et al., 2005). In Raman microscopy, the penetration depth of the excitation light strongly depends on the wavelength of the employed laser. Best penetration depths for biological samples are usually achieved in the near infra-red (NIR). Shorter wavelengths are scattered stronger, the intensity of the scattered light being proportional to the fourth power of the frequency. For longer wavelengths the absorption of water becomes a major problem. In this study, we employed a laser excitation source of 785 nm at constant laser intensity for imaging stratum corneum and the upper layers of the viable epidermis.

Information on intradermal water distribution is relevant as water is a natural carrier for hydrophilic compounds. Beta-carotene is of interest for dermatological applications as it has been suggested to reduce oxidative stresses in the skin related to ultraviolet and infra-red irradiation (Darvin et al., 2011; Stahl and Sies, 2012). Treatment with beta-carotene has also been shown to reduce skin carcinogenesis and is also indicated in the treatment of erythropoietic protoporphyria (Bayerl, 2008). Beta-carotene is often chosen as an example derivative of the carotenoid family, because it exhibits interesting resonance Raman properties. Due to the resonance effects the sensitivity of the Raman measurements is enhanced by several orders of magnitude. Measurements including quantification of β-carotene using resonance Raman effects are well established (Darvin et al., 2012; Ermakov and Gellermann, 2012). Our study provides a relatively simple methodology to non-invasively image the SC for distribution of deuterated water and beta-carotene, following transdermal application.

2. Methods

2.1. Materials

Beta-carotene and dimethyl sulfoxide (DMSO) were purchased from Sigma–Aldrich (Germany). Deuterated water was purchased from Dr. Glaser AG (Basel, Switzerland). Salts used in the preparation of phosphate-buffered saline (PBS), di-sodium hydrogen phosphate, potassium dihydrogen phosphate, sodium chloride and potassium chloride, were purchased from Merck KGaA (Darmstadt, Germany). Mayer's acidic Haemalaun solution and congo red used for staining the cryo-sections of the skin were purchased from Carl Roth GmbH (Germany) and Fluka (Germany) respectively. Euparal used for mounting the sections was purchased from Carl Roth GmbH (Germany). Calcium fluoride slides used for mounting skin cross sections were obtained from Crystal GmbH (Berlin, Germany).

2.2. Human skin preparation

Human skin used in the experiments was obtained from the plastic surgery clinic (Praxisklinik für Plastische Chirurgie, Kassel, Germany) after abdominoplasty. Abdominal skin from a 44-year old Caucasian female was used for all experiments. Immediately following surgery, subcutaneous fat was removed from the dermis with a scalpel and the stratum corneum was cleaned using cotton balls and purified water. Skin was then cut into suitably sized pieces and stored at −26 °C. All the experiments were performed within one year of freezing the skin. Written consent from the patient was obtained before operation for using the excised skin for experiments. The whole process of obtaining skin tissue was approved by the Ethics committee of the University Hospital Jena, Germany.

2.3. Franz-cell experiments

Frozen skin was punched to obtain 30-mm diameter discs which were thawed to room temperature on a Whatman filter paper pre-soaked in PBS. Skin penetration experiments were performed on non-jacketed Franz-cells with a diffusion area of 1.76 cm^2. Temperature of the penetration experiment was controlled by placing the entire Franz-cell assembly in an incubator maintained at 32 °C. In diffusion experiments of deuterated water, 85 $\mu l/cm^2$ of deuterated water was applied to the skin. Due to very poor solubility of beta-carotene in polar solvents, 2.7 mg/ml solutions were prepared in DMSO and 100 $\mu l/cm^2$ of the solution was applied to the skin. Beta-carotene solution was applied to the skin without occlusion. Application of deuterated water was occlusive, the donor compartment of the Franz-cell was covered with Parafilm® to avoid evaporation of deuterated water. After 14 h, the applied substance was removed by repeated, gentle washing of the surface of the skin with purified water upon which the skin was dried with lint-free tissue paper.

2.4. Sample preparation for acquiring XZ-Raman profiles

Sample preparation method was inspired from the Saarbrücken penetration model, originally developed by Loth et al. at the Saarland University, Germany (Blasius, 1985; Borchert, 1994; Hailer, 1981; Wagner et al., 2000). After incubation on the Franz cell, the skin was mounted onto a specially designed aluminium block (tape stripping block) with a central cavity as shown in Fig. 1. The skin was fixed onto the cork discs in the central cavity of the aluminium block with eight stainless steel pins. Sample stability during the Raman imaging was a major concern and sample preparation was optimised so as to minimise the dehydration of the skin. The top most cork disc was covered with aluminium foil to prevent the cork from absorbing water from the skin. In addition, a thin layer of Vaseline was applied on the top cork disc to ensure that moisture did not escape from any cracks or crevices around the cork discs and a Whatman filter paper soaked in PBS was kept under the skin in order to prevent drying of the skin. To minimise exposure of the skin to the environment, an insulating adhesive tape (TESA, Germany) was used as a mask with a 1-cm diameter hole exposing enough skin to perform Raman imaging (Fig. 1B).

Fig. 1. (A) schematic representation of the sample used for acquiring Raman spectral maps. (B) Top view of the sample.

2.5. Cryo-sectioning and Staining

After the diffusion experiment, skin was frozen in liquid nitrogen and 20-μm thick sections were cut with a Reichert-Jung Frigocut-2000 microtome (Germany). Sections were mounted alternately on calcium fluoride slides for Raman mapping and on glass slides for staining. Sections were mounted alternately because during the staining and dehydration processes the sections mounted on calcium fluoride are at risk of being detached. Sections were stained using Mayer's Haemalaun (acidic) and congo red solutions for 7 and 5 min respectively, dehydrated, mounted in euparal and examined using a Leica DMRXP light microscope.

2.6. Raman data acquisition

Raman spectra were acquired using a WITec (Ulm, Germany) Model CRM Alpha-300Rplus confocal Raman microscope. Excitation (approximately 10 mW at the sample) was provided by a 785-nm diode laser (Melles Griot, Carlsbad, CA; Model 532). The exciting laser radiation was coupled to a Zeiss microscope through a wavelength-specific single mode optical fibre. The incident laser beam was collimated *via* an achromatic lens and passed a holographic band pass filter before it was focused onto the sample through the objective of the microscope. A Zeiss 50×/0.9 NA objective was used in the studies reported here. The sample was scanned using a piezo-electrically driven microscope scanning stage with an *x*,*y*-resolution of about 3 nm and a repeatability of ±5 nm, and *z*-resolution of about 0.3 nm and ±2 nm repeatability. The sample was scanned through the laser focus in a continuous line scan at a constant stage speed of fractions of a micrometer per second. Depth profiles were collected employing an *x*,*z*-scan modus starting at the bottom of the image. Spectra were collected with a 1-μm step size and an illumination time of 0.25 s, using a 300/mm grating. The spectral resolution was about 6 cm^{-1} and the spectral window ranged from 300 to 3200 cm^{-1}.

2.7. Image analysis and data processing

Various algorithms for image analysis of hyperspectral datasets have been developed. For extracting spectral information, several factor methods such as principle component analysis (PCA) or vector component analysis (VCA) have shown high potential for the evaluation of Raman datasets (Hedegaard et al., 2011; Miljković et al., 2010). In-house developed spectral unmixing algorithms were used for performing VCA and PCA on the Raman datasets. In principle, these algorithms searched for a basis that describe the spectral variance optimally. Generally, the spectrum of a given image pixel was assumed to be a linear combination of the spectra of individual components:

$$p_{ij} = \sum_k e_{ik} c_{kj},$$

where p_{ij} is the *i*th band of the *j*th pixel, e_{ik} the *i*th band of the *k*th component spectrum and c_{kj} is the mixing proportion for the *j*th pixel of the *k*th component. The mixing proportions were assumed to be percentages and the proportions should add up to one:

$$\sum_k c_{kj} = 1.$$

This new basis then consisted of a few vectors, or in our case Raman spectra, which were used to reconstruct the dataset or image by plotting their individual abundances. The different algorithms varied mainly in what constraints were set for this change of basis. In PCA, for instance, the vectors have to be orthogonal. In VCA the constraint is that the new vectors, usually referred to as endmembers, have to be all positive or real spectra. These endmembers normally represent the most dissimilar spectra within a dataset. For the evaluation of the endmembers an N-FINDR algorithm was employed (Du et al., 2008; Winter, 1999).

3. Results

3.1. Untreated skin

Fig. 2A shows a stained cross section of a human skin sample. The stratum corneum is clearly discernible as the top 20 μm of the cross section. The viable epidermis underneath it consists of a dense cell layer of approximately 50 μm and appears in dark blue. The underlying dermis is mainly composed of connective tissue, i.e. collagen and elastin and has a lower cell density. Fig. 2B is a Raman image of an adjacent 50 × 50 μm^2 cross section of the area indicated in a box in Fig. 2A. The image was generated by integrating the intensities of the C—H stretching vibrations between 2800 and 3100 cm^{-1}, which are predominant for most organic samples. The image mainly reflects a density profile of the tissue. However, very high intensities at the bottom of the image are due to fluorescence contributions. Fig. 2C was reconstructed by the vertex component image analysis described in the methods section while Fig. 2D represents the associated spectral information. In Fig. 2D, spectrum (a) exhibits spectral features typical for proteins, which are discussed in detail in the following section. The distribution of the spectral endmember is plotted in light blue. The colour intensities correspond to high or low abundances. Colour mixing represents the presence of more than one component. Areas with high fluorescence are observed, especially in the lower part of the image bordering the epidermis from about 40 μm down. The fluorescence spectrum is shown in spectrum (b) and areas with high fluorescence are plotted in yellow. For the obtained images

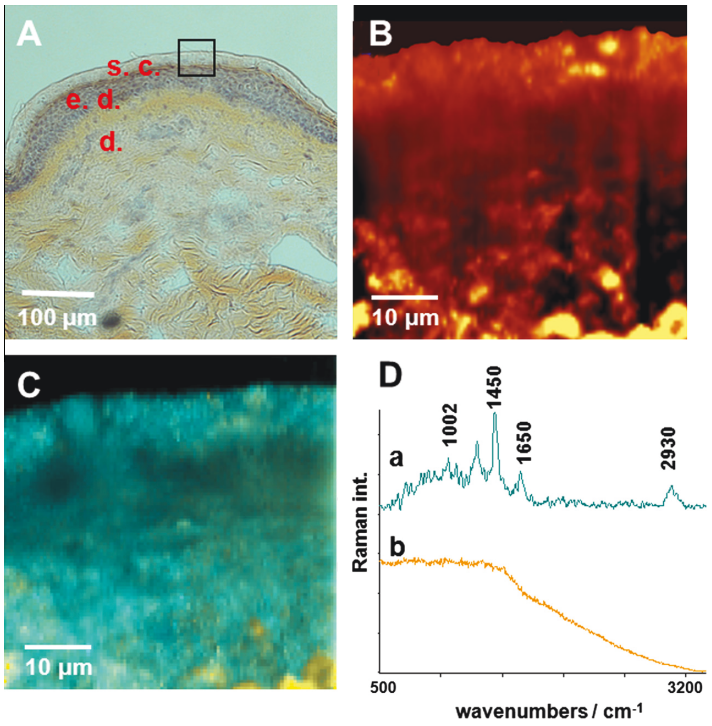

Fig. 2. (A) A Mayer's Haemalaun (acidic) and congo red stained micrograph shows the stratum corneum (s.c.), the epidermis (e.d.) and dermis (d.). (B) Raman image of the region indicated in 1A. The image was reconstructed by plotting the integrated scattering intensities of the C-H stretching region stretching region between 2800 and 3100 cm^{-1}. (C) shows the distribution of proteins (light blue) vs. regions with high fluorescence (yellow). The corresponding spectral information is plotted in (D). (For interpretation of the references to colour in this figure legend, the reader is referred to the web version of this article.)

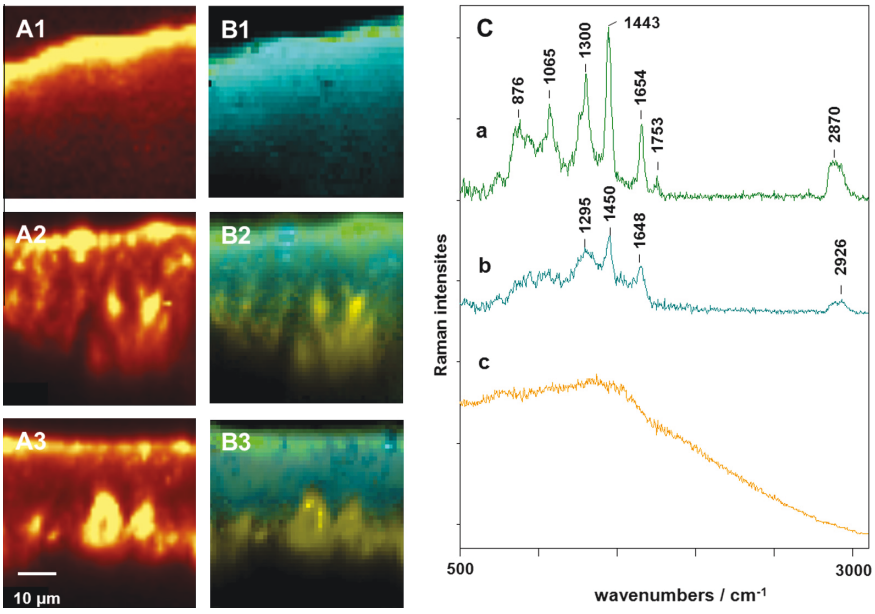

Fig. 3. X,Z-profiles recorded on untreated skin. (A1–3) represents Raman images generated by integrating the signal intensities of C—H stretching vibrations. (B1–3) Images generated by VCA where highest lipid intensities are shown in green while regions in blue show spectral features characteristic for proteins. Fluorescent regions are shown in yellow (C) represents corresponding spectra of the VCA results. (For interpretation of the references to colour in this figure legend, the reader is referred to the web version of this article.)

lower S/N ratios, due to deeper penetration did not affect the VCA analysis.

Fig. 3 shows Raman images of the X,Z-profiles of untreated skin samples measured on the intact tissue after the Franz-cell incubation without cutting or processing. The spectra were measured for areas of 50 × 50 μm^2. Fig. 3A1–3 were generated by integrating the intensities of the C—H stretching vibrations as mentioned earlier. The signal intensities generally drop by a factor 5 comparing the scattering intensities from the top of the stratum corneum with the intensities originating from 50 μm within the tissue. Below 50 μm the signal quality drastically drops, for the described experimental conditions. The Fig. 3B1–3 are the outcome of the vertex component analysis. The associated spectra are shown in 3C using the same colour coding as described before. The light blue spectrum 3C (b) shows all spectral characteristics typical for proteins. Well pronounced are the C—H stretching intensities between 2800 and 3100 cm^{-1} centred at 2930 cm^{-1}. The lower wave-number region between 500 and 1800 cm^{-1} is dominated by scattering intensities of the bonds of the peptide backbones of the tissue components. The band at 1650 cm^{-1} originates from the C=O carbonyl stretch of the peptide bond. The band at 1450 cm^{-1} is caused by scissoring modes of the methylene groups of the peptides, and is followed by other C—H deformations and C—N bending vibrations between 1250 and 1350 cm^{-1}. All other Raman intensities can also be attributed to vibrations of the protein molecules, but are less specific regarding their assignment. Apart from the protein components that can be mainly attributed to the corneocytes of the stratum corneum, there are substantial amounts of lipids shown in green. The spectrum associated with lipids is plotted in 3C (a). The spectrum shows similar features as the protein spectra, such as the C—H stretching and other deformational modes. The stretching of C=C of unsaturated side chains is centred at 1640 cm^{-1} and the C=O stretching of the ester band of lipids is located at 1740 cm^{-1}. Reference spectra and detailed assignments of Raman spectra of biological molecules are described in the literature (De Gelder et al., 2007; Diem et al., 2008; Krafft et al., 2005). Strong Raman signals from lipids are mainly found on the top layer of the stratum corneum and are likely to represent domains of ceramides and fatty acids within the intracellular matrix. Again, substantial spectral contributions from fluorescence are observed in the lower layers of the stratum corneum, which are plotted in yellow. The spectrum is similar to that observed for the cross sectioned sample. The fluorescence is likely caused by pigments such as melanin.

3.2. Diffusion of D_2O

We selected water as one of the candidates for permeation experiments as water penetrates the stratum corneum relatively easily and homogenously. Generally, water has distinct broad Raman band features due to symmetric and anti-symmetric O—H stretching vibrations between 2900 and 4000 cm^{-1}. For technical reasons associated with CCD cameras used for photon counting, the spectral region beyond 3100 cm^{-1} is not accessible for an excitation source of 785 nm. However, it was possible to use deuterated water, which basically has the same chemical properties. Because deuterium is the heavier isotope, O—D stretching vibrations are shifted to a lower wave-number region and appear now in the region between 2200 and 2600 cm^{-1}, where there is no overlap with the Raman bands of organic molecules, hence providing a better spectral contrast. The isotopic labelling also has the advantage that the water of the formulation can be distinguished from the water of the skin. Fig. 4 shows X,Z-Raman profiles of skin samples treated with D_2O on a Franz-Cell over 14 h. Similar to the untreated skin samples we can reconstruct the Raman images based on the main spectral components of the dataset. Images in Fig. 4A1–3 were constructed by integrating the intensities of C—H stretching vibrations between 2800 and 3100 cm^{-1}. In Fig. 4B1–3 lipids and areas with high pigment content are plotted in green and yellow respectively. The endmember spectrum associated with the protein matrix of the skin has now noticeable contributions from the O—D stretching intensities. Deuterated water appeared to penetrate evenly throughout the stratum corneum. The regions rich in lipids also show the presence of D_2O, as can be clearly noticed in the green spectrum.

3.3. Diffusion of Beta-carotene

Due to the high lipophilicity of Beta-carotene it shows poor skin permeability (Grosser et al., 2012). DMSO was employed to facilitate complete dissolution of beta-carotene. Fig. 5 shows X,Z-profiles of three skin samples treated with a beta-carotene solution in DMSO for 14 h on a Franz-Cell. Raman images in Fig. 5A are generated by integrating intensities of C—H stretching vibrations. In Fig. 5B, the distribution of the beta-carotene is shown in red for very high concentrations and purple for lower concentrations, respectively. Penetration of beta-carotene is not homogeneous and generally decreases rapidly with depth. Beta-carotene exhibits special spectroscopic features. Due to the electronic properties of the conjugated double bond sequence it undergoes resonance Raman excitation, whereby an electronic transition and a vibrational excitation occur simultaneously. As a consequence the observed intensities are generally much stronger than the protein scattering intensities. The absorption spectrum of beta-carotene in the visible range of light suggests maximum resonance effects between 450 and 550 nm. However, resonance Raman spectra have also been observed in the pre-resonance region (Gaier et al., 1991). The absorption profile of beta-carotene in the near IR region extends to about 800 nm. The spectrum of β-carotene is dominated by three main bands, which can be assigned to C=C stretches observed at 1510 and 1153 cm^{-1} and a C—CH_3 rocking vibration at 1004 cm^{-1}. The main distribution is conspicuously predominant in the top 10 μm of the stratum corneum, as can be seen in the associated red and pink endmember spectra. However, it is also present in noticeable concentrations throughout the lower regions shown in light blue.

3.4. Discussion

By means of the described method Raman images could be obtained down to 30–40 μm deep into the skin which corresponds to the stratum corneum and the top layers of the viable epidermis. For larger penetration depths, higher laser intensity and higher integration times would be needed to overcome the very low S/N ratios. The lateral resolution of the images was 1 μm. The resolution in the axial direction for the upper regions of the stratum corneum is about 1 μm while axial resolution of the lower regions is less and can only be estimated, because of refraction of the laser beam due to changes in refractive index. The Raman signals from the stratum corneum were to a large extent free of fluorescence. However, deeper regions of the epidermis frequently showed substantial amounts of fluorescence. The fluorescence observed was inhomogenously distributed and was not observed for every XZ profile. The images obtained from cross-sections and the XZ-profiles of intact skin samples are in good agreement. For the cross-sections fluorescence was also observed in the upper region of the epidermis. The full thickness skin samples showed very thin layers of lipids, as shown in Fig. 3B1–3, which we attribute to fatty acids and ceramides of the intra-cellular spaces. The possibility of presence of sebum on the skin surface was rejected as the lipid rich regions were consistent even after thorough cleaning of the stratum corneum (data not shown here). The thin lipid layers were not observed for the measured cross-sections. Rationale for the

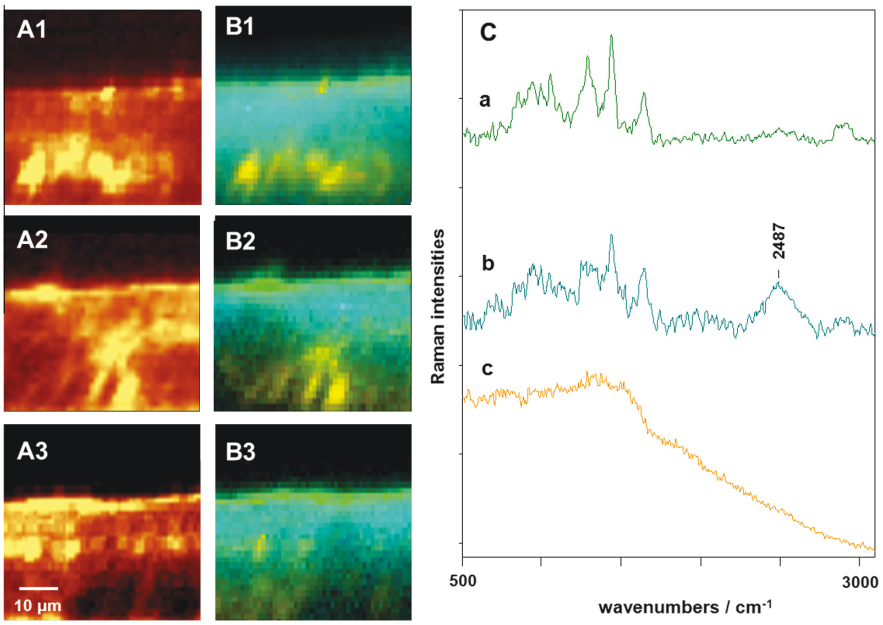

Fig. 4. X,Z-profiles for skin treated with D_2O (A1–3) Raman images generated by integrating the intensities for C—H stretching vibrations (B1–3) Images generated from corresponding Raman maps shown (A1–3) indicating uniform distribution of D_2O throughout the sample. Strong signal due to O—D stretching vibrations can be seen in 2200–2600 cm^{-1}. Green and blue regions correspond to spectra rich in features for lipids and proteins respectively. (C) corresponding spectra generated by the VCA algorithm. (For interpretation of the references to colour in this figure legend, the reader is referred to the web version of this article.)

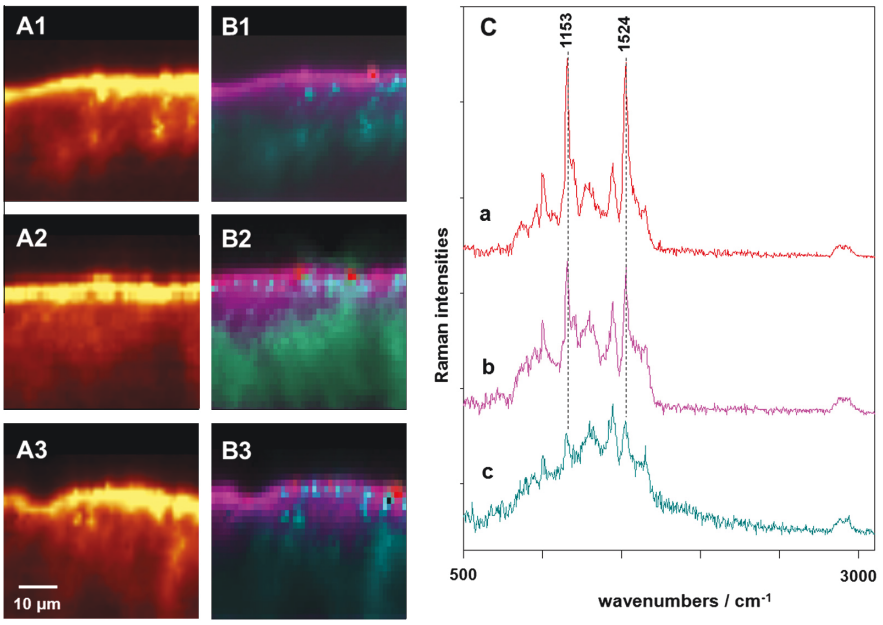

Fig. 5. X,Z-profiles for skin treated with beta-carotene solution (A1–3) Raman images generated by integrating the intensities for C—H stretching vibrations (B1–3) Raman maps generated by VCA indicating inhomogenous distribution of beta-carotene. Concentration of beta-carotene is mapped in red, purple and blue indicating decreasing concentration in that order. (C) shows spectral fratures corresponding to the VCA. Strong Raman bands centering at 1153 and 1524 cm^{-1} are assigned to C=C stretching vibrations. (For interpretation of the references to colour in this figure legend, the reader is referred to the web version of this article.)

absence of this layer in cross sections was not completely clear and further investigations are necessary to look into this matter.

In our experiments, D_2O penetration experiments showed a homogeneous distribution throughout the sample. Effectiveness

of the D_2O in penetrating the SC might be explained the fact that water is a penetration enhancer and water content of the SC is only about 20% of its dry weight. As a result, SC can easily be saturated with water just by occlusion or prolonged contact with water (Van Hal et al., 1996; Williams and Barry, 2004). Van Hal et al. have demonstrated that in water saturated SC, most of the water is absorbed by the corneocytes, which swell as a result while intercellular lipid matrix showed presence of water rich regions without substantial changes to the organisation of lipid domains.

Beta-carotene distribution on the other hand showed a steep gradient, with a rapid decrease in concentration after the first 10 μm. We selected beta-carotene for diffusion experiments because of its high lipophilicity and poor skin permeability (Antille et al., 2004) and, in combination with the strong resonance Raman signal, it was an ideal candidate for these studies. In the past it has been demonstrated that penetration of lipophilic fluorescent markers in the skin is inhomogeneous, when applied in the form of flexible liposomal vesicles. (Schatzlein and Cevc, 1998; van den Bergh et al., 1999; Verma et al., 2003b). Raman images generated in this study exhibit a similar phenomenon with beta-carotene. Beta-carotene on its own does not penetrate the skin very well. However, DMSO is a very well known penetration enhancer and can be effectively employed in increasing penetration of drugs (Christensen et al., 2009; Roth and Shainhouse, 2004; Williams and Barry, 2004). Although mechanism of penetration is not completely understood, DMSO is known to alter the skin barrier by changing the protein conformations in the corneocytes and altering the packing of the lipid domains (Anigbogu et al., 1995). Although DMSO might have assisted beta-carotene in penetration, the localised penetration of beta-carotene remains unclear; possibly it is caused by preferential trans-follicular penetration. Further studies are needed to clarify this.

One challenging aspect of 3D confocal Raman imaging is the quantification of the observed signal intensities. For synthetic mixtures or solutions calibration with known concentrations is possible. In addition ratios of band intensities can be used to internally compare concentrations. However, for depth profiling these evaluations are critical. One aspect is that a change in refractive index will have an effect on both, position and shape of the focal volume (Everall, 2004a,b). Furthermore, the scattering becomes more diffuse with increasing penetration depth. Franzen et al. have recently introduced a semi-solid matrix system to simulate the optical properties of skin, which appears to give reliable results (Franzen et al., 2012).

The most critical aspect of the application of Raman microscopy for direct imaging is the relatively low penetration depth. Although this could be improved by higher laser power and substantially longer integration times, considering the amount of data collected during an image acquisition, long integration times become quickly impractical and higher laser intensities are likely to introduce photo damage. Long measuring times are problematic for imaging applications, because of the associated loss of water. Drying will not only alter the tissue, it also steadily changes the focal plane. Excitation within the red region of light is generally accepted as being least invasive for biological samples (Puppels et al., 1991). However, to the best of the authors knowledge, persistent studies that relate excitation power with photo toxicity have not been published.

For the detection of beta-carotene and other carotenoids resonance Raman effects may be utilised for achieving higher sensitivities. However, previous reports of Raman spectroscopic investigations of human skin are based on single point measurements (Ermakov et al., 2004; Mélot et al., 2009; Pudney et al., 2007; Uragami et al., 2012). Although confocal Raman microscopy for studying skin penetration has already been studied extensively, these studies usually involve either tissue cross sectioning or recording optical biopsies in the *XY* plane at different depths in the skin (Caspers et al., 2001, 2002; Tfayli et al., 2007) which may not generate a sufficiently detailed map of the diffusion pathway taken by the drug. With this in mind, we acknowledge that the method described in this paper might be limited to only the top layers of the epidermis. Key advantage of the proposed methodology is the non-invasiveness of the image acquisition of the stratum corneum, a major barrier in transdermal drug delivery.

Acknowledgements

The authors are grateful to Dr med Lutz Gruhl from the Praxis für Plastische Chirurgie, Kassel, Germany for his assistance in procuring human skin tissue. We would also like to acknowledge Carl Zeiss Foundation, Germany for their financial support.

References

Alvarez-Roman, R., Naik, A., Kalia, Y.N., Fessi, H., Guy, R.H., 2004. Visualization of skin penetration using confocal laser scanning microscopy. European journal of pharmaceutics and biopharmaceutics: official journal of Arbeitsgemeinschaft fur Pharmazeutische Verfahrenstechnik e.V 58, 301–316.

Anigbogu, A.N.C., Williams, A.C., Barry, B.W., Edwards, H.G.M., 1995. Fourier transform Raman spectroscopy of interactions between the penetration enhancer dimethyl sulfoxide and human stratum corneum. Int. J. Pharm. 125, 265–282.

Antille, C., Tran, C., Sorg, O., Saurat, J.H., 2004. Penetration and metabolism of topical retinoids in ex vivo organ-cultured full-thickness human skin explants. Skin Pharmacol. Physiol. 17, 124–128.

Baia, L., Gigant, K., Posset, U., Schottner, G., Kiefer, W., Popp, J., 2002. Confocal micro-Raman spectroscopy: theory and application on a hybrid polymer coating. Appl. Spectrosc. 56, 536.

Bayerl, C., 2008. Beta-carotene in dermatology: does it help? Acta dermatovenerologica Alpina, Panonica, et Adriatica 17 (160–162), 164–166.

Blasius, S., 1985. Sorptionsvermittler—Einfluss auf die Liberation von Indomethacin aus Salben and auf die Arzneistoffaufnahme durch excidierte Haut. Saarland University.

Borchert, D., 1994. Methoden zur Untersuchung der simultanen Penetration von Arzneistoffen and Vehikelbestandteilen aus Salben in exzidierter Humanhaut. Saarland University.

Bouwstra, J.A., Gooris, G.S., van der Spek, J.A., Bras, W., 1991. Structural investigations of human stratum corneum by small-angle X-ray scattering. J. Invest. Dermatol. 97, 1005–1012.

Breternitz, M., Flach, M., Prassler, J., Elsner, P., Fluhr, J.W., 2007. Acute barrier disruption by adhesive tapes is influenced by pressure, time and anatomical location: integrity and cohesion assessed by sequential tape stripping. A randomized, controlled study. Br. J. Dermatol. 156, 231–240.

Carrer, D.C., Vermehren, C., Bagatolli, L.A., 2008. Pig skin structure and transdermal delivery of liposomes: a two photon microscopy study. J. Controlled Release: Official J. Controlled Release Soc. 132, 12–20.

Caspers, P.J., Lucassen, G.W., Carter, E.A., Bruining, H.A., Puppels, G.J., 2001. In Vivo Confocal Raman Microspectroscopy of the Skin: Noninvasive Determination of Molecular Concentration Profiles. J. Invest. Dermatol. 116, 434–442.

Caspers, P.J., Williams, A.C., Carter, E.A., Edwards, H.G., Barry, B.W., Bruining, H.A., Puppels, G.J., 2002. Monitoring the penetration enhancer dimethyl sulfoxide in human stratum corneum in vivo by confocal Raman spectroscopy. Pharm. Res. 19, 1577–1580.

Christensen, E., Skogvoll, E., Viset, T., Warloe, T., Sundstrom, S., 2009. Photodynamic therapy with 5-aminolaevulinic acid, dimethylsulfoxide and curettage in basal cell carcinoma: a 6-year clinical and histological follow-up. J. Eur. Acad. Dermatol. Venereol.: JEADV 23, 58–66.

Chrit, L., Bastien, P., Biatry, B., Simonnet, J.T., Potter, A., Minondo, A.M., Flament, F., Bazin, R., Sockalingum, G.D., Leroy, F., Manfait, M., Hadjur, C., 2007. In vitro and in vivo confocal Raman study of human skin hydration: assessment of a new moisturizing agent, pMPC. Biopolymers 85, 359–369.

Darvin, M.E., Fluhr, J.W., Meinke, M.C., Zastrow, L., Sterry, W., Lademann, J., 2011. Topical beta-carotene protects against infra-red-light-induced free radicals. Exp. Dermatol. 20, 125–129.

Darvin, M., Sandhagen, C., Koecher, W., Sterry, W., Lademann, J., Meinke, M., 2012. Comparison of two methods for noninvasive determination of carotenoids in human and animal skin: Raman spectroscopy versus reflection spectroscopy. J. Biophotonics 5, 550–558.

De Gelder, J., De Gussem, K., Vandenabeele, P., Moens, L., 2007. Reference database of Raman spectra of biological molecules. J. Raman Spectrosc. 38, 1133–1147.

Diem, M., Griffiths, P., Chalmers, J.M., 2008. Vibrational Spectroscopy for Medical Diagnosis. John Wiley & Sons, New York.

Du, Q., Raksuntorn, N., Younan, N.H., King, R.L., 2008. End-member extraction for hyperspectral image analysis. Appl Opt. 47, F77-84.

Ermakov, I., Gellermann, W., 2012. Dermal carotenoid measurements via pressure mediated reflection spectroscopy. J. Biophotonics 5, 559–570.

Ermakov, I.V., Ermakova, M.R., Gellermann, W., Lademann, J., 2004. Noninvasive selective detection of lycopene and beta-carotene in human skin using Raman spectroscopy. J. Biomed. Opt. 9, 332–338.
Everall, N., 2004a. Depth profiling with concocal Raman microscopy, part 1. Spectroscopy 19, 22–27.
Everall, N., 2004b. Depth profiling with concocal Raman microscopy, part 2. Spectroscopy 19, 18–27.
Fink-Puches, R., Hofmann-Wellenhof, R., Smolle, J., Kerl, H., 1995. Confocal laser scanning microscopy: a new optical microscopic technique for applications in pathology and dermatology. J. Cutan. Pathol. 22, 252–259.
Franzen, L., Selzer, D., Fluhr, J., Schaefer, U., Windbergs, M., 2012. Towards drug quantification in human skin with confocal Raman microscopy. Eur. J. Pharm. Biopharm. S0939–6411 (0912), 00383–00389.
Gaier, K., Angerhofer, A., HC, W., 1991. The lowest excited electronic singlet states of all-tras beta-carotene single crystals. Chem. Phys. Lett. 187, 103–109.
Grice, J.E., Zhang, Q., Roberts, M.S., 2010. Chemical structure – skin transport relationships. Toxicol. Skin, 55–68.
Grosser, K., Zedler, L., Schmitt, M., Dietzek, B., Popp, J., Pohnert, G., 2012. Disruption-free imaging by Raman spectroscopy reveals a chemical sphere with antifouling metabolites around macroalgae. Biofouling 28, 687–696.
Hailer, M., 1981. Freisetzung von Salicylsaeure aus Suspensionssalben: Liberation im Membranmodell im Vergleich zur Wirkstoffabgabe an excidierter Haut. Saarland University.
Hedegaard, M., Matthäus, C., Hassing, S., Krafft, C., Diem, M., Popp, J., 2011. Spectral unmixing and clustering algorithms for assessment of single cells by Raman microscopic imaging. Theor. Chem. Acc. 130, 1249–1260.
Krafft, C., Neudert, L., Simat, T., Salzer, R., 2005. Near infrared Raman spectra of human brain lipids. Spectrochim. Acta A Mol. Biomol. Spectrosc. 61, 1529–1535.
Krafft, C., Dietzek, B., Popp, J., 2009. Raman and CARS microspectroscopy of cells and tissues. Analyst 134, 1046–1057.
Mélot, M., Pudney, P., Williamson, A., Caspers, P., Van Der Pol, A., Puppels, G., 2009. Studying the effectiveness of penetration enhancers to deliver retinol through the stratum cornum by in vivo confocal Raman spectroscopy. J. Control Release 138, 32–39.
Miljković, M., Chernenko, T., Romeo, M.J., Bird, B., Matthäus, C., Diem, M., 2010. Label-free imaging of human cells: algorithms for image reconstruction of Raman hyperspectral datasets. Analyst 135, 2002–2013.
Pinkus, H., 1951. Examination of the epidermis by the strip method of removing horny layers. I. Observations on thickness of the horny layer, and on mitotic activity after stripping. J. Invest. Dermatol. 16, 383–386.
Prausnitz, M.R., Langer, R., 2008. Transdermal drug delivery. Nat. Biotechnol. 26, 1261–1268.
Pudney, P., Mélot, M., Caspers, P., Van Der Pol, A., Puppels, G., 2007. An in vivo confocal Raman study of the delivery of trans retinol to the skin. Appl. Spectrosc. 61, 804–811.
Puppels, G., Olminkhof, J., Segers-Nolten, G., Otto, C., de Mul, F., Greve, J., 1991. Laser irradiation and Raman spectroscopy of single living cells and chromosomes: sample degradation occurs with 514.5 nm but not with 660 nm laser light. Exp. Cell Res. 195, 361–367.
Roth, S.H., Shainhouse, J.Z., 2004. Efficacy and safety of a topical diclofenac solution (pennsaid) in the treatment of primary osteoarthritis of the knee: a randomized, double-blind, vehicle-controlled clinical trial. Arch. Int. Med. 164, 2017–2023.
Schatzlein, A., Cevc, G., 1998. Non-uniform cellular packing of the stratum corneum and permeability barrier function of intact skin: a high-resolution confocal laser scanning microscopy study using highly deformable vesicles (Transfersomes). Br. J. Dermatol. 138, 583–592.
Schenke-Layland, K., Riemann, I., Damour, O., Stock, U.A., Konig, K., 2006. Two-photon microscopes and in vivo multiphoton tomographs–powerful diagnostic tools for tissue engineering and drug delivery. Adv. Drug Deliv. Rev. 58, 878–896.
Schmitt, M., Leimeister, B., Baia, L., Weh, B., Zimmermann, I., Kiefer, W., Popp, J., 2003. Characterization of diffusion-processes of pharmacological relevant molecules through pdms-membranes by means of confocal resonance Raman spectroscopy. ChemPhysChem 4, 46.
Stahl, W., Sies, H., 2012. beta-Carotene and other carotenoids in protection from sunlight. Am. J. Clin. Nutr. 96, 1179S–1184S.
Tfayli, A., Piot, O., Pitre, F., Manfait, M., 2007. Follow-up of drug permeation through excised human skin with confocal Raman microspectroscopy. Eur. Biophys. J.: EBJ 36, 1049–1058.
Uragami, C., Yamashita, E., Gall, A., Robert, B., Hashimoto, H., 2012. Application of resonance Raman microscopy to in vivo carotenoid. Acta Biochim. Pol. 59, 53–56.
van den Bergh, B.A., Vroom, J., Gerritsen, H., Junginger, H.E., Bouwstra, J.A., 1999. Interactions of elastic and rigid vesicles with human skin in vitro: electron microscopy and two-photon excitation microscopy. Biochim. Biophys. Acta 1461, 155–173.
Van Hal, D.A., Jeremiasse, E., Junginger, H.E., Spies, F., Bouwstra, J.A., 1996. Structure of fully hydrated human stratum corneum: a freeze-fracture electron microscopy study. J. Invest. Dermatol. 106, 89–95.
Verma, D.D., Verma, S., Blume, G., Fahr, A., 2003a. Liposomes increase skin penetration of entrapped and non-entrapped hydrophilic substances into human skin: a skin penetration and confocal laser scanning microscopy study. European Journal of Pharmaceutics and Biopharmaceutics: Official Journal of Arbeitsgemeinschaft fur Pharmazeutische Verfahrenstechnik e.V 55, 271–277.
Verma, D.D., Verma, S., Blume, G., Fahr, A., 2003b. Particle size of liposomes influences dermal delivery of substances into skin. Int. J. Pharm. 258, 141–151.
Wagner, H., Kostka, K.H., Lehr, C.M., Schaefer, U.F., 2000. Drug distribution in human skin using two different in vitro test systems: comparison with in vivo data. Pharm. Res. 17, 1475–1481.
Walters, K., Brain, K., 2002. Dermatological Formulation and Transdermal Systems, Dermatological and Transdermal Formulations. CRC Press.
Walters, K., Roberts, M., 2002. The Structure and Function of Skin, Dermatological and Transdermal Formulations. CRC Press.
Williams, A.C., Barry, B.W., 2004. Penetration enhancers. Adv. Drug Deliv. Rev. 56, 603–618.
Winter, M.E., 1999. N-FINDR: an algorithm for fast autonomous spectral end-member determination in hyperspectral data. Proc. SPIE 3753, 266–275.
Xiao, C., Moore, D.J., Rerek, M.E., Flach, C.R., Mendelsohn, R., 2005. Feasibility of tracking phospholipid permeation into skin using infrared and Raman microscopic imaging. J. Invest. Dermatol. 124, 622–632.
Yu, B., Kim, K.H., So, P.T., Blankschtein, D., Langer, R., 2003. Visualization of oleic acid-induced transdermal diffusion pathways using two-photon fluorescence microscopy. J. Invest. Dermatol. 120, 448–455.
Zhang, G., Moore, D.J., Sloan, K.B., Flach, C.R., Mendelsohn, R., 2007. Imaging the prodrug-to-drug transformation of a 5-fluorouracil derivative in skin by confocal Raman microscopy. J. Invest. Dermatol. 127, 1205–1209.

3.2.1 Unpublished work

Work that followed the publication-2 is described in this section in brief and also describes difficulties faced. At the moment of writing this thesis, this work is not considered for any publication.

Method development:

Publication-2 presented the first-insights into the method for non-invasive depth profiling of the SC. Depth profiling of the *stratum corneum* and viable epidermis was of interest to study the co-diffusion of liposomal-phospholipid and drug incorporated within the liposomes to comment on the mechanism involved in the drug delivery to skin from topical application of liposomes.

In the second part of this project, further efforts were made to improve the penetration depth achieved during Raman imaging and increase sample stability during the measurements. Increased penetration depth and sample stability were mainly achieved by the combination of following changes;

- A water immersion objective (Nikon, 60x, 1.0 NA, NIR) was used instead of an air immersion objective (Zeiss, 50x, 0.9 NA) as reported in the publication-2
- Skin sample holder proposed in the publication-2 was updated from an open-cell design to a closed-cell design (Figure 5)

Water immersion objectives reduce local heating of skin biopsies which greatly increased the stability of skin samples enabling longer acquisition times for the Raman spectra. Use of water immersion objective prompted us to move away from the open-cell design in order to avoid over-hydrating the skin. A closed cell was implemented by using a thin (thickness = 200 µm) 9 mm diameter quartz window on top of the skin biopsy. Principle design of the sample holder remained similar to the one described previously in publication-2 but rather than aluminum block the assembly was done in a shorter Teflon block to accommodate the larger dimensions of the water immersion objective.

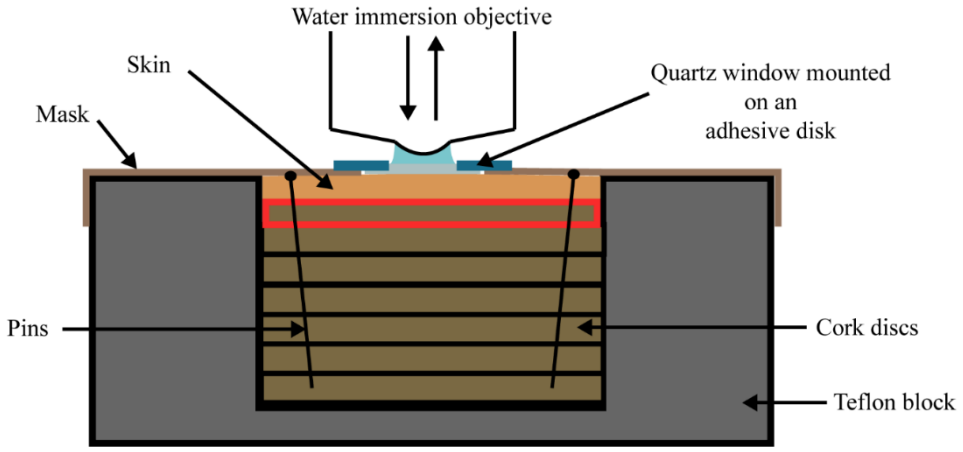

Figure 5: Schematic for the modified closed-cell type sample holder.

Figure 6 and 7 show depth profiles for full thickness untreated human and pig-ear skin respectively. Using the updated version of the method spectra could even be collected at higher acquisition time of 1 or 2 seconds/spectra without any damage to the skin. Vertex component analysis (VCA) of the optical

biopsies shows typical spectral features dominant for proteins and lipids. Spectra at the surface had the highest intensity however, the biggest improvement was for the spectral quality from the deeper focal planes. Compared to the published method, penetration depth achieved was about 60 µm for human skin whereas for pig skin it was approximately 70 µm (Figure 7c). With these results, at least a two fold increase in penetration depth was achieved. It must be pointed out that despite the higher penetration depths achieved, limitations of our method, as discussed in the publication-2, related to quantification and resolution at the deeper focal planes due to change in refractive index are still valid.

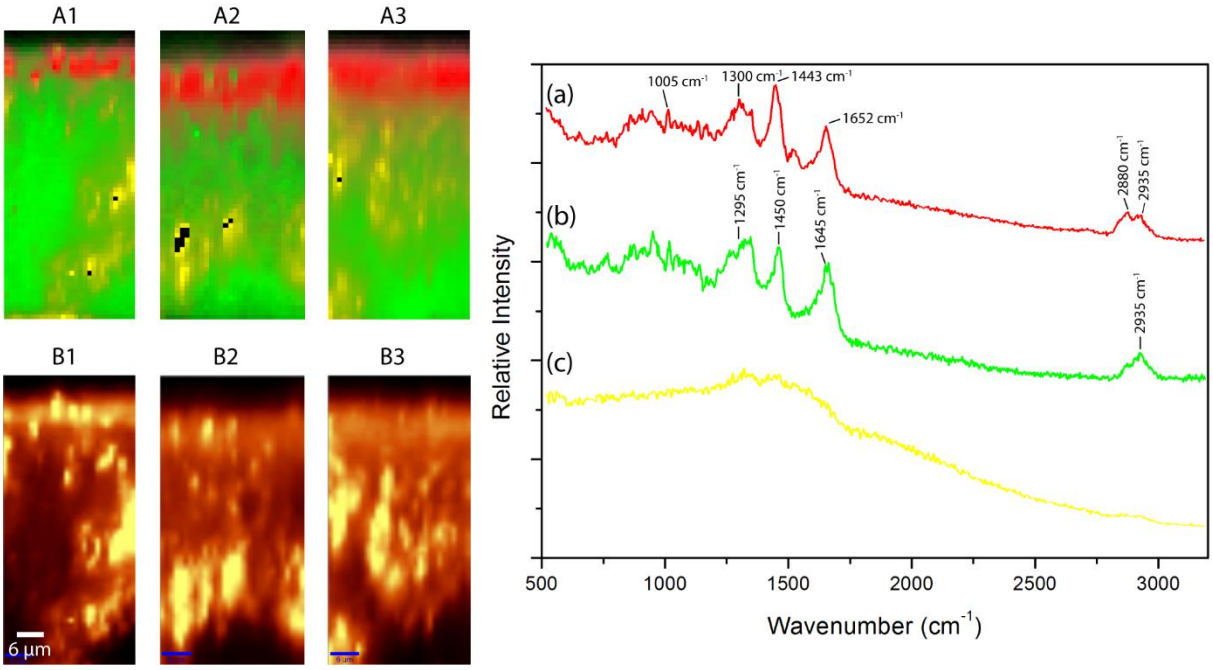

Figure 6: XZ depth profiles of untreated human skin. (A1-3) images generated by VCA where highest intensities showing characteristic spectral features of proteins and lipids (a) are shown in red while regions in green show spectral features characteristic mainly for proteins (b). Fluorescence is represented by yellow (c) in the deeper regions of the skin. (B1-3) represents Raman images generated by integrating the signal intensities for C-H stretching vibrations.

Measurement of diffusion profiles from deuterated liposomes:

Chain deuterated d31-palmitoyl-oleoyl phosphatidylcholine (d31-POPC) was employed for the preparation of liposomal formulations as C-D stretching vibrations can be easily distinguished between the spectral features of skin. For the selection of a model-drug for the diffusion experiments, two criteria were applied. The drug must be able to get incorporated within the liposomes and importantly, should have a strong Raman signature easily identifiable in the skin. A variety of drugs and chemical compounds were scanned, amongst them retinol, beta carotene, tretinoin and ibuprofen were selected

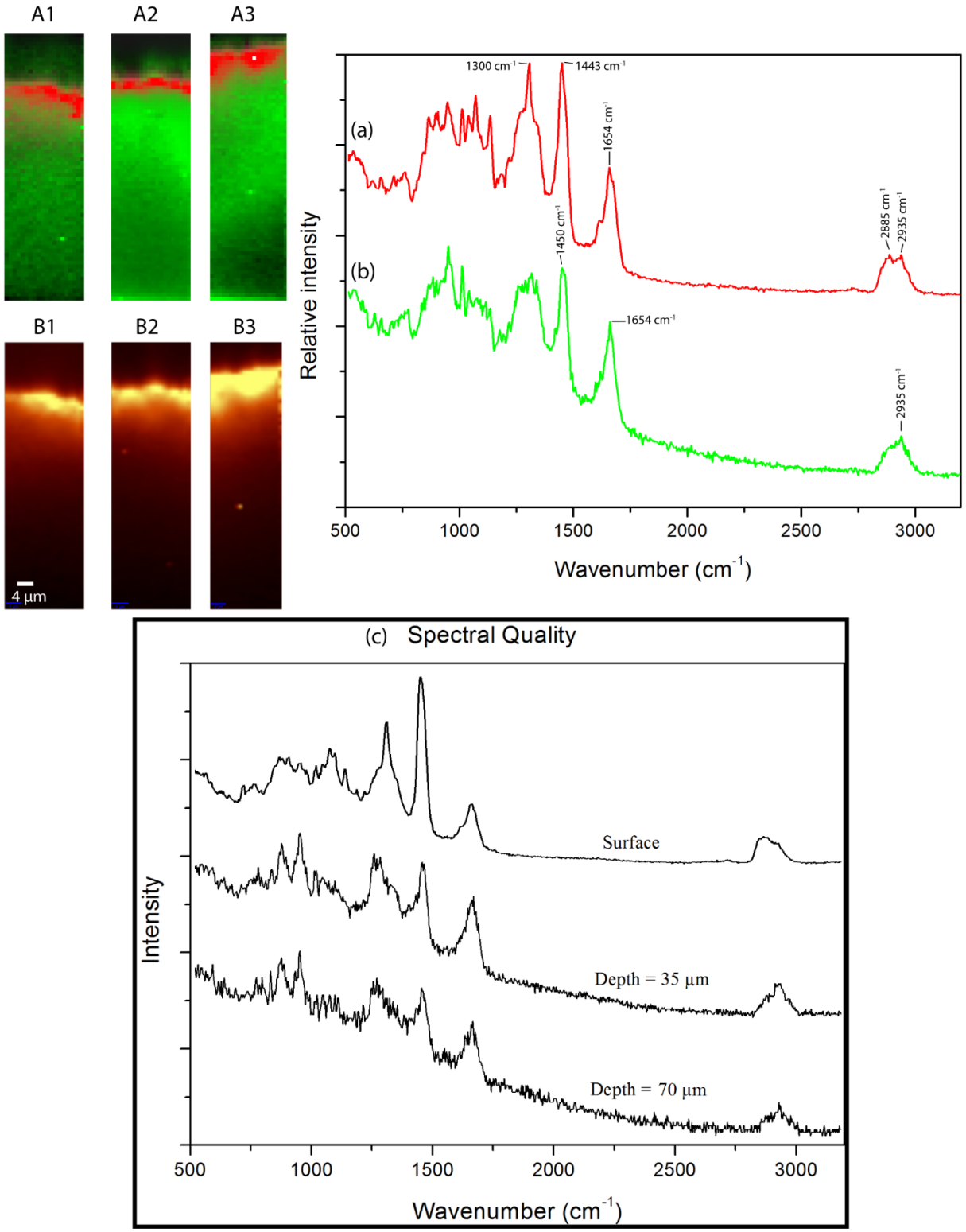

Figure 7: XZ depth profiles of untreated pig-ear skin. (A1-3) images generated by VCA where highest intensities showing characteristic spectral features of proteins and lipids (a) are shown in red while regions in green show spectral features characteristic mainly for proteins (b). (B1-3) represents Raman images generated by integrating the signal intensities for C-H stretching vibrations. (c) spectral quality from various depths of untreated pig skin.

and formulated to form deuterated invasomes. Composition of invasomes was, 9.3% d31-POPC, 0.7% lyso-phosphatidylcholine, 1% terpene and 10% ethanol.

After hydration, MLVs were extruded through 100 nm polycarbonate membrane. Formulations prepared had approximate size of 110 nm and PDI was < 0.1. Full-thickness human skin was mounted on the Franz diffusion cell and a 100 µl/cm² dose was applied non-occlusively on the skin. Diffusion was continued for 14 hours followed by which applied formulation was thoroughly removed from the surface of the skin. Skin was then used without any treatment for the measurement of Raman depth profiles using the sample holder as described in figure 5. For a more detailed explanation of the Franz diffusion experiments and Raman measurements kindly refer to the publication-2.

Hurdles in the measurements of the diffusion profiles:

One of the important objective of the study was to see the diffusion of phospholipid within the skin after topical application of liposomes. Unfortunately in the depth profile measurements, topically applied deuterated phospholipid could not be detected. Rationale behind this observation could be that phospholipids do not penetrate the SC at a sufficient concentration. Coupled this to the intrinsically weak nature of the Raman scattering and challenges of depth profiling, a relatively high concentration of the deuterated phospholipid penetration in the skin might be required for detection.

Another aspect of this problem could be related to the formulation. Addition of drug or labels can have an effect on the bending energy of the phospholipid bilayer and as a result can change the flexibility parameter of the liposomal bilayers. Section 1.3 of this thesis has already highlighted that flexible or deformable liposomes tend to be superior at delivering drugs to/through the skin. Although the flexibility parameter of liposomal formulations was not measured, invasomes without any drug were applied to the skin. Measurement of the depth profiles for empty invasomes revealed no notable improvement in the detection of C-D Raman bands. Another formulation related aspect of this issue could be the selection of phospholipids itself as POPC selected for these experiments is not a representative phospholipid of the soy-phospholipid mixtures usually employed in the preparation of flexible liposomes intended for topical application (see table 3 & 4). However, since it was commercially available it was the preferred choice for these experiments. Issues in tracking of the topically applied phospholipids present a challenge for this study which needs a better understanding of the problem and hopefully these issues will be addressed in the future studies.

3.3 Publication-3

Tip-enhanced Raman scattering
for tracking of invasomes in the stratum corneum

Mukul Ashtikar, Lucas Langelüddecke, Alfred Fahr, Volker Deckert

Manuscript in preparation.

Tip-enhanced Raman scattering for tracking of invasomes in the stratum corneum

Mukul Ashtikar[1*], Lucas Langelüddecke[2*], Alfred Fahr[1], Volker Deckert[2, 3 **]

[1]Institut for Pharmacy, Department for Pharmaceutical Technology, University of Jena, Lessingstraße 8, 07743 Jena, Germany

[2]Institute of Physical Chemistry and Abbe Center of Photonics, University of Jena, Helmholtzweg 4, 07743 Jena, Germany

[3]Leibniz Institute of Photonic Technology, Albert-Einstein-Str. 9, 07745 Jena, Germany

*These authors have contributed equally in this study and in the preparation of this manuscript.

**Corresponding Author:

Prof. Dr. Volker Deckert

Institute of Physical Chemistry and Abbe Center of Photonics,

University of Jena, Helmholtzweg 4, 07743 Jena, Germany

Email: volker.deckert@uni-jena.de

Phone: +49 3641 948347

Abstract:

Stratum corneum is the primary skin barrier to percutaneous absorption. Since 1980, topical liposomal formulations have been proposed and successfully employed for increasing the drug penetration through the skin. There is no clear consensus on the drug penetration mechanism from topically applied liposomes, despite a vast amount of research. Interactions between the stratum corneum and liposomes are at the nanoscale, what makes them difficult to probe. In this study, we have employed tip-enhanced Raman scattering (TERS) to gain a better understanding at the interactions between the human stratum corneum and topically applied invasomes. TERS is capable of imaging at sub nanometer spatial resolution and provides spectral information at nanometer scale. A sample preparation technique was developed and calibrated to enable TERS on complex stratum corneum samples. Invasomes prepared from a head deuterated phospholipid were used to aid identification of topically applied phospholipid in the stratum corneum. The presented results for the first time give strong spectroscopic evidence along with high-resolution images to show intact invasome vesicles in the stratum corneum.

32 **Graphical Abstract:**

33

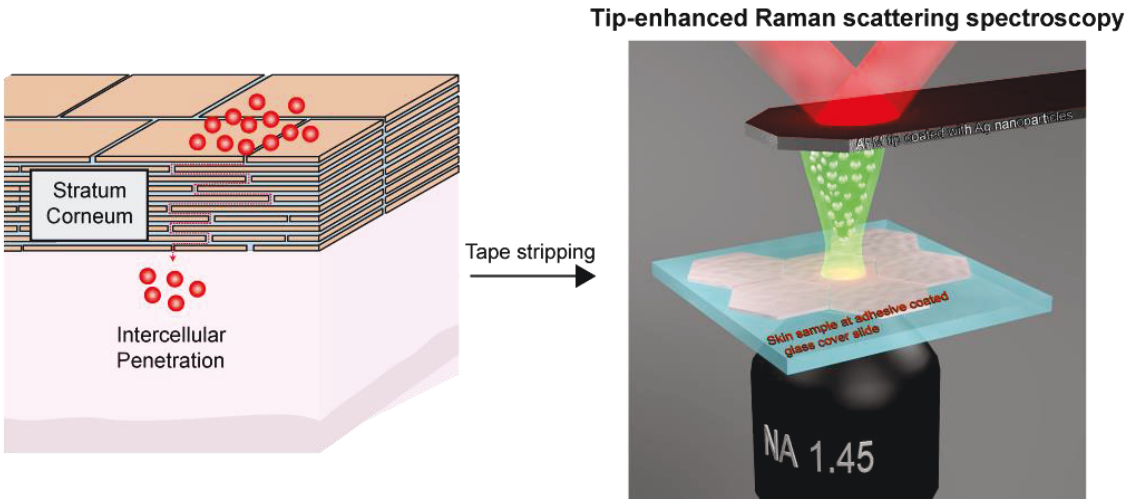

34

35

List of abbreviations

ATR-FTIR – attenuated total reflection Fourier transform infrared spectroscopy

d9-DLPC – 1,2-dilinoleoyl-3-phosphocholine-N,N,N-trimethyl-d9

DMPC – 1,2-dimyristoyl-sn-glycero-3-phosphocholine

DPPC – 1,2-dipalmitoyl-sn-glycero-3-phosphocholine

DSC – differential scanning calorimetry

SAXS – Small angle X-ray scattering

SC – stratum corneum;

Soy-LPC – Soy lyso-phosphatidylcholine

Introduction

Since the emergence of modern medicine, various strategies to deliver drugs to the skin have been explored. Major hurdle in transdermal delivery is the stratum corneum (SC) which forms the uppermost layer of the skin. Current strategies for transdermal drug delivery have been classified into first, second and third generation by Prausnitz and Langer (2008). First generation strategies include traditional delivery systems such as creams and patches which are mainly suitable for a handful of drugs which can penetrate the skin easily. Whereas both, second and third generation strategies focus on increasing the transdermal penetration either chemically, physically or mechanically. Liposomes have an important place in both second and third generation transdermal delivery systems, as phospholipid bilayers form excellent solubilizers and nanocarriers for drugs (Essa *et al.*, 2003; Qiu *et al.*, 2008). Liposomes have been extensively studied for transdermal drug delivery in the last three decades and the superiority of flexible liposomes over its rigid counterpart has been fairly well established in delivering drugs through the skin. Despite decades of studies, there is no clear consensus on how liposomes enhance drug penetration. Working groups around the world have so far proposed five mechanisms to explain drug delivery to skin using liposomes

El Maghraby *et al.* (2006) has proposed five different mechanisms based on different liposome-skin interactions that have been reported. Briefly, '*free drug mechanism*', where liposomes only transport drug up to the SC and drug permeates the skin on its own , '*penetration enhancing mechanism*' suggests that liposomal vesicles cause ultrastructural changes to the SC lipid domains leading to increased drug penetration . '*Vesicle adsorption/fusion theory*' liposomes interact with SC and fuse with the SC lipids leading to drug release. '*Intact vesicular skin penetration mechanism*' suggests liposomes can penetrate through the skin intact and the *'trans-appendageal penetration*' where drug delivery to or via hair follicles is achieved. It is likely that there is no one single mechanism at work responsible for drug delivery to skin but rather multiple mechanisms acting at different levels, depending on vesicle size, charge, mode of application, drug and vesicle composition etc. (Bouwstra and Honeywell-Nguyen, 2002; Cevc and Blume, 1992; Knepp *et al.*, 1987; Knepp *et al.*, 1990; Shah *et al.*, 2015; Verma *et al.*, 2003).

Using ATR-FTIR Hasanovic *et al.* (2011) have reported that *ex vivo* application of DPPC liposomes on human skin resulted in decreased orthothrombic organization in SC lipid domains leading to a decreased barrier function of the SC. Similar findings have also been reported by Zellmer *et al.* (1995) using DSC to study DMPC liposome-treated human skin. Yokomizo and Sagitani (1996) tested penetration-enhancing potential of a range of saturated and unsaturated phospholipids and they demonstrated that highest penetration enhancement achieved was from formulations containing unsaturated phospholipids. Ultrastructural changes to the SC lipid organization followed by application of deformable/elastic liposomal vesicles was also demonstrated by Hofland *et al.* (1995) using freeze fracture transmission electron microscopy and SAXS. Therefore both rigid and flexible liposomes have been demonstrated to

have a penetration enhancing potential, albite to a different degree. Mechanism of phospholipid vesicle interaction with the intercellular lipids is not well understood. Either phospholipid vesicles can fuse with the intercellular lipids followed by passive diffusion of phospholipids through the intercellular lipid domains or penetration of intact liposomes could also affect the organization of intercellular lipids in the SC. In general, the doctrine that intact liposomal vesicles can penetrate the SC has received a lot of skepticism. Using freeze fracture transmission electron microscopy the Bouwstra group has reported changes to the intercellular lipid domains and appearance of flattened vesicular structures in the intercellular lipid domains, *in vitro* as well as *in vivo,* up on treatment with flexible liposomal vesicles (Bouwstra and Honeywell-Nguyen, 2002; Hofland *et al.*, 1995; van den Bergh *et al.*, 1999). Confocal fluorescence microscopy studies have suggested presence of inter-cluster pathways in the SC when skin was treated with fluorescent flexible liposomes (Schatzlein and Cevc, 1998; van den Bergh *et al.*, 1999). Electron microscopic studies from the Bouwstra group presented a case supporting intact penetration of liposomes in the SC. However, given the lack of qualitative evidence and complex nature of the sample preparation in freeze fracture electron microscopic techniques there is still room for speculations. Xiao *et al.* (2005) in separate experiments applied deuterated POPC (liquid crystalline phase) and deuterated DPPC (gel phase) multilamellar liposomes to pig skin and determined the penetration of deuterated phospholipids in the pig skin using infrared and Raman microscopy. POPC penetrated up to 100 μm in the pig skin compared to only 10 – 15 μm for the DPPC, although this study does not provide information about the mechanistic aspect of how phospholipids penetrate these depths in the skin. More recently, Brewer *et al.* (2013) used raster image correlation spectroscopy to study diffusion of liposomes and Transfersomes® in skin. They found that liposomes and Transfersomes® containing twin fluorescent labels showed similar diffusion coefficients as observed for the free fluorescent dyes and concluded that liposomes and Transfersomes® undergo destabilization upon contact with the SC. They also found that in the SC the fluorescent probes did not travel together. This observation was rationalized as 'no intact penetration of liposomes'. However Brewer *et al.* used bulky fluorescent labels in their study and transfer of drugs or compounds to skin from liposomal bilayers can be heavily influenced by the partition coefficient between skin and liposomal bilayers (Shah *et al.*, 2015).

Tracking liposomes in the SC using fluorescence based microscopic techniques is limited by Abbe's diffraction limit (Abbe, 1873) and partition of fluorescent label between the SC and liposomal vesicles needs to be taken in to account. Electron microscopic techniques can get around this problem. However, electron microscopy usually requires extensive sample preparation and qualitative analysis to distinguish externally applied lipids and lipids indigenous to skin is difficult. Using Raman microscopy with isotopic labelling of the phospholipids presents a good opportunity to track nanoparticles with increased contrast to the natural phospholipid. However, this mode of microscopy is also limited by Abbe's diffraction limit and additionally the relatively weak nature of Raman scattering result in longer acquisition times, which can have an adverse effect on the sample stability. To probe liposomal interactions with the SC a technique that can image at high lateral resolution and provide spectroscopic

information at high resolution is desired. Tip-enhanced Raman scattering (TERS) spectroscopy combines high-resolution scanning probe microscopy, atomic force microscopy (AFM) or scanning tunneling microscopy (STM) with surface enhanced Raman scattering (SERS) (Anderson, 2000; Hayazawa *et al.*, 2000; Stöckle *et al.*, 2000b). Raman scattering is a weak inelastic process that can be enhanced using surface plasmon resonances (SPR) of metals like gold (Au) or silver (Ag) as applied in SERS and TERS. With TERS, many different biomaterials have been investigated so far, like model membranes, cells, viruses, bacteria, proteins etc. (Langelüddecke *et al.*, 2014). TERS utilizes metalized or solid metal tips reaching a lateral resolution of less than one nanometer (Zhang *et al.*, 2013). So far, the field enhancements in TERS were reported to be up to 10^{13} and the sensitivity is owing to the sub-nanometer resolution at the single molecule level.(Deckert-Gaudig *et al.*, 2012; Kurouski *et al.*, 2012; Marr and Schultz, 2013; Sonntag *et al.*, 2012; vandenAkker *et al.*, 2015; Zhang *et al.*, 2013).

Invasomes are flexible liposomal formulation containing lyso-PC as edge activator, ethanol and terpenes as penetration enhancers. Invasomes have shown potential to deliver drugs such as temoporfin (Dragicevic-Curic *et al.*, 2008), ferrulic acid (Chen *et al.*, 2010), cyclosporine (Verma and Fahr, 2004), azelaic acid (Shah *et al.*, 2015) etc. In this study, we treated human skin with empty invasomes and post application skin samples were investigated using TERS to track the externally applied head-deuterated phospholipid. Since the interaction between skin and invasomes takes place at molecular scale TERS is a promising tool to probe these interactions and learn about the fate and behavior of invasomes.

MATERIALS AND METHODS

Materials

1,2-dilinoleoyl-3-phosphocholine-N,N,N-trimethyl-d9 (d9-DLPC) was gifted by Cordon Pharma (Switzerland). Purity of d9-DLPC was determined to be > 96 % using UPLC-MS and the phospholipid was used without further purification. TESA SE (Germany) gifted the adhesive used for spin coating the cover slips. Soy lyso-phosphatidylcholine (soy-LPC) was purchased from Avanti Polar Lipids, Inc (USA). Citral, cineol and d-limonene were purchased from Sigma-Aldrich GmbH (Germany). All other chemicals used in the study were of analytical grade.

Preparation of invasomes

Invasomes were prepared by thin lipid film hydration method. In a round bottom flask, a mixture of 4.65 % w/v d9-DLPC with 0.35% w/v soy-LPC was dissolved in a 2:1 mixture of methanol:chloroform. Organic solvent mixture was evaporated using a rotary evaporator (Büchi Labortechnik GmbH, Germany). Lipid film was further dried under flowing nitrogen for 15 minutes. The lipid film was hydrated using a phosphate saline buffer (PBS) containing 10% w/v ethanol and 1% w/v terpene mixture containing citral:cineol:d-linonene (9:9:2). Multilamellar vesicles (MLVs) were prepared by thoroughly vortexing until the entire lipid film was dispersed. MLVs were further bath sonicated for 15 minutes followed by hand extrusion through 100 nm and 50 nm polycarbonate membranes 41 times to prepare the large unilamellar vesicles (LUVs).

Preparation of SERS substrates

SERS substrates were prepared according to Stöckle *et al.* (2000a) by evaporating glass cover slides with 6 nm silver and annealing for 60 seconds at 290°C. Before evaporative coating, glass cover slips were cleaned by placing them for 150 minutes in a mixture of HNO_3/H_2O_2 (3:1) and thoroughly washed afterwards to assure sufficient cleanliness.

Preparation of supported membrane bilayers

Supported membrane bilayers were prepared on cleaned glass cover slips to measure TER spectra originating from invasomes alone. Prior to any lipid deposition, glass cover slips were cleaned using a mixture containing concentrated HNO_3 : 30% H_2O_2 (3:1) for 2 hours followed by a series of distilled water washes. Cleaned cover slips were dried under vacuum. Invasomal LUVs prepared above were diluted with PBS to get final lipid concentration of 1 mg/ml. 20 µl of the diluted lipid dispersion was spread on a cleaned glass cover slip and was allowed to air dry. Excess lipid was removed by gently washing the cover slip three times with ultrapure water (Milli-Q® Advantage A10). Washed cover slip was then air dried and imaged using AFM to ensure successful bilayer formation. AFM tip was then replaced with a TERS tip and TER spectra are measured as described below.

Preparation of adhesive coated cover slips:

In tape stripping experiments, it is common practice to use commercially available adhesive tapes like TESA kristal klar® (Germany), Transpore® 3M (USA), D-squame® CuDerm (USA), for sampling of the SC. However, in this study application of commercially available adhesive tapes was not a feasible solution as imaging with an AFM requires sample mounted on a solid substrate. In our preliminary studies, a kristal klar® TESA adhesive tape was fixed on a glass cover slip using a double sided adhesive tape however this approach had a major disadvantage as it led to high internal reflections and scattering leading to poor TERS signal quality. To overcome this we developed a method to coat glass cover slips with a very thin layer of adhesive. These adhesive covered cover slips could directly be used for sampling the SC in place of adhesive tapes.

TESA adhesive mixture typically used in the preparation of kristal klar® adhesive tapes was used for coating the glass cover slips. A uniform coating of the adhesive was achieved with the help of an in-house custom built spin coating device. Prior to spin coating cover slips were cleaned as described above. A spin coating protocol was optimized by varying the duration of coating, RPM and amount of the adhesive placed on the cover slip at the beginning of the coating cycle to ensure thin, clear and uniform glue coverage on the glass surface. The adhesive was mixed well to ensure a uniform dispersion and 60 µl of the adhesive was spread uniformly on a glass cover slip attached to the sample holder of the spin coater. Cover slip was then accelerated uniformly at 85 RMP/sec till 3000 RPM and maintained for 30 seconds. After coating, cover slips were incubated at 40 °C for 12 hours. Adhesive coated cover slips were always prepared fresh before the experiment and were used within 48 hours after preparation. Amount of SC removed by individual adhesive cover slip was assessed by IR-densitometry using D-Squame Scan 850A (CuDerm, USA) as described previously (Franzen *et al.*, 2012; Klang *et al.*, 2011; Voegeli *et al.*, 2007).

Skin sample preparation:

To study the interactions between invasomes and the SC preliminary experiments were carried out on excised human skin using a Franz diffusion model. However, we shifted to *in vivo* model as removal of the SC using adhesive cover slips was much more consistent and uniform *in vivo* compared to the *ex vivo* model. Penetration experiments were performed on the volar surface of the left forearm of a representative subject (male, 30 years old). Area of the forearm was carefully shaved at least four hours prior to the start of the experiment and was washed again gently with tap water before start of the experiment. 100 µl/cm² of invasomes were applied to the skin with the help of a pipette. Formulation was contained in the applied area with the help of a polypropylene disc (with a 14 mm diameter hole) that was securely glued to the skin. Formulation was applied to the skin for a period of four hours after which the residual formulation was removed by gently washing the skin under tap water and then carefully wiping the skin with a lint-free tissue paper until the skin was dry. SC was removed

progressively using the adhesive coated cover slips. To limit the area for removal of the SC a mask made of nylon mesh (80 µm pore size, 130 µm thickness) with 14 mm diameter central hole was used. To ensure good contact between skin and adhesive coated cover slip, a 2 kg weight was placed on top of the cover slip for 10 seconds. The cover slip was ripped off in one uniform motion along with the nylon mask. Nylon mask was then removed and the cover slip was stored carefully. The process was repeated 10 times and samples were measured with AFM first followed by TERS. Pseudo absorption before and after sampling the SC was measured using D-Squame Scan 850A densitometer (Cuderm, USA). Experiments were approved by the ethical committee of the Friedrich-Schiller-Universität Jena, Germany. In case of untreated or control experiments, equivalent PBS was applied to the skin and rest of the sample preparation was carried out exactly like treated samples.

TERS measurements:

The TERS setup has the bottom illumination/bottom collection geometry as described before (Rasmussen and Deckert, 2006; Stöckle *et al.*, 2000b). In brief, our TERS setup consisted of Nanowizard III AFM (JPK Instruments AG, Germany) mounted on an inverted Raman microscope (IX71, Olympus, Germany). The excitation laser (532 nm) was focused onto the TERS tip and sample from below using an oil immersion objective (40x; 1.35 NA). Enhanced Raman signal was collected by the same objective and was directed towards the spectrometer (SP2750A, Acton Advanced, Princeton Instruments Roper Scientific, USA) through a dichroic beam splitter and a series of mirrors. Spectra were finally recorded using a CCD camera (Pixis 400, Princeton Instruments Roper Scientific, USA). Skin samples were mounted on a XY scanning piezo stage (P-733.2DD, Physik Instrumente, Germany). For all AFM and TERS measurements, AFM was operated in the intermittent contact mode. For standard AFM operation commercially available tips were used (Budget Sensors, Tap190Al-G) whereas the tips were evaporated with 25 nm silver for TERS experiments and stored under argon until usage. Skin samples were first imaged using AFM to gain an understanding of the topographical features of the sample. Post imaging, the AFM tip was replaced with a TERS tip. Tip-setting was done by aligning and then fixing the TERS tip in the focus of the excitation laser. After tip-setting, samples were scanned using the piezo sample scanner while the TERS tip recorded the topography. TER spectra were recorded by setting a grid of points on the region of interest on the scanned image. The measurement procedure and technique is described in great detail within a recent publication (Langelüddecke *et al.*, 2015).
During TERS measurements, laser power at sample was approximately 500 µW and acquisition time for each spectra varied between 3-5 seconds.

Data analysis:

Raw spectra were analyzed using IGOR Pro 6.36. AFM images were treated with JPK Data Processing software applying plane leveling and subtracting a polynomial fit from each line independently.

RESULTS AND DISCUSSION

Calibration of adhesive coated cover slips and sample preparation

Spin coating protocol used was consistent in producing thin and uniform adhesive coated cover slips. Average thickness of the adhesive film was 17.6 ± 2.85 µm (n = 15). Among different protocols tested, the protocol described above offered the best compromise between adhesiveness and film clarity. In general, subjecting cover slips to a smaller centrifugal force lead to thicker and more adhesive surfaces but such films were often not transparent. After tape stripping, microscopic evaluation showed an even distribution of corneocyte clusters on the surface of adhesive coated cover slips. However, clusters were less dense compared to the kristal klar® TESA tapes. For a quantitative comparison between the two adhesive devices, pseudo-absorption was measured before and after tape stripping using IR densitometry to measure the amount of stratum corneum removed during tape stripping. Figure 1 shows cumulative pseudo-absorption profiles of adhesive coated cover slips compared with kristal klar® TESA adhesive tapes. Linear profiles with small standard deviation indicate that adhesive cover slips were consistent at removing similar amounts of SC proteins. Average pseudo-absorption values for adhesive coated cover slips were 5.60 ± 1.74 units as compared to 9.0 ± 2.8 units for krystal klar® TESA tape, indicating our in-house adhesive coated cover slips were approximately 62 % as efficient at removing the stratum corneum compared to the kristal klar® TESA tape.

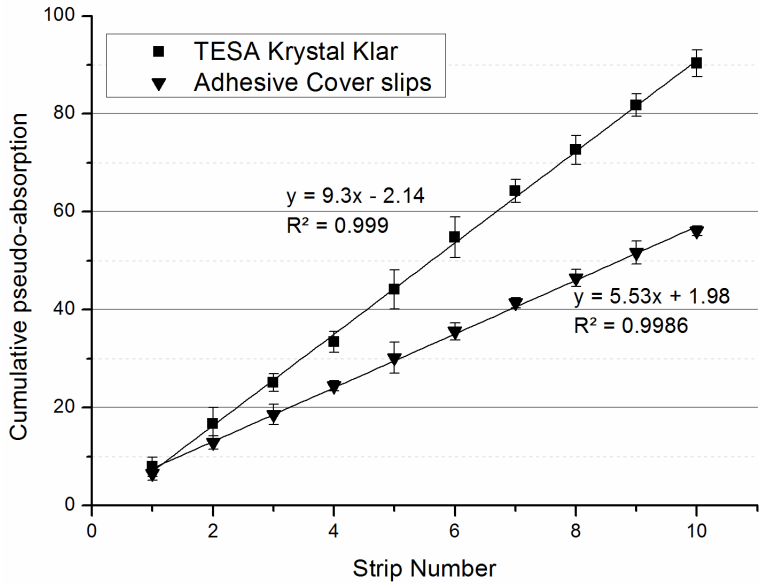

Figure 1: Pseudo-absorption profiles measured at 850 nm using D-Squame Scan 850A densitometer (n = 50).

Atomic force microscopy of treated and untreated skin:

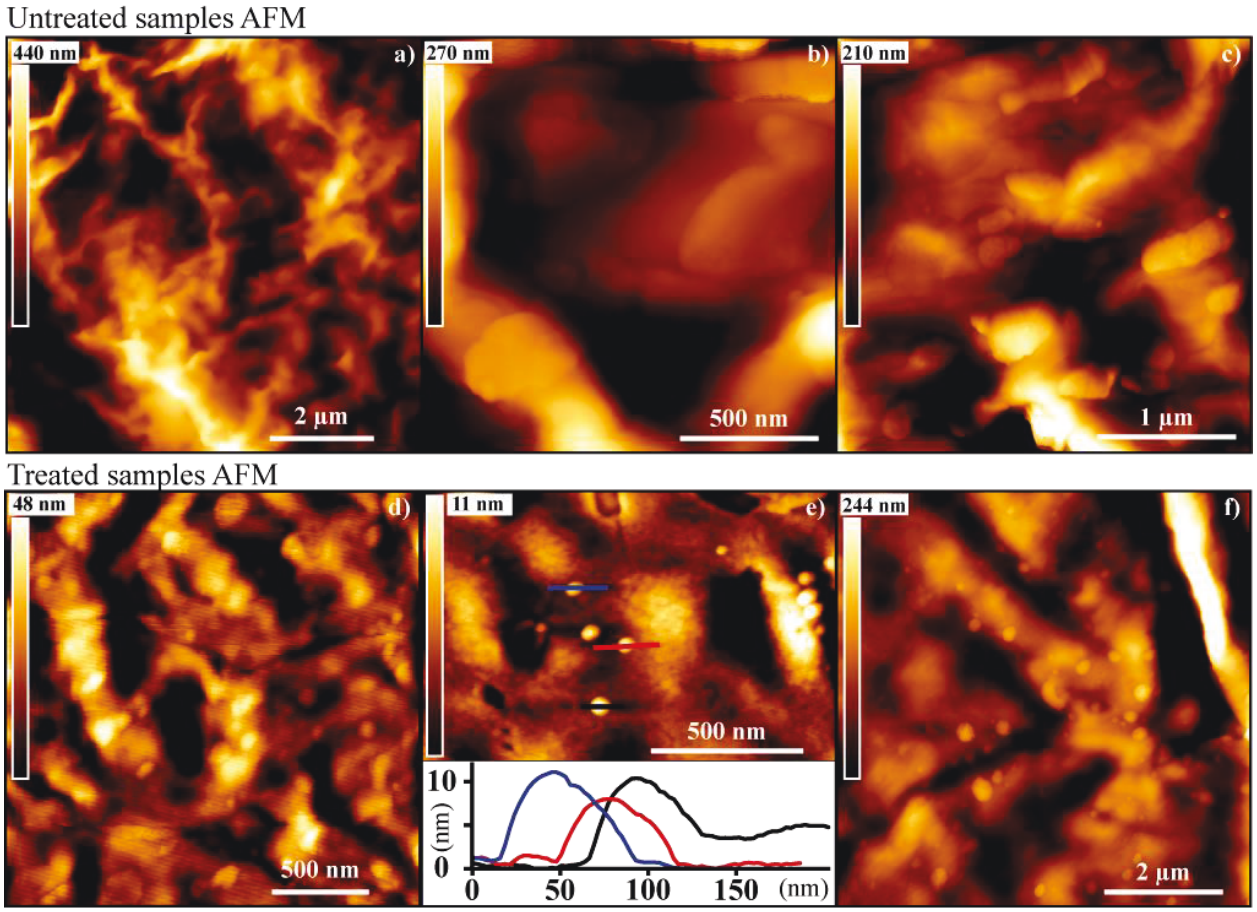

Figure 2: AFM images of stripped samples of untreated (top) and treated skin (bottom); a) and d) representing layer 1, b) and e) representing layer 5; and c) and f) representing layer 10, respectively; Inset in e) shows height profile for three flattened vesicles.

Average diameter for different batches of invasomes were in the range of 80-90 nm with polydispersity index of < 0.1. SC was progressively removed as explained in the methods section and all layers were analyzed using AFM to understand the topography of the samples and identify the regions of interest for TERS measurements. Figure 2 shows typical topographical features observed in untreated (Fig. 2 a-c) and treated (Fig. 2 d-f) stripped skin samples. Considerable differences were observed between untreated and treated samples, most notable was the persistent appearance of vesicular structures on the surface of corneocytes. This was a dominant feature observed in all treated samples especially in the deeper layers. Dimensions of these vesicular structures varied between 50 nm to 300 nm indicating some invasomal vesicles might have fused. Based on the height profiles, most of the vesicles appeared to be flattened. The inset in Fig. 2e shows height profiles for flattened invasomal vesicles from layer 5, which suggests the height of these structures to be between 5 to 10 nm indicating vesicles might consist of one or two phospholipid bilayers. It is possible that flat vesicular structures originated from the liposomal vesicles that managed to penetrate intact in the skin, however upon tape stripping intact liposomes would lose their aqueous contents as the samples were not frozen or fixed.

Treated and untreated skin samples also showed large oval structures with granular topography (shown by black arrows in Fig 3a). These structures were likely to be corneodesmosomes, which act as rivets between the neighboring corneocytes. These structures had size ranging from 150 – 600 nm and had heights between 15 – 80 nm, these figures agree with the dimensions of corneodesmosomes that were reported in the literature (Chapman and Walsh, 1990; Harding, 2004). Bouwstra group also reported such structures in the freeze fracture electron microscopic studies however they anticipate these structures to be corneodesmosomes or swollen keratin filaments perpendicular to the surface of corneocytes (Loan Honeywell-Nguyen *et al.*, 2002; van den Bergh *et al.*, 1999). Nevertheless, given the differences in the sample preparation methods, we consider over-hydration unlikely in our samples and the frequency of the feature's occurrence is more consistent with corneodesmosomes than keratin filaments. Invasomal vesicles could be distinguished from desmosomes based on shape and height profile. The oval-granular structures of desmosomes were not investigated in detail mainly because they do not significantly play a role in liposome penetration. Schatzlein and Cevc (1998) while studying penetration of Transfersomes® in murine skin using confocal laser scanning microscopy described intercorneocyte pathways between clusters of corneocytes. Loan Honeywell-Nguyen *et al.* (2002) have also reported similar channels in treated and untreated human stratum corneum. The Cevc group has hypothesized that these channels play a role in penetration of transfersomes into the SC. Although we did not find a substantial evidence for this claim, we did find channels or ridges in both untreated and treated samples. These channels are highlighted using black lines in Fig 3b in an untreated sample of layer-8. Black arrows in Fig 3b indicate the intercorneocyte boundary and it can be seen that these channels were not limited by the corneocyte boundaries. Fig 3c shows a small channel on layer 5 of a treated sample with three flattened vesicles. We would like to emphasize that although many 'channels' were observed on the surface of corneocytes, presence of vesicles in them as shown in Fig 3c was quiet rare.

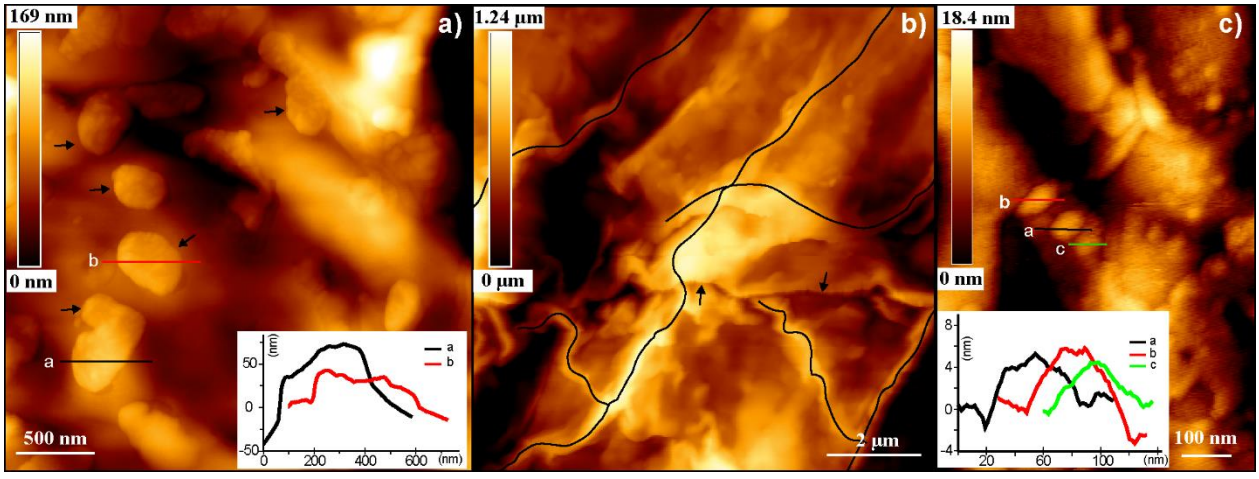

Figure 3: AFM images showing a) oval-granular structures as observed in layer 9 of untreated skin b) channels shown by black lines in layer 5 of an untreated skin, arrows indicate intercorneocyte boundary c) channel showing three flattened invasomal vesicles in layer 5 of invasome treated skin.

Flattened invasomal vesicles could be found in all 10 layers of the treated samples that were investigated however, they were more abundant in the lower layers especially from layer 5 to 10. Once regions of interest were identified in the layer, AFM tip was switched for a TERS tip and TER spectra were measured on the invasomal vesicles and regions of interest.

TER – spectra of head deuterated invasomes

Deuterated lipids in Raman spectroscopy enable the utilization of the C-D signal at around 2000-2300 cm^{-1} in the cell silent region. In our case, a big contrast between skin (lipids and proteins) and invasomal lipids is created. In order to keep the manipulation of the lipid as less as possible we prepare our invasomes from head-deuterated (d9) lipids. In addition, we think that using d9-lipids is the most convenient way to use SERS and TERS enhancement in our sample system. SERS and TERS make use of a strongly distance dependent near-field effect to enhance Raman signals by several orders of magnitude. In our study, a head-deuterated phospholipid was employed for preparation of invasomes as the lipid head groups are closest to the SERS substrate or TERS tip. This allows for easier detection in the experiments compared to chain deuterated phospholipids. The SER spectrum of adsorbed d9-DLPC bilayers (Fig 4b) shows a similar pattern as the Raman spectrum (Fig 4a) and is strongly enhanced under SERS/TERS conditions. The most prominent bands of d9-DLPC are marked and assigned in the SER and Raman spectra according to Bunow and Levin (1977) , which are 1) 2272 cm^{-1} (CD_3 asym. str.); 2) 2181 cm^{-1} (overtone, combination modes of acyl chains); 3) 2080 cm^{-1} (CD_3 sym. str.); 4) 1763 cm^{-1} (C=O str.); 5) 1655 cm^{-1} (C=C str.); 6) 1435 cm^{-1} (CH_2 deform.); 7) 1299 cm^{-1} (CH_2 twist deform.); 8) 1259 cm^{-1} (PO^-_2 asym. str.) and 9) 1077 cm^{-1} (PO^-_2 sym. str.). For further reference purposes we investigated supported bilayers of d9-DLPC adsorbed on glass with TERS and found that the TER spectral pattern differed from standard Raman and SERS. Fig 4c shows a TER spectra measured on d9-DLPC bilayers and it shows only one C-D peak compared to the four peaks seen in the SERS and Raman spectra. We believe the disparity between the SER/ Raman on the one hand and TER spectra on the other hand can be explained based on polarization effects due to the strong field gradient in TERS that results in an unusual polarization geometry (Deckert-Gaudig *et al.*, 2010; Meng *et al.*, 2015; Ossikovski *et al.*, 2007). Despite such peculiarities, TERS nevertheless allows the detection of the lipid head-deuteration, which is the main message from this experiment.

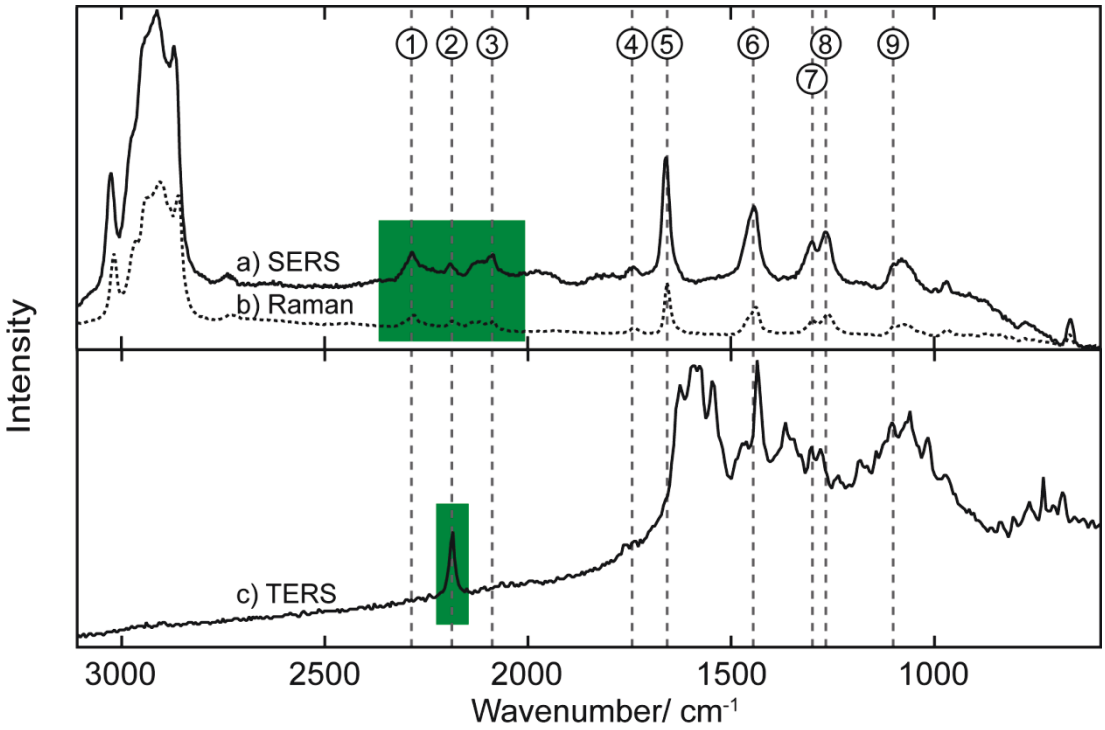

Figure 4: a) SER spectrum (bilayers; t_{acq}=10 sec), b) single Raman spectrum (powder; t_{acq}=25 sec) and c) TER spectrum (bilayers; t_{acq}=2 sec) from d9-DLPC; Raman and SER spectra show similar spectral patterns with enhanced signal in SERS and C-D bands at around 2200 cm^{-1}; the TER spectrum shows only one C-D band; marked bands in Raman and SERS are listed in the text.

Measurement of TER spectra on stratum corneum samples:

After identifying the regions-of-interest, TER spectra were mainly measured on the channels found on the surface of corneocytes (Figure 3b) and on flattened vesicles described in Figure 2b. TERS results shown in Figure 5 and 6 are split in two panels, respectively. Left panels show the sample topography on which the TERS grids were measured while the right panel shows the TER spectra. TER spectra were measured for each point on the TERS grid one at a time and the dotted arrows indicate the direction in which the TERS tip moved along the sample to measure the TER spectra. Figure 5a shows a channel with a TERS measurement grid placed on it and the first twenty TER spectra are plotted on the right. Spectra number 5-12 and 14-15 exhibit a C-D sym. str. peak at around 2150 cm^{-1} which is evidence for topically applied d9-DLPC present at these particular grid points. Nevertheless, sample topography around the grid is indicative of a lack of intact invasome vesicle and the lack of continuity in C-D positive spectra indicates that head-deuterated phospholipids from topically applied invasomes had diffused into the SC. Such a diffusion might be a result of the 'penetration enhancing mechanism' suggested by Maghraby *et al.* (2006). Such interactions might be a result of lipid exchange between the invasomal bilayer and SC lipids. The cholesterol peak at 700 cm^{-1} appearing in the spectra indicates that the TER spectra were measured on the SC intercorneocyte lipids as cholesterol forms a major fraction

of the SC lipids. An even more conclusive result indicating the phospholipid diffusion is presented in Figure 5b where a TERS grid was measured on a channel in the 5th layer. Analysis of the TER spectra revealed that the measurement points with C-D positive spectra were even further scattered over the measurement grid. An interesting facet of the result showed that the C-D active bands shifted within the TERS grid, which might be attributed to the polarization effects due to the TERS probe or even orientation of the phospholipid with respect to the TERS tip. Combined with the topography from the AFM and spectral analysis, it seems conclusive that (deuterated) phospholipids did diffuse in the SC.

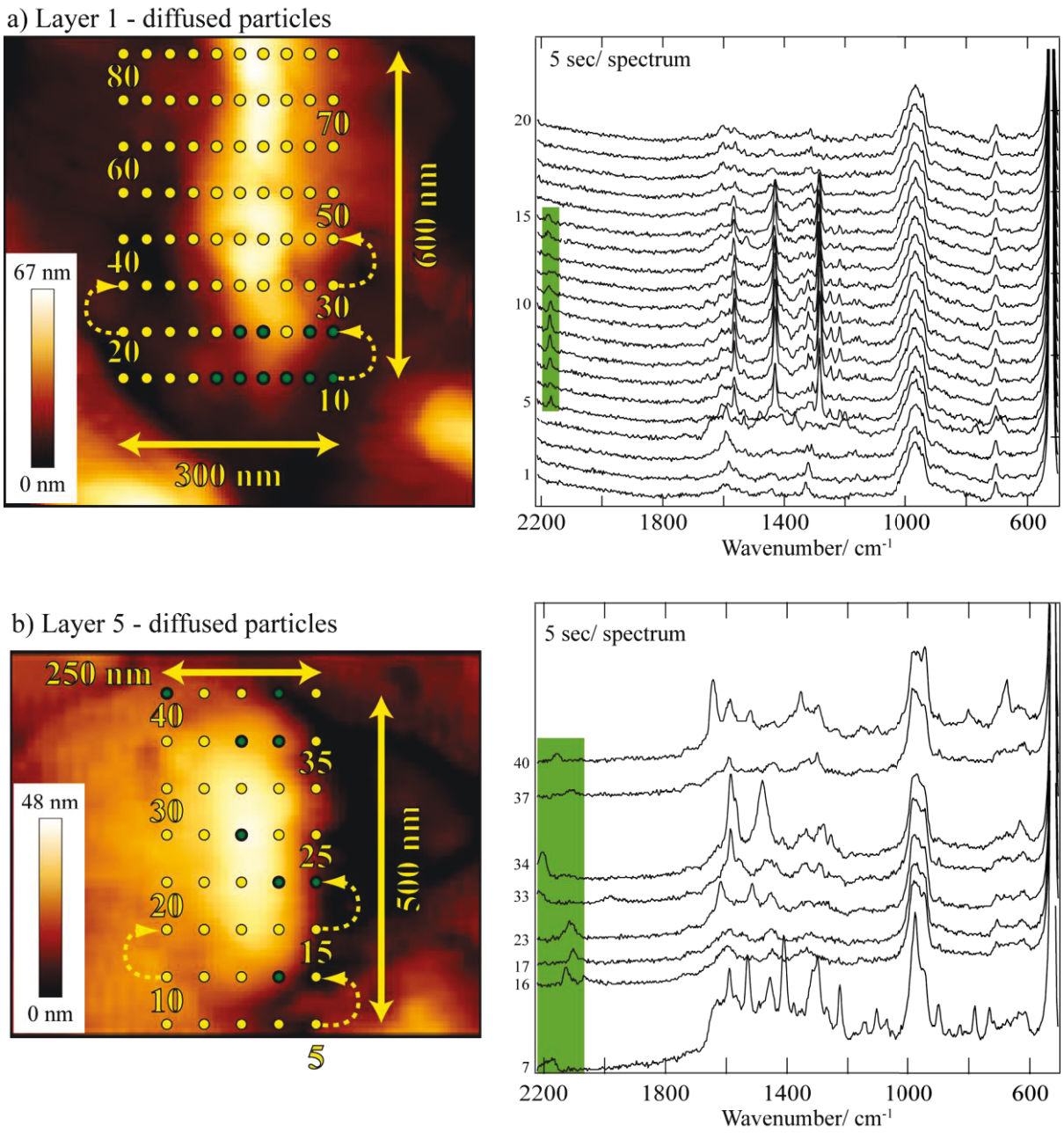

Figure 5:

a) AFM image of treated skin (Layer 1) showing a channel-like structure; a typical TERS measurement grid (8x10 points; Δx=30 nm, Δy=75 nm) is superimposed; topography differs from expected shape of a

flattened invasomal vesicle and showing locally concentrated C-D positive spectra (marked in green); result indicates diffusion of head-deuterated phospholipid from invasomes into the stratum corneum.

b) AFM image of a skin structure (treated skin) on Layer-5; TERS grid is superimposed (5x8 points; Δx=50 nm, Δy=62.5 nm); C-D positive spectra are marked in green in the AFM image; spectra correlated with topography are indicating diffused phospholipids from invasomes.

Figure 6a shows two flattened vesicles from the 7th layer of the stratum corneum. Four C-D positive TER spectra are observed in a 10x10 points measurement grid on the lower edges of the particles. In this image, we present two adjacent spectra to the C-D positive spectra in order to show the intactness of our TERS tip during the experiment. To show the intactness of our TERS tip we have presented two adjacent TER spectra to the C-D positive spectra. Usually, the C-D negative spectra show typical features from skin-own lipids and proteins such as amide II (~1560 cm^{-1}), CH_2 deform. (~1430 cm^{-1}), Amide III α-helix (~1280 cm^{-1}), PO_2^- asym. str. (~1250 cm^{-1}) and cholesterol str. ring (~700 cm^{-1}), respectively.

In Fig. 6b another flattened invasomal vesicle from the 5th layer of treated skin was investigated by measuring TER spectra at 25 points on a grid. We observed 6 C-D positive spectra in this grid. These six spectra can be nicely correlated with the topography and let us conclude that we probed an intact invasomal vesicle that penetrated down to the 5th layer of the *stratum corneum*.

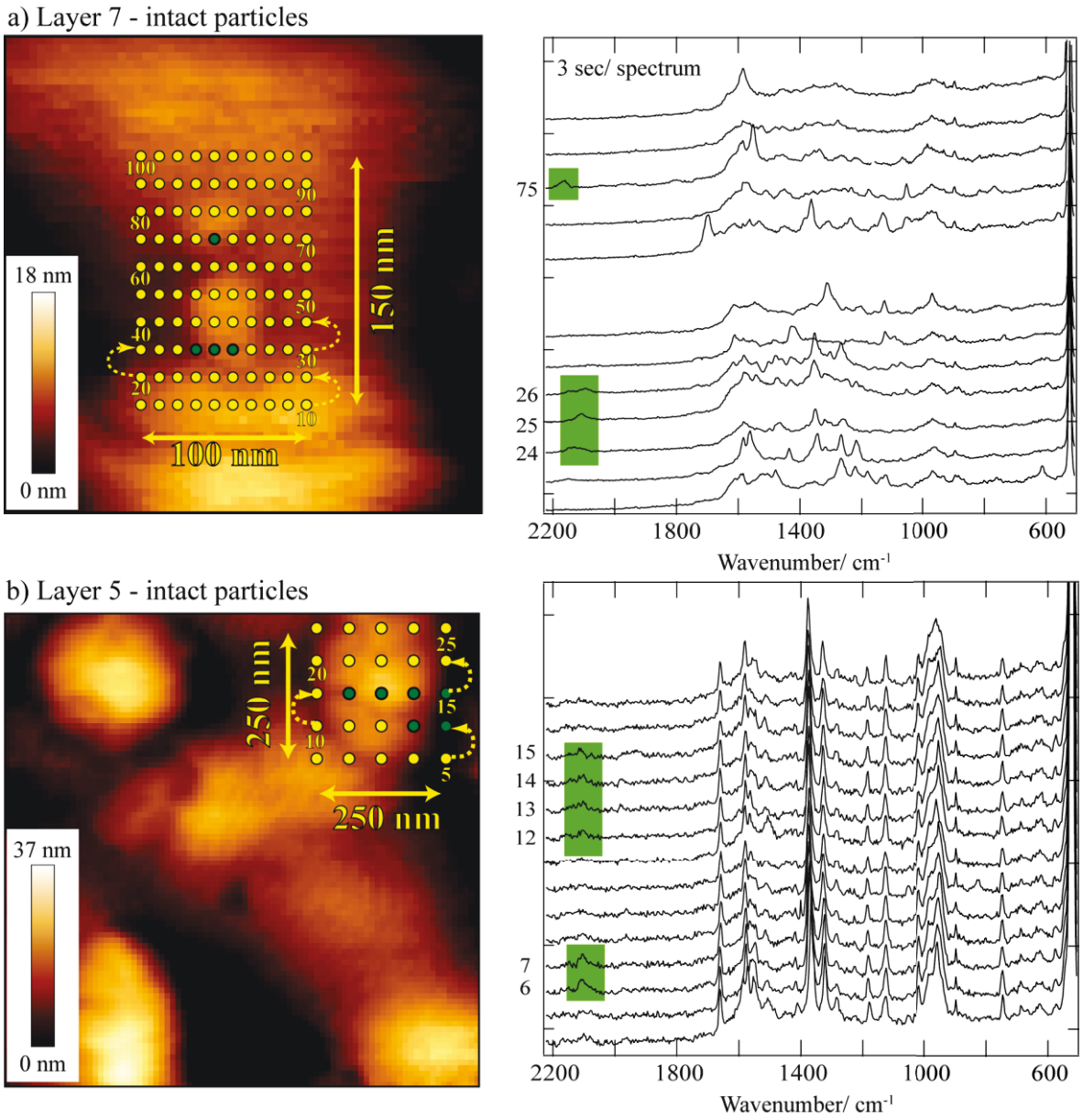

Figure 6:

a) AFM image of layer 7 from treated skin with superimposed TERS measurement grid (10x10 points; Δx=10 nm, Δy=15 nm); two flattened particles are visible; correlation of topography with C-D positive spectra show that an intact vesicle was probed; the position of the C-D positive spectra (at the bottom of each particle) can be explained by the non-uniformity of the enhanced field resulting from the tip geometry.

b) AFM image of layer 5 from treated skin with superimposed TERS measurement grid (5x5 points; Δx=50 nm, Δy=50 nm); an intact vesicle was probed; the continuity and position of C-D positive spectra are evidence that an intact particle was probed during experiment.

General Discussion

Motivation for the current study originated from the quest to understand the mechanism of liposomal drug delivery to the skin. Interactions between skin and liposomes have already been probed using

techniques like ATR-FTIR, DSC, SAXS, electron microscopy etc. TERS provides a unique opportunity to image and to detect deuterated invasomal phospholipids in the stratum corneum. Theoretically, based on the mechanisms discussed earlier there were three possible outcomes of the TERS study; a) no detection of d9-DLPC in the SC b) presence of diffused d9-DLPC in the SC or c) presence of intact invasomes in the SC. Based on these assumptions we measured TER spectra at multiple points on the surface of corneocytes. Grids measured on the corneocytes rarely showed presence of d9-DLPC and only in a few instances we had a strong indication of diffused d9-DLPC in the SC. In all the instances, the diffused d9-DLPC was detected on the channel-like structures found on the corneocytes. We should point out that detecting the phospholipid diffused after application of invasomes in the SC was like 'looking for a needle in a haystack' because there are no topographical structures to guide the placement of the TERS grids. Although the fact that it was harder to detect the deuterated phospholipid on the surface of the *stratum corneum* might point to either a very particular pathway or more likely point to the fact that only a small fraction of the applied phospholipid on the skin makes it in to the skin. Highlight of the present study was the demonstration of imaging and identifying invasomal vesicles penetrated deep into the SC after topical application. Although presence of flattened vesicles in the SC after liposomal application was also demonstrated by Hofland *et al.* (1995); and Loan Honeywell-Nguyen *et al.* (2002), our study presents, for the first time a spectroscopic evidence to identify the penetrating phospholipid vesicles. Based on the AFM studies, a higher density of vesicles was observed for the deeper layers (layer 5 to 10). Reason behind this observation was not clear but one might speculate that this phenomenon was either a result of rigorous washing of the skin to remove the residual formulation or that the formulation penetrates only in the first few minutes after application.

Discrepancies in the quantity of SC removed during tape stripping protocols are well documented (Holbrook and Odland, 1974; Jacobi *et al.*, 2005; Lademann *et al.*, 2009; Lindemann *et al.*, 2003; Marttin *et al.*, 1996). We would also like to point out that, it is rather difficult to predict how deep we can sample the SC using our stripping technique. Based on our densitometry results and our experience with tape stripping we would conservatively speculate that by layer 10 we should be at least 5 μm deep in the SC. From all the AFM data analyzed for layer 10, we estimated approximately 130 vesicles per 100 μm^2 of the SC. This number might seem large however, assuming a homogenous distribution of vesicles and an average invasome diameter of 80 nm, it means only 0.0003% of the invasomes applied topically reach the 10^{th} layer. In our opinion, this estimate only emphasizes the barrier function of the SC. In this study, we employed empty invasomes to shed a light on the role of phospholipid in delivery to the skin.

Based on our results transdermal drug delivery from liposomally entrapped drug is likely to be a multifaceted phenomenon that is likely to include intact liposomal penetration and decreased barrier function of the SC due to disturbed arrangement of intercorneocyte lipid domains. Given the small

fraction of invasomes that were observed on the 10th layer it is obvious that these two are not the only mechanisms involved in transdermal drug penetration. These results also highlight the importance of physicochemical properties of the drug and the partition coefficient of the drug between the SC and phospholipid bilayers. The simplicity in the sample preparation presented here coupled with the fact that samples can be measured at ambient conditions make TERS a very promising tool in carrying out such investigative studies in the SC.

Conclusions:

We have successfully demonstrated application of TERS to study the penetration mechanism of topically applied invasomes. After the invasome treatment, presence of flattened vesicles was observed on the surface of corneocytes. A head deuterated phospholipid was employed in the preparation of invasomes to distinguish the externally applied invasomes from endogenous contents of the SC. We successfully measured C-D TERS bands on the flattened vesicles confirming that invasomes can penetrate into the SC. Apart from invasomal vesicles we also found evidence of diffused deuterated phospholipid on the surface of corneocytes.

References:

Abbe E (1873) Beiträge zur Theorie des Mikroskops und der mikroskopischen Wahrnehmung. *Archiv f mikrosk Anatomie* 9:413-8.

Anderson MS (2000) Locally enhanced Raman spectroscopy with an atomic force microscope. *Appl Phys Lett* 76:3130-2.

Bouwstra JA, Honeywell-Nguyen PL (2002) Skin structure and mode of action of vesicles. *Adv Drug Deliv Rev* 54 Suppl 1:S41-55.

Brewer J, Bloksgaard M, Kubiak J*, et al.* (2013) Spatially resolved two-color diffusion measurements in human skin applied to transdermal liposome penetration. *J Invest Dermatol* 133:1260-8.

Bunow MR, Levin IW (1977) Raman spectra and vibrational assignments for deuterated membrane lipids: 1,2-Dipalmitoyl phosphatidylcholine-d9 and -d62. *Biochim Biophys Acta* 489:191-206.

Cevc G, Blume G (1992) Lipid vesicles penetrate into intact skin owing to the transdermal osmotic gradients and hydration force. *Biochim Biophys Acta* 1104:226-32.

Chapman SJ, Walsh A (1990) Desmosomes, corneosomes and desquamation. An ultrastructural study of adult pig epidermis. *Archives of Dermatological Research* 282:304-10.

Chen M, Liu X, Fahr A (2010) Skin delivery of ferulic acid from different vesicular systems. *Journal of biomedical nanotechnology* 6:577-85.

Deckert-Gaudig T, Kämmer E, Deckert V (2012) Tracking of nanoscale structural variations on a single amyloid fibril with tip-enhanced Raman scattering. *J Biophotonics* 5:215-9.

Deckert-Gaudig T, Rauls E, Deckert V (2010) Aromatic Amino Acid Monolayers Sandwiched between Gold and Silver: A Combined Tip-Enhanced Raman and Theoretical Approach. *J Phys Chem C* 114:7412-20.

Dragicevic-Curic N, Scheglmann D, Albrecht V*, et al.* (2008) Temoporfin-loaded invasomes: Development, characterization and in vitro skin penetration studies. *J Controlled Release* 127:59-69.

El Maghraby GM, Williams AC, Barry BW (2006) Can drug-bearing liposomes penetrate intact skin? *J Pharm Pharmacol* 58:415-29.

Essa EA, Bonner MC, Barry BW (2003) Electroporation and ultradeformable liposomes; human skin barrier repair by phospholipid. *J Control Release* 92:163-72.

506 Franzen L, Windbergs M, Hansen S (2012) Assessment of Near-Infrared Densitometry for in situ
507 Determination of the Total Stratum Corneum Thickness on Pig Skin: Influence of Storage Time. *Skin*
508 *Pharmacol Physiol* 25:249-56.

509
510 Harding CR (2004) The stratum corneum: structure and function in health and disease. *Dermatol Ther*
511 17 Suppl 1:6-15.

512
513 Hasanovic A, Winkler R, Resch GP*, et al.* (2011) Modification of the conformational skin structure by
514 treatment with liposomal formulations and its correlation to the penetration depth of aciclovir. *Eur J*
515 *Pharm Biopharm* 79:76-81.

516
517 Hayazawa N, Inouye Y, Sekkat Z*, et al.* (2000) Metallized tip amplification of near-field Raman
518 scattering. *Opt Commun* 183:333-6.

519
520 Hofland HE, Bouwstra JA, Bodde HE*, et al.* (1995) Interactions between liposomes and human
521 stratum corneum in vitro: freeze fracture electron microscopical visualization and small angle X-ray
522 scattering studies. *Br J Dermatol* 132:853-66.

523
524 Holbrook KA, Odland GF (1974) Regional Differences in the thickness (cell layers) of the human
525 stratum corneum: an ultrastructural analysis. *J Investig Dermatol* 62:415-22.

526
527 Jacobi U, Weigmann HJ, Ulrich J*, et al.* (2005) Estimation of the relative stratum corneum amount
528 removed by tape stripping. *Skin Res Technol* 11:91-6.

529
530 Klang V, Schwarz JC, Hartl A*, et al.* (2011) Facilitating in vitro Tape Stripping: Application of Infrared
531 Densitometry for Quantification of Porcine Stratum Corneum Proteins. *Skin Pharmacol Physiol*
532 24:256-68.

533
534 Knepp VM, Hinz RS, Szoka Jr FC*, et al.* (1987) Controlled drug release from a novel liposomal delivery
535 system. I. Investigation of transdermal potential. *J Controlled Release* 5:211-21.

536
537 Knepp VM, Szoka Jr FC, Guy RH (1990) Controlled drug release from a novel liposomal delivery
538 system. II. Transdermal delivery characteristics. *J Controlled Release* 12:25-30.

539
540 Kurouski D, Deckert-Gaudig T, Deckert V*, et al.* (2012) Structure and composition of insulin fibril
541 surfaces probed by TERS. *J Am Chem Soc* 134:13323-9.

542
543 Lademann J, Jacobi U, Surber C*, et al.* (2009) The tape stripping procedure--evaluation of some
544 critical parameters. *Eur J Pharm Biopharm* 72:317-23.

545
546 Langelüddecke L, Deckert-Gaudig T, Deckert V (2014) Spectroscopic Imaging of Biological Samples
547 Using Near-Field Methods. In: *Infrared and Raman Spectroscopic Imaging* (Salzer R, Siesler HW, eds)
548 Vol. -, Weinheim, Germany: Wiley-VCH Verlag GmbH & Co. KGaA, 477-512.

549
550 Langelüddecke L, Singh P, Deckert V (2015) Exploring the Nano Scale - 15 Years of Tip-Enhanced
551 Raman Spectroscopy. *Appl Spectrosc* accepted.

552
553 Lindemann U, Weigmann HJ, Schaefer H*, et al.* (2003) Evaluation of the Pseudo-Absorption Method
554 to Quantify Human Stratum corneum Removed by Tape Stripping Using Protein Absorption. *Skin*
555 *Pharmacol Physiol* 16:228-36.

556
557 Loan Honeywell-Nguyen P, de Graaff AM, Wouter Groenink HW*, et al.* (2002) The in vivo and in vitro
558 interactions of elastic and rigid vesicles with human skin. *Biochimica et Biophysica Acta (BBA)-*
559 *General Subjects* 1573:130-40.

560
561 Marr JM, Schultz ZD (2013) Imaging Electric Fields in SERS and TERS Using the Vibrational Stark Effect.
562 *J Phys Chem Lett* 4:3268-72.

563
564 Marttin E, Neelissen-Subnel MTA, De Haan FHN*, et al.* (1996) A Critical Comparison of Methods to
565 Quantify Stratum corneum Removed by Tape Stripping. *Skin Pharmacol Physiol* 9:69-77.

566
567 Meng L, Yang Z, Chen J*, et al.* (2015) Effect of Electric Field Gradient on Sub-nanometer Spatial
568 Resolution of Tip-enhanced Raman Spectroscopy. *Sci Rep* 5:9240.

569
570 Ossikovski R, Nguyen Q, Picardi G (2007) Simple model for the polarization effects in tip-enhanced
571 Raman spectroscopy. *Phys Rev B* 75:045412.

572
573 Prausnitz MR, Langer R (2008) Transdermal drug delivery. *Nat Biotechnol* 26:1261-8.

574
575 Qiu Y, Gao Y, Hu K*, et al.* (2008) Enhancement of skin permeation of docetaxel: a novel approach
576 combining microneedle and elastic liposomes. *J Control Release* 129:144-50.

577
578 Rasmussen A, Deckert V (2006) Surface- and tip-enhanced Raman scattering of DNA components. *J*
579 *Raman Spectrosc* 37:311-7.

580
581 Schatzlein A, Cevc G (1998) Non-uniform cellular packing of the stratum corneum and permeability
582 barrier function of intact skin: a high-resolution confocal laser scanning microscopy study using highly
583 deformable vesicles (Transfersomes). *Br J Dermatol* 138:583-92.

584
585 Shah SM, Ashtikar M, Jain AS*, et al.* (2015) LeciPlex, invasomes, and liposomes: A skin penetration
586 study. *Int J Pharm* 490:391-403.

587
588 Sonntag MD, Klingsporn JM, Garibay LK*, et al.* (2012) Single-Molecule Tip-Enhanced Raman
589 Spectroscopy. *J Phys Chem C* 116:478-83.

590

591 Stöckle RM, Deckert V, Fokas C*, et al.* (2000a) Controlled Formation of Isolated Silver Islands for
592 Surface-Enhanced Raman Scattering. *Appl Spectrosc* 54:1577-83.

593
594 Stöckle RM, Suh YD, Deckert V*, et al.* (2000b) Nanoscale chemical analysis by tip-enhanced Raman
595 spectroscopy. *Chem Phys Lett* 318:131-6.

596
597 van den Bergh BA, Vroom J, Gerritsen H*, et al.* (1999) Interactions of elastic and rigid vesicles with
598 human skin in vitro: electron microscopy and two-photon excitation microscopy. *Biochim Biophys*
599 *Acta* 1461:155-73.

600
601 vandenAkker CC, Deckert-Gaudig T, Schleeger M*, et al.* (2015) Nanoscale Heterogeneity of the
602 Molecular Structure of Individual hIAPP Amyloid Fibrils Revealed with Tip-Enhanced Raman
603 Spectroscopy. *Small* 11:4131-9.

604
605 Verma DD, Fahr A (2004) Synergistic penetration enhancement effect of ethanol and phospholipids
606 on the topical delivery of cyclosporin A. *J Control Release* 97:55-66.

607
608 Verma DD, Verma S, Blume G*, et al.* (2003) Particle size of liposomes influences dermal delivery of
609 substances into skin. *Int J Pharm* 258:141-51.

610
611 Voegeli R, Heiland J, Doppler S*, et al.* (2007) Efficient and simple quantification of stratum corneum
612 proteins on tape strippings by infrared densitometry. *Skin Res Technol* 13:242-51.

613
614 Xiao C, Moore DJ, Rerek ME*, et al.* (2005) Feasibility of tracking phospholipid permeation into skin
615 using infrared and Raman microscopic imaging. *J Invest Dermatol* 124:622-32.

616
617 Yokomizo Y, Sagitani H (1996) The effects of phospholipids on the percutaneous penetration of
618 indomethacin through the dorsal skin of guinea pig in vitro. 2. The effects of the hydrophobic group
619 in phospholipids and a comparison with general enhancers. *J Controlled Release* 42:37-46.

620
621 Zellmer S, Pfeil W, Lasch J (1995) Interaction of phosphatidylcholine liposomes with the human
622 stratum corneum. *Biochim Biophys Acta* 1237:176-82.

623
624 Zhang R, Zhang Y, Dong ZC*, et al.* (2013) Chemical mapping of a single molecule by plasmon-
625 enhanced Raman scattering. *Nature* 498:82-6.

626

627

3.4 Publication-4

LeciPlex, invasomes, and liposomes: A skin penetration study

Sanket M. Shah, Mukul Ashtikar, Ankitkumar S. Jain, Dinesh T. Makhija, Yuvraj Nikam, Rajiv P. Gude, Frank Steiniger, Aarti A. Jagtap, Mangal S. Nagarsenker, Alfred Fahr

International Journal of Pharmaceutics, Vol 490 (2015) 391-403.
Published on 19th May 2015.

International Journal of Pharmaceutics 490 (2015) 391–403

Contents lists available at ScienceDirect

International Journal of Pharmaceutics

journal homepage: www.elsevier.com/locate/ijpharm

LeciPlex, invasomes, and liposomes: A skin penetration study

Sanket M. Shah[a,1], Mukul Ashtikar[b,1], Ankitkumar S. Jain[a], Dinesh T. Makhija[c], Yuvraj Nikam[d], Rajiv P. Gude[d], Frank Steiniger[e], Aarti A. Jagtap[c], Mangal S. Nagarsenker[a,*], Alfred Fahr[b]

[a] Department of Pharmaceutics, Bombay College of Pharmacy, Kalina, Santacruz (East), 400098 Mumbai, India
[b] Friedrich-Schiller-Universität Jena, Institut für Pharmazie, Lehrstuhl für Pharmazeutische Technologie, Lessingstraße 8, 07743 Jena, Germany
[c] Department of Pharmacology, Bombay College of Pharmacy, Kalina, Santacruz (East), 400098 Mumbai, India
[d] Advanced Centre for Treatment, Research and Education in Cancer, Kharghar, 410210 Navi Mumbai, India
[e] Elektronenmikroskopisches Zentrum, Universitätsklinikum Jena, Ziegelmühlenweg 1, D07743 Jena, Germany

ARTICLE INFO

Article history:
Received 18 March 2015
Received in revised form 14 May 2015
Accepted 15 May 2015
Available online 19 May 2015

Keywords:
Skin delivery
Invasomes
LeciPlex
Liposomes
Cationic surfactants
Propionibacterium acne

ABSTRACT

The present study compares three vesicular systems, cationic LeciPlex, invasomes, and conventional liposomes for their ability to deliver drugs deep into the skin. Skin penetration ability of the three vesicular systems was studied for two drugs namely idebenone (antioxidant/anticancer) and azelaic acid (antiacne). All systems showed sizes in nanometer range with small polydispersity indices. Vesicular systems were characterized by CryoTEM studies to understand the differences in morphology of the vesicular systems. *Ex vivo* human skin penetration studies suggested a pattern in penetration of drugs in different layers of the skin: LeciPlex showed higher penetration for idebenone whereas invasomes showed higher penetration of azelaic acid. *Ex vivo* study using a fluorescent dye (DiI) was performed to understand the differences in the penetration behavior of the three vesicular systems on excised human skin. *In vitro* cytotoxicity studies on B16F10 melanoma cell lines revealed, when loaded with idebenone, LeciPlex formulations had the superior activity followed by invasomes and liposomes. *In vitro* antimicrobial study of azelaic acid loaded systems on *Propionibacterium acne* revealed high antimicrobial activity for DDAB leciplex followed by almost equal activity for invasomes and CTAB LeciPlex followed by liposomes. Whereas antiacne efficacy study in rats for azelaic acid loaded systems, invasomes exhibited the best antiacne efficacy followed by liposomes and LeciPlex.

1. Introduction

Drug delivery directed to skin layers is the most sought after and successful approach in treatment of various conditions like acne, eczema, psoriasis, keratinization, and skin cancer. Conventional transdermal dosage forms like ointments and gels, although easier to formulate, are not ideal formulation strategies for lipophilic drugs. Although creams can incorporate lipophilic drugs they tend to localize the drug in stratum corneum (Higuchi, 1960). Liposomal vesicular systems on the other hand have an advantage of incorporating both hydrophilic and lipophilic drugs still retaining the hydrophilic nature of the system aiding in penetration of the incorporated active agent and patient compliance. For any compound applied topically there are two basic mechanisms that have been suggested *viz.* transepidermal wherein the penetration is through the stratum corneum mainly following the trans-cellular route and trans-appendageal route wherein the permeation is through the sweat glands and across the hair follicles (Barry, 2006).

Liposomes are phospholipid based vesicular systems that have been extensively explored for skin delivery of drugs (Cevc, 1996; Mezei and Gulasekharam, 1980; Michel et al., 1992; Schaeffer and Krohn, 1982; Skalko et al., 1992). Advantages of using liposomes for skin delivery of drugs are well documented. Liposomes have been shown to have penetration enhancing effect and deliver a range of drugs with different physicochemical properties and

Abbreviation: Soy PC, soy phosphatidylcholine; Lyso PC, lyso phosphatidylcholine; PEG, polyethylene glycol; CTAB, cetyl trimethyl ammonium bromide; DDAB, didodecyl dimethyl ammonium bromide; PL90G, Phospholipon® 90G; PL90H, Phospholipon® 90H; PBS, phosphate buffer saline; CryoTEM, cryo transmission electron microscopy; SUV, small unilamellar vesicles; LUV, large unilamellar vesicles; DSPC, distearoylphosphatidylcholine; DPPC, dipalmitoylphosphatidylcholine; DMPC, dimyristoylphosphatidylcholine; RBF, round bottom flask.

* Corresponding author at: Bombay College of Pharmacy, Kalina, Santacruz (East), Mumbai 400098, Maharashtra, India. Tel.: +91 22 2667 0871; fax: +91 22 2667 0816.
E-mail addresses: mangal.nagarsenker@gmail.com, mangal_nag511@yahoo.co.in (M.S. Nagarsenker).

[1] These authors have contributed equally in preparation of the manuscript.

http://dx.doi.org/10.1016/j.ijpharm.2015.05.042
0378-5173/

even serve as a depot for sustained delivery of drugs that require local deposition (Gonzalez-Rodriguez and Rabasco, 2011). Factors affecting drug penetration from vesicular systems include lipid composition, size, lamellarity, mode of application whether occlusive or non-occlusive, lipid concentration *etc.* (Cevc and Blume, 1992; Weiner et al., 1989). Verma et al. (2003c) studied the effect of liposomal size on the penetration behavior of a hydrophilic and lipophilic fluorescent dye carboxyfluorescein and DiI respectively and concluded that the penetration was inversely proportional to the size of liposomal vesicles. Another important factor for dermal delivery is the fluidity of vesicle membrane. Many authors have reported that increasing the deformability or elasticity of vesicles lead to deeper penetration of the drug. This penetration enhancing effect has been attributed to mixing of the liposomal bilayer lipids with the intracellular lipids in the stratum corneum (Cevc et al., 1998a; Egbaria et al., 1991; Guo et al., 2000; Loan Honeywell-Nguyen et al., 2002; Paul et al., 1998; Planas et al., 1992; van den Bergh et al., 1999). Different theories for enhanced penetration of drugs delivered from liposomal systems have been proposed and reviewed (El Maghraby et al., 2008). These assumed penetration mechanisms can roughly be classified into five pathways. The 'free drug mechanism' proposes that the drug permeates through the skin independently after exiting from the vesicles (Ganesan et al., 1984). The 'penetration enhancing mechanism' suggests that lecithin causes ultrastructural changes in the stratum corneum leading to the enhanced transdermal passage of drug. The mechanism of 'vesicle adsorption to and/or fusion with the stratum corneum lipids' suggests that the vesicles adsorb/fuse with the stratum corneum leading to increased drug partitioning in the skin (Bouwstra and Honeywell-Nguyen, 2002). Whereas 'intact vesicular skin penetration' mechanism proposes the penetration of intact vesicles, especially in case of ultra-deformable liposomes called transfersomes (Cevc et al., 1998b; Cevc et al., 2003). The 'trans-appendageal passage' once disregarded has also received a lot of attention in the last decade as a primary penetration pathway (Andrea, 2005; El Maghraby et al., 2006; Patzelt and Lademann, 2013).

Cationic liposomes have been explored for delivery of many drugs. The mechanism for enhanced penetration is thought to be interactions between positively charged liposomal components with negatively charged components of the stratum corneum, which induce transfer between the liposome and skin (Kitagawa and Kasamaki, 2006). Cationic liposomes have been shown to improve skin delivery of drugs like retinoic acid (Kitagawa and Kasamaki, 2006), heparin (Song and Kim, 2006), meloxicam (Duangjit et al., 2013), fluorescent dye rhodamine (Katahira et al., 1999), acyclovir, and minoxidil (Hasanovic et al., 2010). Kitagawa and Kasamaki, (2006) demonstrated, up to 3.7 fold increase in penetration of retinoic acid from cationic liposomes in excised pig ear skin compared to its neutral counterpart.

LeciPlex is a positively charged phospholipid based vesicular system that has been explored for oral delivery of quercetin (Date et al., 2011a,b). The major components of a LeciPlex system are soy PC, a cationic agent, and a bio-compatible solvent like PEG 300, PEG 400, Transcutol® HP (diethylene glycol monoethyl ether), glycofurol (tetrahydrofurfuryl alcohol polyethylene glycol ether), Soluphor® P (2-pyrrolidone) or Pharmasolve™ (*N*-methyl-2-pyrrolidone) (Date et al., 2011a). The physicochemical properties of these bio-compatible solvents have been extensively reviewed (Shah et al., 2014). Earlier, LeciPlex have shown good improvement in oral bioavailability of quercetin with improved *in vivo* anticancer activity (Date et al., 2011b). The advantage of LeciPlex over conventional vesicular systems is in simplicity of preparation as it is a one-step fabrication process that yields nanosized vesicular systems by simple mixing (Date et al., 2011a). This is the first study that explores its potential in skin delivery of actives.

Invasome is a flexible, neutrally charged, phospholipid based vesicular system containing a mixture of soy PC, lyso PC, terpenes, and ethanol. This system has shown to improve skin penetration of hydrophilic and lipophilic drugs (Chen et al., 2011; Dragicevic-Curic et al., 2008a; Dragicevic-Curic et al., 2009; Verma and Fahr, 2004; Verma et al., 2003b). Flexibility of the bilayer membrane is mainly due to the lyso PC acting as an edge activator. Ethanol is a good penetration enhancer while terpenes have also shown potential to increase the penetration of many drugs by disrupting the tight lipid packing of the stratum corneum. (Ogiso et al., 1995; Ota et al., 2002; Puglia et al., 2001; Vaddi et al., 2002).

Vesicular systems have been studied extensively in conditions like skin cancer due to their potential to improve skin penetration and clinical efficacy of drugs like gemcitabine (Moog et al., 2002), vincristine (Guthlein et al., 2002), 5-Fluorouracil (Kaiser et al., 2003). According to the World Health Organization (WHO), skin cancer is one in every three cancers diagnosed with between 2 to 3 million non-melanoma skin cancers and 132,000 melanoma skin cancer cases occurring globally every year (WHO, 2014). Acne, a skin condition caused by *Propionibacterium acnes* infection is not a life threatening disease but certainly has a significant physical and psychological ramification such as permanent scarring, poor self-image, social inhibition, depression, anxiety, and in extreme cases suicidal tendency (Date et al., 2005; Gupta and Gupta, 1998).

The objective of this study was to test and compare the ability of LeciPlex, invasomes, and conventional liposomes to deliver drug into the deeper layers of human skin. Conventional liposomes, (referred as liposomes throughout the text) were chosen as a control to compare the skin penetration ability of LeciPlex formulations with respect to flexible liposomal formulation (invasomes). Idebenone (Fig. 1), a coenzyme Q10 analogue, has antioxidant free radical scavenging properties and has implications in management of melanoma (Wempe et al., 2009). Azelaic acid (Fig. 1), an aliphatic nine carbon dicarboxylic acid, is employed in the management of *P. acne* induced inflammation of acne (Date et al., 2005; Gollnick, 1993). LeciPlex, invasomes, and liposomes loaded with idebenone were investigated *ex vivo* to determine the extent of penetration on excised human skin and for their *in vitro* cytotoxicity on melanoma cell line. The vesicular systems loaded with azelaic acid were evaluated *ex vivo* to determine the extent of penetration on excised human skin, *in vitro* antimicrobial activity, and *in vivo* efficacy study on *P. acne* induced inflammation in rats.

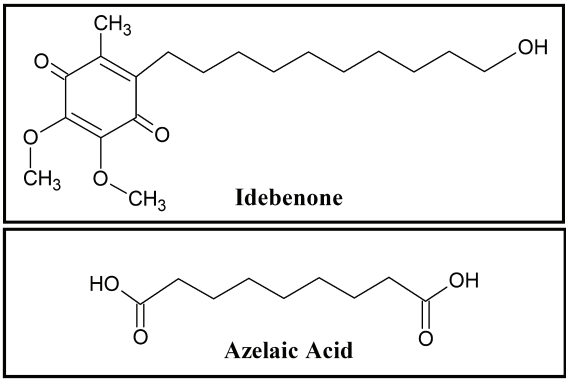

Fig. 1. Chemical structures of idebenone and azelaic acid.

2. Materials and methods

2.1. Materials

Idebenone and azelaic acid were purchased from Rxn Chemicals, India; and Sigma–Aldrich, India, respectively. Phospholipon® 90G and Phospholipon® 90H were gift samples from Lipoid GmbH, Germany. Transcutol® HP was a gift sample from Gattefossè India Pvt. Ltd., India. Cationic surfactant cetyltrimethylammonium bromide (CTAB) and didodecyldimethyl ammonium bromide (DDAB) were purchased from Sigma–Aldrich, India. NAT8539 (ethanolic solution containing 75% by weight soybean phospholipid. Phospholipid fraction contained phosphatidylcholine >73%, lyso PC < 7%, phosphatidylethanolamine < 7%, phosphatidylinositol < 5%, phosphatidic acid < 7%) was purchased from Lipoid GmbH, Germany. Limonene, citral, and cineole were purchased from Sigma–Aldrich, Germany. Actinomyces broth was purchased from Himedia Laboratories, India. Freeze dried *P. acne* strains were procured from Microbial Type Cell Culture and Gene Bank (MTCC), India. B16F10 melanoma cell line was procured from ATCC, USA. All the other chemicals and reagents used were of analytical grade unless otherwise specified.

2.2. Analytical method development

2.2.1. Idebenone

Idebenone was analyzed from skin samples on Hibar® Purospher™ STAR RP-18e HPLC column (250 mm, 4.6 mm × 5 μm, Merck KGaA, Germany) using a Shimadzu (Japan) LC-20AD liquid chromatography system and a Shimadzu SPD-M20A diode array detector. Mobile phase consisting of water and methanol in 20:80 ratio was maintained at a flow of 1 mL/min (Amorim et al., 2009). An injection volume of 20 μL was injected and the chromatograms were recorded at 279 nm using benzophenone as an internal standard. Chromatograms were recorded and processed using LC Solutions data management software.

2.2.2. Azelaic acid

Azelaic acid was analyzed from skin samples on Kromasil® 100-5C18 column (150 mm, 4.6 mm × 5 μm, Kromasil, Sweden) using a JASCO PU-2089 plus quaternary pump, JASCO AS-2055 plus intelligent sampler, and a JASCO MD-2018 plus photodiode array detector (Jasco corporation, Japan). Chromatograms were recorded and processed using ChromNAV CFR v1.18.06 software. Mobile phase (0.3885 g Ammonium acetate in water:methanol ratio of 60:40, pH was adjusted to 5.0 using glacial acetic acid) was maintained at a flow of 1 mL/min (Mansour and Ibrahiem, 2002). 100 μL samples were injected and chromatograms were recorded at 220 nm using sebacic acid (Sigma–Aldrich, Germany) as an internal standard.

2.3. Formulation of nanocarriers

2.3.1. LeciPlex

LeciPlex were prepared using a one-step fabrication process (Date et al., 2011a,b). DDAB LeciPlex were prepared by dissolving PL90G, DDAB, and drug in Transcutol® HP (see Table 1 for further details). To aid in dissolution, mixture was heated briefly to 70 °C in a water bath. Aqueous phase maintained at 70 °C was added to the transcutol solution under vortexing (Tarson SPINIX-VORTEX shaker, India) to form DDAB LeciPlex. To form CTAB LeciPlex (see Table 1), PL90G along with drug was dissolved in Transcutol® HP by heating the mixture briefly to 70 °C in water bath. CTAB was dissolved in water and maintained at 70 °C and was added to the Transcutol® HP solution under vortexing to form CTAB LeciPlex.

2.3.2. Invasomes

Drug was weighed into a RBF and dissolved in about 3 mL mixture of chloroform:methanol (2:1) along with NAT8539 (Table 1). The lipid film was formed with the help of Rotavapor® (Buechi, Germany) with gradual pump down sequence of 500 mbar (5 min), 200 mbar (5 min), 100 mbar (5 min), and 40 mbar (1 h at room temperature). This film was further dried under nitrogen for 15 min. To the lipid film, mixture of terpenes was added followed by addition of filtered saline phosphate buffer pH 7.4 (PBS) and ethanol. The lipid film was thoroughly vortexed to form multilamellar vesicles (MLVs). MLVs were extruded 41 times through polycarbonate membranes (Armatis, Germany) with pore diameter of 100 nm to ensure homogenous dispersion.

2.3.3. Liposomes

Liposomes were prepared by lipid film hydration technique. Briefly, PL90G, and PL90H were dissolved in chloroform along with the drug (Table 1). Organic phase was slowly removed on a Rotavapor® (Buechi, Switzerland) maintained at 40 °C and at speed of 100 rpm with a pump down sequence of 600 mbar (5 min), 400 mbar (5 min), 200 mbar (5 min), and 60 mbar (1 h). The dried lipid film was hydrated using Milli-Q® water (Merck Millipore Direct-Q®3, Germany) and MLVs were allowed to anneal. Size reduction of liposomes was performed using a bath sonicator (Trans-O-sonic, D250/IH, India) for a total duration of 10 min at 25 °C.

2.4. Formulation of nanocarriers gel

All three systems *viz.* LeciPlex, invasomes, and liposomes had low viscosity, hence for *in vivo* experiments, vesicular formulations were dispersed into a suitable gel. Carbopol® 940, Methocel™ K4M, and Polaxamer 188 were investigated for their ability to improve topical applicability. To prepare gels of LeciPlex, Liposome, and Invasome systems, gelling agents at 2% w/v concentration were added in small aliquots under agitation to

Table 1
Formulation details of vesicular systems LeciPlex, invasomes, and liposomes.

Components	CTAB LeciPlex	DDAB LeciPlex	Invasomes	Liposomes
PL90G	31 mg/mL	18.6 mg/mL	–	27.4 mg/mL
PL90H	–	–	–	3.1 mg/mL
NAT8539	–	–	133 mg/mL	–
Terpenes (Cineole:Citral:D-limonene in ratio 4.5:4.5:1.0)	–	–	10 mg/mL	–
Ethanol	–	–	100 mg/mL	–
CTAB	2.9 mg/mL	–	–	–
DDAB	–	15.1 mg	–	–
Transcutol® HP	50 μL/mL	50 μL/mL	–	–
Drug (Idebenone or azelaic acid)	2.5 mg/mL	2.5 mg/mL	2.5 mg/mL	2.5 mg/mL
Dispersion medium	Milli-Q® water	Milli-Q® water	PBS, pH 7.4	Milli-Q® water

the vesicular systems. Gels were prepared just before application in the *in vivo* study and were allowed to hydrate for 1 h before use.

2.5. Characterization of nanocarriers

2.5.1. Particle size distribution

Particle size distribution was measured by photon correlation spectroscopy (N5 Submicron particle size analyzer, Beckman Coulter Inc., USA) employing a 25 mW He–Ne laser (wavelength 632.8 nm) incident on the sample at an angle of 90°. LeciPlex, and liposomes were diluted with Milli-Q® water and invasomes were diluted with filtered PBS pH 7.4 (0.22 μm, Ultipor®N68 Nylon 6,6 membrane, Pall Life Science, Mumbai) to achieve optimal scattering intensity ($(1–10) \times 10^5$ counts/s). Samples were equilibrated at 24 °C before measuring particle size.

2.5.2. Zeta potential

Zeta potential of LeciPlex, invasomes, and liposomes was evaluated using a Zetasizer (Nano ZS; Malvern, UK) and analyzed using the Nano ZS version 6.34. Briefly, Leciplex and liposomes were appropriately diluted with 10 mM sodium chloride solution and zeta potential was measured using a disposable zeta cell DTS 1060C (Malvern, UK). For measuring the zeta potential of invasomes, PBS was used as a dilution medium.

2.5.3. Entrapment efficiency

Entrapment efficiency was determined by diluting the delivery system with saturated sodium chloride solution followed by ultracentrifugation at 80000 rpm for 45 min at 4 °C. The supernatant was analyzed by using the HPLC method described earlier in Section 2.2 and % entrapment efficiency was calculated.

2.5.4. CryoTEM

Cryo TEM study of various formulations was undertaken to study the morphology of systems under investigation. For the electron microscopic investigations, 5 μL of each sample was applied to Quantifoil® copper grids R1.2/1.3 (Quantifoil, Germany), coated with a perforated (circular holes with 1.2 μm in diameter) carbon film. The grids were mounted on a plunger, blotted (blotting time 2 s) and vitrified in liquid ethane at −180 °C. After plunging, the samples were transferred immediately with a Gatan 626 (Gatan Inc., USA) cryo holder to the Philips (Philips, Netherland) CM120 transmission cryoelectron microscope (LaB_6 cathode source operated at 120 kV accelerating voltage and stage maintained at –178 °C). Images were recorded with a 1 k × 1 k Fast Scan-F114CCD Camera (TVIPS GmbH, Germany). In order to minimize the noise, five images were recorded and averaged to one image.

2.6. Ex vivo human skin penetration study

2.6.1. Preparation of human skin

Excised human skin from female patients who had undergone abdominal plastic surgery (Praxis für Plastische Chirurgie, Kassel, Germany) was used to study the *ex vivo* penetration of idebenone and azealic acid from different delivery systems. Immediately after the abdominoplasty, subcutaneous fat was removed and skin was cleaned to remove any debris of blood or fat. Skin was cut into manageable pieces and wrapped in aluminum foil and stored at −26 °C for later use. Integrity of the skin was checked visually and by measuring trans-epithelial water loss (Vapometer®, Delfin Technologies Ltd., Finland). All protocols and standard operating procedures for acquiring and processing of the human skin were approved by the ethics committee of University Hospital-Jena, Germany.

2.6.2. Ex vivo penetration experiments

Vertical Franz diffusion cells with diffusion area of 3.14 cm^2 and diffusion volume of 15 mL were used for this study. Just before the penetration experiment, skin discs were punched, thawed for 1 h and then hydrated using PBS for another hour. PBS was used as an acceptor medium in the Franz cells. PBS was degassed under low pressure for 30 min just before mounting the skin on to the Franz cells. Skin was mounted with stratum corneum side up. During mounting, caution was exercised to remove all the air bubbles between the dermis and diffusion medium. Skin was stretched uniformly to avoid any wrinkles. Skin surface was maintained at 32 °C by circulating water at 37 °C through the outer jackets of the Franz diffusion chambers. Formulations were applied to the skin non-occlusively (infinite dosing, 100 μL/cm^2) with the help of a pipette. Using an inoculation loop, the dose was distributed uniformly on the skin surface. The applied formulation was thoroughly removed 6 h after application of dose. For dose removal, the remaining formulation was gently wiped off with a cotton swab and then the skin surface was further cleaned by rinsing the surface with 1 mL of MilliQ® water three to five times as required, followed by cleaning with a cotton swab.

2.6.3. Tape stripping

After dose removal, skin was mounted on to a tape stripping block with the help of cork discs and stainless steel pins. Skin was gently stretched to remove any wrinkles. With the help of a teflon mask of diameter 1.5 cm, a fixed area of stratum corneum was removed progressively using 10 adhesive tapes (Kristall Klar® Tesa, Germany). An adhesive tape was placed on the skin and a weight of 2 kg was placed gently on the tape for 10 s to ensure uniform contact between the skin and adhesive tape. After 10 s, the weight was removed and adhesive tape was removed in one quick motion. Tape strip was transferred to a suitably sized glass vial for further extraction. For ease of analysis, tape number 1 to 5 and 6 to 10 were pooled together.

2.6.4. Extraction of drug from skin samples

After tape stripping, viable epidermis (referred to as epidermis from here on) was removed by careful scraping with the help of a scalpel. Dermis was then cut into small pieces and collected into 2 mL homogenization vials (PEQLAB Ltd., Germany). Each homogenization vial was preloaded with a combination of 1.4 and 2.8 mm zirconium beads. The extraction solvent used was a mixture of PBS and methanol in 1:1 ratio. 2 mL extraction solvent was used for tape strips and 1 mL for epidermis and each dermis sample. Vials containing the tape strips were kept in a bench shaker at room temperature for 24 h. Epidermis and dermis samples were homogenized using three 6000 rpm cycles (Precellys® 24, Bertin Technologies, France). Post extraction, homogenate was collected in microcentrifuge tubes and centrifuged at 13000 rpm (Mini-Spin®, Eppendorf, Germany) for 10 min and the supernatant was analyzed by analytical methods described earlier.

2.7. Confocal microscopy study for determining distribution of DiI in human skin

Formulations with lipophilic fluorescent dye DiI [(2Z)-2-[(E)-3-(3,3-dimethyl-1-octadecylindol-1-ium-2-yl)prop-2-enylidene]-3,3-dimethyl-1-octadecylindole perchlorate] were prepared to analyze the penetration behavior of different vesicular systems and to see if any information pertaining to the penetration mechanism can be obtained. Vesicular formulations were prepared as described earlier with 0.65 mg/mL of DiI in each vesicular system. The fluorescent formulations were applied to human skin mounted on a Franz diffusion cells for duration of 12 h. After the penetration experiment, residual dose from surface of the skin was

removed as described earlier. Skin was cut into small manageable pieces and plunged into liquid nitrogen. Vitrified skin was then mounted onto a cryotome sample holder and 20 μm sections were taken perpendicular to the surface of the skin. The cut sections were placed on a glass slide and maintained at −26 °C until observation by confocal laser scanning microscopy (CLSM). Confocal imaging was performed using a Zeiss LSM 510 (Zeiss, Germany) inverted microscope using an argon laser line at 488 nm as an excitation source. HFT UV/488-5 dichroic mirror was used for splitting the beam and the reflected beam from the sample was passed through LP560 emission filter before detection. All images were recorded using constant gain and incident intensity. The raw images were processed using ImageJ software 1.48 v (Rasband, 1997–2014).

2.8. In vitro cytotoxicity study for idebenone formulations

Delivery systems loaded with idebenone were evaluated for their cytotoxicity potential using B16F10 melanoma cell line. Cell lines were grown in Dulbecco's modified eagle's medium (DMEM) containing 10% fetal bovine serum and 2 mM L-glutamine at 37 °C, 5% CO_2, 95% air and 100% relative humidity for 24 h prior to addition of formulations. Idebenone solution was prepared in 30% v/v Transcutol® HP and sterile filtered. Formulations were incubated for 72 h with the cells. After incubation, the microtitre plates were centrifuged and the supernatant was discarded. The cells that adhered to the bottom were treated with [3-(4,5-dimethylthiazolyl-2)-2,5-diphenyltetrazolium bromide] (yellow tetrazolium MTT) and were incubated for another 4 h. Post incubation, the purple colored formazan crystals were dissolved in 100 μL of DMSO and the plate was read on a microplate reader at 570 nm.

2.9. In vitro antimicrobial study for azelaic acid formulations

P. acne (1×10^5 CFU/mL) was cultured in actinomyces broth as described by Nakatsuji et al. (2009). Dilutions of azelaic acid formulations were added to a sterile 96 well plate (90 μL bacterial culture + 10 μL azelaic acid formulation) such that the concentration of azelaic acid ranged from 10^{-4} M to 10^{-7} M. Blank medium was used as a negative control. The plates were incubated under anaerobic conditions at 37 °C for 72 h. Post incubation plates were read on a plate reader (MODULUS microplate reader, Turner Biosystems, USA) at 600 nm. % bacterial cell viability was determined using the readings for untreated control and respective treated formulation groups (Nakatsuji et al., 2009).

2.10. In vivo efficacy study for azelaic acid formulations

Female Wistar rats (8–10 weeks old) in weight range of 200–250 g were used for the to study. After appropriate dilution with physiological saline, *P. acne* strain was injected (20 μL equivalent to 1.5×10^7 CFU) using a 30 gauge needle intradermally into the mid-ventral side of right ear of ether-anaesthetized rats. Ear thickness was measured using a micrometer screw gauge at different time points to determine the progression of acne in different animal groups. Vesicular systems of azelaic acid were dispersed into gels, as explained in Section 2.4 and were topically applied 1 day after injection of *P. acne* and the change in development of acne was studied for a total period of 10 days. Azelaic acid suspension (2.5 mg/mL) was used as a control and was also dispersed into a gel as explained in Section 2.4. The reduction in the thickness (mm) of acne was used to evaluate effectiveness of the formulations. Animal study was approved by the institutional ethics committee (protocol # CPCSEA/BCP/2010/05).

2.11. Statistical analysis

Data were expressed as mean ± standard error of mean (SEM) of multiple determinations along with Student's t-test using GraphPad Prism 5 (GraphPad Software, Inc., USA). The differences were considered statistically significant if $p < 0.05$.

3. Results

3.1. Analytical method development

Reverse phase HPLC methods adopted could successfully separate idebenone and azelaic acid from the skin components. Skin components eluted by 4 min of the run time for the given HPLC conditions and for all samples, the drug eluted after the skin components.

3.1.1. Idebenone

The retention time for idebenone (LOD: 30 ng/mL; LOQ: 100 ng/mL) and internal standard benzophenone were 10.9 and 6.9 min, respectively with benzophenone having a relative retention time of 0.65. Linearity of response ($r^2 = 0.99$) was observed from 0.5 μg/mL to 10 μg/mL.

3.1.2. Azelaic acid

The retention time for azelaic acid (LOD: 0.2 μg/mL; LOQ: 0.6 μg/mL) and internal standard sebacic acid was 7.8 and 17.1 min, respectively with sebacic acid having a relative retention time of 2.20. Linearity of response ($r^2 = 0.99$) was observed from 1.0 μg/mL to 50 μg/mL.

3.2. Characterization of nanocarriers

3.2.1. Particle size

All the delivery systems were nanosized as observed by dynamic light scattering (Table 2) and were in accordance with the size obtained by CryoTEM (Fig. 2 and Fig. 3). LeciPlex formulations had average sizes ranging from 250 nm to 350 nm and PDI from 0.2 to 0.4. Invasomes had a size of about 140 nm with

Table 2
Characterization of nanocarriers.

Drug	Formulations	Particle size (nm) ± Std Dev/PDI ± Std Dev	Zeta potential (mV) ± Std Dev	% Entrapment efficiency
Idebenone	CTAB LeciPlex	350.5 ± 3.8/0.436 ± 0.044	+66.8 ± 0.8	95.75
	DDAB LeciPlex	352.0 ± 4.4/0.197 ± 0.100	+64.3 ± 1.0	98.15
	Invasomes	134.4 ± 1.267/0.093 ± 0.003	−14.8 ± 1.61	93.6
	Liposomes	288.3 ± 0.2/0.400 ± 0.127	−1.6 ± 2.1	98.18
Azelaic acid	CTAB LeciPlex	263.8 ± 1.6/0.453 ± 0.002	+64.9 ± 6.7	97.3
	DDAB LeciPlex	296.8 ± 3.0/0.208 ± 0.020	+64.7 ± 8.0	95.2
	Invasomes	139.2 ± 0.080/0.072 ± 0.006	−13.6 ± 1.05	92.1
	Liposomes	147.0 ± 0.4/0.433 ± 0.056	+3.6 ± 3.0	97.2

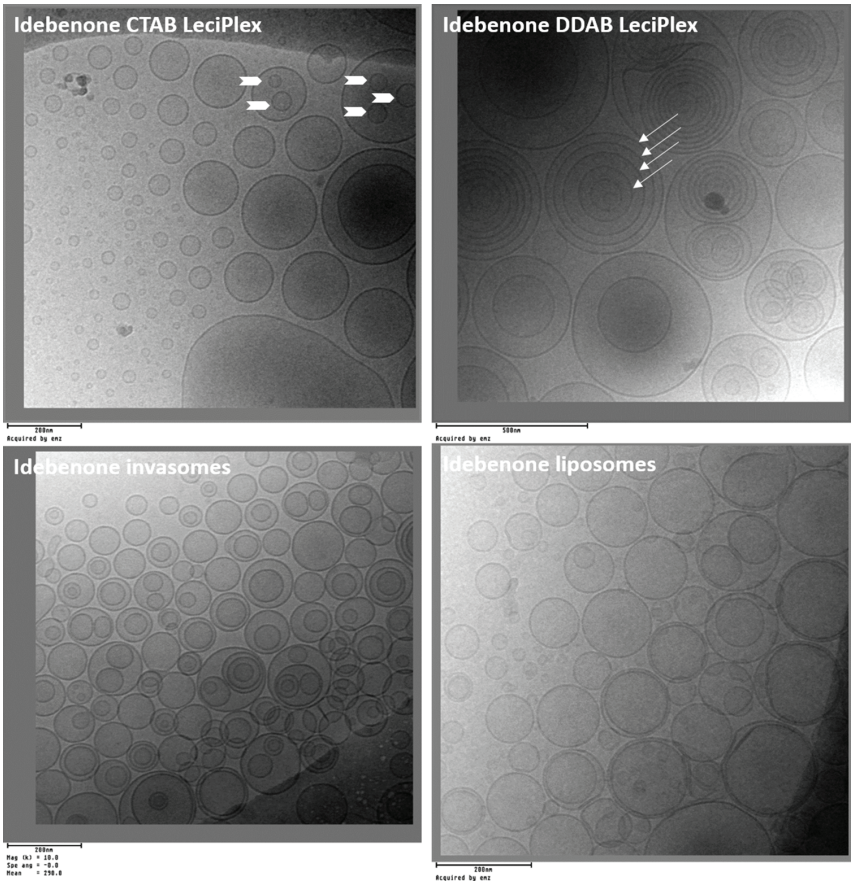

Fig. 2. CryoTEM investigation of LeciPlex, invasomes, and liposome loaded with idebenone. A unique feature of LeciPlex prepared using CTAB is presence of multivesicular liposomes (white solid filled arrows), which are unilamellar in nature. A unique feature of LeciPlex prepared with DDAB is the presence of well differentiated concentric rings of each lamella (white arrows) suggesting presence of special plurilamellar vesicles.

PDI <0.1. Idebenone liposomes had an average size of 288 nm with PDI of 0.4 while azelaic acid liposomes were smaller at 147 nm and with a PDI of 0.4. Higher sizes and PDIs of LeciPlex formulations were because they were mainly prepared using a single step mixing without homogenization.

3.2.2. Zeta potential

The zeta potential for both idebenone and azelaic acid loaded-CTAB LeciPlex or DDAB LeciPlex was more than +60 mV (Table 2). High positive zeta potential for LeciPlex system gives it a good colloidal stability. Liposomal formulations were neutral as there were no charge imparting components. Idebenone loaded liposomes had a zeta potential of −1.6 mV and azelaic acid loaded liposomes had a zeta potential of +3.6 mV. Invasomes had slightly negative zeta potential around −13 mV which was probably due to the presence of phosphatidic acid and phosphatidylinositol present in NAT8539.

3.2.3. Nanocarrier gels

For *in vivo* experiments, azelaic acid vesicles were incorporated into a 2% Methocel™ K4M gel. Governing choice in selection of the gelling agent was ease of gel formation, adequate viscosity and homogeneity of the final gel formulation. Although we did not measure the viscosity of the final vesicular gels, viscosity was acceptable for topical application and had adequate applicability in an *in vivo* efficacy study.

3.2.4. % Entrapment efficiency

The entrapment efficiency for both idebenone and azelaic acid-loaded vesicular systems was more than 90% (Table 2). Idebenone as well as azelaic acid were loaded in liposomes, invasomes, and LeciPlex at a concentration of 2.5 mg/mL, despite different drug to lipid ratios, all formulations were loaded with equal amount of drug to keep the same concentration gradient of drug for *ex vivo* skin penetration study.

3.2.5. CryoTEM

CryoTEM images of vesicular systems loaded with idebenone and azelaic acid are shown in Fig. 2 and Fig. 3. LeciPlex had a very unique and a distinguishable feature. CTAB LeciPlex showed mostly unilamellar and plurilamellar vesicles. DDAB Leciplex showed well-defined special plurilamellar systems, with the lamellas arranged in a definitive pattern resembling concentric rings, which are characteristically apart from each other. This system is different from the multilamellar liposomes in which the lamellas are very closely packed. These special structures could be triggered by the presence of CTAB or DDAB as formulation components and Transcutol® HP as a biocompatible cosolvent.

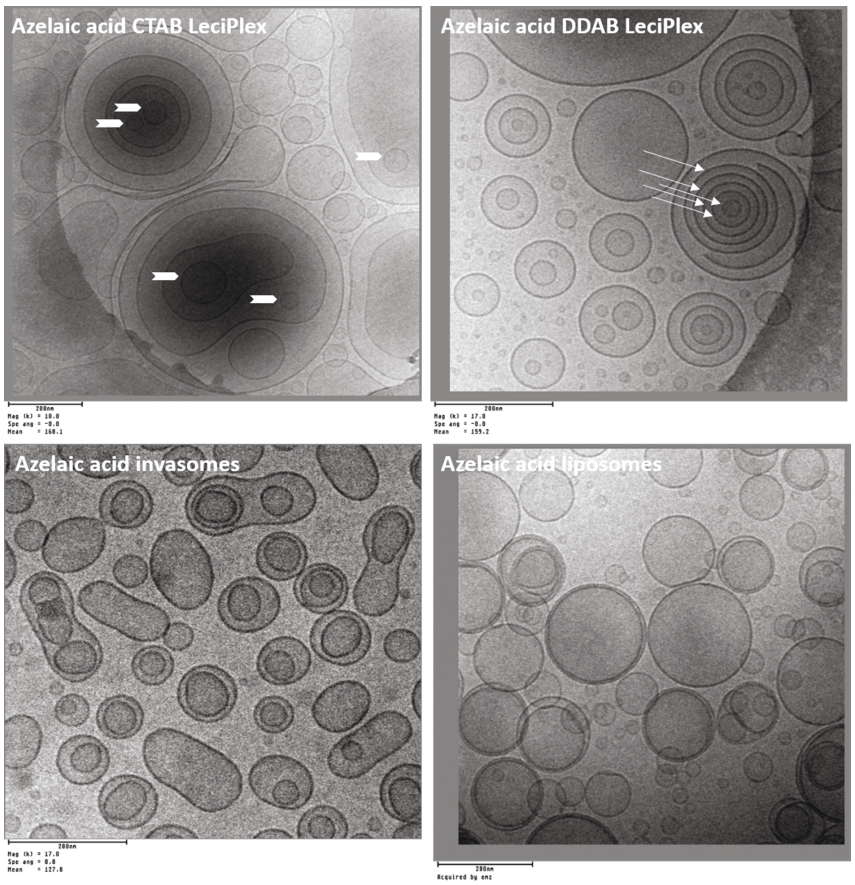

Fig. 3. CryoTEM investigation of LeciPlex, invasomes, and liposome loaded with azelaic acid. Both cationic formulations exhibited mixture of unilamellar and plurilamellar vesicles.

Liposomes and invasomes showed the traditional morphology of soy PC vesicles. Invasomes were mostly unilamellar showing a mixture of SUVs and LUVs, although a few vesicles were oligolamellar. Liposomes were mostly unilamellar vesicles with a few oligolamellar structures. Incorporation of drug did not seem to affect the shape of the vesicular systems under study.

3.3. Ex vivo human skin penetration study

3.3.1. Idebenone

Total idebenone penetration in the skin (Fig. 4B) in descending order was from CTAB LeciPlex, DDAB LeciPlex, liposomes and invasomes, respectively. Total idebenone delivered by CTAB LeciPlex was significantly higher than that of invasomes. In the

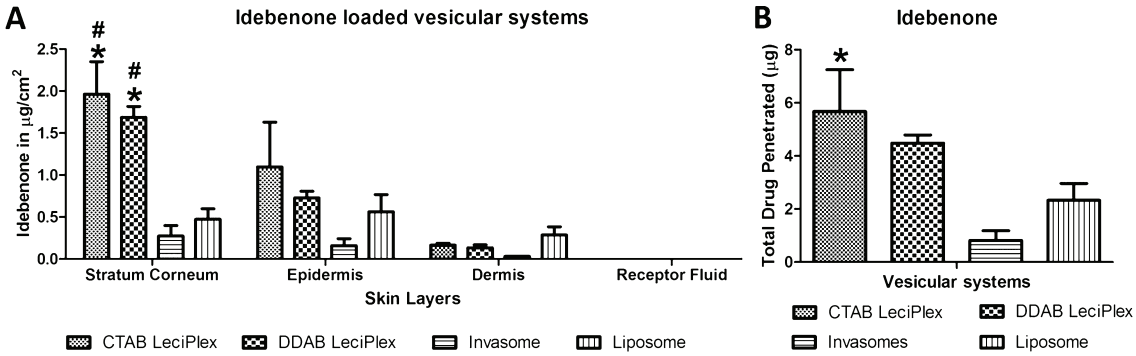

Fig. 4. (A) *Ex vivo* human skin penetration ($\mu g/cm^2$) of vesicular systems loaded with idebenone. Significant difference in idebenone content between invasomes (*), liposomes (#) and CTAB LeciPlex, DDAB LeciPlex was observed. (B) Total idebenone (μg) recovered from all layers of the skin. Significant difference between invasomes (*) and CTAB LeciPlex. Error bars represent SEM ($n = 6$).

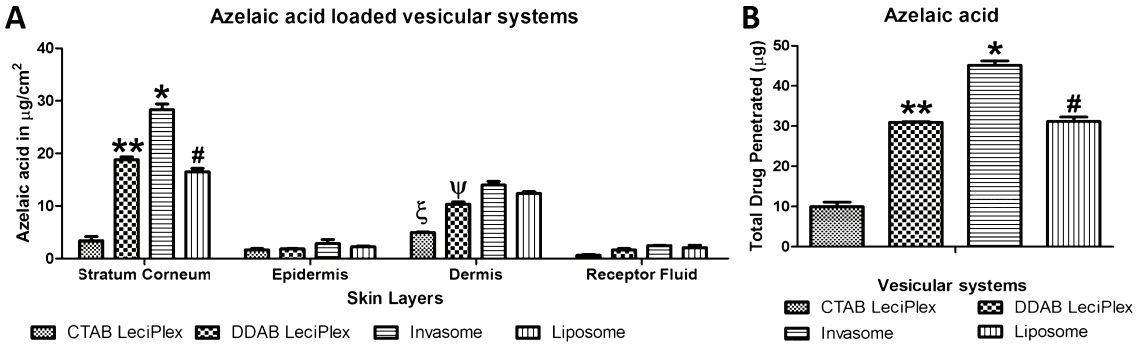

Fig. 5. (A) *Ex vivo* human skin penetration (μg/cm^2) of vesicular systems loaded with azelaic acid. A significant difference in azelaic acid content in stratum corneum between invasomes (*) and all other vesicular systems was observed as well as in stratum corneum between liposome (#) and CTAB LeciPlex; DDAB LeciPlex (**) and CTAB LeciPlex. In dermis, significant difference between CTAB LeciPlex (ξ) and liposome, invasomes, and DDAB LeciPlex (Ψ). (B) Total azelaic acid penetration from all layers of the skin. A significant difference between invasomes (*) and other vesicular systems was detected as well as between liposome (#) and CTAB LeciPlex, DDAB LeciPlex (**) and CTAB LeciPlex. Error bars represent SEM ($n = 6$).

stratum corneum (Fig. 4A), CTAB LeciPlex delivered the highest concentration of idebenone. In the epidermis, a trend similar to that of stratum corneum was observed for penetration of idebenone, with no statistically significant differences. In dermis, maximum idebenone penetration was achieved by liposomes followed by CTAB LeciPlex, DDAB LeciPlex, and invasomes, however, no statistically significant differences were observed among the formulations at the 5% significance niveau. Idebenone was not detected in the receptor fluid. CTAB LeciPlex deposited the highest amount of idebenone with 0.7% of the total applied drug reaching different layers of the skin.

3.3.2. Azelaic acid

Total azelaic acid deposition in the skin from different formulations (in descending order) was from, invasomes, liposomes, DDAB LeciPlex, and CTAB LeciPlex (Fig. 5B). There were significant differences between all vesicular systems except among liposomes and DDAB LeciPlex. In the stratum corneum, azelaic acid from invasomes penetrated the most, followed by DDAB LeciPlex, liposomes, and CTAB LeciPlex. Azelaic acid from invasomes showed a significantly higher penetration compared to all formulations. There was a significant difference between azelaic acid quantity delivered into the skin by liposomes and CTAB LeciPlex as well as between the two LeciPlex systems. In epidermis and receptor fluid, highest azelaic acid was delivered from invasomes followed by liposomes, DDAB and CTAB LeciPlex, without significant differences. Dermis also showed a similar trend although with significant differences in amount delivered by liposomes, invasomes and CTAB LeciPlex as well as between CTAB LeciPlex and DDAB LeciPlex. Although it appears that azelaic acid penetration was higher in dermis than in epidermis, the trend can be explained by the fact that dermis is a much thicker tissue compared to the epidermis (thickness of dermis was approximately 2 mm compared to approximately 100 μm for epidermis). Azelaic acid loaded invasomes deposited 5.75% of the total drug applied and could be detected in different layers of the skin.

3.4. Ex vivo human skin distribution using confocal microscopy

Ex vivo distribution of DiI monitored using CLSM revealed a marked contrast in the penetration behavior of different vesicular systems. Fluorescence intensity observed was highest for the cationic LeciPlex formulations followed by invasomes and liposomes. Cationic LeciPlex particles appeared to have followed a transfollicular route of penetration which resulted in deeper penetration and accumulation of fluorescent dye in the dermis as evident from Fig. 6. There is an intense fluorescence of DiI in the stratum corneum for CTAB and DDAB LeciPlex. Although the DiI fluorescence is not as intense for invasomes, they did appear to reach the deep hair follicles although in much lower concentration. Liposomes on the other hand, showed only a weak fluorescence intensity in the stratum corneum. The fluorescence intensity was semi-quantitatively blind-scored (Verma et al., 2003c; Waring et al., 1993) by four colleagues and scored as: (0) no fluorescence; (1) very weak fluorescence; (2) weak fluorescence; (3) medium fluorescence; and (4) bright fluorescence. A summary of final score for all the formulations is presented in Table 3.

3.5. In vitro cytotoxicity study of idebenone formulations

In vitro cytotoxicity study was conducted to determine the cytotoxic potential of different vesicular systems loaded with idebenone on B16F10 melanoma cell line. Formulations containing idebenone in the range of 0.001 μM to 10 μM were applied to the cells (Fig. 7). High cytotoxicity was observed for LeciPlex formulations at all the idebenone concentrations tested. There were significant difference between all the systems at all concentrations except between invasomes and DDAB LeciPlex at 10 μM idebenone and between invasomes and CTAB LeciPlex at 0.1 μM idebenone. DDAB LeciPlex had the highest cytotoxicity while liposomes had the least cytotoxicity for all the concentrations.

3.6. In vitro antimicrobial assay of azelaic acid formulations

As azelaic acid is indicated against acne, *in vitro* microbial assay was performed for formulations containing azelaic acid. All the formulations showed minimum to no antimicrobial activity at concentrations of 0.1 and 1 μM of azelaic acid. However, as concentration of azelaic acid increased to 10 and 100 μM a relatively stronger antimicrobial activity could be seen. DDAB LeciPlex showed the maximum antibacterial activity, with invasomes and CTAB LeciPlex showing similar antibacterial activity at 10 μM and 100 μM azelaic acid concentration (Fig. 8). Liposomes showed the lowest antimicrobial activity. At azelaic acid concentration of 10 μM and 100 μM, significant differences were observed between all the delivery systems except between CTAB LeciPlex and invasomes, and azelaic acid solution and liposomes.

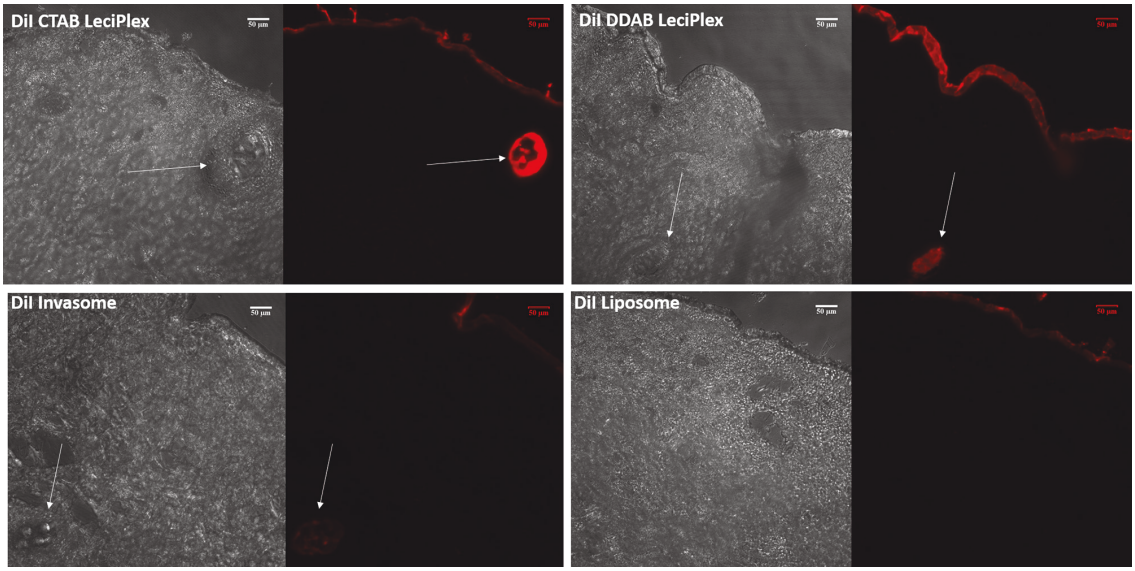

Fig. 6. Fluorescence micrographs showing cross sections of human skin treated with different formulations loaded with DiI. Every image is divided in two parts, the left image is a brightfield image and the one on the right shows fluorescence image. White arrows indicate the accumulation of the DiI in the hair follicle/sweat gland.

3.7. In vivo efficacy study of azelaic acid formulations

Azelaic acid invasomal gels showed the highest *in vivo* activity, with liposomal gels and DDAB LeciPlex gels showing similar activity and CTAB LeciPlex gels showing the least activity (Fig. 9). There were significant differences between the azelaic acid-treated formulations and the untreated control on all days except day 1. Invasomal gels showed significantly faster and better activity as compared to other delivery systems from day 2 through day 7. By day 10, all the delivery systems had achieved similar antiacne activity but at different rates. Drug suspension had the least anti-acne activity which might be due to slow diffusion in the stratum corneum. Even untreated control showed reduced inflammation which is expected as the immune system of the animal fights against the infection. All the systems had statistically significant better *in vivo* activity when compared to azelaic acid suspension.

4. Discussion

In this study, we evaluated three fundamentally different types of vesicular systems *viz* cationic LeciPlex, invasomes, and liposomes for their ability to deliver idebenone and azelaic acid using *in vitro*,*ex vivo*, and *in vivo* models. In *ex vivo* human skin penetration study, idebenone vesicular systems followed a descending order of idebenone deposition in different skin layers starting with CTAB LeciPlex, DDAB LeciPlex, liposomes, and invasomes. When the vesicular systems were loaded with azelaic acid, under similar set of conditions the results were reversed. This was an interesting result as although the two drugs were loaded at the same concentration into same vesicular systems and were evaluated under the same set of conditions for *ex vivo* studies, marked differences were observed in penetration behavior of the two drugs. This difference in the penetration behavior was an indication either that different penetration mechanisms were involved in the skin penetration of both drugs or that the two drugs change the carrier system characteristics in different ways. The first rationale was substantiated by the CLSM studies where both cationic LeciPlex formulations showed much higher fluorescence in the hair follicles. Although in this study we did not quantify the fluorescence intensity in the hair follicles, fluorescence intensity was an order of magnitude higher for LeciPlex formulations followed by invasomes, while for control liposome formulation, no fluorescence was detected in the hair follicles. From this observation, we can predict that LeciPlex employs a dual pathway for skin delivery-transfollicular and intercellular compared to mainly intercellular pathway for invasomes and control liposomes. This finding is also supported by the findings from Jung et al. (2006) where they compared different liposomal formulations with a conventional cream for the delivery of fluorescent dyes carboxyfluorescein and curcumin to hair follicles. According to Jung et al. (2006), surface charge, especially cationic, was an important parameter for follicle delivery whereas size of vesicles and transition temperature of phospholipids were of relatively less importance.

Idebenone deposition in skin was significantly higher from CTAB and DDAB LeciPlex compared to invasomes. This contrast might be explained by the interaction of idebenone with the phospholipid membrane. Idebenone is a small molecule (molecular weight 338 Da) which is practically insoluble in water and with a pK_a value of 15.19 (Li and Ge, 2012), it will have a neutral charge within the phospholipid membrane and will prefer a lipophilic environment. Fresta et al. (1998) have shown that idebenone is fully inserted into a phospholipid membrane. The interaction of idebenone with membranes is further enhanced by negatively charged headgroups, which are present in the NAT8539 in the form of phosphatidic acid and phosphatidylinositol. They also observed a phase segregation in DMPC and DPPC liposomes containing idebenone beyond a molar fraction of 0.09. Above a certain drug:

Table 3
Summarized blind average intensity scoring from confocal study described in Section 3.4 for different vesicular systems using DiI as the fluorophore on excised human skin.

Delivery System	Stratum corneum	Epidermis	Dermis	Total Score
CTAB LeciPlex	3	2.25	3.5	8.75
DDAB LeciPlex	3.25	3	2.5	8.75
Invasomes	1.25	1.5	2	4.75
Liposomes	2.5	1.75	0.75	5

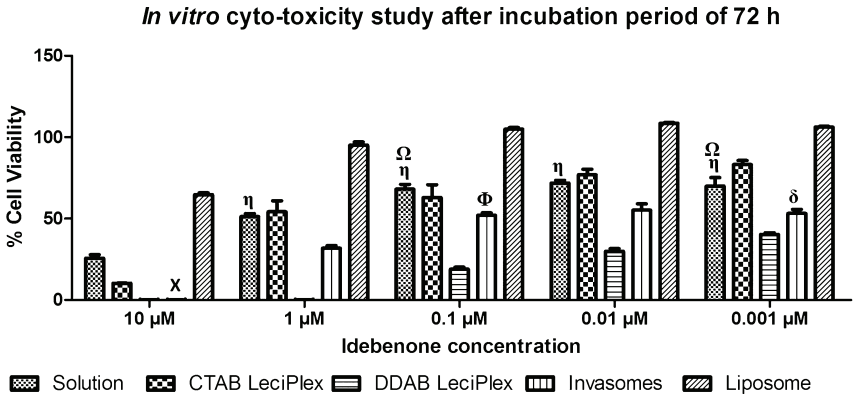

Fig. 7. *In vitro* cyto-toxicity of idebenone solution and idebenone loaded CTAB LeciPlex, DDAB LeciPlex, invasomes, and liposomes at different molar concentrations of idebenone. Significant differences were observed between all vesicular systems at all concentrations except at 10 μM between invasomes and DDAB LeciPlex (X); at 1 μM, 0.1 μM, 0.01 μM, 0.001 μM idebenone between solution and CTAB LeciPlex (η); at 0.1 μM, 0.001 μM idebenone between solution and invasomes (Ω); at 0.1 μM between invasomes and CTAB LeciPlex (Φ); and at 0.001 μM between invasomes and DDAB LeciPlex (δ). Error bars represent SEM ($n = 6$).

lipid ratio, both idebenone rich and poor domains could therefore be expected in the liposomal formulations. In CTAB and DDAB LeciPlex, the idebenone molar fraction is 0.15 and 0.13, respectively, compared to 0.056 for invasomes. This difference in the drug: lipid ratio will have a big impact on the dynamics of drug transfer from liposomal membranes to biological membranes. Drug release from vesicles is an important step and it can influence transdermal flux (Chen et al., 2010; Honeywell-Nguyen and Bouwstra, 2003). *Fresta et al.* have also shown that the rate-limiting step for idebenone transfer from liposomal membrane to biological membrane is diffusion through the aqueous compartment. Due to higher drug:lipid ratio, idebenone will readily partition out of the phospholipid membrane compared to invasomes and its diffusion across the aqueous compartment might be facilitated by presence of transcutol in LeciPlex formulations. Both these factors explain higher deposition of idebenone from the cationic LeciPlex formulations. Although liposomes had high drug:lipid ratio like Leciplex formulations, liposomes did not perform equally to the cationic formulations suggesting the presence of cationic surfactants had a crucial role in increased deposition of idebenone from Leciplex.

Azelaic acid (molecular weight 188 Da) is a dicarboxylic acid which is slightly soluble in water. Bossi et al. (1990) have shown that in distearoylphospocholine (DSPC) bilayers, azelaic acid gets completely inserted into the bilayers. Geometry of these bilayers was found to be dependent on the drug:lipid molar ratio and temperature. Below the transition temperature and above drug: lipid molar ratio of 0.2, an interdigitated lamellar gel phase with lamellar repeat distance of 5.25 nm (decreased from 6.83 nm for conventional Lβ phase) was witnessed. Above the transition temperature, however, Lα lamellar phase was observed at all drug: lipid ratios. They have also shown that azelaic acid strongly interacts with phosphate in the phospholipid head groups and only weakly interacts with the fatty acid chains, therefore chain melting in DSPC was relatively unaffected by the presence of azelaic acid. Due to the nature of phospholipids employed in the present study, all the azelaic acid vesicular systems at experimental conditions can be expected to be in Lα lamellar phase. In the *ex vivo* penetration study, azelaic acid penetrated to the highest extent when applied by loading in invasomes followed by liposomes, DDAB LeciPlex, and CTAB LeciPlex. Lower penetration of azelaic acid from LeciPlex formulations might be due to interactions between the cationic surfactants and carboxylic groups of the azelaic acid which would retard partitioning of azelaic acid out of the LeciPlex vesicles. Differences between CTAB-LeciPlex and DDAB-LeciPlex are difficult to explain and we can only speculate that they might have been due to differential skin penetration enhancement abilities of individual surfactants. *Duangjit et al.* investigated the link between chain length of cationic surfactants and skin penetration by studying skin penetration ability of

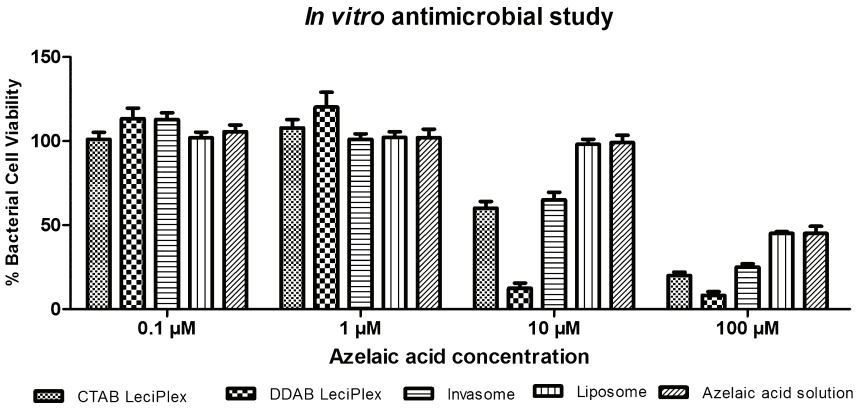

Fig. 8. *In vitro* anti-microbial study of CTAB LeciPlex, DDAB LeciPlex, invasomes, and liposome loaded with azelaic acid. Error bars represent standard error of mean ($n = 6$). Blank medium served as control with % cell viability of 100%.

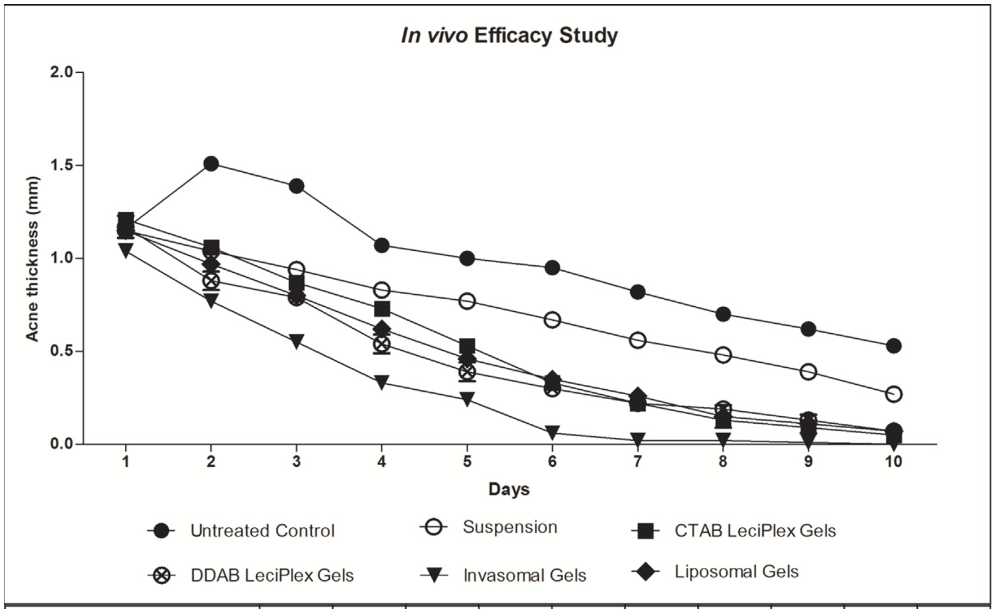

Bonferroni's multiple Comparison test	Day 1	Day 2	Day 3	Day 4	Day 5	Day 6	Day 7	Day 8	Day 9	Day 10
CTAB LeciPlex vs DDAB LeciPlex	No	Yes	No	Yes	No	No	No	No	No	No
CTAB LeciPlex vs Liposomes	No	No	No	No	No	No	No	No	No	No
CTAB LeciPlex vs Invasomes	No	Yes	Yes	Yes	Yes	Yes	Yes	Yes	No	No
DDAB LeciPlex vs Liposomes	No	No	No	No	No	No	No	No	No	No
DDAB LeciPlex vs Invasomes	No	No	Yes	Yes	Yes	Yes	Yes	Yes	Yes	Yes
Liposomes vs Invasomes	No	Yes	Yes	Yes	Yes	Yes	Yes	Yes	No	No

Fig. 9. *In vivo* efficacy study of CTAB LeciPlex, DDAB LeciPlex, invasomes, and liposome loaded with azelaic acid. Bonferroni's multiple comparison test was applied to determine statistical difference between delivery systems on different days, which are tabulated. Error bars represent SEM ($n = 6$).

meloxicam loaded cationic liposomes. They found that liposomes containing 16 carbon chain surfactant penetrated better than liposomes containing 12 carbon chain surfactant (Duangjit et al., 2014). Our results however, are at variance with their findings as DDAB-LeciPlex (C_{12}) showed higher penetration of azelaic acid than CTAB-LeciPlex (C_{16}). However we must point out that Duangjit et al. (2014) have used alkyl pyridinium based surfactants compared to CTAB and DDAB tested in this study. To gain an understanding into the differences in the penetration behavior of CTAB and DDAB LeciPlex, further systematic studies are required. In the past, *Fahr et al.* have successfully demonstrated that invasomes can deliver hydrophilic and lipophilic drugs deeper into the skin layers (Dragicevic-Curic et al., 2008b, 2009; Verma and Fahr, 2004; Verma et al., 2003a). The penetration ability of invasomes is believed to be due to higher deformability of the vesicles. Deformability to invasomes vesicles is imparted by terpenes and by lyso PC which is one of the components of the NAT8539. Effect of lyso PC on bending elasticity of phosphatidylcholine membrane is well known (Fuller and Rand, 2001; Vitkova et al., 2014), effect of terpenes on the fluidity of the invasomes was investigated using electron spin resonance spectroscopy and a 1% mixture of citral:cineole:limonene (4.5:4.5:1) was found to be optimal for topical delivery of temoporfin to deeper layers of skin (Dragicevic-Curic et al., 2011; Dragicevic-Curic et al., 2008b).

In vitro cytotoxicity study of idebenone loaded vesicular systems on B16F10 melanoma cell line gave an indication of superior activity of LeciPlex followed by invasomes and liposomes. An important contributing factor to the superior activity of LeciPlex is the presence of cationic surfactant CTAB or DDAB, which are known to have cytotoxic activity (Cui et al., 2006). Blank formulations of invasomes, CTAB LeciPlex, and DDAB LeciPlex showed weak cytotoxic activity in the cell line investigated (Data not shown). Cytotoxicity of blank invasomes could be due to the presence of ethanol.

All azelaic acid formulations showed antimicrobial activity above 10 μM and 100 μM azelaic acid concentration except liposomes which did not show any significant antimicrobial activity at 10 μM azelaic acid concentration. Highest activity was seen for DDAB LeciPlex at 10 μM and 100 μM azelaic acid concentration. *In vitro* antimicrobial study on *P. acne* revealed that at concentration of 10 μM and 100 μM, significant differences were observed between all the delivery systems except between CTAB LeciPlex and invasomes, and between liposomes and azelaic acid solution. *In vivo* antiacne efficacy study showed significant differences in the effectiveness of different azelaic acid loaded delivery systems. Invasomal gels were the best performing delivery system followed by liposomes and DDAB LeciPlex gels, while CTAB LeciPlex gels was the slowest to exert its antiacne effect. *P. acne* is often found in the microcomedone that is a precursor of acne vulgaris, which is characterized by hyperkeratinisation, formation of keratin plug, and increase in sebum production by sebaceous glands. *P. acne* stimulates the production of pro-inflammatory cytokines (Nakatsuji et al., 2011). Because of increased penetration facilitated by invasomes which is also evident from *ex vivo* penetration study, more amount of azelaic acid could have been available at the site of inflammation of *P. acne* leading to faster therapeutic action. There were significant differences between all the vesicular systems and untreated control on all days starting from day 2. A significant difference between activity of azelaic acid as invasomes and liposome from day 2 through day 7 was

observed, after which the baseline activity was attained for both systems. Liposomal gels were closely followed in activity by DDAB LeciPlex gels which were followed by CTAB LeciPlex gels. In essence, although CTAB LeciPlex performed well in the *in vitro* antimicrobial study, it was the slowest of all formulations in *in vivo* efficacy study. This slow response for cationic formulations is likely due to the fact that CTAB and DDAB are known to cause some inflammation on topical application (Smith and Maibach, 2006) and acne being a condition where skin is inflamed due to inflammatory cytokines, the therapeutic efficacy of azelaic acid could have been reduced due to inflammation caused by CTAB or DDAB itself. A few factors that need careful consideration while correlating *ex vivo* and *in vivo* efficacy are (a) the *ex vivo* penetration study was performed on intact excised human abdominal skin, (b) the *in vivo* efficacy was performed on rat ear skin, and (c) the *in vivo* studies are performed in *P. acne* induced inflamed skin. Human skin is less permeable than rat skin (Van Ravenzwaay and Leibold, 2004) and this physiological difference could also be a determining factor. An important correlation observed in these studies was that azelaic acid loaded in invasomes penetrated the most in *ex vivo* study on human skin and also showed high *in vivo* efficacy compared to other vesicular systems.

5. Conclusion

In this bicentric study, vesicular systems loaded with two actives differing in physicochemical properties were successfully developed and characterized. LeciPlex increased delivery of idebenone whereas invasomes increased delivery of azelaic acid in *ex vivo* experiments. *In vivo* efficacy study for azelaic acid formulations supported this hypothesis. Intracutaneous delivery of actives is presented based on drug properties, properties of formulation components, and properties of the formulation as a whole.

Acknowledgements

Sanket M. Shah, Mukul Ashtikar, Mangal S. Nagarsenker, and Alfred Fahr are thankful to Indian Council of Medical Research (ICMR), New Delhi, India and Bundesministerium für Bildung und Forschung (BMBF), Bonn, Germany for financial assistance, travel, and accommodation. We are grateful to Dr. Gruhl (Kassel, Germany) for providing the human abdominal skin for *ex vivo* studies. Authors thank Erica D'aguanno for her help in confocal imaging and Dr. Jana Thamm for the assistance in CryoTEM imaging.

References

Amorim, C., Netz, D.A., Couto, A., Freitas, R., Bresolin, T.B., 2009. Stability-indicating LC-PDA method for determination of idebenone in nanoparticles based on chitosan and *N*-carboxymethylchitosan. Chromatographia 70, 1411–1415.
Andrea, C.L., 2005. Percutaneous drug delivery to the hair follicle. Percutaneous Absorption. CRC Press, Boca Raton, pp. 429–437.
Barry, B.W., 2006. Penetration enhancer classification, In: Smith, E., Maibach, H.I. (Eds.), Percutaneous Penetration Enhancers. 2nd ed. Taylor and Francis Group, Boca Raton London New York, pp. 3–16.
Bossi, G., Dubini, B., Mariani, P., Ponzi Bossi, M.G., Rustichelli, F., Phadke, R.S., 1990. Azelaic acid in model membranes: a thermodynamical and structural study. Il Nuovo Cimento D 12, 1293–1308.
Bouwstra, J.A., Honeywell-Nguyen, P.L., 2002. Skin structure and mode of action of vesicles. Adv. Drug Delivery Rev. 54, S41–S55.
Cevc, G., 1996. Transfersomes, liposomes and other lipid suspensions on the skin: permeation enhancement, vesicle penetration, and transdermal drug delivery. Critical Reviews™ in Therapeutic Drug Carrier Systems 13.
Cevc, G., Blume, G., 1992. Lipid vesicles penetrate into intact skin owing to the transdermal osmotic gradients and hydration force. Biochim. Biophys. Acta, Biomembr. 1104, 226–232.
Cevc, G., Gebauer, D., Stieber, J., Schaetzlein, A., Blume, G., 1998a. Ultraflexible vesicles transfersomes, have an extremely low pore penetration resistance and transport therapeutic amounts of insulin across the intact mammalian skin. Biochim. Biophys. Acta, Biomembr. 1368, 201–215.
Cevc, G., Gebauer, D., Stieber, J., Schatzlein, A., Blume, G., 1998b. Ultraflexible vesicles transfersomes, have an extremely low pore penetration resistance and transport therapeutic amounts of insulin across the intact mammalian skin. Biochim. Biophys. Acta Biomembr. 1368, 201–215.
Cevc, G., Schatzlein, A.G., Richardsen, H., Vierl, U., 2003. Overcoming semipermeable barriers, such as the skin, with ultradeformable mixed lipid vesicles, transfersomes, liposomes, or mixed lipid micelles. Langmuir 19, 10753–10763.
Chen, M., Liu, X., Fahr, A., 2010. Skin delivery of ferulic acid from different vesicular systems. J. Biomed. Nanotechnol. 6, 577–585.
Chen, M., Liu, X., Fahr, A., 2011. Skin penetration and deposition of carboxyfluorescein and temoporfin from different lipid vesicular systems: in vitro study with finite and infinite dosage application. Int. J. Pharm. 408, 223–234.
Cui, Z., Qiu, F., Sloat, B.R., 2006. Lecithin-based cationic nanoparticles as a potential DNA delivery system. Int. J. Pharm. 313, 206–213.
Date, A.A., Naik, B., Nagarsenker, M.S., 2005. Novel drug delivery systems: potential in improving topical delivery of antiacne agents. Skin Pharmacol. Physiol. 19, 2–16.
Date, A.A., Srivastava, D., Nagarsenker, M.S., Mulherkar, R., Panicker, L., Aswal, V., Hassan, P.A., Steiniger, F., Thamm, J., Fahr, A., 2011a. Lecithin-based novel cationic nanocarriers (LeciPlex) I: fabrication, characterization and evaluation. Nanomedicine (Lond.) 6, 1309–1325.
Date, A.A., Nagarsenker, M.S., Patere, S., Dhawan, V., Gude, R.P., Hassan, P.A., Aswal, V., Steiniger, F., Thamm, J., Fahr, A., 2011b. Lecithin-based novel cationic nanocarriers (Leciplex) II: improving therapeutic efficacy of quercetin on oral administration. Mol. Pharm. 8, 716–726.
Dragicevic-Curic, N., Grafe, S., Albrecht, V., Fahr, A., 2008a. Topical application of temoporfin-loaded invasomes for photodynamic therapy of subcutaneously implanted tumours in mice: a pilot study. J. Photochem. Photobiol. B 91, 41–50.
Dragicevic-Curic, N., Scheglmann, D., Albrecht, V., Fahr, A., 2008b. Temoporfin-loaded invasomes: development, characterization and in vitro skin penetration studies. J. Control. Release 127, 59–69.
Dragicevic-Curic, N., Scheglmann, D., Albrecht, V., Fahr, A., 2009. Development of different temoporfin-loaded invasomes-novel nanocarriers of temoporfin: characterization, stability and in vitro skin penetration studies. Colloids Surf. B 70, 198–206.
Dragicevic-Curic, N., Friedrich, M., Petersen, S., Scheglmann, D., Douroumis, D., Plass, W., Fahr, A., 2011. Assessment of fluidity of different invasomes by electron spin resonance and differential scanning calorimetry. Int. J. Pharm. 412, 85–94.
Duangjit, S., Opanasopit, P., Rojanarata, T., Ngawhirunpat, T., 2013. Evaluation of meloxicam-loaded cationic transfersomes as transdermal drug delivery carriers. AAPS PharmSciTech 14, 133–140.
Duangjit, S., Pamornpathomkul, B., Opanasopit, P., Rojanarata, T., Obata, Y., Takayama, K., Ngawhirunpat, T., 2014. Role of the charge, carbon chain length, and content of surfactant on the skin penetration of meloxicam-loaded liposomes. Int. J. Nanomed. 9, 2005–2017.
Egbaria, K., Ramachandran, C., Weiner, N., 1991. Topical application of liposomally entrapped ciclosporin evaluated by in vitro diffusion studies with human skin. Skin Pharmacol. Physiol. 4, 21–28.
El Maghraby, G.M., Williams, A.C., Barry, B.W., 2006. Can drug-bearing liposomes penetrate intact skin? J. Pharm. Pharmacol. 58, 415–429.
El Maghraby, G.M., Barry, B.W., Williams, A.C., 2008. Liposomes and skin: from drug delivery to model membranes. Eur. J. Pharm. Sci. 34, 203–222.
Fresta, M., Ventura, C.A., Mezzasalma, E., Puglisi, G., 1998. A calorimetric study on the idebenone–phospholipid membrane interaction. Int. J. Pharm. 163, 133–143.
Fuller, N., Rand, R.P., 2001. The influence of lysolipids on the spontaneous curvature and bending elasticity of phospholipid membranes. Biophys. J. 81, 243–254.
Ganesan, M.G., Weiner, N.D., Flynn, G.L., Ho, N.F.H., 1984. Influence of liposomal drug entrapment on percutaneous absorption. Int. J. Pharm. 20, 139–154.
Gollnick, H., 1993. Azelaic acid-pharmacology, toxicology and mechanisms of action on keratinization in vitro and in vivo. J. Dermatolo. Treat. 4, S3–S7.
Gonzalez-Rodriguez, M.L., Rabasco, A.M., 2011. Charged liposomes as carriers to enhance the permeation through the skin. Expert Opin. Drug Deliv. 8, 857–871.
Guo, J., Ping, Q., Sun, G., Jiao, C., 2000. Lecithin vesicular carriers for transdermal delivery of cyclosporin A. Int. J. Pharm. 194, 201–207.
Gupta, M.A., Gupta, A.K., 1998. Depression and suicidal ideation in dermatology patients with acne, alopecia areata, atopic dermatitis and psoriasis. Brit. J. Dermatol. 139, 846–850.
Guthlein, F., Burger, A.M., Brandl, M., Fiebig, H.-H., Schubert, R., Unger, C., Massing, U., 2002. Pharmacokinetics and antitumor activity of vincristine entrapped in vesicular phospholipid gels. Anti-Cancer Drugs 13, 797–805.
Hasanovic, A., Hollick, C., Fischinger, K., Valenta, C., 2010. Improvement in physicochemical parameters of DPPC liposomes and increase in skin permeation of aciclovir and minoxidil by the addition of cationic polymers. Eur. J. Pharm. Biopharm. 75, 148–153.
Higuchi, T., 1960. Physical chemical analysis of percutaneous absorption process from creams and ointments. J. Soc. Cosmet. Chem. 11, 85–97.
Honeywell-Nguyen, P.L., Bouwstra, J.A., 2003. The in vitro transport of pergolide from surfactant-based elastic vesicles through human skin: a suggested mechanism of action. J. Control. Release 86, 145–156.
Jung, S., Otberg, N., Thiede, G., Richter, H., Sterry, W., Panzner, S., Lademann, J., 2006. Innovative liposomes as a transfollicular drug delivery system: penetration into porcine hair follicles. J. Invest. Dermatol. 126, 1728–1732.

Kaiser, N., Kimpfler, A., Massing, U., Burger, A.M., Fiebig, H.H., Brandl, M., Schubert, R., 2003. 5-Fluorouracil in vesicular phospholipid gels for anticancer treatment: entrapment and release properties. Int. J. Pharm. 256, 123–131.
Katahira, N., Murakami, T., Kugai, S., Yata, N., Takano, M., 1999. Enhancement of topical delivery of a lipophilic drug from charged multilamellar liposomes. J. Drug Targeting 6, 405–414.
Kitagawa, S., Kasamaki, M., 2006. Enhanced delivery of retinoic acid to skin by cationic liposomes. Chem. Pharm. Bull. 54, 242–244.
Li, B., Ge, Z.Q., 2012. Nanostructured lipid carriers improve skin permeation and chemical stability of idebenone. AAPS PharmSciTech 13, 276–283.
Loan Honeywell-Nguyen, P., de Graaff, A.M., Wouter Groenink, H.W., Bouwstra, J.A., 2002. The in vivo and in vitro interactions of elastic and rigid vesicles with human skin. Biochim. Biophys. Acta 1573, 130–140.
Mansour, A.M., Ibrahiem, M.M., 2002. Simultaneous determination of azelaic and benzoic acids in topical preparations by liquid chromatography. Chromatographia 55, 435–437.
Mezei, M., Gulasekharam, V., 1980. Liposomes-a selective drug delivery system for the topical route of administration I. Lotion dosage form. Life Sci. 26, 1473–1477.
Michel, C., Purmann, T., Mentrup, E., Seiller, E., Kreuter, J., 1992. Effect of liposomes on percutaneous penetration of lipophilic materials. Int. J. Pharm. 84, 93–105.
Moog, R., Burger, A., Brandl, M., Schüler, J., Schubert, R., Unger, C., Fiebig, H., Massing, U., 2002. Change in pharmacokinetic and pharmacodynamic behavior of gemcitabine in human tumor xenografts upon entrapment in vesicular phospholipid gels. Cancer Chemoth. Pharmacol. 49, 356–366.
Nakatsuji, T., De-chu, C.T., Zhang, L., Gallo, R.L., Huang, C.-M., 2011. Propionibacterium acnes CAMP factor and host acid sphingomyelinase contribute to bacterial virulence: potential targets for inflammatory acne treatment. PLoS One 6, e14797.
Nakatsuji, T., Kao, M.C., Fang, J.-Y., Zouboulis, C.C., Zhang, L., Gallo, R.L., Huang, C.-M., 2009. Antimicrobial property of lauric acid against propionibacterium acnes: its therapeutic potential for inflammatory acne vulgaris. J. Invest. Dermatol. 129, 2480–2488.
Ogiso, T., Iwaki, M., Paku, T., 1995. Effect of various enhancers on transdermal penetration of indomethacin and urea, and relationship between penetration parameters and enhancement factors. J. Pharm. Sci. 84, 482–488.
Ota, Y., Hamada, A., Nakano, M., Saito, H., 2002. Evaluation of percutaneous absorption of midazolam by terpenes. Drug Metab. Pharmacokinet. 18, 261–266.
Patzelt, A., Lademann, J., 2013. Drug delivery to hair follicles. Expert Opin. Drug Deliv. 10, 787–797.
Paul, A., Cevc, G., Bachhawat, B.K., 1998. Transdermal immunisation with an integral membrane component, gap junction protein, by means of ultradeformable drug carriers, transfersomes. Vaccine 16, 188–195.
Planas, M.E., Gonzalez, P., Rodriguez, L., Sanchez, S., Cevc, G., 1992. Noninvasive percutaneous induction of topical analgesia by a new type of drug carrier: and prolongation of local pain insensitivity by anesthetic liposomes. Anesth. Analg. 75, 615–621.
Puglia, C., Bonina, F., Trapani, G., Franco, M., Ricci, M., 2001. Evaluation of in vitro percutaneous absorption of lorazepam and clonazepam from hydro-alcoholic gel formulations. Int. J. Pharm. 228, 79–87.
W.S. Rasband ImageJ. U.S. National Institutes of Health, Bethesda, Maryland, USA, 1997–2014.
Schaeffer, H.E., Krohn, D.L., 1982. Liposomes in topical drug delivery. Invest. Ophthalmol. Visual Sci. 22, 220–227.
Shah, S.M., Jain, A.S., Kaushik, R., Nagarsenker, M.S., Nerurkar, M.J., 2014. Preclinical formulations: insight, strategies, and practical considerations. AAPS PharmSciTech 1–17.
Skalko, N., Cajkovac, M., Jalsenjak, I., 1992. Liposomes with clindamycin hydrochloride in the therapy of acne vulgaris. Int. J. Pharm. 85, 97–101.
Smith, E.W., Maibach, H.I., 2006. Percutaneous Penetration Enhancers, 2nd ed. CRC Press Taylor & Francis Group LLC, Boca Raton London New York.
Song, Y.-K., Kim, C.-K., 2006. Topical delivery of low-molecular-weight heparin with surface-charged flexible liposomes. Biomaterials 27, 271–280.
Vaddi, H.K., Ho, P.C., Chan, Y.W., Chan, S.Y., 2002. Terpenes in ethanol: haloperidol permeation and partition through human skin and stratum corneum changes. J. Controlled Release 81, 121–133.
van den Bergh, B.A.I., Bouwstra, J.A., Junginger, H.E., Wertz, P.W., 1999. Elasticity of vesicles affects hairless mouse skin structure and permeability. J. Controlled Release 62, 367–379.
Van Ravenzwaay, B., Leibold, E., 2004. A comparison between in vitro rat and human and in vivo rat skin absorption studies. Hum. Exp. Toxicol. 23, 421–430.
Verma, D.D., Fahr, A., 2004. Synergistic penetration enhancement effect of ethanol and phospholipids on the topical delivery of cyclosporin A. J. Control. Release 97, 55–66.
Verma, D.D., Verma, S., Blume, G., Fahr, A., 2003a. Liposomes increase skin penetration of entrapped and non-entrapped hydrophilic substances into human skin: a skin penetration and confocal laser scanning microscopy study. Eur. J. Pharm. Biopharm. 55, 271–277.
Verma, D.D., Verma, S., Blume, G., Fahr, A., 2003b. Liposomes increase skin penetration of entrapped and non-entrapped hydrophilic substances into human skin: a skin penetration and confocal laser scanning microscopy study. Eur. J. Pharm. Biopharm. 55, 271–277.
Verma, D.D., Verma, S., Blume, G., Fahr, A., 2003c. Particle size of liposomes influences dermal delivery of substances into skin. Int. J. Pharm. 258, 141–151.
Vitkova, V., Mitkova, D., Staneva, G., 2014. Lyso-and omega-3-containing phosphatidylcholines alter the bending elasticity of lipid membranes. Colloids Surf. A: Physicochem. Eng. Asp. 460, 191–195.
Waring, M.J., Monger, L., Hollingsbee, D.A., Martin, G.P., Marriott, C., 1993. Assessment of corticosteroid-induced skin blanching: evaluation of the minolta chromameter CR200. Int. J. Pharm. 94, 211–222.
Weiner, N., Williams, N., Birch, G., Ramachandran, C., Shipman, C., Flynn, G., 1989. Topical delivery of liposomally encapsulated interferon evaluated in a cutaneous herpes guinea pig model. Antimicrob. Agents Chemother. 33, 1217–1221.
Wempe, M.F., Lightner, J.W., Zoeller, E.L., Rice, P.J., 2009. Investigating idebenone and idebenone linoleate metabolism: in vitro pig ear and mouse melanocyte studies. J. Cosmet. Dermatol. 8, 63–73.
WHO, 2014. Skin cancers, in: WHO (Ed.), Ultraviolet radiation and the INTERSUN Programme: How common is skin cancer? WHO.

4. Discussion

The last couple of decades have seen an enormous growth in microscopic techniques available for biomedical research. Adopting such new technologies, various secrets of nature can be revealed. The first application of liposomes for drug delivery to skin was demonstrated back in 1980 by Mezei and Gulasekharam (Mezei and Gulasekharam, 1980) and even after 35 years, mechanism for liposomal drug delivery to skin still remains ambiguous. Studies presented in this thesis were designed to probe the mechanisms of drug delivery to skin from topically applied liposomes. Studies presented in publication-2 and 3 not only probe the liposome-skin interactions but also present relatively easy sample preparation techniques which could be adopted easily by the scientific community to expand their research further.

4.1 Application of confocal Raman microscopy to probe liposome-skin interactions

Theoretically there are five mechanisms by which liposomal drug delivery to the skin can be envisaged. In brief, these mechanisms include a) *free drug penetration mechanism*, where liposomes only act as carriers of the drug up to the skin and drug penetrates on its own; b) *penetration enhancing mechanism*, where liposomal components cause an ultrastructural change to the SC structure resulting in enhanced drug penetration; c) *vesicle adsorption or fusion*, where liposomes are adsorbed or fused with the surface of the SC releasing the drug in the *stratum corneum*; d) *intact penetration*, liposomal vesicles penetrate the skin intact carrying the drug along with them and e) *transfollicular penetration*, liposomal penetration via the follicles where drug is released. Given the vast variation in the penetration mechanisms, experiments described in this thesis were designed to probe the liposome-skin interactions and gain a better understanding of the possible penetration mechanisms for the drug delivery from topical application of invasomes. Mendelsohn's group using infrared and Raman microscopy has previously mapped phospholipids in pig skin following topical application of deuterated liposomes (Xiao *et al.*, 2005a; Xiao *et al.*, 2005b). However, their approach involved cryo-sectioning the skin before the measurements, an approach which is rather difficult to employ for high resolution Raman imaging. Lunter and Daniels (2014) have employed a similar technique for investigating delivery of procaine in the pig skin.

Understanding the diffusion of phospholipid along with the drug can be a crucial part of the puzzle in understanding the mechanism of drug delivery to skin from liposomes especially as each mechanism points to subtle differences in the drug-phospholipid diffusion profiles. The 'penetration enhancing mechanism' and 'intact penetration mechanism' suggest a relatively high penetration of phospholipid at least in the upper SC. In both mechanisms, phospholipid and drug would diffuse together. If liposomal drug delivery followed 'the free drug mechanism' then the SC should not have any phospholipid but the drug should be relatively uniformly distributed in the SC. 'Vesicle adsorption or fusion mechanism' would have shown the uppermost layers of the SC to have a very high phospholipid deposition and a

relatively homogenous distribution of the drug in the deeper *stratum corneum*. If the primary mechanism of penetration was 'transfollicular' then diffusion of phospholipid should exhibit a columnar diffusion and should be relatively diffused around the follicles deeper in the SC or in viable epidermis.

Many scientific groups have studied the interactions between liposomes and skin in the past. Most notable microscopic techniques employed were confocal fluorescence microscopy (Alvarez-Roman *et al.*, 2004; Schatzlein and Cevc, 1998; van Kuijk-Meuwissen *et al.*, 1998; Verma *et al.*, 2003), two-photon microscopy (Carrer *et al.*, 2008; van den Bergh *et al.*, 1999) and freeze fracture electron microscopy (Bouwstra and Honeywell-Nguyen, 2002; Hofland *et al.*, 1995; van den Bergh *et al.*, 1999). Freeze fracture electron microscopy although can provide high magnification images, sample preparation is extremely complicated which makes FFTEM rather unsuitable for studying the liposome-skin interactions. Fluorescence based techniques on the other hand have to rely on fluorescent labels. Fluorescent labels tend to be bulky and can also partition out of the liposomal membrane and diffuse independently in the SC.

Confocal Raman microscopy (CRM) on the other hand allows for a label-free imaging of the biological tissues and can even produce spectral mapping of the sample, which can be useful in determining the penetration profiles of the liposomal contents. However, high resolution non-invasive Raman depth profiling of *ex vivo* human skin is quiet challenging as long acquisition times required for Raman imaging can result in very high-energy transfer to the skin, which affects sample stability. Publication-2 presents for the first time a method with minimum sample preparation for acquiring high resolution non-invasive Raman depth maps of treated and untreated *ex vivo* human skin. Using the method described Raman mapping down to approximately 30 µm deep in the full thickness human skin was possible. Improvements in the penetration depth would require higher laser power or increased acquisition times, both of which compromise sample stability. To achieve this, two important changes were made to the method: 1) a water immersion objective was employed and 2) closed cell-design was used which not only reduced the skin dehydration rates but also tissue damages due to local heating was reduced as heat can dissipate more efficiently. Closed-cell design approach also avoids over-hydration of the SC from the water required for the water immersion objective. Figure 8 presents a comparison of the two methods. Using the closed-cell design Raman depth mapping up to a depth of 60 µm for full thickness human skin and up to 70 µm for full thickness pig skin was possible. At deepest focal planes the quality of Raman spectra did deteriorate. Lateral resolution achieved with this method was 1 µm whereas axial resolution at least for the upper SC was 1 µm however for deeper focal planes due to changes in the refractive index (Xiao *et al.*, 2004) the resolution was lower than 1 µm.

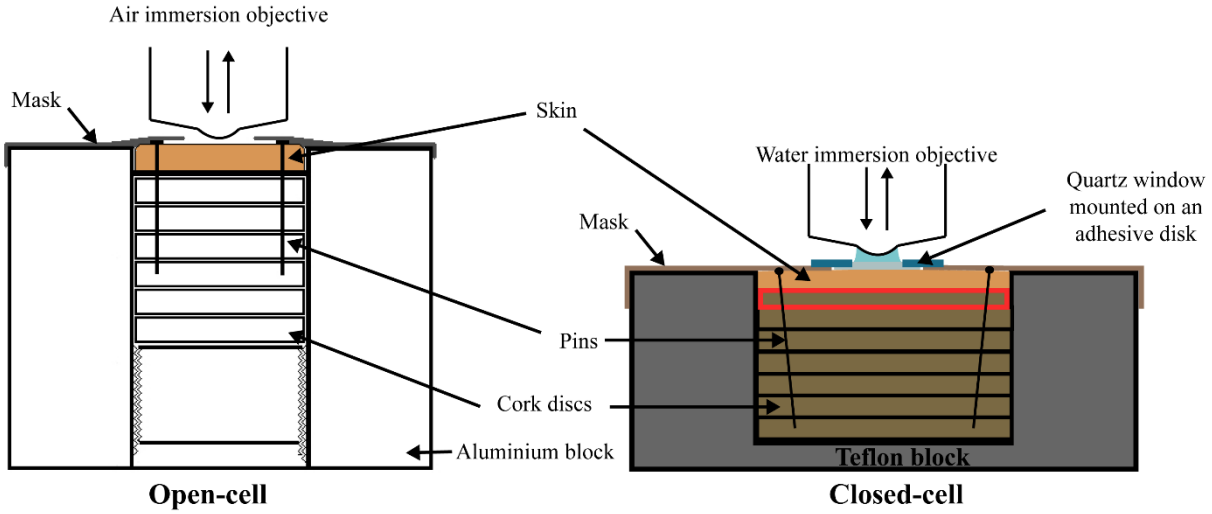

Figure 8: A schematic showing comparison of an open-cell (taken from publication-2) and a closed-cell sample holder design used for in the measurement of Raman depth profiles.

Publication-2 demonstrated that method can be employed for diffusion mapping of beta-carotene and deuterated water. Penetration of deuterated water in the Raman depth profiles appears to be uniform which was no surprise as water is known to penetrate the skin very well. However, application of beta-carotene solubilized in DMSO to human skin showed non-homogenous penetration of beta-carotene. Reason for such non-homogeneity from a solution was not completely obvious. But one can speculate that it might be a function of localized concentration of DMSO and water as beta-carotene precipitates quickly in presence of water.

An interesting aspect observed in the depth profile measurements was the presence of localized fluorescence in human skin. In human skin, *stratum corneum* was always fluorescence free however at about 15-20 µm in the skin isolated islands of fluorescence were observed. These patches of fluorescence were probably originating from the skin pigments present in the viable epidermis. Another interesting aspect was observed during human skin selection. During the course of the experiments human skin from different patients was used and skins which appeared to have a spray tan showed much greater levels of fluorescence to an extent that measurements even in the SC were heavily affected. Similar results were observed even for dark-toned skin. Therefore for the Raman depth profiling, untanned Caucasian skin was preferable.

Raman depth maps obtained constitute a complex dataset and spatial distribution of various spectral components was determined by vertex component analysis (VCA). In untreated human skin samples, the endmembers obtained mainly consisted of spectral features typical of proteins, lipids and fluorescence (kindly refer publication-2, page-67, for specific band assignments). In pig skin no fluorescence was observed as pig skin naturally lacks melanin pigments which are main source of fluorescence in human skin especially at 785 nm. For beta-carotene treated human skin samples, VCA

was able to map high-low concentrations of beta-carotene in the skin along with intrinsic components of the skin such as proteins, lipids and fluorescent pigments.

All the above results demonstrated that the method had the technical capability to determine the co-diffusion of the drug and liposomal-phospholipid from a topical application to skin. However, upon treating human skin with invasomes containing deuterated phospholipids (for composition of invasomes kindly refer to section 3.2.1), we could not detect diffusion of deuterated phospholipid in the skin. In order to reason with this issue, dose of deuterated invasomes applied to the skin was increased coupled with to increased diffusion time on the Franz cells however it did not make a significant difference. Possible rationale for this observation are;

- Only a small amount of phospholipid penetrates the SC and CRM is not sensitive enough to detect the phospholipid that has penetrated in the SC.
- Deuterated phospholipid (d31-POPC) employed for preparation of invasomes in this study was not an ideal phospholipid and does not impart a significant penetration enhancing effect on the skin.

If phospholipids do not penetrate the SC at all then skin penetration mechanism for invasomes points at a 'free drug mechanism' for delivering drug to the skin. However this is rather unlikely as there is an evidence that invasomes increase penetration of hydrophilic compounds in the skin (Chen *et al.*, 2010; Verma *et al.*, 2003) compared to their aqueous solutions. Also given the vast amount of literature suggesting that liposomes can cause changes to the SC lipid organization (Bouwstra and Honeywell-Nguyen, 2002; Hasanovic *et al.*, 2011; Hofland *et al.*, 1991; Honeywell-Nguyen and Bouwstra, 2005; Loan Honeywell-Nguyen *et al.*, 2002; van den Bergh *et al.*, 1999), it is more likely that the CRM is not sensitive enough to detect the d31-POPC that has penetrated the full thickness human skin.

4.2 Tip-enhanced Raman scattering spectroscopy to probe the interactions between skin and invasomes

While confocal Raman microscopy was employed to explore diffusion of phospholipids, tip-enhanced Raman scattering (TERS) allowed to probe the liposome-stratum corneum interactions at resolution much greater than a Raman or infrared microscope would allow. TERS experiments in the publication-3 were inspired by the work of the Bouwstra group who has demonstrated, using freeze fracture electron microscopy, that liposome treated skin shows changes in the intercellular lipids and also shows penetration of intact liposomal vesicles in the *stratum corneum* (Bouwstra and Honeywell-Nguyen, 2002). Although freeze fracture microscopy can provide a very good lateral resolution, it cannot qualitatively identify the externally applied phospholipid. Also extensive sample preparation required for freeze fracture technique makes it rather vulnerable to introduction of artifacts. Therefore, an ambition in this study was to keep the sample preparation to a minimum so as to minimize the risk of introduction of any artifacts and measure in ambient conditions to avoid issues with sample stability.

TERS presented a unique opportunity where samples could be imaged at ambient conditions with sub-nanometer lateral resolution and also provided spectroscopic information at high resolution. Findings of these experiments would allow us to comment on the interactions between the SC and invasomes. One of the biggest challenge in the TERS measurements was the sample preparation. AFM-head required the sample to be rigid and the bottom illumination for TERS meant sample had to be transparent in order to allow for the collection of TERS signal (Deckert *et al.*, 2015). These requirements eliminated the possibility of measuring a full thickness skin directly and tape-stripping was chosen for sampling of the SC. To take in to account the requirements of the TERS setup, a protocol for spin coating glass cover slips using a proprietary adhesive was developed successfully in-house. Using the adhesive coated glass cover slips, the *stratum corneum* could be progressively removed just like in case of tape stripping (Lademann *et al.*, 2009). However extreme care was required during tape stripping as any excess force and the adhesive glass cover slip cracked. To overcome this issue a Teflon mesh was introduced in the form of a mask on to the skin which not only limited the area of sampling the SC but also aided in smooth and fast removal of the adhesive cover slip. Based on densitometry data for 50 adhesive cover slips, the in-house developed stripping technique was about 62% as effective in removing SC as krystal klar® TESA adhesive tape which is regularly used for tape stripping.

In order to identify topically applied phospholipid, invasomes were prepared using a head deuterated phospholipid 1,2-dilinoleoyl-3-phosphocholine-N,N,N-trimethyl-d9 (d9-DLPC) (kindly refer to publication-3 page 83, for formulation details). d9-DLPC was selected for preparation of invasomes because, enhancement of Raman signal in TERS is strongly distance dependent and deuteration at the head groups allowed for a higher enhancement factor compared to chain deuterated phospholipid bilayers in our preliminary experiments. Another factor in lipid selection was that 1,2-dilinoleoyl phosphatidylcholine represents a major fraction (~ 65%) of natural soy-phosphatidylcholine NAT8539 which is employed in the preparation of invasomes (kindly refer to table 4 for composition of NAT8539).

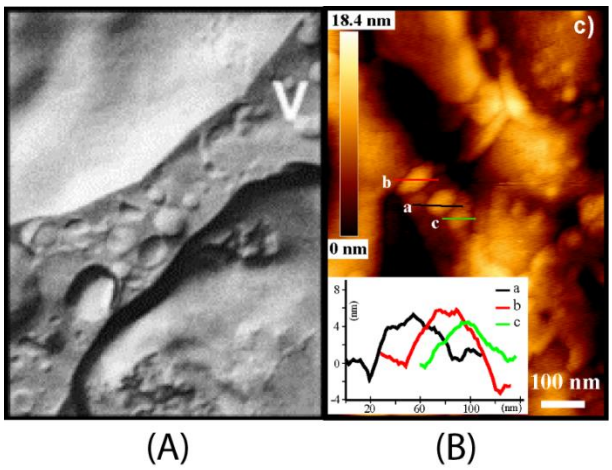

Figure 9: Comparison of the flattened vesicles in stratum corneum followed by treatment with liposomes reported by (A) Bouwstra and Honeywell-Nguyen (2002) using freeze fracture electron transmission electron microscopy (B) AFM image of invasome vesicles on the surface of corneocyte reported in publication-3.

To demonstrate the proof of concept, TER spectra were measured on supported lipid bilayers and compared with Raman and surface enhanced Raman scattering (SERS) spectra. In all three techniques bands observed between 2000 – 2300 cm-1 were representative of the C-D vibrational modes. Differences between Raman/SERS and TERS spectra were due to the inhomogeneity of the field enhancement and polarization effects in TERS (Deckert-Gaudig *et al.*, 2010). Due to these phenomena not all bonds experience equal enhancement effect in TERS which often gives rise to a disparity between Raman and TERS spectra.

After 4 hour application of invasomes, skin was thoroughly cleaned under running water to ensure complete removal of topically applied formulation. After removal of 10 layers of SC, all the layers were first subjected to atomic force microscopy (AFM) to identify the regions of interest and were followed by TERS measurements for identification of structures of interest. In the AFM measurements, a marked difference between the treated and untreated samples was observed. In invasome treated samples, there was a persistent presence of flattened vesicles throughout all the samples. Such flattened vesicles were about 5-10 nm in height indicating vesicles were flattened and consisted of one or two phospholipid bilayers. Although, whether vesicles penetrated in flattened state or vesicles were flattened after stripping of the SC could not be established based on the current studies. These flattened vesicles were very similar to the features reported by Bouwstra's group (Figure 9) in human SC treated with deformable liposomes (Bouwstra and Honeywell-Nguyen, 2002). Since studies by Bouwstra's group were carried using freeze fracture electron microscopy, there was no opportunity for a qualitative analysis, as in freeze fracture technique the original sample is destroyed (Severs, 2007). Flattened vesicles were present on the surface of corneocytes in all 10 layers analyzed. Apart from vesicles, corneodesmosomes were observed in both treated and untreated samples and could be easily distinguished from flattened vesicles on the basis dimensions.

AFM analysis identified the regions of interest in the skin samples and was followed by TERS measurements. The biggest advantage of the current study was that the skin samples could be qualitatively measured by investigating the figure print spectra of the invasomal head deuterated phospholipid. TER spectra were measured mainly on the flattened vesicles and channels or ridges on the surface of corneocytes. TER spectra measured on the surface of the vesicles showed Raman bands positive for C-D vibrations. When spectra were measured on adjacent points outside the vesicles, Raman bands typical for proteins and lipids in the skin were observed without any C-D bands. This observation established the integrity of the TERS tip and also confirmed that the flattened vesicles present on the surface of the corneocytes were indeed topically applied invasomes. TER spectra were also measured on ridges and surface of corneocytes where there were no vesicular structures present. These measurements were intended to quench the curiosity to find deuterated phospholipid that might have diffused from topically applied invasomes. It must be stressed that such measurements were like searching for a needle in a haystack as there were no topographical features to guide the placement of TERS grids like in case of measurements on vesicles. Despite the odds, on few occasions deuterated phospholipid was detected on the ridge like structures in corneocytes. Points where deuteration was detected did not have any topographical feature resembling a vesicle. On one occasion, along with deuteration spectra were also positive for 700 cm^{-1} cholesterol band indicating that these spectra were measured in the intercorneocyte lipids.

TERS results together with the high resolution AFM studies presented in publication-3 give a strong evidence that invasomes can in fact penetrate the human SC although not in a great number as only a very small fraction of the topically applied vesicles could be identified in the skin. One limitation of the study was that actual penetration depth for the invasomal vesicles was rather difficult to predict. A rather conservative speculation is that by 10^{th} layer the sampling technique has reached depth of at least 5 µm in the SC. *Stratum corneum* of the forearm in healthy humans is about 10 to 20 cell layers thick (Ya-Xian *et al.*, 1999) with *stratum disjunctum* accounting for the first 3-5 cell layers. Therefore it was very likely that sampling technique described here was able to also probe the stratum compactum present below the *stratum disjunctum*.

TERS is a very complex technique and has been shown to have capability to detect even single molecules (Treffer *et al.*, 2011). Ideally for TERS, samples should be as flat as possible as this ensures easy access for the TERS tip to the sample surface. Skin samples measured in the current study were far from ideal samples and despite this we could demonstrate application of TERS on complex skin samples. In this study a sample preparation technique was developed and interactions between the SC and invasomes were successfully probed. However, few answers raise more questions. A more comprehensive study to compare different topical liposomal formulations and a thorough investigation to see how deep intact vesicles can be seen in the SC makes a quiet appealing outlook for this project.

4.3 Mechanism behind invasomal drug delivery to skin

Based on the results published in this thesis, it is foreseeable that mechanism involved in drug penetration from topical invasomal application would involve a combination of 'penetration of intact vesicles' and 'penetration enhancement mechanism'. The above predictions are mainly based on the publication-3 where effect of empty invasomes on the *stratum corneum* was studied. Although, Hofland *et al.* (1995) provided the first evidence for intact liposomes penetrating the SC using freeze fracture electron mcroscopy, we have presented for the first time a strong spectroscopic evidence along with imaging to support the claim. Although intact invasomal vesicles were observed in the SC, a claim cannot be made that this is the main mechanism for drug penetration in the skin. This skepticism arises from the fact that only a very small fraction of vesicles could be detected in the SC, compared to what was applied topically to the skin. If this small fraction is able to make a big enough impact on the SC barrier function is not clear. Also the state in which these vesicles penetrate the SC was not clear and whether they would be able to carry drug deeper along with them will need future investigations. The TERS study also points towards the 'penetration enhancement mechanism' which is one of the well accepted mechanism for liposomal drug penetration (El Maghraby *et al.*, 2006). In this mechanism components which make up the liposomal vesicles penetrate the intercorneocyte lipids either in the form of individual molecules or in smaller molecular arrangement.

Studies in publication-4 emphasized that, during formation development a close attention should be given to the interactions between the drug and phospholipid bilayer. For highest drug penetration in the skin, it will be important for the drug to partition out of the lipid bilayer and enter the intercorneocyte lipids. Once the drug has partitioned out, further movement of the drug will be determined by 1) physicochemical properties of the drug 2) components of the liposomes. Components of the liposomes play an important role as they would influence the extent of disruption of the intercorneocyte lipids. Higher the extent of disruption, higher will be the drug penetration. However first the drug must be able to partition out of the liposome bilayer and into the SC lipids. If drug is involved in electrostatic interactions with the liposomal bilayer as seen in the publication-4 or if the drug is so lipophilic that it prefers to stay associated with the bilayer then using a liposomal system for delivering such drugs would rather hamper the drug delivery rather than enhancing it.

In general, liposomes in topical delivery do not offer a 'one-stop' solution. For example, ibuprofen gel with penetration enhancers would far outweigh ibuprofen-liposome system. Cost factors and long term stability also make topical liposomal formulation a little impractical. Topical liposomal systems would be rather more suitable in instances where conventional systems cannot be applied successfully.

5. Summary

Stratum corneum forms the most significant part of the skin barrier for topically applied substances. Various invasive and non-invasive strategies such as chemical penetration enhancers, iontophoresis, microneedles etc. can be employed to increase drug penetration through the skin. Liposomes have also been shown to enhance the penetration of a variety of drugs in the skin. Invasomes is a soy-phosphatidylcholine based liposomal system that was developed by the Fahr group for drug delivery to skin. When drug substances are applied on the skin in solution form, drug penetration mainly depends on the physicochemical properties of the drug however, incorporation of drugs in the liposomes results in a rather complex interaction between the *stratum corneum*, phospholipid membrane and drug. Studies in this thesis were designed to probe the interactions between the *stratum corneum* and invasomes in order to gain a better understanding of the mechanisms involved in the drug delivery to skin from invasomes.

Confocal Raman microscopy was employed to study the co-diffusion of liposomally entrapped drugs and the phospholipids forming the liposomal bilayers. The study was based on a premise that if diffusion patterns of both, drug and phospholipid could be studied in the skin then it might allow us to comment on the underlying mechanism responsible for penetration of drug as each mechanism should give rise to a different diffusion profile. Confocal Raman microscopy was the preferred choice of imaging technique as it facilitated possibility of a label-free identification. Biggest challenge in such measurements was to keep the sample stable. A method was developed to obtain non-invasive Raman depth profiles in *ex vivo* human skin. Optical biopsies of untreated skin were measured along with diffusion profiles of skin treated with beta-carotene and deuterated water. The maximum penetration depth achieved for the optical biopsies was about 30-35 µm, which was subsequently improved to increase the penetration depth achieved to about 60 µm. This method was unfortunately not sensitive enough to measure the diffusion of deuterated phospholipid applied topically in the form of invasomes.

A more sensitive method to probe the interactions between liposomes and the *stratum corneum* was required. Tip-enhanced Raman scattering (TERS) was the tool of choice as TERS is not limited by the Abbe's resolution limit and is an excellent tool for providing chemical and structural information. Conventional tape stripping technique was adopted to allow application of TERS. *In vivo* human skin was treated with deuterated invasomes and the *stratum corneum* was progressively removed. TERS and atomic force microscopy measurements revealed that intact invasome vesicles did penetrate the *stratum corneum*. Vesicular structures were flattened and were observed in all 10 layers which were analyzed in the measurements. For the first time spectroscopic evidence along with high resolution imaging confirmed that intact liposomes can penetrate the human *stratum corneum*.

Further, in a bicentric study, three vesicular systems viz. cationic LeciPlex, amphoteric invasomes and conventional liposomes were compared for their ability to deliver idebenone and azelaic acid into the deeper layers of human skin. All formulations were also characterized and their efficacy was measured using *in vitro* cell assays and *in vivo* animal model. Observations were discussed based on the drug-liposomal membrane interactions.

Based on results of studies discussed in this dissertation, it is anticipated that drug delivery to skin from topically applied invasomes would encompass a combination of mechanism of penetration enhancement and transport by intact vesicle penetration.

Zusammenfassung

Das S*tratum corneum* bildet den wichtigsten Bestandteil der Hautbarriere für topisch applizierte Substanzen. Verschiedene invasive und nicht-invasive Strategien, wie z.B. chemische Penetrationsverstärker, Iontophorese, Mikronadeln usw., können angewandt werden, um die Wirkstoffpenetration durch die Haut zu verbessern. Es wurde auch gezeigt, dass Liposomen die Penetration einer Vielzahl von Medikamenten durch die Haut verbessern können. Invasomen sind ein auf Soja-Phosphatidylcholin basierendes Liposomensystem, das von der Arbeitsgruppe um A. Fahr für den Wirkstofftransport durch die Haut entwickelt wurde. Werden Wirkstoffe in Form einer Lösung auf die Haut appliziert, hängt die Penetration hauptsächlich von den physikochemischen Eigenschaften der Substanz ab. Werden sie dagegen in Liposomen eingearbeitet, führt dies zu einer ziemlich komplexen Wechselwirkung zwischen dem *Stratum corneum*, der Phospholipidmembran und dem Wirkstoff. Die in dieser Arbeit durchgeführten Studien wurden konzipiert, um die Wechselwirkungen zwischen *Stratum corneum* und Invasomen zu untersuchen, um dadurch ein besseres Verständnis der Mechanismen zu erhalten, die an der Wirkstoffabgabe aus den Invasomen in die Haut beteiligt sind.

Konfokale Raman-Mikroskopie wurde verwendet, um die Codiffusion von liposomal eingeschlossenem Wirkstoff und den dazugehörigen, den liposomalen Bilayer formenden, Phospholipiden zu untersuchen. Diese Studie basiert auf der Voraussetzung, dass man, falls das Diffusionsmuster von Wirkstoff und Phospholipid in der Haut untersucht werden kann, eine Erklärung darüber äußern kann, welche Mechanismen für die Penetration des Wirkstoffes verantwortlich sind, da jeder Mechanismus ein unterschiedliches Diffusionsprofil hervorruft. Konfokale Raman-Mikroskopie war dabei das bevorzugte Bildgebungsverfahren, da es eine Identifikation ohne vorherige Substanzmarkierung ermöglicht. Die größte Herausforderung bei solchen Messungen war es, die Probe stabil zu halten. Es wurde ein Verfahren entwickelt, um nicht-invasive Raman-Tiefenprofile in menschlicher Haut *ex vivo* zu erhalten. Optische Biopsien von unbehandelter Haut und ein Diffusionsprofil von, mit Beta-Carotin und deuteriertem Wasser, behandelter Haut wurden aufgenommen. Die maximale Eindringtiefe, die bei dieser Gewebeuntersuchung anfänglich erreicht wurde, lag bei ungefähr 30-35 µm und wurde anschließend auf ungefähr 60 µm verbessert. Dennoch war diese Methode leider nicht sensitiv genug, um die Diffusion von deuterierten Phospholipiden, die topisch in Form von Invasomen appliziert wurden, zu messen.

Daher wurde eine empfindlichere Methode benötigt, um die Interaktionen zwischen Liposomen und *Stratum corneum* zu untersuchen. Tip-Enhanced Raman Scattering (TERS) war das Mittel der Wahl, da TERS nicht durch das Auflösungsvermögen nach Abbe limitiert ist und ein exzellentes Werkzeug liefert, um chemische und strukturelle Informationen zu erhalten. Die konventionelle Tape-Stripping-Methode wurde modifiziert, um die Anwendung von TERS zu ermöglichen. Dabei wurde menschliche Haut *in vivo* mit deuterierten Invasomen behandelt und das *Stratum corneum* anschließend schrittweise

entfernt. TERS und Atomkraftmikroskopie (AFM) zeigten, dass intakte Invasomvesikel das *Stratum corneum* penetrieren können. Vesikuläre Strukturen wurden abgeflacht und konnten in allen 10 Schichten, die in den Studien untersucht wurden, beobachtet werden. Dadurch konnte erstmals mit Hilfe von spektroskopischen Hinweisen, in Kombination mit einer hochauflösenden Bildtechnik, bestätigt werden, dass intakte Liposomen das menschliche *Stratum corneum* penetrieren können.

In einer bizentrischen Studie wurden drei vesikuläre Systeme – kationische LeciPlex, amphotere Invasomen und herkömmliche Liposomen – auf ihre Fähigkeit untersucht, Idebenon und Azelainsäure in die tieferen Schichten menschlicher Haut zu transportieren. Alle Formulierungen wurden entsprechend charakterisiert und ihre Wirksamkeit mit Hilfe von *in vitro*-Zellassays und *in vivo*-Tiermodellen gemessen. Die hierbei gemachten Beobachtungen wurden auf Grundlage von Wechselwirkungen zwischen Wirkstoff und liposomaler Membran diskutiert.

Auf Grundlage der Ergebnisse aller Untersuchungen dieser Arbeit ist anzunehmen, dass der Mechanismus für die Wirkstoffabgabe topisch applizierter Invasomen in die menschliche Haut eine Kombination aus Penetrationsbeschleunigung und der Penetration intakter Vesikel umfasst.

6. References

Aalto-Korte K (1995) Improvement of skin barrier function during treatment of atopic dermatitis. *Journal of the American Academy of Dermatology* 33:969-72.

Alvarez-Roman R, Naik A, Kalia YN*, et al.* (2004) Visualization of skin penetration using confocal laser scanning microscopy. *European journal of pharmaceutics and biopharmaceutics : official journal of Arbeitsgemeinschaft fur Pharmazeutische Verfahrenstechnik eV* 58:301-16.

Anderson MS (2000) Locally enhanced Raman spectroscopy with an atomic force microscope. *Applied Physics Letters* 76:3130-2.

Ashtikar M, Matthäus C, Schmitt M*, et al.* (2013) Non-invasive depth profile imaging of the stratum corneum using confocal Raman microscopy: First insights into the method. *European Journal of Pharmaceutical Sciences* 50:601-8.

Atkinson JP, Maibach HI, Dragicevic N (2015) Targets in dermal and transdermal delivery and classification of penetration enhancement methods. In: *Percutaneous penetration enhancers Chermical methods in penetration enhancement* (Dragicevic N, Maibach HI, eds) Vol. 1: Springer, 94-108.

Bachhav YG, Heinrich A, Kalia YN (2013) Controlled intra- and transdermal protein delivery using a minimally invasive Erbium:YAG fractional laser ablation technology. *European journal of pharmaceutics and biopharmaceutics : official journal of Arbeitsgemeinschaft fur Pharmazeutische Verfahrenstechnik eV* 84:355-64.

Bailo E, Deckert V (2008) Tip-Enhanced Raman Spectroscopy of Single RNA Strands: Towards a Novel Direct-Sequencing Method. *Angewandte Chemie* 47:1658-61.

Barber PW, Chang RK, Massoudi H (1983) Surface-Enhanced Electric Intensities on Large Silver Spheroids. *Physical Review Letters* 50:997-1000.

Barenholz Y, Lasic DD (1996) *Handbook of Nonmedical Applications of Liposomes*. Taylor & Francis.

Barry BW (2001) Novel mechanisms and devices to enable successful transdermal drug delivery. *European journal of pharmaceutical sciences : official journal of the European Federation for Pharmaceutical Sciences* 14:101-14.

Barry BW (2005) Penetration Enhancer Classification. In: *Percutaneous Penetration Enhancers, Second Edition* (CRC Press, 3-15.

Benson HA (2005) Transdermal drug delivery: penetration enhancement techniques. *Curr Drug Deliv* 2:23-33.

Benson HA (2009) Elastic liposomes for topical and transdermal drug delivery. *Curr Drug Deliv* 6:217-26.

Blagus T, Markelc B, Cemazar M*, et al.* (2013) In vivo real-time monitoring system of electroporation mediated control of transdermal and topical drug delivery. *Journal of controlled release : official journal of the Controlled Release Society* 172:862-71.

Blum C, Opilik L, Atkin JM*, et al.* (2014) Tip-enhanced Raman spectroscopy – an interlaboratory reproducibility and comparison study. *Journal of Raman Spectroscopy*:n/a-n/a.

Boskey A, Mendelsohn R (2005) Infrared analysis of bone in health and disease. *Journal of biomedical optics* 10:031102.

Bouwstra JA, Gooris GS, van der Spek JA*, et al.* (1991) Structural investigations of human stratum corneum by small-angle X-ray scattering. *The Journal of investigative dermatology* 97:1005-12.

Bouwstra JA, Honeywell-Nguyen PL (2002) Skin structure and mode of action of vesicles. *Adv Drug Deliv Rev* 54 Suppl 1:S41-55.

Bramson J, Dayball K, Evelegh C*, et al.* (2003) Enabling topical immunization via microporation: a novel method for pain-free and needle-free delivery of adenovirus-based vaccines. *Gene therapy* 10:251-60.

Carrer DC, Vermehren C, Bagatolli LA (2008) Pig skin structure and transdermal delivery of liposomes: a two photon microscopy study. *Journal of controlled release : official journal of the Controlled Release Society* 132:12-20.

Celia C, Cilurzo F, Trapasso E*, et al.* (2012) Ethosomes(R) and transfersomes(R) containing linoleic acid: physicochemical and technological features of topical drug delivery carriers for the potential treatment of melasma disorders. *Biomedical microdevices* 14:119-30.

Cevc G (2003) Transdermal drug delivery of insulin with ultradeformable carriers. *Clinical pharmacokinetics* 42:461-74.

Cevc G, Blume G (2001) New, highly efficient formulation of diclofenac for the topical, transdermal administration in ultradeformable drug carriers, Transfersomes. *Biochimica et biophysica acta* 1514:191-205.

Cevc G, Blume G (2003) Biological activity and characteristics of triamcinolone-acetonide formulated with the self-regulating drug carriers, Transfersomes. *Biochimica et biophysica acta* 1614:156-64.

Cevc G, Gebauer D, Stieber J*, et al.* (1998) Ultraflexible vesicles, Transfersomes, have an extremely low pore penetration resistance and transport therapeutic amounts of insulin across the intact mammalian skin. *Biochimica et Biophysica Acta (BBA)-Biomembranes* 1368:201-15.

Cevc G, Mazgareanu S, Rother M*, et al.* (2008) Occlusion effect on transcutaneous NSAID delivery from conventional and carrier-based formulations. *Int J Pharm* 359:190-7.

Cevc G, Vierl U (2010) Nanotechnology and the transdermal route: A state of the art review and critical appraisal. *Journal of controlled release : official journal of the Controlled Release Society* 141:277-99.

Chen M, Liu X, Fahr A (2010) Skin delivery of ferulic acid from different vesicular systems. *Journal of biomedical nanotechnology* 6:577-85.

Cheong H-A, Choi H-K (2003) Effect of ethanolamine salts and enhancers on the percutaneous absorption of piroxicam from a pressure sensitive adhesive matrix. *European Journal of Pharmaceutical Sciences* 18:149-53.

Chi S-C, Park E-S, Kim H (1995) Effect of penetration enhancers on flurbiprofen permeation through rat skin. *International Journal of Pharmaceutics* 126:267-74.

Date AA, D. S, S. NM*, et al.* (2011) Lecithin-based novel cationic nanocarriers (LeciPlex) I: fabrication, characterization and evaluation. *Nanomedicine (Lond)* 6:1309-25.

Deckert-Gaudig T, Deckert V (2011) Nanoscale structural analysis using tip-enhanced Raman spectroscopy. *Current opinion in chemical biology* 15:719-24.

Deckert-Gaudig T, Rauls E, Deckert V (2010) Aromatic Amino Acid Monolayers Sandwiched between Gold and Silver: A Combined Tip-Enhanced Raman and Theoretical Approach. *The Journal of Physical Chemistry C* 114:7412-20.

Deckert V, Deckert-Gaudig T, Diegel M*, et al.* (2015) Spatial resolution in Raman spectroscopy. *Faraday discussions* 177:9-20.

Denet AR, Preat V (2003) Transdermal delivery of timolol by electroporation through human skin. *Journal of controlled release : official journal of the Controlled Release Society* 88:253-62.

Denet AR, Vanbever R, Preat V (2004) Skin electroporation for transdermal and topical delivery. *Adv Drug Deliv Rev* 56:659-74.

Deo MR, Sant VP, Parekh SR*, et al.* (1997) Proliposome-based transdermal delivery of levonorgestrel. *Journal of biomaterials applications* 12:77-88.

Dragicevic-Curic N, Fahr A (2012) Liposomes in topical photodynamic therapy. *Expert opinion on drug delivery* 9:1015-32.

Dragicevic-Curic N, Grafe S, Albrecht V*, et al.* (2008) Topical application of temoporfin-loaded invasomes for photodynamic therapy of subcutaneously implanted tumours in mice: a pilot study. *Journal of photochemistry and photobiology B, Biology* 91:41-50.

El Maghraby GM, Barry BW, Williams AC (2008a) Liposomes and skin: from drug delivery to model membranes. *European journal of pharmaceutical sciences : official journal of the European Federation for Pharmaceutical Sciences* 34:203-22.

El Maghraby GM, Barry BW, Williams AC (2008b) Liposomes and skin: From drug delivery to model membranes. *European Journal of Pharmaceutical Sciences* 34:203-22.

El Maghraby GM, Williams AC, Barry BW (2006) Can drug-bearing liposomes penetrate intact skin? *The Journal of pharmacy and pharmacology* 58:415-29.

Elias PM (1983) Epidermal lipids, barrier function, and desquamation. *The Journal of investigative dermatology* 80 Suppl:44s-9s.

Elsayed MM, Abdallah OY, Naggar VF*, et al.* (2007) Lipid vesicles for skin delivery of drugs: reviewing three decades of research. *Int J Pharm* 332:1-16.

Ermakov IV, Ermakova MR, Gellermann W*, et al.* (2004) Noninvasive selective detection of lycopene and beta-carotene in human skin using Raman spectroscopy. *Journal of biomedical optics* 9:332-8.

Eroschenko VP, Fiore MSHd (2013) *diFiore's atlas of histology with functional correlations*, 12th edn. Wolters Kluwer Health/Lippincott Williams & Wilkins: Philadelphia, xx, 603 p.

Escribano E, Calpena AC, Queralt J*, et al.* (2003) Assessment of diclofenac permeation with different formulations: anti-inflammatory study of a selected formula. *European journal of pharmaceutical sciences : official journal of the European Federation for Pharmaceutical Sciences* 19:203-10.

Fahr A, Muller R (2003) Invasomes for therapy of disorders, their preparation and use. (Office USPaT ed): USA.

Fang L, Xi H, Cun D (2015) Formation of ion pairs and complex coacervates. In: *Percutaneous penetration enhancers Chermical methods in penetration enhancement* (Dragicevic N, Maibach HI, eds) Vol. 1: Springer, 175-87.

Fartasch M (1996) The nature of the epidermal barrier: structural aspects. *Advanced Drug Delivery Reviews* 18:273-82.

Feldmann RJ, Maibach HI (1965) PENETRATION OF 14C HYDROCORTISONE THROUGH NORMAL SKIN: THE EFFECT OF STRIPPING AND OCCLUSION. *Arch Dermatol* 91:661-6.

Flynn GL, Weiner ND (1991) Topical and transdermal delivery - provinces of realism. In: *Dermal and transdermal delivery* (Teubner GR, ed), Stuttgart: Wissenschaftliche Verlafsgesellschaft GmbH, 33-64.

Foldvari M, Gesztes A, Mezei M (1990) Dermal drug delivery by liposome encapsulation: clinical and electron microscopic studies. *Journal of microencapsulation* 7:479-89.

Fresta M, Puglisi G (1996) Application of liposomes as potential cutaneous drug delivery systems. In vitro and in vivo investigation with radioactively labelled vesicles. *Journal of drug targeting* 4:95-101.

Garson JC, Doucet J, Leveque JL*, et al.* (1991) Oriented structure in human stratum corneum revealed by X-ray diffraction. *The Journal of investigative dermatology* 96:43-9.

Gesztes A, Mezei M (1988) Topical anesthesia of the skin by liposome-encapsulated tetracaine. *Anesthesia and analgesia* 67:1079-81.

Gill HS, Prausnitz MR (2007) Coating formulations for microneedles. *Pharm Res* 24:1369-80.

Gniadecka M, Philipsen PA, Sigurdsson S*, et al.* (2004) Melanoma Diagnosis by Raman Spectroscopy and Neural Networks: Structure Alterations in Proteins and Lipids in Intact Cancer Tissue. *J Investig Dermatol* 122:443-9.

Goldsmith LA, Fitzpatrick TB (2012) *Fitzpatrick's dermatology in general medicine*, 8th edn. McGraw-Hill Professional: New York, p.

Gomez C, Costela A, Garcia-Moreno I*, et al.* (2008) Laser treatments on skin enhancing and controlling transdermal delivery of 5-fluorouracil. *Lasers in surgery and medicine* 40:6-12.

Gregoriadis G (2006) *Liposome Technology: Liposome Preparation and Related Techniques*. CRC Press.

Gupta PN, Mishra V, Singh P*, et al.* (2005) Tetanus toxoid-loaded transfersomes for topical immunization. *Journal of Pharmacy and Pharmacology* 57:295-301.

Gwak HS, Chun IK (2002) Effect of vehicles and penetration enhancers on the in vitro percutaneous absorption of tenoxicam through hairless mouse skin. *Int J Pharm* 236:57-64.

Hamishehkar H, Rahimpour Y, Kouhsoltani M (2012) Niosomes as a propitious carrier for topical drug delivery. *Expert opinion on drug delivery* 10:261-72.

Hasanovic A, Winkler R, Resch GP*, et al.* (2011) Modification of the conformational skin structure by treatment with liposomal formulations and its correlation to the penetration depth of aciclovir. *European journal of pharmaceutics and biopharmaceutics : official journal of Arbeitsgemeinschaft fur Pharmazeutische Verfahrenstechnik eV* 79:76-81.

Hayazawa N, Inouye Y, Sekkat Z*, et al.* (2001) Near-field Raman scattering enhanced by a metallized tip. *Chemical Physics Letters* 335:369-74.

Herrmann F, Mandol L (1955) Studies of Ph of Sweat Produced by Different Forms of Stimulation1. *The Journal of investigative dermatology* 24:225-46.

Higuchi WI (1962) Analysis of data on the medicament release from ointments. *J Pharm Sci* 51:802-4.

Hofland HE, Bouwstra JA, Bodde HE*, et al.* (1995) Interactions between liposomes and human stratum corneum in vitro: freeze fracture electron microscopical visualization and small angle X-ray scattering studies. *The British journal of dermatology* 132:853-66.

Hofland HE, van der Geest R, Bodde HE*, et al.* (1994) Estradiol permeation from nonionic surfactant vesicles through human stratum corneum in vitro. *Pharm Res* 11:659-64.

Hofland HEJ, Bouwstra JA, Ponec M*, et al.* (1991) Interactions of non-ionic surfactant vesicles with cultured keratinocytes and human skin in vitro: a survey of toxicological aspects and ultrastructural changes in stratum corneum. *Journal of Controlled Release* 16:155-67.

Honeywell-Nguyen PL, Bouwstra JA (2005) Vesicles as a tool for transdermal and dermal delivery. *Drug Discovery Today: Technologies* 2:67-74.

Horwitz E, Pisanty S, Czerninski R*, et al.* (1999) A clinical evaluation of a novel liposomal carrier for acyclovir in the topical treatment of recurrent herpes labialis. *Oral surgery, oral medicine, oral pathology, oral radiology, and endodontics* 87:700-5.

Hosafci G, Klein O, Oremek G*, et al.* (2007) Clinical chemistry without reagents? An infrared spectroscopic technique for determination of clinically relevant constituents of body fluids. *Analytical and bioanalytical chemistry* 387:1815-22.

Iwai I, Han H, den Hollander L*, et al.* (2012) The human skin barrier is organized as stacked bilayers of fully extended ceramides with cholesterol molecules associated with the ceramide sphingoid moiety. *The Journal of investigative dermatology* 132:2215-25.

Jona JA, Dittert LW, Crooks PA*, et al.* (1995) Design of novel prodrugs for the enhancement of the transdermal penetration of indomethacin. *International Journal of Pharmaceutics* 123:127-36.

Jung S, Otberg N, Thiede G*, et al.* (2006) Innovative Liposomes as a Transfollicular Drug Delivery System: Penetration into Porcine Hair Follicles. *The Journal of investigative dermatology* 126:1728-32.

Kasting G, Smith R, Cooper E (1987) Effect of lipid solubility and molecular size on percutaneous absorption. In: *Pharmacology and the skin* (Shroot B, Schaefer H, eds) Vol. 1, Basel: Karger, 138-53.

Kenneth AW, Michael SR (2002) The Structure and Function of Skin. In: *Dermatological and Transdermal Formulations* (CRC Press.

Kitagawa S, Kasamaki M (2006) Enhanced delivery of retinoic acid to skin by cationic liposomes. *Chemical and pharmaceutical bulletin* 54:242-4.

Knepp VM, Hadgraft J, Guy RH (1987) Transdermal drug delivery: problems and possibilities. *Critical reviews in therapeutic drug carrier systems* 4:13-37.

Kodali DR, Small DM, Powell J*, et al.* (1991) Infrared Micro-imaging of Atherosclerotic Arteries. *Applied Spectroscopy* 45:1310-7.

Krafft C, Salzer R (2008) Neuro-oncological applications of infrared and Raman spectroscopy. In: *Vibrational spectroscopy for medical diagnosis* (Diem M, Chalmers JM, Griffiths PR, eds): John Wiley & Sons Ltd.

Kranz G, Schaefer H, Zesch A (1977) Hydrocortisone (cortisol) concentration and penetration gradient. *Acta Derm Venereol* 57:269-73.

Krause K, Foitzik K (2006) Biology of the hair follicle: the basics. *Semin Cutan Med Surg* 25:2-10.

Krishnan G, Edwards J, Chen Y*, et al.* (2010) Enhanced skin permeation of naltrexone by pulsed electromagnetic fields in human skin in vitro. *J Pharm Sci* 99:2724-31.

Lademann J, Jacobi U, Surber C*, et al.* (2009) The tape stripping procedure--evaluation of some critical parameters. *European journal of pharmaceutics and biopharmaceutics : official journal of Arbeitsgemeinschaft fur Pharmazeutische Verfahrenstechnik eV* 72:317-23.

Lakshmi PK, Devi GS, Bhaskaran S*, et al.* (2007) Niosomal methotrexate gel in the treatment of localized psoriasis: phase I and phase II studies. *Indian journal of dermatology, venereology and leprology* 73:157-61.

Lasch P, Beekes M, Schmitt J*, et al.* (2007) Detection of preclinical scrapie from serum by infrared spectroscopy and chemometrics. *Anal Bioanal Chem* 387:1791-800.

Lavrijsen AP, Oestmann E, Hermans J*, et al.* (1993) Barrier function parameters in various keratinization disorders: transepidermal water loss and vascular response to hexyl nicotinate. *The British journal of dermatology* 129:547-53.

Levin G, Gershonowitz A, Sacks H*, et al.* (2005) Transdermal delivery of human growth hormone through RF-microchannels. *Pharm Res* 22:550-5.

Levin J, Friedlander SF, Del Rosso JQ (2013) Atopic Dermatitis and the Stratum Corneum: Part 2: Other Structural and Functional Characteristics of the Stratum Corneum Barrier in Atopic Skin. *The Journal of Clinical and Aesthetic Dermatology* 6:49-54.

Li L, Hoffman RM (1997) Topical liposome delivery of molecules to hair follicles in mice. *J Dermatol Sci* 14:101-8.

Lieber CA, Majumder SK, Billheimer D*, et al.* (2008) Raman microspectroscopy for skin cancer detection in vitro. *Journal of biomedical optics* 13:024013.

Loan Honeywell-Nguyen P, de Graaff AM, Wouter Groenink HW*, et al.* (2002) The in vivo and in vitro interactions of elastic and rigid vesicles with human skin. *Biochimica et Biophysica Acta (BBA)-General Subjects* 1573:130-40.

Lucille A, Le Grand R, Martinon F (2014) Electroporation-Mediated Intradermal Delivery of DNA Vaccines in Nonhuman Primates. In: *Electroporation Protocols: Preclinical and Clinical Gene Medicine* (Li S, Cutrera J, Heller R, Teissie J, eds) 1 ed.: Humana Press, 309-13.

Lunter D, Daniels R (2014) Confocal Raman microscopic investigation of the effectiveness of penetration enhancers for procaine delivery to the skin. *Journal of biomedical optics* 19:126015.

Madison KC, Swartzendruber DC, Wertz PW*, et al.* (1987) Presence of intact intercellular lipid lamellae in the upper layers of the stratum corneum. *The Journal of investigative dermatology* 88:714-8.

Maheshwari C, Pandey RS, Chaurasiya A*, et al.* (2011) Non-ionic surfactant vesicles mediated transcutaneous immunization against hepatitis B. *International immunopharmacology* 11:1516-22.

Malkinson FD. (1963) Radioactive agents and radioisotopes in dermatology: Investigative applications. In: PILLSBURY DM, LIVINGOOD CS (eds) *Proceedings of the Conference Radioactive agents and radioisotopes in dermatology: Investigative applications;* 1963 1962; Washington DC. Excerpta Medica Foundation: Amsterdam.

Manosroi A, Kongkaneramit L, Manosroi J (2004) Stability and transdermal absorption of topical amphotericin B liposome formulations. *Int J Pharm* 270:279-86.

Manosroi A, Ruksiriwanich W, Abe M*, et al.* (2012) Transfollicular enhancement of gel containing cationic niosomes loaded with unsaturated fatty acids in rice (Oryza sativa) bran semi-purified fraction. *European journal of pharmaceutics and biopharmaceutics : official journal of Arbeitsgemeinschaft fur Pharmazeutische Verfahrenstechnik eV* 81:303-13.

Markets Ma (2013) Drug Delivery Technologies Market (Metered Dose Inhalers, Needle-Free Injectors, Auto-Injectors, Nasal Sprays, Transdermal Patches, Nebulizers, Infusion Pumps, Drug Eluting Stents, Sustained Release, Ocular Implants) - Global Forecasts To 2017.

Masukawa Y, Narita H, Shimizu E*, et al.* (2008) Characterization of overall ceramide species in human stratum corneum. *J Lipid Res* 49:1466-76.

Mateus R, Abdalghafor H, Oliveira G*, et al.* (2013) A new paradigm in dermatopharmacokinetics – Confocal Raman spectroscopy. *International Journal of Pharmaceutics* 444:106-8.

Mezei M, Gulasekharam V (1980) Liposomes--a selective drug delivery system for the topical route of administration. Lotion dosage form. *Life Sci* 26:1473-7.

Miller JM, Dahan A, Gupta D*, et al.* (2009) Quasi-equilibrium analysis of the ion-pair mediated membrane transport of low-permeability drugs. *Journal of controlled release : official journal of the Controlled Release Society* 137:31-7.

Mishra D, Dubey V, Asthana A*, et al.* (2006) Elastic liposomes mediated transcutaneous immunization against Hepatitis B. *Vaccine* 24:4847-55.

Moskovits M (1985) Surface-enhanced spectroscopy. *Reviews of Modern Physics* 57:783-826.

Murthy SN, Sammeta SM, Bowers C (2010) Magnetophoresis for enhancing transdermal drug delivery: Mechanistic studies and patch design. *Journal of controlled release : official journal of the Controlled Release Society* 148:197-203.

Narasimha Murthy S, Shivakumar HN (2010) CHAPTER 1 - Topical and Transdermal Drug Delivery. In: *Handbook of Non-Invasive Drug Delivery Systems* (Kulkarni VS, ed), Boston: William Andrew Publishing, 1-36.

Ng KW, Lau WM (2015) Skin deep: The basics of human skin structure and drug penetration. In: *Percutaneous Penetration Enhancers: Chemical Methods in Penetration Enhancement* (Dragicevic N, Maibach HI, eds) Vol. I: Springer-Verlag, 4-11.

Nijssen A, Maquelin K, Santos LF*, et al.* (2007) Discriminating basal cell carcinoma from perilesional skin using high wave-number Raman spectroscopy. *Journal of biomedical optics* 12:034004.

Nolano M, Simone DA, Wendelschafer-Crabb G*, et al.* (1999) Topical capsaicin in humans: parallel loss of epidermal nerve fibers and pain sensation. *Pain* 81:135-45.

Paolino D, Lucania G, Mardente D*, et al.* (2005) Ethosomes for skin delivery of ammonium glycyrrhizinate: in vitro percutaneous permeation through human skin and in vivo anti-inflammatory activity on human volunteers. *Journal of controlled release : official journal of the Controlled Release Society* 106:99-110.

Park JH, Lee JW, Kim YC*, et al.* (2008) The effect of heat on skin permeability. *Int J Pharm* 359:94-103.

Patzelt A, Lademann J (2013) Drug delivery to hair follicles. *Expert opinion on drug delivery* 10:787-97.

Polat BE, Hart D, Langer R*, et al.* (2011) Ultrasound-mediated transdermal drug delivery: mechanisms, scope, and emerging trends. *Journal of controlled release : official journal of the Controlled Release Society* 152:330-48.

Prausnitz MR, Langer R (2008) Transdermal drug delivery. *Nat Biotechnol* 26:1261-8.

Röding J, Artmann C (1992) The Fate of Liposomes in Animal Skin. In: *Liposome Dermatics* (Braun-Falco O, Korting H, Maibach H, eds): Springer Berlin Heidelberg, 185-94.

Schaefer H, Redelmeier T (1996) Structure and dynamics of the skin barrier. In: *Skin Barrier: Principles of Percutaneous Absorption* (Basel: Karger), 1-42.

Schaefer H, Zesch A, Stättgen G (1982) Skin Permeability. In: *Skin Permeability* (Springer Berlin Heidelberg, 541-845.

Schatzlein A, Cevc G (1998) Non-uniform cellular packing of the stratum corneum and permeability barrier function of intact skin: a high-resolution confocal laser scanning microscopy study using highly deformable vesicles (Transfersomes). *The British journal of dermatology* 138:583-92.

Scheuplein RJ, Blank IH (1971) Permeability of the skin. *Physiol Rev* 51:702-47.

Severs NJ (2007) Freeze-fracture electron microscopy. *Nat Protocols* 2:547-76.

Shah SM, Ashtikar M, Jain AS*, et al.* (2015) LeciPlex, invasomes, and liposomes: A skin penetration study. *International Journal of Pharmaceutics* 490:391-403.

Sharma G, Deckert-Gaudig T, Deckert V (2015) Tip-enhanced Raman scattering—Targeting structure-specific surface characterization for biomedical samples. *Advanced Drug Delivery Reviews* 89:42-56.

Sinico C, Manconi M, Peppi M*, et al.* (2005) Liposomes as carriers for dermal delivery of tretinoin: in vitro evaluation of drug permeation and vesicle-skin interaction. *Journal of controlled release : official journal of the Controlled Release Society* 103:123-36.

Sivamani RK, Liepmann D, Maibach HI (2007) Microneedles and transdermal applications. *Expert opinion on drug delivery* 4:19-25.

Skerrow CJ, Clelland DG, Skerrow D (1989) Changes to desmosomal antigens and lectin-binding sites during differentiation in normal human epidermis: a quantitative ultrastructural study. *Journal of cell science* 92 (Pt 4):667-77.

Sloan KB, Synovec J, Wasdo SC (2015) Selection of a Proper Prodrug for Penetration Enhancement. In: *Percutaneous Penetration Enhancers: Chemical Methods in Penetration Enhancement* (Dragicevic N, Maibach HI, eds) Vol. I: Springer-Verlag, 137-50.

Stöckle RM, Suh YD, Deckert V*, et al.* (2000) Nanoscale chemical analysis by tip-enhanced Raman spectroscopy. *Chemical Physics Letters* 318:131-6.

Stott PW, Williams AC, Barry BW (1998) Transdermal delivery from eutectic systems: enhanced permeation of a model drug, ibuprofen. *Journal of controlled release : official journal of the Controlled Release Society* 50:297-308.

Takahashi K, Rytting JH (2001) Novel approach to improve permeation of ondansetron across shed snake skin as a model membrane. *The Journal of pharmacy and pharmacology* 53:789-94.

Tezel A, Mitragotri S (2003) Interactions of inertial cavitation bubbles with stratum corneum lipid bilayers during low-frequency sonophoresis. *Biophysical journal* 85:3502-12.

Tfaili S, Gobinet C, Josse G*, et al.* (2013) Vibrational spectroscopies for the analysis of cutaneous permeation: experimental limiting factors identified in the case of caffeine penetration. *Anal Bioanal Chem* 405:1325-32.

Tfayli A, Piot O, Pitre F*, et al.* (2007) Follow-up of drug permeation through excised human skin with confocal Raman microspectroscopy. *European Biophysics Journal* 36:1049-58.

Torchilin V, Weissig V (2003) *Liposomes: A Practical Approach*. OUP Oxford.

Touitou E, Chow DD, Lawter JR (1994) Chiral β-blockers for transdermal delivery. *International Journal of Pharmaceutics* 104:19-28.

Touitou E, Dayan N, Bergelson L*, et al.* (2000) Ethosomes - novel vesicular carriers for enhanced delivery: characterization and skin penetration properties. *Journal of controlled release : official journal of the Controlled Release Society* 65:403-18.

Trauer S, Richter H, Kuntsche J*, et al.* (2014) Influence of massage and occlusion on the ex vivo skin penetration of rigid liposomes and invasomes. *European Journal of Pharmaceutics and Biopharmaceutics* 86:301-6.

Treffer R, Bohme R, Deckert-Gaudig T*, et al.* (2012) Advances in TERS (tip-enhanced Raman scattering) for biochemical applications. *Biochemical Society transactions* 40:609-14.

Treffer R, Lin X, Bailo E*, et al.* (2011) Distinction of nucleobases - a tip-enhanced Raman approach. *Beilstein journal of nanotechnology* 2:628-37.

Valjakka-Koskela R, Hirvonen J, Monkkonen J*, et al.* (2000) Transdermal delivery of levosimendan. *European journal of pharmaceutical sciences : official journal of the European Federation for Pharmaceutical Sciences* 11:343-50.

van den Bergh BA, Vroom J, Gerritsen H*, et al.* (1999) Interactions of elastic and rigid vesicles with human skin in vitro: electron microscopy and two-photon excitation microscopy. *Biochimica et biophysica acta* 1461:155-73.

van Kuijk-Meuwissen ME, Junginger HE, Bouwstra JA (1998) Interactions between liposomes and human skin in vitro, a confocal laser scanning microscopy study. *Biochimica et biophysica acta* 1371:31-9.

Verma DD, Verma S, Blume G*, et al.* (2003) Liposomes increase skin penetration of entrapped and non-entrapped hydrophilic substances into human skin: a skin penetration and confocal laser scanning microscopy study. *European journal of pharmaceutics and biopharmaceutics : official journal of Arbeitsgemeinschaft fur Pharmazeutische Verfahrenstechnik eV* 55:271-7.

Verma DD, Verma S, McElwee KJ*, et al.* (2004) Treatment of alopecia areata in the DEBR model using Cyclosporin A lipid vesicles. *European journal of dermatology : EJD* 14:332-8.

Vogt A, Mandt N, Lademann J*, et al.* (2005) Follicular targeting--a promising tool in selective dermatotherapy. *The journal of investigative dermatology Symposium proceedings / the Society for Investigative Dermatology, Inc [and] European Society for Dermatological Research* 10:252-5.

von Zglinicki T, Lindberg M, Roomans GM*, et al.* (1993) Water and ion distribution profiles in human skin. *Acta Derm Venereol* 73:340-3.

Vyumvuhore R, Tfayli A, Duplan H*, et al.* (2013) Effects of atmospheric relative humidity on Stratum Corneum structure at the molecular level: ex vivo Raman spectroscopy analysis. *Analyst* 138:4103-11.

Washitake M, Yajima T, Anmo T*, et al.* (1973) Studies on percutaneous absorption of drugs. 3. Percutaneous absorption of drugs through damaged skin. *Chemical & pharmaceutical bulletin* 21:2444-51.

West PA, Bostrom MP, Torzilli PA*, et al.* (2004) Fourier transform infrared spectral analysis of degenerative cartilage: an infrared fiber optic probe and imaging study. *Appl Spectrosc* 58:376-81.

White SH, Mirejovsky D, King GI (1988) Structure of lamellar lipid domains and corneocyte envelopes of murine stratum corneum. An X-ray diffraction study. *Biochemistry* 27:3725-32.

Winkelmann RK, Breathnach AS (1973) THE MERKEL CELL. *J Investig Dermatol* 60:2-15.

Wo Y, Zhang Z, Zhang Y*, et al.* (2011) Preparation of ethosomes and deformable liposomes encapsulated with 5-fluorouracil and their investigation of permeability and retention in hypertrophic scar. *Journal of nanoscience and nanotechnology* 11:7840-7.

Wokaun A, Gordon JP, Liao PF (1982) Radiation Damping in Surface-Enhanced Raman Scattering. *Physical Review Letters* 48:957-60.

Xi H, Cun D, Wang Z*, et al.* (2012) Effect of the stability of hydrogen-bonded ion pairs with organic amines on transdermal penetration of teriflunomide. *Int J Pharm* 436:857-61.

Xiao C, Flach CR, Marcott C*, et al.* (2004) Uncertainties in depth determination and comparison of multivariate with univariate analysis in confocal Raman studies of a laminated polymer and skin. *Appl Spectrosc* 58:382-9.

Xiao C, Moore DJ, Flach CR*, et al.* (2005a) Permeation of dimyristoylphosphatidylcholine into skin—Structural and spatial information from IR and Raman microscopic imaging. *Vibrational Spectroscopy* 38:151-8.

Xiao C, Moore DJ, Rerek ME*, et al.* (2005b) Feasibility of tracking phospholipid permeation into skin using infrared and Raman microscopic imaging. *The Journal of investigative dermatology* 124:622-32.

Ya-Xian Z, Suetake T, Tagami H (1999) Number of cell layers of the stratum corneum in normal skin – relationship to the anatomical location on the body, age, sex and physical parameters. *Archives of dermatological research* 291:555-9.

Yu H-Y, Liao H-M (1996) Triamcinolone permeation from different liposome formulations through rat skin in vitro. *International Journal of Pharmaceutics* 127:1-7.

Zhang YT, Shen LN, Wu ZH*, et al.* (2014) Comparison of ethosomes and liposomes for skin delivery of psoralen for psoriasis therapy. *Int J Pharm* 471:449-52.

List of abbreviations

AFM – Atomic force microscopy

AmB – Amphotericin B

Chol. – Cholesterol,

CRM – Confocal Raman microscopy

d31-POPC – 1-palmitoyl-d31-2-oleoyl-sn-glycero-3-phosphocholine

d9-DLPC – 1,2-dilinoleoyl-3-phosphocholine-N,N,N-trimethyl-d9

DC-chol. – 3β-[N-(dimethylaminoethane) carbamoyl]cholesterol

DMPC – 1,2-dimyristoyl-sn-glycero-3-phosphocholine

DOTAP – 1,2-dioleoyl-3-trimethylammonium-propane

DPPC – 1,2-dipalmitoyl-sn-glycero-3-phosphocholine

DPPG – 1,2-dipalmitoyl-sn-glycero-3-phosphoglycerol

HPC – Hydrogenated soya phosphatidylcholine,

MLV – Multilamellar vesicles

PC – Phosphatidylcholine

Rh-DOPE – 1,2-Dioleoyl-sn-glycero-3-phosphoethanolamine-N-(lissamine rhodamine B)

SC – Stratum corneum

SERS – Surface enhanced Raman scattering

SPM – Scanning probe microscope

STM – Scanning tunneling microscope

SUV – Small unilamellar vesicles,

TERS – Tip-enhanced Raman scattering

TES – Trimethylammonium methyl sulfate

VCA – Vertex component analysis

Acknowledgements

I would like to thank my advisor Prof Fahr for giving me an opportunity to be part of his research group. Even today, almost six years later I still remember our first meeting in Boston and I distinctly remember thinking to myself after the meeting how nice it would be to work with him, and I am really glad I moved to Jena. I would always be thankful to him for his unreserved help, trust and guidance throughout my Ph.D. I owe the perspective I have today, to his unlimited zeal for science and constant encouragement I received from him during my postgraduate research. It is hard to overstate my gratitude to him.

I must express my sincere gratitude to Prof Deckert for his guidance on TERS. Without his enthusiasm, genius suggestions and support it would not have been possible to conduct this research. I am also extremely grateful to Dr.Christian Matthäus for our nice collaboration and for introducing me to the wonderful world of Raman spectroscopy. I have learned a great deal from him and I will never forget his kindness. Christian, your friendly advice and constructive discussions helped me a lot to improve my understanding of Raman spectroscopy. I am also grateful to Prof. Mangal Nagarsenkar for always being there to answer my (most of the time silly) questions. I thoroughly enjoyed three years of collaborative science we did together and look forward for many more to come.

I am extremely thankful to Lucas Langelüddecke for the collaborative work on TERS measurements and to Dr Sanket Shah for the collaborative work on the ICMR-BMBF project. It was really fun working with you guys.

I would also like to thank my colleagues; Stephan Holzschuh, Erica D'Aguano, Markus Rabenhold, Georg Pester, Marius Bauer, Khaled Shalaby, Kewei Yang, Ming Chen, Ronny Rüger, Keda Zhang, Maximillian Sperlich, Christiane Decker, Amaraporn Roopdee, Florian Schlenk , Yaser Alkhatib, Kathrin Kaeß and Hossam Hefesha. All wonderful memories we had in lab, conferences, Christmas markets and lunch breaks made my time at PhT very memorable. Special thanks to Jana Thamm, Christine Steinbach, Ramona Brabetz, Angela Herre and Alexander Mohn for their kind help and support throughout my time in Jena.

I would also like to thank my thesis committee for their time and patience.

Finally, I wish to express my appreciation to my family, for their endless support and encouragement in all of my endeavors. Special thanks to my wife for being there with me in all the ups and downs.

I would like to dedicate this dissertation to my parents,

Sandhya and Arun Ashtikar.

Curriculum Vitae

Personal Information

Name:	Mukul Ashtikar
Date of Birth:	April 26, 1985
Nationality:	Indian
Address:	Lessingstr. 8 (Pharm), 07743 Jena, Germany
Telephone:	+ 49 3641 949907 (office)
E-mail:	mukul-arun.ashtikar@uni-jena.de

Education

PhD candidate (December. 2009 – Present)	**Friedrich-Schiller-University Jena**, Germany Thesis title: 'Studies on the penetration mechanisms of topical liposomal formulations'
Masters of Pharmaceutical Sciences **(**September 2007 – May 2009**)**	**Northeastern University**, Boston, USA Concentration: Pharmaceutics and drug delivery systems
Bachelor of Pharmaceutical Sciences **(**October 2002 - July 2006**)**	**University of Mumbai**, Mumbai, India

Research Experience

Doctoral Research:

- Study of interaction of liposomes with human skin using Tip-enhanced Raman spectroscopy
- Developing novel methodology to using confocal Raman microscopy, for taking high resolution non-invasive optical biopsies in intact human and pig skin.
- Preparation and characterization of anti-cancer liposomal formulations using in vitro, ex vivo and in vivo models to understand their ability to deliver drugs to deeper layers of skin.
- Development of novel methodology for preparation of cochleate formulations with uniform size distribution.

Past Research experience:

- Determination of solubility of 181 drugs and drug-like compounds in a variety of simulated GI Fluids. Project with Simulations Plus Inc, California. Duration: Jan 2008 to Oct 2009.
- Diffusion studies on intestinal mucus: Project focused on finding out permeability characteristics of porcine intestinal mucus. Duration: June 2008 to 2009.
- Effect of food on drug dissolution, in-vitro modeling. Duration: September 2008 to May 2009.
- Drug precipitation kinetics, modeling in-vitro precipitation kinetics of basic drugs as they transition from stomach to intestine. Duration: September 2008 to March 2009

Publications

1. **Ashtikar M.**, Verma D., Fahr A. Confocal microscopy for visualization of skin penetration - Book Chapter, Percutaneous Penetration Enhancers, 3rd edition - In Press
2. Nagarsekar K., **Ashtikar M.**, Thamm J., Steiniger F., Schacher F., Fahr A., May S. Electron Microscopy and Theoretical Modeling of Cochleates. Langmuir 2014, 30, 13143-13151.
3. **Ashtikar M.**, Matthäus C., Schmitt M., Krafft C., Fahr A., Popp J. Non-invasive depth profile imaging of the stratum corneum using confocal Raman microscopy: First insights into the method. European Journal of Pharmaceutical Sciences 2013, 50, 601-608
4. Shah S., ****Ashtikar M.**, Jain A., Makhija D., Nikam Y., Gude R., Steiniger F., Jagtap A., Nagarsenker M., Fahr A. LeciPlex, invasomes and liposomes: A skin penetration study. International Journal of Pharmaceutics 2015, 490, 391-403.
5. Gamsiz E., **Ashtikar M.**, Crison J., Woltosz W., Bolger M., Carrier R. Predicting the Effect of Fed-State Intestinal Contents on Drug Dissolution. Pharmaceutical Research 2010, 27, 2646-2656.
6. Nagarsekar K., ****Ashtikar M.**, Steiniger F., Thamm J., Schacher F., Fahr A. Understanding cochleate formation: Insight into structural evolution. Manuscript under review in Soft Matter
7. Nagarsekar K., ****Ashtikar M.**, Steiniger F., Thamm J., Fahr A. Microspherical cochleate composites: Method development for monodispersed system. Under review in the Journal of Liposome Research.
8. **Ashtikar M.**, Langelüddecke L., Fahr A., Deckert V. Interactions of liposomes with human skin - A Tip-enhanced Raman Spectroscopy study. Manuscript in preparation

****Equal first authorship**

Presentations

1. TERS investigations on invasome treated human skin, poster presentation at Liposome Research Days, Copenhagen, Denmark, 4-7 August 2014.
2. Can liposomes penetrate skin? AFM-TERS investigations on invasome treated skin. Oral presentation at the 23rd Mountain / Sea Liposome workshop, Oberjoch, Germany, 24 - 28 March 2014.
3. AFM-TERS investigations on Invasome treated skin, poster presentation at the 3rd Symposium on Phospholipids in Pharmaceutical Research, Heidelberg, Germany, 16-17 September 2013
4. AFM-TERS investigations in invasome treated skin, poster presentation at 2013 European Conferences on Biomedical Optics, Munich, Germany, 12-16 May 2013.
5. PEGylated invasomes for dermal delivery. Oral presentation at 22nd Mountain / Sea workshop at Ameland, Netherlands, 24-28 September 2012.
6. Non-invasive imaging of transdermal penetration profiles in skin using Raman microscopy. Poster presentation at 9th International conference and workshop on Biological Barriers, Saarbrücken, Germany, 29 February - 9 March 2012.
7. Comparison of percutaneous penetration of ibuprofen from cream and gel. Oral presentation at 21st Mountain / Sea Liposome workshop at Oberjoch, Germany, 28 March - 1 April 2011
8. Measurement of solubility in simulated gastrointestinal fluids for a diverse set of 160 molecules. Poster presentation at AAPS Annual meeting and Exposition, Los Angeles, USA, 8-12 November 2009.

Declaration

I would like to acknowledge that I am familiar with the 'Promotionsordnung' of the Faculty of Biology and Pharmacy in the Friedrich-Schiller-University Jena. All chapters of this dissertation were produced by myself. This dissertation does not contain any material previously submitted for any degree or diploma at any other University. Also this dissertation does not contain any material previously written or published by any other person, except where due acknowledgement or reference has been made in the text. I would also like to declare that I did not enlist the assistance of any 'dissertation-counseling agent' and that I did not provide any direct or indirect monetary benefit to any third party for work connected to my dissertation.

Mukul Ashtikar

Jena, 23/10/2015